POWER SYSTEM INTERCONNECTION

(TRANSMISSION PROBLEMS)

Also by

H. RISSIK

THE CALCULATION OF UNSYMMETRICAL SHORT CIRCUITS

A practical introduction to the use of symmetrical components in fault studies of three-phase networks. **7s. 6d.** net.

"*Admirably suited to the needs of those students already familiar with the subject who require a practical reference work.*"—INSTITUTION OF ELECTRICAL ENGINEERS' STUDENTS QUARTERLY JOURNAL.

MERCURY-ARC CURRENT CONVERTORS

An introduction to the theory of vapour-arc discharge devices and to the study of rectification phenomena. It deals with the subject in a way which meets the needs of students at Universities, Technical Colleges, etc., who are grappling with the subject for the first time, and also assists the engineer who is primarily interested in practical applications. **25s.** net.

Published by
PITMAN

POWER SYSTEM INTERCONNECTION

(TRANSMISSION PROBLEMS)

BY

H. RISSIK, Hons. B.Sc. (Eng.)

A.M.I.E.E., M.A.I.E.E.

SECOND EDITION

LONDON

SIR ISAAC PITMAN & SONS, LTD.

First published 1940
Second Edition 1950

SIR ISAAC PITMAN & SONS, LTD.
PITMAN HOUSE, PARKER STREET, KINGSWAY, LONDON, WC.2
THE PITMAN PRESS, BATH
PITMAN HOUSE, LITTLE COLLINS STREET, MELBOURNE
27 BECKETTS BUILDINGS, PRESIDENT STREET, JOHANNESBURG

ASSOCIATED COMPANIES
PITMAN PUBLISHING CORPORATION
2 WEST 45TH STREET, NEW YORK
205 WEST MONROE STREET, CHICAGO
SIR ISAAC PITMAN & SONS (CANADA), LTD.
(INCORPORATING THE COMMERCIAL TEXT BOOK COMPANY)
PITMAN HOUSE, 381–383 CHURCH STREET, TORONTO

MADE IN GREAT BRITAIN AT THE PITMAN PRESS, BATH
Eo—(T.180)

TO

ANN RISSIK

Αἰὲν ἀριστεύειν καὶ ὑπείροχον ἔμμεναι ἄλλων

—*Homer.*

PREFACE

THE present work is not just another treatise on the apparently inexhaustible subject of electric power. It is neither intended to survey existing practice in the generation, transmission, or distribution of alternating current, nor concerned with the many problems associated with the design and operation of individual power stations and distribution networks. Both these aspects of electric power are adequately dealt with in a number of already standard textbooks and works of reference. On the contrary, the object of this new book is to acquaint the practising engineer, as well as the advanced student, with the several analytical and semi-graphical methods that have been developed, during the last two decades, for calculating the performance of interconnected power systems. And it has been the author's aim throughout to present in this volume just the bare minimum of theoretical material necessary not only to an understanding of the special problems involved in power system interconnection, but also to the formulation of appropriate solutions to these problems.

The view is commonly expressed that, as the British "Grid" is, in effect, a vast 132 kV. busbar system, it does not lend itself to study from this particular aspect of power system operation, and that in consequence those studies of power system interconnection which are usually associated with the transport of electricity on a continental scale can only be of academic interest so far as this country is concerned. Such a point of view is, to say the least, short-sighted. It completely overlooks the fact that the linking up of large selected stations through the medium of the "Grid" can, and sometimes does, reproduce conditions which are a commonplace, say, in America. The fact that the Boulder Dam line is 270 miles long and operates at 287 kV. does not mean to say that the problems connected with its operation are fundamentally different from those arising in the case of the interconnection of, say, Hams Hall and Nechells. Although there exists a wide difference in order of magnitude, the relative scale to which system behaviour must be referred is more or less the same for both.

As indicated by its sub-title, the present volume has been

purposely limited in scope to a consideration of the basic transmission problems underlying the technique of power system interconnection as we know and understand it to-day. That technique, however, is intimately bound up with the solution of other no less vital problems centring upon a variety of extraneous factors which involve the operational behaviour of electrical machines *per se*. Although these aspects are not stressed, the present volume gives a sufficiently comprehensive treatment of the subject as a whole to enable an adequate quantitative examination to be made of any but the most complicated interconnected systems.

The bulk of the material included in the book has been based on articles by the author which have already appeared in the technical press, and upon notes on the subject collected by him during recent years. The treatment of power limits in Chapter III is nevertheless original, and, in particular, the analysis underlying the geometrical construction of the power-limit parabola and of the power-circle envelope has not been previously published. Where the work of others has been drawn upon, due acknowledgment is made at the end of the chapter concerned. In addition, to facilitate further study of the subject, a bibliography of all the most important references in the English language, together with a few foreign references, has been compiled and arranged in chronological sequence.

H. R.

1949.

CONTENTS

CHAPTER VI

INSETS

LIST OF SYMBOLS

Vector Representation

$\mathbf{A}$ . . .	Vector or complex quantity. $= A\lvert\underline{\alpha} = A_1 + jA_2 = A\varepsilon^{j\alpha}$.
A . . .	Modulus of **A**.
α . . .	Argument of **A**.
A_1 . .	Datum-axis component of **A**.
A_2 . .	Quadrature-axis component of **A**.
j . . .	Anticlockwise 90°-operator.
$\mathbf{A}'$ . . .	Conjugate of **A**. $= A\lvert\underline{-\alpha} = A_1 - jA_2 = A\varepsilon^{-j\alpha}$.

Network Quantities

$\mathbf{A} = A\lvert\underline{\alpha} = A_1 + jA_2$ $\mathbf{B} = B\lvert\underline{\beta} = B_1 + jB_2$ $\mathbf{C} = C\lvert\underline{\gamma} = C_1 + jC_2$ $\mathbf{D} = D\lvert\underline{\delta} = D_1 + jD_2$	General network constants or parameters.
$B = j\omega C$.	Shunt susceptance.
C . . .	Shunt capacitance.
G . . .	Shunt leakance.
L . . .	Series inductance.
R . . .	Series resistance.
$X = j\omega L$.	Series reactance.
$\mathbf{Y} = G + jB$.	Shunt admittance.
$\mathbf{Z} = R + jX$.	Series impedance.
$\mathbf{Z}_r = Z_r\lvert\underline{\rho_r}$.	Receiving-end driving-point impedance.
$\mathbf{Z}_s = Z_s\lvert\underline{\rho_s}$.	Sending-end driving-point impedance.
$\mathbf{Z}_t = Z_t\lvert\underline{\rho_t}$.	Transfer impedance.
$\mathbf{Z}_0 = \sqrt{(\mathbf{Z}/\mathbf{Y})}$.	Characteristic impedance.
$\Theta = \sqrt{(\mathbf{ZY})}$.	Complex line angle.
ρ . . .	Impedance angle.
$\sigma = \frac{1}{2}\pi - \rho$.	Complement of impedance angle.
$\omega = 2\pi f$.	Angular frequency.

Voltages, Currents, Powers and Mechanical Quantities

D . . .	Transmission distance.
$\mathbf{E} = E\lvert\underline{\theta}$.	E.m.f. or voltage.

H	Energy stored per unit of rating.
$\mathbf{I} = I\lfloor\underline{\psi}$	Current.
J	Moment of inertia.
M	Inertia constant.
N	Synchronous speed.
P	Power.
Q	Reactive volt-amperes.
T	Torque.
T	Power ratio.
t	Time.
W	Kinetic energy stored at synchronous speed.
ΔP	Power differential.
δP	Power increment.
η	Efficiency.
λ	Torque angle.
μ	Displacement angle.
ϕ	External power-factor angle.
ψ	Internal power-factor angle.
τ	Generalized time.
$\omega = 2\pi f$	Angular frequency.
ω	Angular velocity.

SUFFICES

r, s	Receiving-, sending-end *line-to-neutral* or phase values in V, A., W. and VAr.
R, S	Receiving-, sending-end *line* values in kV., A., MW. and MVAr.
E	Electrical.
	Limiting.
G	Generator.
Go	Generator loss.
I	Interconnector.
L	Line.
	Loss (line).
M	Maximum.
	Mechanical.
	Motor.
Mo	Motor loss.
R	Receiving-end (line).
S	Sending-end (line).
	Synchronizing.
SC	Short-circuit.

T . . .	Transfer.
	Transformer.
U . . .	Critical.
l . . .	Loss (phase).
m . . .	Maximum.
	Maximum transfer.
n . . .	Rated.
o . . .	Open-circuit.
p . . .	Phase component.
q . . .	Quadrature component.
r . . .	Receiving-end (phase).
ro . . .	Receiving-end driving-point.
s . . .	Sending-end.
so . . .	Sending-end driving-point.
0 . . .	Characteristic.
	Initial.
	Separating.
1 . . .	Primary.
	First.
2 . . .	Secondary.
	Second.
3 . . .	Tertiary.
	Third.

POWER SYSTEM INTERCONNECTION

CHAPTER I

[FUNDAMENTAL CONCEPTIONS AND PRINCIPLES]

WHEN considering the transmission of electric power in general it is necessary at the outset to distinguish between *synchronous* and *asynchronous* transmission systems. By the term "transmission system" is to be understood the composite electrical system formed by a generating station, a distant load network, and the overhead line or underground cable (including terminal transformers) constituting the intervening power-transmitting link.

The majority of power transmission problems discussed in standard texts on generation and transmission are concerned with essentially asynchronous systems, that is to say, transmission systems of the type represented by a synchronous generator supplying power, through a circuit combination of series impedance and shunt admittance, to an asynchronous load consisting, say, partly of static impedance (e.g. lighting) and partly of dynamic impedance (e.g. induction motors). The characteristic feature of such a transmission system is that the terminal voltage at the load is not an independent factor, but is determined by the induced e.m.f. of the generator as well as by the amount of power transmitted. The general behaviour of an asynchronous transmission system is accordingly conditioned by the fundamental characteristics of a generator supplying a simple impedance load. As the result, problems which centre upon this type of transmission system may be solved with the aid of vector diagrams and their attendant analysis—in short, by the straightforward application of conventional a.c. theory.

Problems of power system interconnection, on the other hand, concern a transmission system which is essentially synchronous in character. The very term "interconnection" implies a linking-up of power systems having independent

existence. And when two such systems are linked by a general network of series impedance and shunt admittance, the aggregation constitutes a synchronous transmission system. In its most elementary form such a system comprises a synchronous generator supplying power to a synchronous motor through a simple reactive tie. But the most general form of a synchronous transmission system is typified by two otherwise independent synchronous systems connected together by a power-transmitting link of some kind, e.g. a busbar, a cable interconnector, or a transmission line. The characteristic feature of such a transmission system is that the voltages at the two ends of the power link exist independently of one another as well as of the amount of power interchanged between the terminal systems. The general behaviour of a synchronous transmission system is accordingly determined by the characteristic mode of power flow between individual synchronous machines. Consequently the problems peculiar to power system interconnection cannot usefully be approached from the standpoint of conventional a.c. theory, nor can they be solved by the methods usually associated with vector analysis.

It is the purpose of this opening chapter to outline the several elements of the analytical framework within which such problems can be readily confined, and their solution in consequence becomes a matter of the routine application of certain principles and methods of attack. Some of these methods are of a graphical nature; others, again, are purely analytical. All, however, involve concepts that are often foreign to the average engineer who, while being *au fait* with the many problems of everyday electrical practice, is, as a rule, not familiar with the theoretical approach that is characteristic of power transmission technique. This general unfamiliarity with power transmission, considered as a special branch of electrical engineering practice, is all the more unfortunate in that many of the analytical tools employed, e.g. equivalent circuits and circle diagrams, are only too well known in their application to the solution of the more common electrical power problems. Particularly is this the case, for example, in determining the power limit of a synchronous transmission system operating under normal steady-load conditions. For this important problem lends itself, as will be shown later on, to a semi-graphical method of solution that

makes a ready appeal to the electrical engineer versed in the diagrammatic representation of technical questions in general.

Representation of Vector Quantities. In nearly all problems connected with power system interconnection the main variables are vector quantities, that is to say, alternating quantities which can be represented graphically by means of rotating vectors. The conventional method of vector analysis employed in a.c. theory makes use of the so-called symbolic or algebraic method of vector notation in which vector quantities are represented by complex numbers. By this method a vector quantity is defined completely, i.e. in magnitude and direction, with reference to a system of rectangular or x/y co-ordinates in which the abscissae (x) represent "datum" values and the ordinates (y) represent "quadrature" values, that is, "datum" values operated upon by a 90° anticlockwise rotation. This unit operator is customarily denoted by the symbol j, algebraically equivalent to $\sqrt{-1}$.

This system of notation is illustrated in Fig. 1 (a), in which the vector quantity **A*** is regarded as the resultant of two component vector quantities—the one along datum and of magnitude A_1, the other in quadrature and of magnitude A_2. The vector quantity is thus completely defined by the relation

$$\mathbf{A} = A_1 + jA_2 \quad . \quad . \quad . \quad (1)$$

In this system of notation the *conjugate* $\mathbf{A}'$ of the vector **A** is defined by the corresponding relation

$$\mathbf{A}' = A_1 - jA_2 \quad . \quad . \quad . \quad (2)$$

and is represented in Fig. 1 (a) by the image of the vector **A** as seen reflected in the x- or datum-axis.

It is seen from Fig. 1 (a) that the quadrature component jA_2 of the vector quantity **A** is obtained by rotating a vector representing the datum quantity A_2 in the positive (anticlockwise) direction of rotation through the angle $\pi/2$. Operation by j thus denotes the rotation of a vector through a positive right angle. Conversely, division by the unit operator j denotes rotation through a negative right angle, since $1/j = j/j^2 = -j$. For example, referring to Fig. 1 (a), the quadrature component $-jA_2$ of the conjugate vector quantity $\mathbf{A}'$ is obtained by rotating a vector representing the datum quantity

* All vector quantities and vector operators are indicated by Clarendon type, thus: **E, z, B, i.**

A_2 in the negative (clockwise) direction of rotation through the angle $\pi/2$.

This conception of rotating vectors at once leads to the trigonometric method of vector notation, illustrated in Fig. 1 (*b*), by which a vector is completely defined with reference to a system of polar or r-θ co-ordinates. In this system the radius vector A represents the *modulus*, while its angular displacement α from the zero axis of vector reference represents the *argument* of the complex quantity $\mathbf{A} = A_1 + jA_2$. Comparing diagrams (*a*) and (*b*) of Fig. 1 it is evident that $A_1 = A \cos \alpha$ and

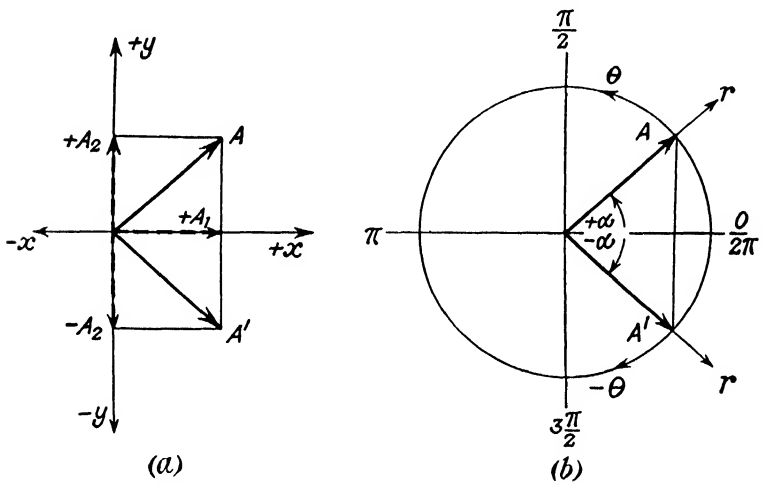

FIG. 1. CONVENTIONS IN VECTOR REPRESENTATION
(*a*) Rectangular co-ordinate system.
(*b*) Polar co-ordinate system.

$A_2 = A \sin \alpha$, so that the vector quantity $\mathbf{A}$ is completely defined by the relation

$$\begin{aligned} \mathbf{A} &= A_1 + jA_2 = A \cos \alpha + jA \sin \alpha \\ &= A (\cos \alpha + j \sin \alpha) = A\varepsilon^{j\alpha} \quad . \quad . \quad (3) \end{aligned}$$

Multiplication by the operator $\varepsilon^{j\alpha}$ thus signifies rotation of a vector representing the real quantity A through the positive angle α. Hence the operator $\varepsilon^{j\pi/2}$ must be identical with the unit operator j. That this is actually the case may be shown by putting $A = 1$ and $\alpha = \pi/2$ in equation (3). Similarly, application of the operator $\varepsilon^{-j\alpha}$ signifies the rotation of a

vector through the angle $-\alpha$. For example, the conjugate vector quantity $\mathbf{A}'$ is defined by the relation

$$\begin{aligned}\mathbf{A}' &= A_1 - jA_2 = A\cos\alpha - jA\sin\alpha \\ &= A[\cos(-\alpha) + j\sin(-\alpha)] = A\,\varepsilon^{-j\alpha} \quad . \quad (4)\end{aligned}$$

The operator $\varepsilon^{j\theta}$ is customarily abbreviated to $\underline{|\,\theta}$, so that the vector $\mathbf{A}$ is written $A\,\underline{|\,\alpha}$ and its conjugate $\mathbf{A}'$ is similarly written $A\,\underline{|-\alpha}$. The advantage of this trigonometric notation is that it facilitates the multiplication and division of vector quantities. Take the case of the voltage vector $\mathbf{E} = E\,\underline{|\,\theta}$ and the current vector $\mathbf{I} = I\,\underline{|\,\psi}$. The vector impedance is then simply

$$\begin{aligned}\mathbf{Z} = \frac{\mathbf{E}}{\mathbf{I}} &= \frac{E\,\underline{|\,\theta}}{I\,\underline{|\,\psi}} = \frac{E}{I}\cdot\frac{\varepsilon^{j\theta}}{\varepsilon^{j\psi}} = \frac{E}{I}\cdot\varepsilon^{j(\theta-\psi)} = \frac{E}{I}\,\underline{|\,(\theta-\psi)} \\ &= Z\,\underline{|\,\phi} \text{ (where } Z = E/I \text{ and } \phi = \theta - \psi) \\ &= R + jX \text{ (where } \sqrt{(R^2 + X^2)} = Z \text{ and } \tan^{-1}(X/R) = \phi)\end{aligned}$$

Provided $\theta > \psi$, that is, provided the voltage leads the current, the impedance angle ϕ is positive and the reactance X is then inductive. Conversely, a negative value of ϕ corresponds to a leading current and thus to capacitive reactance.

On considering power as the product of voltage and current it is found, however, that the vector power is given *not* by the product of the current vector $\mathbf{I}$ and the voltage vector $\mathbf{E}$ but by the vector product of $\mathbf{I}$ and $\mathbf{E}'$, the conjugate of $\mathbf{E}$, because we then have—

$$\begin{aligned}\textbf{Vector power} = \mathbf{E}'\mathbf{I} &= E\,\underline{|-\theta} \times I\,\underline{|\,\psi} \\ &= E\varepsilon^{-j\theta} \times I\varepsilon^{j\psi} = EI\varepsilon^{j(\psi-\theta)} \\ &= EI\cos(\psi-\theta) + jEI\sin(\psi-\theta) \\ &= P + jQ\end{aligned}$$

where $P = EI\cos(\psi - \theta)$ is the active power, and $Q = EI\sin(\psi - \theta)$ is the reactive power. In this case Q is positive if $\psi > \theta$, that is, provided the current $\mathbf{I}$ leads the voltage $\mathbf{E}$. This is the converse of the impedance case, where X is positive so long as $\theta > \psi$.

In other words, *an impedance* $(R \pm jX)$ *corresponds to a vector power* $(P \mp jQ)$. Positive or inductive reactance $(+X)$ thus corresponds to negative or lagging reactive power $(-Q)$; while negative or capacitive reactance $(-X)$ in turn corresponds to positive or leading reactive power $(+Q)$.

The General Transmission Network. To appreciate the nature of power transmission problems as a whole it is necessary not only to be clear as to the electrical behaviour of a transmission system, when regarded as a vehicle for the transport of electrical energy in bulk, but also to visualize the kind of picture which such a system presents when looked upon as an electrical circuit pure and simple. In fact, unless and until one can represent a given transmission system by a comparatively simple and familiar circuit diagram, any analysis of specific power transmission problems becomes unnecessarily difficult.

The starting-point in the solution of problems relating to power system interconnection is therefore the reduction of the transmission system to an equivalent network. In the last analysis, the power-transmitting element of a synchronous system is a generalized circuit, compounded of series impedance and shunt admittance, to one end of which—the so-called *sending end*—power is supplied, and at whose other end—termed the *receiving end*—power is withdrawn. Such a generalized circuit is known as a *network*, and the points where power is supplied and withdrawn are called the *terminals* of the network.[1]* No matter how complicated its structure, provided that all the elements of a network are inert and linear and that it has two sets of terminals, then the current and voltage at one end can be expressed as simple linear functions of the current and voltage at the other end. A synchronous transmission system may therefore be represented by an electrical network connecting two pairs of terminals across which are applied voltages that are quite independent as regards magnitude and phase relationship, but are interdependent in the sense that they are synchronous. At the same time, the corresponding currents flowing into and out of the network are not independent, for they are determined as much by the magnitudes and phases of the terminal voltages as by the electrical characteristics of the network. The several current and voltage relations of this general transmission network may be explained with reference to Fig. 2. In diagram (*a*) the sending-end and receiving-end terminals are designated by (*S*) and (*R*) respectively. If $\mathbf{E}_s$ and $\mathbf{I}_s$ denote the vector voltage and current at the sending end, and $\mathbf{E}_r$ and $\mathbf{I}_r$ those at the receiving end, then the electrical characteristics of the network determining the relation between them can be expressed in

* All numbered references are given at the end of each chapter.

terms of four constants, **A**, **B**, **C**, and **D**, through the fundamental *network equations*—

$$\mathbf{E}_s = \mathbf{A}\mathbf{E}_r + \mathbf{B}\mathbf{I}_r \quad . \quad . \quad . \quad (5a)$$

$$\mathbf{I}_s = \mathbf{C}\mathbf{E}_r + \mathbf{D}\mathbf{I}_r \quad . \quad . \quad . \quad (5b)$$

or their equivalents—

$$\mathbf{E}_r = \mathbf{D}\mathbf{E}_s - \mathbf{B}\mathbf{I}_s \quad . \quad . \quad . \quad (6a)$$

$$\mathbf{I}_r = -\mathbf{C}\mathbf{E}_s + \mathbf{A}\mathbf{I}_s \quad . \quad . \quad . \quad (6b)$$

In the above equations $\mathbf{E}_s$ and $\mathbf{E}_r$ are the independent variables and $\mathbf{I}_s$ and $\mathbf{I}_r$ the corresponding dependent variables. The four vector operators, **A**, **B**, **C**, and **D**, which take into account the composition of the power transmitting circuit as well as the electrical frequency of the synchronous system, are complex constants of the type $\mathbf{A} = (A_1 + jA_2)$, and are known as the *general network constants* or *parameters* of the transmission system.

It is clear that **A** and **D** are complex numeric operators, whereas **B** is a vector impedance and **C** is a vector admittance. For, referring to equation (5*a*), if $\mathbf{I}_r = 0$, then $\mathbf{A} = \mathbf{E}_s/\mathbf{E}_r$; that is to say, the constant **A** is the vector ratio of the sending-end voltage to the receiving-end voltage when the receiving end is open-circuited. Similarly, from equation (5*b*), if $\mathbf{E}_r = 0$, then $\mathbf{D} = \mathbf{I}_s/\mathbf{I}_r$. In other words, the constant **D** is the vector ratio of the sending- and receiving-end currents when the receiving end is short-circuited. Again, by the same reasoning, **B** is the ratio of the sending-end voltage to the receiving-end current when the receiving end is short-circuited. This vector impedance is known as the *transfer impedance* of the system and, as will be shown later, is a factor of vital importance in limiting the amount of power which can be transmitted between (*S*) and (*R*). Finally, the constant **C** is the ratio of the sending-end current to the receiving-end voltage when the receiving end is open-circuited, and is accordingly termed the *transfer admittance* of the system. These four network constants are bound by the universal relation

$$\mathbf{AD} - \mathbf{BC} \equiv 1 \quad . \quad . \quad . \quad . \quad (7)$$

so that only three of the four are independent.*

Two further relations of importance are to be derived from

* The equivalence of equations (5) and (6) is based on this relation.

equations (5*a*) and (5*b*). If the receiving end is short-circuited, so that $\mathbf{E}_r = 0$, then the sending-end impedance becomes

$$\mathbf{Z}_s = \frac{\mathbf{E}_s}{\mathbf{I}_s} = \frac{\mathbf{B}}{\mathbf{D}} \quad . \quad . \quad . \quad (8)$$

Similarly, if the sending end is short-circuited, so that $\mathbf{E}_s = 0$, then the receiving-end impedance becomes

$$\mathbf{Z}_r = \frac{\mathbf{E}_r}{-\mathbf{I}_r} = \frac{\mathbf{B}}{\mathbf{A}} \quad . \quad . \quad . \quad (9)$$

The minus sign in front of $\mathbf{I}_r$ indicates that, as seen from the receiving end, the direction of power flow through the network

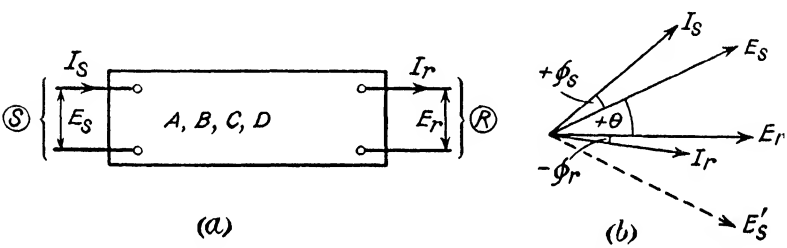

FIG. 2. THE GENERAL TRANSMISSION NETWORK
(*a*) Network diagram.
(*b*) Vector diagram.

is reversed. These two impedances are termed the *driving-point impedances* of the system.

The vector diagram for the general transmission network is shown in Fig. 2 (*b*). It is customary to take the receiving-end voltage as being along the datum of vector reference, so that $\mathbf{E}_r = E_r|\underline{0} = E_r$. The vector angle θ between $\mathbf{E}_s$ and $\mathbf{E}_r$ is commonly known as the *transmission angle*. The sending-end voltage is thus $\mathbf{E}_s = E_s|\underline{\theta}$. The power-factor angles of the currents at the sending and receiving ends are respectively ϕ_s and ϕ_r, so that the currents are $\mathbf{I}_s = I_s|\underline{(\theta + \phi_s)}$ and $\mathbf{I}_r = I_r|\underline{\phi_r}$. The receiving-end power output is consequently

$$P_r + jQ_r = \mathbf{E}_r'\mathbf{I}_r = E_r I_r|\underline{\phi_r} \quad . \quad . \quad (10a)$$

while the vector power input at the sending end is

$$P_s + jQ_s = \mathbf{E}_s'\mathbf{I}_s = E_s I_s|\underline{\phi_s} \quad . \quad . \quad (10b)$$

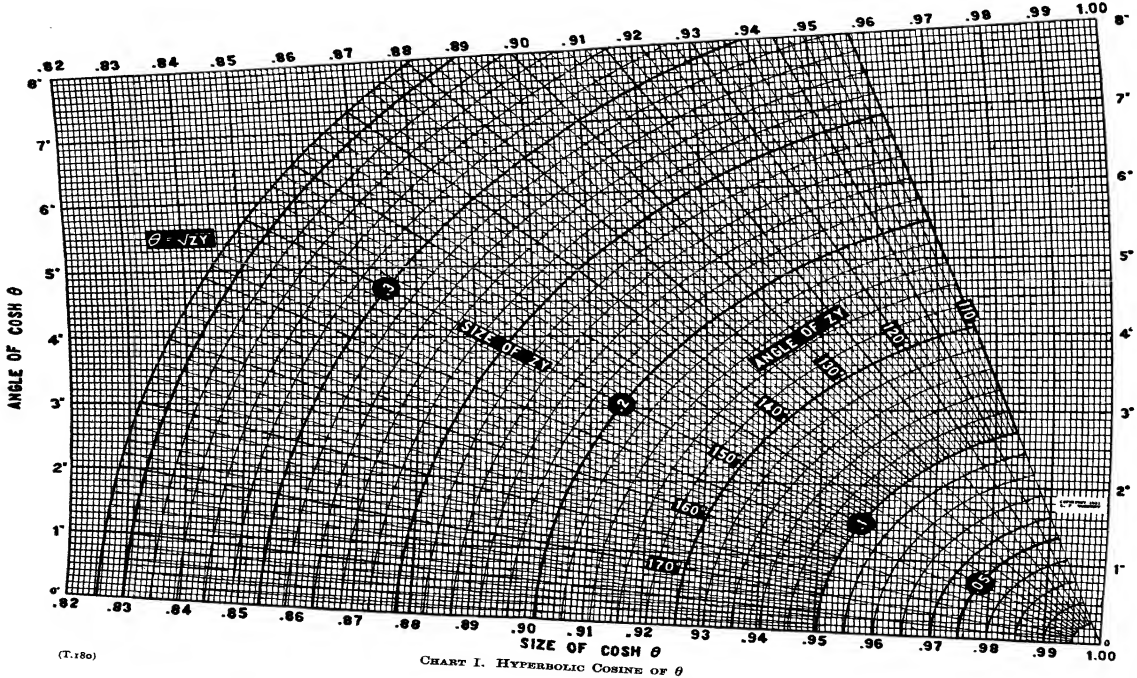

(T.180)

CHART I. HYPERBOLIC COSINE OF θ

Transmission-line Constants. The fundamental voltage and current equations for a long transmission line with uniformly distributed constants are—

$$\mathbf{E}_s = \mathbf{E}_r \cosh \Theta + \mathbf{Z}_0 \mathbf{I}_r \sinh \Theta \quad . \quad . \quad (11a)$$

$$\mathbf{I}_s = \frac{\mathbf{E}_r}{\mathbf{Z}_0} \sinh \Theta + \mathbf{I}_r \cosh \Theta \quad . \quad . \quad (11b)$$

where $\Theta = \sqrt{(\mathbf{ZY})}$ is the complex angle subtended by the line and $\mathbf{Z}_0 = \sqrt{(\mathbf{Z/Y})}$ is its characteristic impedance.[2] Here $\mathbf{Z} = (R + jX)$ is the total series impedance and $\mathbf{Y} = (G + jB)$ is the total shunt admittance of the line. Comparing equations (11) and (5) it is evident that the network constants of the transmission line are—

$$\left.\begin{aligned} \mathbf{A} = \mathbf{D} &= \cosh \Theta = \cosh \sqrt{(\mathbf{ZY})} \\ \mathbf{B} &= \mathbf{Z}_0 \sinh \Theta = \mathbf{Z} \frac{\sinh \Theta}{\Theta} = \mathbf{Z} \frac{\sinh \sqrt{(\mathbf{ZY})}}{\sqrt{\mathbf{ZY}}} \\ \mathbf{C} &= \frac{\sinh \Theta}{\mathbf{Z}_0} = \mathbf{Y} \frac{\sinh \Theta}{\Theta} = \mathbf{Y} \frac{\sinh \sqrt{(\mathbf{ZY})}}{\sqrt{(\mathbf{ZY})}} \end{aligned}\right\} . \quad (12)$$

Charts I and II* provide a rapid means of determining the complex values of $\cosh \Theta$ and $(\sinh \Theta)/\Theta$, as they are plotted in terms of $\mathbf{ZY} = \Theta^2$, instead of Θ as in the case of Kennelly's unique *Chart Atlas of Complex Hyperbolic and Circular Functions*. These two charts cover a transmission range up to 350 miles at 50 cycles.[3]

As an example of their use, consider the case of a single-circuit 132 kV. grid line, 100 miles in length, for which $\mathbf{Z} = 71{\cdot}45\underline{|69{\cdot}4^\circ}$ vector ohms and $\mathbf{Y} = 0{\cdot}0004425\ \underline{|90^\circ}$ vector mhos.[4] We have

$$\mathbf{ZY} = 71{\cdot}45\underline{|69{\cdot}4^\circ} \times 4{\cdot}425 \times 10^{-4}\underline{|90^\circ} = 0{\cdot}0316\underline{|159{\cdot}4^\circ}$$

Entering Chart I with this value of $\mathbf{ZY}$, we find that $\cosh \Theta = 0{\cdot}9853\underline{|0{\cdot}32^\circ}$. Similarly, Chart II gives $(\sinh \Theta)/\Theta = 0{\cdot}9951\ \underline{|0{\cdot}11^\circ}$.

In the case of short lines, i.e. under about 50 miles in length at 50 c/s, $\cosh \Theta$ and $(\sinh \Theta)/\Theta$ may be taken as being equal to unity. Also both the capacitive susceptance $B = \omega C$ and the conductance G (due to leakage and corona) are

* Reprinted by permission from *Electric Power Transmission*, by L. F. Woodruff (John Wiley & Sons Inc.).

negligible, so that $\mathbf{Y} = 0$. The network constants then become simply—

$$\left.\begin{aligned} \mathbf{A} &= \mathbf{D} = 1 \\ \mathbf{B} &= \mathbf{Z} = R + jX \\ \mathbf{C} &= 0 \end{aligned}\right\} \quad . \quad . \quad . \quad (13)$$

and hence $\mathbf{E}_s = (\mathbf{E}_r + \mathbf{ZI}_r)$ and $\mathbf{I}_s = \mathbf{I}_r$. Under these circumstances the transmission line may be represented by a series circuit containing only the lumped impedance $\mathbf{Z}$.

Transformer Constants. The equivalent circuit of a transformer is shown in Fig. 3. It is an asymmetrical $\mathbf{T}$ circuit with lumped impedances in the two arms and lumped admittance

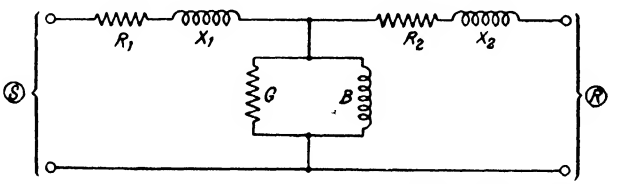

FIG. 3. EQUIVALENT T CIRCUIT OF A TRANSFORMER (EXACT)

in the staff. $\mathbf{Z}_1 = (R_1 + jX_1)$ represents the primary impedance due to resistance and leakage reactance, $\mathbf{Z}_2 = (R_2 + jX_2)$ the secondary impedance, and $\mathbf{Y} = (G - jB)$ the no-load admittance of the transformer.*

Denoting the voltage across the staff by $\mathbf{E}$, we have

$$\mathbf{E} = \mathbf{E}_r + \mathbf{Z}_2\mathbf{I}_r; \quad \mathbf{E}_s = \mathbf{E} + \mathbf{Z}_1\mathbf{I}_s; \quad \mathbf{I}_s = \mathbf{I}_r + \mathbf{YE}$$

Consequently

$$\mathbf{I}_s = \mathbf{I}_r + \mathbf{Y}(\mathbf{E}_r + \mathbf{Z}_2\mathbf{I}_r) = \mathbf{YE}_r + (1 + \mathbf{Z}_2\mathbf{Y})\mathbf{I}_r$$

and

$$\begin{aligned} \mathbf{E}_s &= (\mathbf{E}_r + \mathbf{Z}_2\mathbf{I}_r) + \mathbf{Z}_1[\mathbf{YE}_r + (1 + \mathbf{Z}_2\mathbf{Y})\mathbf{I}_r] \\ &= (1 + \mathbf{Z}_1\mathbf{Y})\mathbf{E}_r + (\mathbf{Z}_1 + \mathbf{Z}_2 + \mathbf{Z}_1\mathbf{Z}_2\mathbf{Y})\mathbf{I}_r \end{aligned}$$

Hence the network constants for the transformer are—

$$\left.\begin{aligned} \mathbf{A} &= 1 + \mathbf{Z}_1\mathbf{Y} \\ \mathbf{B} &= \mathbf{Z}_1 + \mathbf{Z}_2 + \mathbf{Z}_1\mathbf{Z}_2\mathbf{Y} \\ \mathbf{C} &= \mathbf{Y} \\ \mathbf{D} &= 1 + \mathbf{Z}_2\mathbf{Y} \end{aligned}\right\} \quad . \quad . \quad (14)$$

As the primary and secondary impedances of the transformer are as a rule not obtainable from test data, it is permissible to

* The minus sign indicates that the magnetizing susceptance B is *inductive*.

put $\mathbf{Z}_1 = \mathbf{Z}_2 = \mathbf{Z}/2$, where $\mathbf{Z} = (R + jX)$ is the equivalent transformer impedance. In that case equations (14) become—

$$\left.\begin{aligned} \mathbf{A} &= \mathbf{D} = 1 + \mathbf{ZY}/2 \\ \mathbf{B} &= \mathbf{Z}\,(1 + \mathbf{ZY}/4) \\ \mathbf{C} &= \mathbf{Y} \end{aligned}\right\} \quad . \quad . \quad . \quad (15)$$

These formal expressions for the general network constants are, however, cumbersome to use in practice. They are greatly

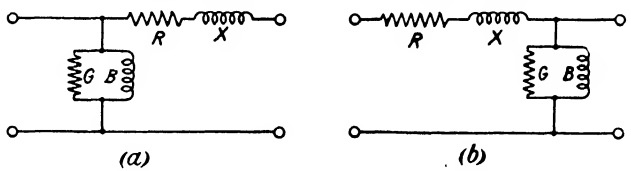

FIG. 4. EQUIVALENT CANTILEVER CIRCUIT OF A TRANSFORMER (APPROXIMATE)
(*a*) Sending end. (*b*) Receiving end.

simplified when the transformer is represented by its approximate "cantilever" circuit as shown in Fig. 4. The errors introduced by this simplification are less than 1 per cent, so that the approximation is justifiable in practical calculations. In the case of the sending-end transformer of Fig. 4 (*a*) the network constants are—

$$\left.\begin{aligned} \mathbf{A} &= 1 & \mathbf{B} &= \mathbf{Z} \\ \mathbf{C} &= \mathbf{Y} & \mathbf{D} &= 1 + \mathbf{ZY} \end{aligned}\right\} \quad . \quad . \quad (16)$$

For the receiving-end transformer of Fig. 4 (*b*) they are—

$$\left.\begin{aligned} \mathbf{A} &= 1 + \mathbf{ZY} & \mathbf{B} &= \mathbf{Z} \\ \mathbf{C} &= \mathbf{Y} & \mathbf{D} &= 1 \end{aligned}\right\} \quad . \quad . \quad . \quad (17)$$

The values of $\mathbf{Z} = (R + jX)$ and $\mathbf{Y} = (G - jB)$ are found from the usual transformer data as follows—

$$R = \frac{10 \times (\%\ I^2R \text{ loss}) \times (\text{kV.})^2}{\text{Transformer kVA.}} \text{ ohms},$$

$$X = \frac{10 \times (\%\ \text{reactance}) \times (\text{kV.})^2}{\text{Transformer kVA.}} \text{ ohms},$$

$$G = \frac{(\%\ \text{core loss}) \times \text{kVA.}}{(\text{kV.})^2 \times 10^5} \text{ mhos},$$

$$B = \frac{(\%\ \text{magnetizing current}) \times \text{kVA.}}{(\text{kV.})^2 \times 10^5} \text{ mhos}.$$

Synchronous Machine Constants. The equivalent circuits of synchronous machines are shown in Fig. 5, in which R is the series resistance representing armature copper loss, X_s is the series reactance representing the synchronous reactance of the machine, and G is the shunt conductance representing iron loss at no load. For the synchronous generator, Fig. 5 (a) gives—

$$\left.\begin{aligned} \mathbf{A} &= 1 & \mathbf{B} &= R + jX_s \\ \mathbf{C} &= G & \mathbf{D} &= 1 + G(R + jX_s) \end{aligned}\right\} \quad . \quad (18)$$

while, in the case of the synchronous motor, Fig. 5 (b) gives—

$$\left.\begin{aligned} \mathbf{A} &= 1 + G(R + jX_s) & \mathbf{B} &= R + jX_s \\ \mathbf{C} &= G & \mathbf{D} &= 1 \end{aligned}\right\} \quad . \quad . \quad (19)$$

The values of R, X_s, and G may be found in the same way as for a transformer.

Series and Parallel Networks. If $\mathbf{A}_1, \mathbf{B}_1, \mathbf{C}_1, \mathbf{D}_1$ are the constants of one network and $\mathbf{A}_2, \mathbf{B}_2, \mathbf{C}_2, \mathbf{D}_2$ are those of a second network

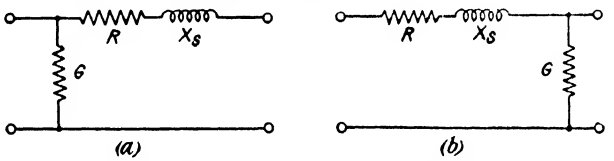

FIG. 5. EQUIVALENT CIRCUITS OF SYNCHRONOUS MACHINES
(a) Generator. (b) Motor.

connected in series with it, then the network constants of the series combination are—

$$\left.\begin{aligned} \mathbf{A} &= \mathbf{A}_1\mathbf{A}_2 + \mathbf{B}_1\mathbf{C}_2 \\ \mathbf{B} &= \mathbf{A}_1\mathbf{B}_2 + \mathbf{B}_1\mathbf{D}_2 \\ \mathbf{C} &= \mathbf{C}_1\mathbf{A}_2 + \mathbf{D}_1\mathbf{C}_2 \\ \mathbf{D} &= \mathbf{C}_1\mathbf{B}_2 + \mathbf{D}_1\mathbf{D}_2 \end{aligned}\right\} \quad . \quad . \quad . \quad (20)$$

In the case of two networks connected in parallel, the general network constants become—

$$\left.\begin{aligned} \mathbf{A} &= \frac{\mathbf{A}_1\mathbf{B}_2 + \mathbf{A}_2\mathbf{B}_1}{\mathbf{B}_1 + \mathbf{B}_2} \\ \mathbf{B} &= \frac{\mathbf{B}_1\mathbf{B}_2}{\mathbf{B}_1 + \mathbf{B}_2} \\ \mathbf{C} &= \mathbf{C}_1 + \mathbf{C}_2 - \frac{(\mathbf{A}_1 - \mathbf{A}_2)(\mathbf{D}_1 - \mathbf{D}_2)}{\mathbf{B}_1 + \mathbf{B}_2} \\ \mathbf{D} &= \frac{\mathbf{B}_1\mathbf{D}_2 + \mathbf{B}_2\mathbf{D}_1}{\mathbf{B}_1 + \mathbf{B}_2} \end{aligned}\right\} \quad . \quad . \quad (21)$$

It is useful to note that, if the two parallel networks are identical (e.g. a double-circuit transmission line), the constants become **A**, **B**/2, 2**C**, and **D**.

A frequently recurring case is that of three networks in series. Here the general network constants are—

$$\left.\begin{aligned}
\mathbf{A} &= \mathbf{A}_1(\mathbf{A}_2\mathbf{A}_3 + \mathbf{B}_2\mathbf{C}_3) + \mathbf{B}_1(\mathbf{C}_2\mathbf{A}_3 + \mathbf{D}_2\mathbf{C}_3)\\
\mathbf{B} &= \mathbf{A}_1(\mathbf{A}_2\mathbf{B}_3 + \mathbf{B}_2\mathbf{D}_3) + \mathbf{B}_1(\mathbf{C}_2\mathbf{B}_3 + \mathbf{D}_2\mathbf{D}_3)\\
\mathbf{C} &= \mathbf{C}_1(\mathbf{A}_2\mathbf{A}_3 + \mathbf{B}_2\mathbf{C}_3) + \mathbf{D}_1(\mathbf{C}_2\mathbf{A}_3 + \mathbf{D}_2\mathbf{C}_3)\\
\mathbf{D} &= \mathbf{C}_1(\mathbf{A}_2\mathbf{B}_3 + \mathbf{B}_2\mathbf{D}_3) + \mathbf{D}_1(\mathbf{C}_2\mathbf{B}_3 + \mathbf{D}_2\mathbf{D}_3)
\end{aligned}\right\} \quad (22)$$

An example of this particular case is afforded by what is probably the most common type of transmission circuit, viz. a long transmission line with transformers at each end. Such a circuit may be regarded as an "equivalent transmission line" having constants which are simple functions of the constants of the actual transmission line and of its terminal transformers. If the actual line constants are $\mathbf{A}_L$, $\mathbf{B}_L$, $\mathbf{C}_L$, $\mathbf{D}_L$, and if the sending- and receiving-end transformers have series impedances $\mathbf{Z}_{TS}$, $\mathbf{Z}_{TR}$ and shunt admittances $\mathbf{Y}_{TS}$, $\mathbf{Y}_{TR}$ respectively, then the network constants of the equivalent line become—

$$\left.\begin{aligned}
\mathbf{A}_L' &= \mathbf{A}_L(1 + \mathbf{Z}_{TR}\mathbf{Y}_{TR}) + \mathbf{B}_L\mathbf{Y}_{TR}\\
&\quad + \mathbf{C}_L\mathbf{Z}_{TS}(1 + \mathbf{Z}_{TR}\mathbf{Y}_{TR}) + \mathbf{D}_L\mathbf{Z}_{TS}\mathbf{Y}_{TR}\\
\mathbf{B}_L' &= \mathbf{A}_L\mathbf{Z}_{TR} + \mathbf{B}_L + \mathbf{C}_L\mathbf{Z}_{TS}\mathbf{Z}_{TR} + \mathbf{D}_L\mathbf{Z}_{TS}\\
\mathbf{C}_L' &= \mathbf{A}_L\mathbf{Y}_{TS}(1 + \mathbf{Z}_{TR}\mathbf{Y}_{TR}) + \mathbf{B}_L\mathbf{Y}_{TS}\mathbf{Y}_{TR}\\
&\quad + \mathbf{C}_L(1 + \mathbf{Z}_{TS}\mathbf{Y}_{TS})(1 + \mathbf{Z}_{TR}\mathbf{Y}_{TR})\\
&\quad + \mathbf{D}_L\mathbf{Y}_{TR}(1 + \mathbf{Z}_{TS}\mathbf{Y}_{TS})\\
\mathbf{D}_L' &= \mathbf{A}_L\mathbf{Z}_{TR}\mathbf{Y}_{TS} + \mathbf{B}_L\mathbf{Y}_{TS} + \mathbf{C}_L\mathbf{Z}_{TR}(1 + \mathbf{Z}_{TS}\mathbf{Y}_{TS})\\
&\quad + \mathbf{D}_L(1 + \mathbf{Z}_{TS}\mathbf{Y}_{TS})
\end{aligned}\right\} \quad (23)$$

Moreover, if, as is usually the case, the actual line is symmetrical, so that $\mathbf{A}_L = \mathbf{D}_L$, and if, in addition, the terminal transformers are identical, so that $\mathbf{Z}_{TS} = \mathbf{Z}_{TR} = \mathbf{Z}_T$ and $\mathbf{Y}_{TS} = \mathbf{Y}_{TR} = \mathbf{Y}_T$, then the above expressions for the equivalent line constants reduce to the form—

$$\left.\begin{aligned}
\mathbf{A}_L' &= \mathbf{D}_L' = \mathbf{A}_L(1 + 2\mathbf{Z}_T\mathbf{Y}_T) + \mathbf{B}_L\mathbf{Y}_T + \mathbf{C}_L\mathbf{Z}_T(1 + \mathbf{Z}_T\mathbf{Y}_T)\\
\mathbf{B}_L' &= 2\mathbf{A}_L\mathbf{Z}_T + \mathbf{B}_L + \mathbf{C}_L\mathbf{Z}_T^2\\
\mathbf{C}_L' &= 2\mathbf{A}_L\mathbf{Y}_T(1 + \mathbf{Z}_T\mathbf{Y}_T) + \mathbf{B}_L\mathbf{Y}_T^2 + \mathbf{C}_L(1 + \mathbf{Z}_T\mathbf{Y}_T)^2
\end{aligned}\right\} \quad (24)$$

The Equivalent T and Π Circuits. In the same way that it is possible to represent the electrical characteristics of any

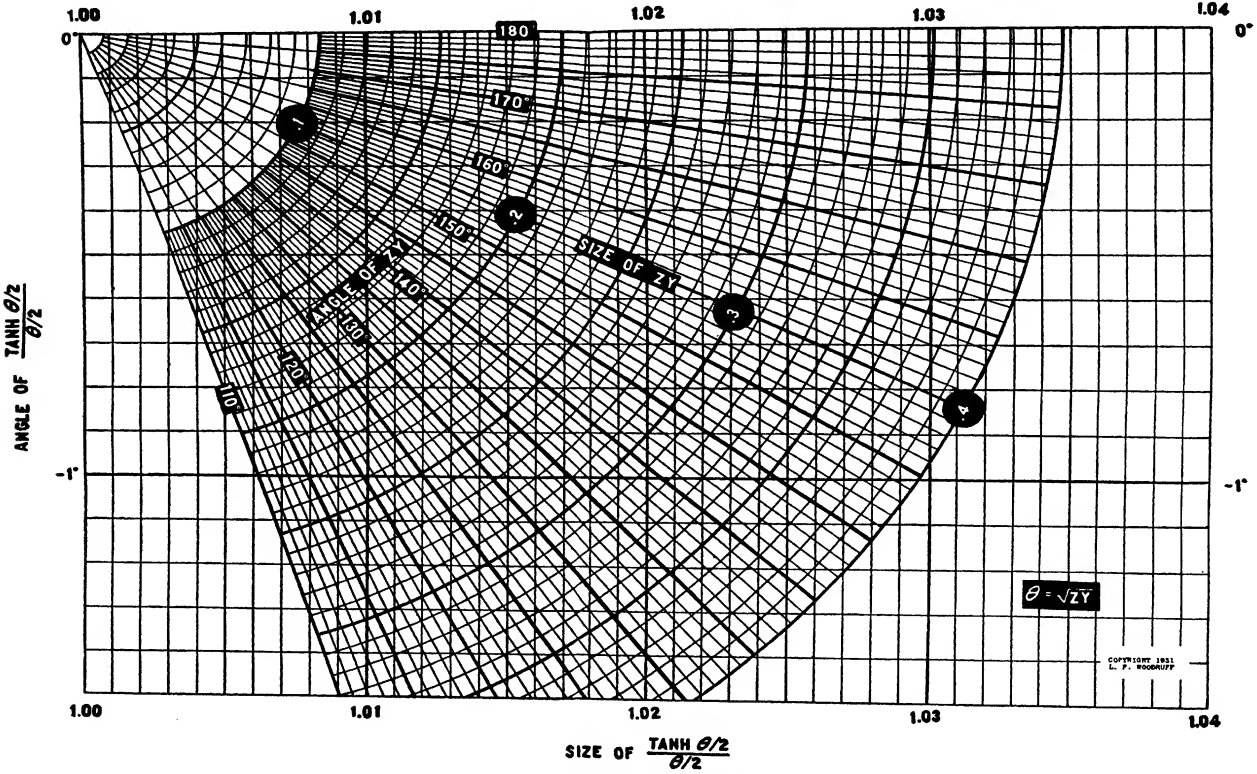

CHART III. HYPERBOLIC TANGENT $\frac{\theta/2}{\theta/2}$

(T.180)

denotes the equivalent series impedance and $\mathbf{Y}'$ the equivalent shunt admittance of such a line, then equations (25) give—

$$\frac{\mathbf{Z}'}{2} = \mathbf{Z}_0 \frac{\cosh \Theta - 1}{\sinh \Theta} = \mathbf{Z}_0 \frac{2 \cosh^2 \frac{1}{2}\Theta}{2 \sinh \frac{1}{2}\Theta \cosh \frac{1}{2}\Theta}$$

$$= \mathbf{Z}_0 \tanh \tfrac{1}{2}\Theta = \frac{\mathbf{Z}}{2} \cdot \frac{\tanh \frac{1}{2}\Theta}{\frac{1}{2}\Theta} \quad . \quad . \quad . \quad (28a)$$

$$\mathbf{Y}' = \frac{\sinh \Theta}{\mathbf{Z}_0} = \mathbf{Y} \frac{\sinh \Theta}{\Theta} \quad . \quad . \quad . \quad . \quad (28b)$$

while equations (27) give the corresponding relations—

$$\mathbf{Z}' = \mathbf{Z}_0 \sinh \Theta = \mathbf{Z} \frac{\sinh \Theta}{\Theta} \quad . \quad . \quad . \quad . \quad (29a)$$

$$\frac{\mathbf{Y}'}{2} = \frac{\cosh \Theta - 1}{\mathbf{Z}_0 \sinh \Theta} = \frac{\mathbf{Y}}{2} \cdot \frac{\tanh \frac{1}{2}\Theta}{\frac{1}{2}\Theta} \quad . \quad . \quad . \quad (29b)$$

Charts [3] II and III* enable values of the correction factors $(\sinh \Theta)/\Theta$ and $(\tanh \frac{1}{2}\Theta)/\frac{1}{2}\Theta$ to be obtained directly in terms of the product $\mathbf{ZY} = \Theta^2$.

In the case of short transmission lines, i.e. under about 50 miles in length, these correction factors differ negligibly from unity, so that then $\mathbf{Z}' = \mathbf{Z}$ and $\mathbf{Y}' = \mathbf{Y}$. Figs. 6 (*a*) and 6 (*b*) in this case become the circuits of the so-called *nominal* **T** and **Π** lines in which the electrical constants are lumped instead of being uniformly distributed.

The Star/Delta and Delta/Star Transformations. In the simplification of complicated networks it is often a great convenience to be able to replace a star-connected group of three impedances by an electrically equivalent group of three delta-connected impedances, and vice versa. Particularly is this the case when determining the transfer impedance of a transmission system under fault conditions.†

The general equivalence of three-cornered star and mesh circuits was first established by Kennelly,[5] and the principle was subsequently extended by Rosen[6] to the general transformation from a star circuit to a mesh circuit. In the general case, however, the converse transformation from a mesh circuit to a star circuit is no longer possible. If the star has *n* rays of

* Reprinted by permission from *Electric Power Transmission*, by L. F. Woodruff (John Wiley & Sons Inc.).

† *Cf.* Chapter V.

impedance $\mathbf{Z}_1$, $\mathbf{Z}_2$, $\mathbf{Z}_3$, . . . $\mathbf{Z}_n$, then the impedances of the $\frac{1}{2}n\,(n-1)$ sides of the equivalent mesh are given by—

$$\mathbf{Z}_{mn} = \mathbf{Z}_m\mathbf{Z}_n\left(\frac{1}{\mathbf{Z}_1} + \frac{1}{\mathbf{Z}_2} + \cdots \frac{1}{\mathbf{Z}_n}\right) = \mathbf{Z}_m\mathbf{Z}_n \sum_{1}^{n}\left(\frac{1}{\mathbf{Z}_n}\right) \quad (30)$$

Equation (30) expresses the so-called *star/mesh transformation* in its most general form.

For the particular case where $n = 3$ it becomes the *star/delta* transformation—

$$\left.\begin{aligned} \mathbf{Z}_{12} &= \mathbf{Z}_1 + \mathbf{Z}_2 + \frac{\mathbf{Z}_1\mathbf{Z}_2}{\mathbf{Z}_3} \\ \mathbf{Z}_{23} &= \mathbf{Z}_2 + \mathbf{Z}_3 + \frac{\mathbf{Z}_2\mathbf{Z}_3}{\mathbf{Z}_1} \\ \mathbf{Z}_{31} &= \mathbf{Z}_3 + \mathbf{Z}_1 + \frac{\mathbf{Z}_3\mathbf{Z}_1}{\mathbf{Z}_2} \end{aligned}\right\} \quad . \quad . \quad . \quad (31)$$

The corresponding *delta/star* transformation is as follows—

$$\left.\begin{aligned} \mathbf{Z}_1 &= \frac{\mathbf{Z}_{31}\mathbf{Z}_{12}}{\mathbf{Z}_{12} + \mathbf{Z}_{23} + \mathbf{Z}_{31}} \\ \mathbf{Z}_2 &= \frac{\mathbf{Z}_{12}\mathbf{Z}_{23}}{\mathbf{Z}_{12} + \mathbf{Z}_{23} + \mathbf{Z}_{31}} \\ \mathbf{Z}_3 &= \frac{\mathbf{Z}_{23}\mathbf{Z}_{31}}{\mathbf{Z}_{12} + \mathbf{Z}_{23} + \mathbf{Z}_{31}} \end{aligned}\right\} \quad . \quad . \quad . \quad (32)$$

As an example illustrating the use of these transformations [7] let us take the case of the equivalent **T** line. This is a simple star circuit in which, from equations (28*a*) and (28*b*),

$$\mathbf{Z}_1 = \mathbf{Z}_2 = \frac{\mathbf{Z}'}{2} = \mathbf{Z}_0\left(\frac{\cosh\Theta - 1}{\sinh\Theta}\right); \quad \mathbf{Z}_3 = \frac{1}{\mathbf{Y}'} = \frac{\mathbf{Z}_0}{\sinh\Theta}$$

The architrave of the equivalent **II** line, which in turn is a simple delta circuit, is then given by equations (31) as—

$$\begin{aligned} \mathbf{Z}_{12} &= \frac{\mathbf{Z}'}{2} + \frac{\mathbf{Z}'}{2} + \mathbf{Y}'\left(\frac{\mathbf{Z}'}{2}\right)^2 \\ &= 2\mathbf{Z}_0\left(\frac{\cosh\Theta - 1}{\sinh\Theta}\right) + \frac{\sinh\Theta}{\mathbf{Z}_0}\,\mathbf{Z}_0{}^2\left(\frac{\cosh\Theta - 1}{\sinh\Theta}\right)^2 \\ &= \frac{\mathbf{Z}_0}{\sinh\Theta}\,(\cosh^2\Theta - 1) = \mathbf{Z}_0 \sinh\Theta, \end{aligned}$$

which is the same result as equation (29*a*), as is to be expected. Similarly, the pillars of the equivalent **II** line are given by—

$$\mathbf{Z}_{23} = \mathbf{Z}_{31} = \frac{\mathbf{Z}'}{2} + \frac{1}{\mathbf{Y}'} + \frac{\mathbf{Z}'}{2\mathbf{Y}'} \cdot \frac{2}{\mathbf{Z}'} = \frac{\mathbf{Z}'}{2} + \frac{2}{\mathbf{Y}'}$$
$$= \mathbf{Z}_0\left(\frac{\cosh\Theta - 1}{\sinh\Theta}\right) + \frac{2\mathbf{Z}_0}{\sinh\Theta}$$
$$= \mathbf{Z}_0\left(\frac{\cosh\Theta + 1}{\sinh\Theta}\right) = \frac{\mathbf{Z}_0 \sinh\Theta}{\cosh\Theta - 1};$$

alternatively—

$$\mathbf{Y}_{23} = \mathbf{Y}_{31} = \frac{\cosh\Theta - 1}{\mathbf{Z}_0 \sinh\Theta} = \frac{1}{\mathbf{Z}_0}\tanh\tfrac{1}{2}\Theta;$$

which, in turn, is the same result as equation (29*b*). Conversely, taking the case of the equivalent **II** line, the lumped constants of this simple delta circuit are—

$$\mathbf{Z}_{12} = \mathbf{Z}' = \mathbf{Z}_0 \sinh\Theta; \quad \mathbf{Y}_{23} = \mathbf{Y}_{31} = \frac{\mathbf{Y}'}{2} = \frac{\cosh\Theta - 1}{\mathbf{Z}_0 \sinh\Theta}.$$

The arms of the equivalent **T** line, which in turn is a simple star circuit, are then given by equations (32) as—

$$\mathbf{Z}_1 = \mathbf{Z}_2 = \frac{\mathbf{Z}' \,.\, 2/\mathbf{Y}'}{\mathbf{Z}' + \frac{2}{\mathbf{Y}'} + \frac{2}{\mathbf{Y}'}} = \frac{2\mathbf{Z}'}{4 + \mathbf{Z}'\mathbf{Y}'}$$
$$= \frac{\mathbf{Z}_0 \sinh\Theta}{2 + \mathbf{Z}_0 \sinh\Theta\left(\frac{\cosh\Theta - 1}{\mathbf{Z}_0 \sinh\Theta}\right)} = \frac{\mathbf{Z}_0 \sinh\Theta}{\cosh\Theta + 1}$$
$$= \mathbf{Z}_0\left(\frac{\cosh\Theta - 1}{\sinh\Theta}\right) = \mathbf{Z}_0 \tanh\tfrac{1}{2}\Theta$$

which is the same result as equation (28*a*). Similarly the staff of the equivalent **T** line is given by—

$$\mathbf{Z}_3 = \frac{2/\mathbf{Y}' \,.\, 2/\mathbf{Y}'}{\mathbf{Z}' + \frac{2}{\mathbf{Y}'} + \frac{2}{\mathbf{Y}'}} = \frac{4}{\mathbf{Y}'(4 + \mathbf{Z}'\mathbf{Y}')}$$
$$= \frac{\mathbf{Z}_0 \sinh\Theta}{\cosh^2\Theta - 1} = \frac{\mathbf{Z}_0}{\sinh\Theta};$$

alternatively, $\mathbf{Y}_3 = \sinh\Theta/\mathbf{Z}_0$, which in turn is the same result as equation (28*b*).

References

[1] For a practical discussion of network theory, see Chapter V of *Electrical Power Transmission and Interconnection*, by C. Dannatt and J. W. Dalgleish (Pitman, London, 1930).

[2] *Cf.* H. Waddicor: *The Principles of Electric Power Transmission* (fourth edition) (Chapman & Hall, London, 1939), Chapter V, particularly pp. 69–74. A rapid method of calculating the voltage and current along a transmission line under any conditions of receiving-end load has been given by H. Rissik in "Transmission Line Analysis," *Electrician*, 29th April, 1938, p. 539; and *ibid.*, 20th May, 1938, p. 633.

[3] These charts are due to L. F. Woodruff, and were first published in an article by him describing their compilation, and entitled "Hyperbolic Function Charts," appearing in *Electrical Engineering*, May, 1935, p. 550.

[4] *Vide* H. Rissik: "Transmission Line Analysis," *Electrician*, 20th May, 1938, p. 633.

[5] *Vide* A. E. Kennelly: "The Equivalence of Triangles and Three-pointed Stars in Conducting Networks," *Elec. World and Eng.*, 1899, Vol. 34, p. 413.

[6] *Vide* A. Rosen: "A New Network Theorem," *Journ. I.E.E.*, 1924, Vol. 62, p. 916.

[7] An elementary proof of these two transformations is given in Appendix II, pp. 465–7, of A. T. Starr's *Generation, Transmission, and Utilization of Electrical Power* (Pitman, London, 1937).

CHAPTER II

CIRCLE DIAGRAMS IN POWER SYSTEM STUDIES

JUST as the vector diagram is the key to the solution of practically every normal a.c. circuit problem, so the circle diagram is a *sine qua non* in the quantitative as well as qualitative analysis of kindred phenomena occurring in the realm of power transmission and, in particular, of power system interconnection. The representation of circuit phenomena in graphical form by means of a circle diagram, that is, a diagram consisting of a family of circles each of which is the terminal locus of a vector, is of course a familiar means of studying the behaviour of the induction motor and the synchronous motor. At the same time it is seldom realized that the circle diagram of the induction motor, or the family of so-called O-curves of the synchronous motor, are but highly specialized forms of the general circle diagram of a linear network. From the point of view of power transmission problems the most important applications of this fundamental network diagram are derived from that particular form of it known as the *power-circle diagram*.

The power-circle diagram of a transmission line was first developed by Philip,[1] but in a form restricting its application to the study of short lines in which the effects of shunt capacitance could be neglected. This new analytical method was later extended by Dwight [2] to include the general case of the long transmission line with uniformly distributed constants. Dwight [3] subsequently developed the power-circle diagram to a still further stage, while Evans and Sels [4] presented the results of a semi-graphical analysis in a series of articles published in the *Electric Journal* at about the same time. Mention should also be made of an independent development of network circle diagrams by Thielemans,[5] outlined in a slightly earlier series of articles published in the *Revue générale de l'électricité*. Later still, Fortescue and Wagner [6] gave a proof of the power-circle diagram of a transmission system in which the idea of an angular displacement between the sending-end and receiving-end voltages was maintained, and which constituted a marked step forward in the analytical study of

power system interconnection. Finally, Terman [7] has co-ordinated the graphical and mathematical methods of constructing the power-circle diagram in an important paper which discusses *inter alia* a generalized circle diagram on which may be drawn circles representing almost any conceivable locus, the construction being carried out with the aid of computations made from relatively simple formulae. Terman has indicated how any errors in the mathematical or graphical work that lead to an incorrect diagram can be simply and quickly uncovered by applying the numerous geometrical checks given in the paper. The result is a diagram easy to obtain, almost error-proof, and of extreme usefulness.

The Fundamental Power Equations. The network voltage equations (5*a*) and (6*a*) may be put in the form

$$\mathbf{I}_r = \frac{\mathbf{E}_s}{\mathbf{B}} - \frac{\mathbf{A}\mathbf{E}_r}{\mathbf{B}}$$

$$= \frac{\mathbf{E}_s}{\mathbf{Z}_t} - \frac{\mathbf{E}_r}{\mathbf{Z}_r} \quad . \quad . \quad . \quad . \quad (33)$$

and

$$\mathbf{I}_s = \frac{\mathbf{D}\mathbf{E}_s}{\mathbf{B}} - \frac{\mathbf{E}_r}{\mathbf{B}}$$

$$= \frac{\mathbf{E}_s}{\mathbf{Z}_s} - \frac{\mathbf{E}_r}{\mathbf{Z}_t} \quad . \quad . \quad . \quad . \quad (34)$$

where $\mathbf{Z}_t = Z_t|\underline{\rho_t} = B|\underline{\beta} = \mathbf{B}$, the *transfer impedance* of the system; $\mathbf{Z}_r = Z_r|\underline{\rho_r} = (B/A)\ |\underline{(\beta - \alpha)} = \mathbf{B/A}$, the *receiving-end driving-point impedance*; and $\mathbf{Z}_s = Z_s|\underline{\rho_s} = B/D\ |\underline{(\beta - \delta)} = \mathbf{B/D}$, the *sending-end driving-point impedance.*

As was explained in the preceding chapter, vector power is given by the product of the vector current and the *conjugate* of the vector voltage. The receiving-end vector power is accordingly found from equation (33) to be—

$$P_r + jQ_r = \mathbf{E}_r'\mathbf{I}_r = \frac{\mathbf{E}_s\mathbf{E}_r'}{\mathbf{Z}_t} - \frac{\mathbf{E}_r\mathbf{E}_r'}{\mathbf{Z}_r}$$

$$= \frac{E_sE_r}{Z_t}\ |\underline{(\theta - \rho_t)} - \frac{E_r^2}{Z_r}\ |\underline{-\rho_r} \quad . \quad . \quad . \quad (35a)$$

$$= \left[\frac{E_sE_r}{Z_t}\cos(\theta - \rho_t) - \frac{E_r^2}{Z_r}\cos\rho_r\right]$$

$$+ j\left[\frac{E_sE_r}{Z_t}\sin(\theta - \rho_t) + \frac{E_r^2}{Z_r}\sin\rho_r\right]$$

$$= \left[\frac{E_s E_r}{Z_t} \sin(\theta + \sigma_t) - \frac{E_r^2}{Z_r} \sin \sigma_r\right] + j\left[\frac{E_r^2}{Z_r} \cos \sigma_r - \frac{E_s E_r}{Z_t} \cos(\theta + \sigma_t)\right]$$

$$= [P_m \sin(\theta + \sigma_t) - P_{ro}] + j[Q_{ro} - P_m \cos(\theta + \sigma_t)] \quad . \quad . \quad . \quad (35b)$$

where $\sigma_t = (\pi/2 - \rho_t) = (\pi/2 - \beta)$, and $\sigma_r = (\pi/2 - \rho_r) = (\pi/2 + \alpha - \beta)$. Similarly, the sending-end vector power is found from equation (34) to be—

$$P_s + jQ_s = \mathbf{E}_s'\mathbf{I}_s = \frac{\mathbf{E}_s'\mathbf{E}_s}{\mathbf{Z}_s} - \frac{\mathbf{E}_s'\mathbf{E}_r}{\mathbf{Z}_t}$$

$$= \frac{E_s^2}{Z_s}\underline{|-\rho_s} - \frac{E_s E_r}{Z_t}\underline{|-(\theta + \rho_t)} \quad . \quad . \quad (36a)$$

$$= \left[\frac{E_s^2}{Z_s} \cos \rho_s - \frac{E_s E_r}{Z_t} \cos(\theta + \rho_t)\right] + j\left[\frac{E_s E_r}{Z_t} \sin(\theta + \rho_t) - \frac{E_s^2}{Z_s} \sin \rho_s\right]$$

$$= \left[\frac{E_s^2}{Z_s} \sin \sigma_s + \frac{E_s E_r}{Z_t} \sin(\theta - \sigma_t)\right] + j\left[\frac{E_s E_r}{Z_t} \cos(\theta - \sigma_t) - \frac{E_s^2}{Z_s} \cos \sigma_s\right]$$

$$= [P_{so} + P_m \sin(\theta - \sigma_t)] + j[P_m \cos(\theta - \sigma_t) - Q_{so}] \quad . \quad (36b)$$

where $\sigma_s = (\pi/2 - \rho_s) = (\pi/2 + \delta - \beta)$, and $\sigma_t = (\pi/2 - \rho_t) = (\pi/2 - \beta)$ as before. Equations (35*b*) and (36*b*) finally give the following expressions for the receiving- and sending-end powers, P_r and P_s—

$$P_r = \frac{E_s E_r}{Z_t} \sin(\theta + \sigma_t) - \frac{E_r^2}{Z_r} \sin \sigma_r$$

$$= P_m \sin(\theta + \sigma_t) - P_{ro} \quad . \quad . \quad . \quad (37)$$

$$P_s = \frac{E_s^2}{Z_s} \sin \sigma_s + \frac{E_s E_r}{Z_t} \sin(\theta - \sigma_t)$$

$$= P_{so} + P_m \sin(\theta - \sigma_t) \quad . \quad . \quad . \quad (38)$$

in which $P_m = E_s E_r / Z_t$ is the *maximum transfer power* of the system, and P_{ro} and P_{so} are the *driving-point powers* at the receiving and sending ends respectively. These relations

between the transfer and driving-point powers of a general transmission network are shown diagrammatically in Fig. 7.

It ought here to be pointed out that in actuality the transfer impedance $\mathbf{Z}_t$ and the driving-point impedances $\mathbf{Z}_r$ and $\mathbf{Z}_s$ are predominantly reactive. As the result, the angles σ_t, σ_r, and σ_s are all very small, of the order of a few degrees only. Moreover, in the case of the shorter transmission distances, where the effects of line capacitance and conductance (due to corona and insulator leakage) may be neglected, the transmission network

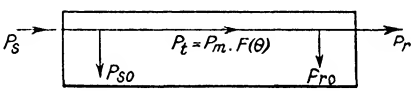

FIG. 7. POWER FLOW IN A TRANSMISSION SYSTEM

approximates very closely to a simple circuit containing series impedance only, and for which $\mathbf{A} = \mathbf{D} = 1$, $\mathbf{B} = \mathbf{Z}$, and $\mathbf{C} = 0$. Under these circumstances the system impedances $\mathbf{Z}_t$, $\mathbf{Z}_r$, and $\mathbf{Z}_s$ are all equal to the series impedance $\mathbf{Z} = Z\underline{/\rho} = (R + jX)$, so that equations (37) and (38) reduce to the simple form—

$$P_r = P_m \left[\sin(\theta + \sigma) - \frac{E_r}{E_s} \sin \sigma \right]$$

and

$$P_s = P_m \left[\frac{E_s}{E_r} \sin \sigma + \sin(\theta - \sigma) \right]$$

These are at once recognized as expressing the same relations as those which obtain between the external and internal powers and the load angle θ of a synchronous generator.[8] In that case E_s is the air-gap voltage or induced e.m.f. of the machine, E_r is the terminal voltage, $\mathbf{Z} = \sqrt{(R^2 + X_s^2)}$ is the synchronous impedance, and $\sigma = \tan^{-1}(R/X_s)$ is the complement of the impedance angle. This particular case is of interest in that it illustrates the applicability of network analysis to purely machine problems. In fact, and as Terman has shown,[9] the general network circle diagram based on equations (35) and (36) can be applied to any machine problem by substituting the equivalent network of Fig. 2 for the conventional equivalent circuit of the machine.

It is seen from equations (37) and (38) that the *average transmitted power* is

$$P = \tfrac{1}{2}(P_r + P_s) = \tfrac{1}{2}(P_{so} - P_{ro}) + P_m \cos \sigma_t \sin \theta \,. \quad (39)$$

In the case of a symmetrical transmission network, such as a transmission line with identical transformers at each end, for which $\mathbf{A} = \mathbf{D}$, and if $E_s = E_r = E$, say, then $P_{so} = P_{ro}$, so that the above expression reduces to

$$P = P_m \cos \sigma_t \sin \theta = \frac{E^2 \cos \sigma_t}{Z_t} \sin \theta$$
$$= \frac{E^2 \sin \theta}{X_t\left(1 + \frac{R_t^2}{X_t^2}\right)} \quad . \quad . \quad . \quad . \quad . \quad . \quad (40)$$

where $R_t = Z_t \sin \sigma_t$ and $X_t = Z_t \cos \sigma_t$. R_t is the *transfer resistance* and X_t the *transfer reactance* of the transmission network. Furthermore, if the transmission network contains series impedance only, then R_t is the total series resistance R and X_t the total series reactance X of the power transmitting link. Finally, if the resistance of the link be neglected, then equation (40) reduces to the simple form

$$P = \frac{E^2}{X} \sin \theta \quad . \quad . \quad . \quad . \quad . \quad . \quad . \quad (41)$$

On referring to equations (37) and (38) it is seen that this last relation is but a particular case of the general relation

$$P_r = P_s = P_m \sin \theta = \frac{E_s E_r}{X} \sin \theta \quad . \quad . \quad . \quad (42)$$

expressing the synchronizing power transmitted by a simple reactive tie in terms of the angle between the voltages at its two ends. Because if the resistance R is assumed to be zero, the driving-point powers P_{ro} and P_{so} also become zero, so that the sending- and receiving-end powers are then both equal to the transfer power $P_m \sin \theta$. Equation (42) is of fundamental importance, as it leads directly to the so-called *power/angle* diagram of a synchronous system in its simplest possible form.

Equations (37) and (38) similarly give rise to an expression for the *power loss*, namely—

$$P_l = P_s - P_r = (P_{so} + P_{ro}) - 2 P_m \sin \sigma_t \cos \theta \quad . \quad (43)$$

In the case of a simple series-impedance network this expression reduces to

$$P_l = \frac{R}{R^2 + X^2}(E_s^2 + E_r^2 - 2 E_s E_r \cos \theta) = I^2 R \quad . \quad (44)$$

since then $\mathbf{I}_s = \mathbf{I}_r = \mathbf{I}$ (say), and $\mathbf{IZ} = \mathbf{E}_s - \mathbf{E}_r$. Equation (43) is of importance in that it forms the basis of the so-called straight-line loss diagram discussed towards the end of the present chapter.

The Basic Vector Diagrams. The fundamental transmission network equations (5) and (6) may be represented graphically in the form of voltage and current vector diagrams. The relation expressed by equation (5*a*), for example, gives rise to the receiving-end voltage vector diagram of Fig. 8. Here the

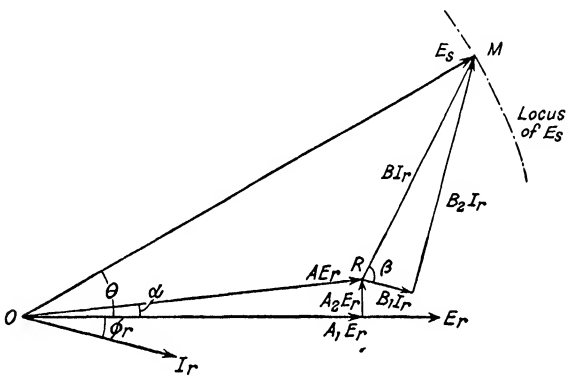

FIG. 8. RECEIVING-END VOLTAGE VECTOR DIAGRAM

receiving-end voltage is taken as the vector datum, so that $\mathbf{E}_r = E_r \underline{|0}$. The vector OR then represents the open-circuit sending-end voltage $\mathbf{E}_{so} = \mathbf{AE}_r = E_r \,.\, A \underline{|\alpha} = E_r\,(\mathrm{A}_1 + jA_2)$, and is thus the vector sum of a datum component A_1E_r and a quadrature component jA_2E_r. The vector RM in turn represents the transfer impedance voltage $\mathbf{BI}_r = \mathbf{I}_r \,.\, B \underline{|\beta} = \mathbf{I}_r\,(B_1 + jB_2)$, and may be regarded as the vector sum of a voltage component $B_1\mathbf{I}_r$ in phase with $\mathbf{I}_r$, and a voltage component $jB_2\mathbf{I}_r$ in leading quadrature with $\mathbf{I}_r$. The vector resultant OM then represents the sending-end voltage under load conditions, $\mathbf{E}_s = E_s \underline{|\theta}$.

Assuming E_s and E_r to be fixed in magnitude, then any variation of the load current I_r must be simultaneously in magnitude and phase such as will cause the terminus of the sending-end voltage vector to follow the circular locus shown dotted in Fig. 8. These conditions are represented by a synchronous transmission system in which the sending-end voltage

is held constant by appropriate generator field regulation, and the receiving-end voltage is similarly held constant by field regulation of the synchronous machines—whether generators, motors, or synchronous phase modifiers*—at the receiving end.

Fig. 9 shows the corresponding sending-end voltage vector diagram derived from equation (6*a*). In this case the sending-end voltage is taken as the vector datum, so that $\mathbf{E}_s = E_s \underline{|0}$. The vector OS then represents the receiving-end voltage when the sending-end current is zero, namely, $\mathbf{E}_{r0} = \mathbf{D}\mathbf{E}_s = E_s \,.\, D \underline{|\delta} = E_s\,(D_1 + jD_2)$, while the vector SN represents the transfer

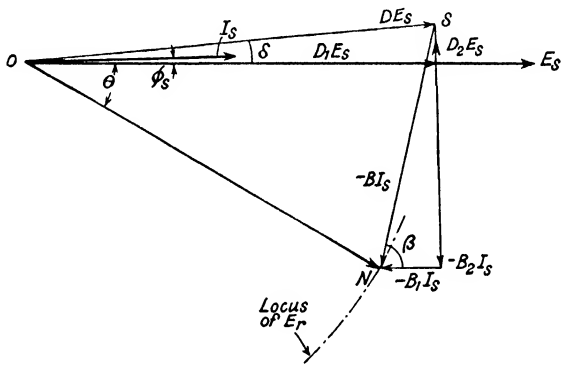

FIG. 9. SENDING-END VOLTAGE VECTOR DIAGRAM

impedance voltage $-\mathbf{B}\mathbf{I}_s = -\mathbf{I}_s \,.\, B \underline{|\beta} = -\mathbf{I}_s\,(B_1 + jB_2)$, comprising the in-phase and quadrature components $-B_1\mathbf{I}_s$ and $-jB_2\mathbf{I}_s$ respectively. The vector resultant ON then represents the receiving-end voltage, $\mathbf{E}_r = E_r \underline{|-\theta}$.

In the same way equations (5*b*) and (6*b*) can be represented by corresponding current vector diagrams, but as these are relatively unimportant they will not be considered here.

An interesting modification of Figs. 8 and 9 arises in the case of a network containing series impedance only, for which $\mathbf{I}_s = \mathbf{I}_r$ (= $\mathbf{I}$, say), because it leads to a semi-graphical method

* The general term "synchronous phase modifier" signifies a synchronous machine designed to supply only reactive volt-amperes to a transmission system. When the reactive VA. to be supplied is lagging—as is generally the case—the machine is termed a "synchronous condenser." When leading reactive VA. is to be supplied—as in the case of a long transmission line on open circuit—the machine is usually referred to as a "synchronous reactor," although the term "synchronous inductor" would be more explicit.

of determining the power relation expressed by equation (40). The vector diagram illustrating this particular case—e.g. a short transmission line in which the effects of capacitance and conductance are negligible—is shown in Fig. 10. The current $\mathbf{I} = (I_p - jI_q)$ lags the receiving-end voltage by the power-factor angle ϕ. If the transfer impedance of the network (i.e. the series impedance in this case) be $\mathbf{Z}_t = (R_t + jX_t)$, then the vector impedance drop (RM in Fig. 10) between the sending and receiving ends is—

$$\begin{aligned}\mathbf{e} = \mathbf{E}_s - \mathbf{E}_r &= \mathbf{IZ}_t = (I_p - jI_q)(R_t + jX_t) \\ &= (I_pR_t + I_qX_t) + j(I_pX_t - I_qR_t) \\ &= e + j\varepsilon\end{aligned}$$

Here e is the "magnitude" difference and ε the "displacement" difference between the sending-end voltage E_s and the receiving-end voltage E_r. If E_s and E_r are the same and equal to E,

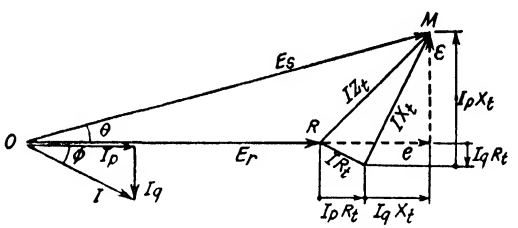

Fig. 10. Vector Diagram for an Impedance Tie

say, then $e \simeq 0$ and $\varepsilon \simeq E \sin\theta$; that is to say $(I_pR_t + I_qX_t) \simeq 0$ and $(I_pX_t - I_qR_t) \simeq E \sin\theta$. The first relation gives $I_q = -I_p(R_t/X_t)$. Substituting this value of I_q in the second relation then gives $I_p(X_t + R_t^2/X_t) = E \sin\theta$. The power transmitted to the receiving end is $P = E_rI \cos\phi$, and is thus equal to EI_p. Hence—

$$P = \frac{E^2 \sin\theta}{X_t\left(1 + \frac{R_t^2}{X_t^2}\right)}$$

which is the same result as equation (40).

In its simplest possible form Fig. 10 becomes Fig. 11, which shows the vector diagram of a purely reactive transmission

circuit. The average power transmitted and the sending- and receiving-end powers are in this case all equal, so that $P = E_s I \cos \phi_s = E_r I \cos \phi_r$.* But from the trigonometry of the vector diagram we have

$$\frac{IX}{\sin \theta} = \frac{E_s}{\sin (\pi/2 + \phi_r)} = \frac{E_r}{\sin (\pi/2 - \phi_s)}$$

The transmitted power is consequently given by

$$P = \frac{E_s E_r}{X} \sin \theta$$

which is the same result as equation (42).*

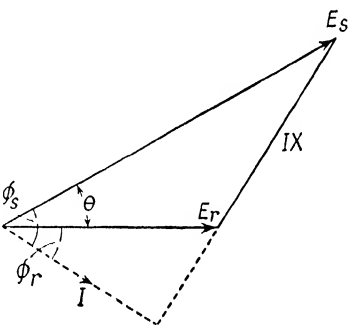

FIG. 11. VECTOR DIAGRAM FOR A SIMPLE REACTIVE TIE

The Power-circle Diagram. The fundamental vector diagrams of the general transmission network given in Figs. 8 and 9 lead, by way of a simple transformation, to two modified vector diagrams, which in turn form the basis of the all-important *power-circle diagram* of a synchronous transmission system. It has long been recognized that graphical or semi-graphical methods constitute one of the most valuable means available to the electrical engineer for attacking the many problems with which he is constantly faced. In no field of operation is this more true than in that of power system interconnection. In fact, many problems arising in this branch of electrical engineering practice are so complex, and the number of possible variables in a given problem are often so large, that purely analytical methods of solution are totally inadequate or, at best, involve a disproportionate amount of valuable time and labour. The power-circle diagram of a transmission system, along with its subsidiary loss- and efficiency- circle diagrams, provides a graphical method of solution to power transmission problems which is as elegant as it is labour-saving and which, moreover, can be made to give results of an accuracy comparable to that of the data on which the problem is founded.

* A little consideration will show that in all cases the power transmitted is equal to twice the area of the voltage vector triangle divided by the system reactance.

The analytical approach to the power-circle diagram given here is not that usually followed in textbooks on power transmission,[10] but is one which does not—as does the orthodox method of approach—lose sight of the main feature of synchronous power transmission, namely, the angular displacement between the independently generated voltages at the two ends of the transmission system. Consider for a moment the fundamental vector diagram of Fig. 8. If the scale of the diagram is altered by dividing each vector by the complex quantity $\mathbf{B} = B\underline{/\beta}$, the modified diagram of Fig. 12 is obtained. It is seen that the diagram as a whole is thereby rotated through the angle $-\beta$, so that the active component of the receiving-end current now becomes the zero axis of vector reference. As the result, the dotted circle is now the locus of the end of the current vector $\mathbf{I}_r$. The modified diagram is thus a receiving-end *current-circle diagram* in which the current vectors corresponding to different receiving-end load conditions all radiate from a common point and terminate on a circle whose radius is proportional to the sending-end voltage, and the position of whose centre is fixed by the receiving-end voltage. Not only so, but the common point of origin of the current vectors is actually the origin of a system of rectangular co-ordinates in which the abscissae represent active current and the ordinates represent reactive current.

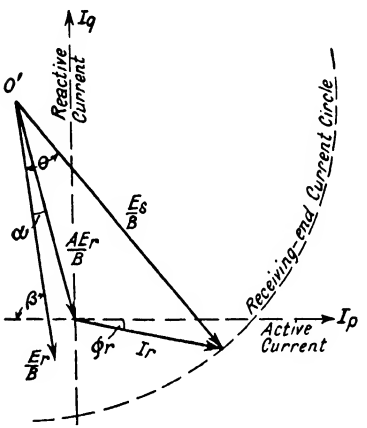

FIG. 12. THE RECEIVING-END CURRENT-CIRCLE DIAGRAM

The significance of these relationships is perhaps best realized by stating them somewhat differently. If the sending-end and receiving-end voltages are fixed in magnitude, then, in a system of active and reactive current co-ordinates, the vector representing the receiving-end current is constrained to terminate on a circle whose radius is proportional to the sending-end voltage and whose centre is determined by the receiving-end voltage. Referring to Fig. 12, it is seen that the radius of any receiving-end current circle is E_s/B; while the centre O' of the

circle lies at the end of the vector $-\mathbf{AE}_r/\mathbf{B}=(AE_r/B)\,\underline{|(\pi+\alpha-\beta)}$ and thus has the co-ordinates $I_p = -(AE_r/B)\,.\cos(\beta-\alpha)$ and $I_q = (AE_r/B)\,.\sin(\beta-\alpha)$.

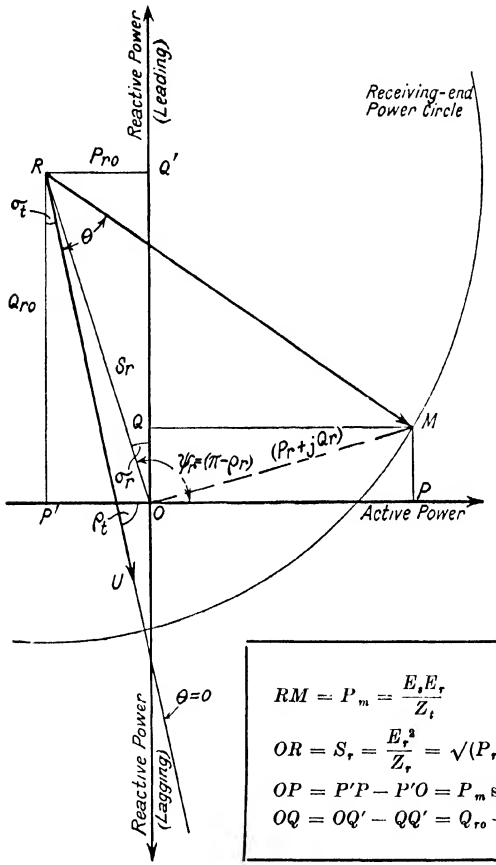

$$RM = P_m = \frac{E_s E_r}{Z_t} \qquad RU = \frac{E_r^2}{Z_t}$$

$$OR = S_r = \frac{E_r^2}{Z_r} = \sqrt{(P_{ro}^2 + Q_{ro}^2)}$$

$$OP = P'P - P'O = P_m \sin(\theta+\sigma_t) - P_{ro}$$

$$OQ = OQ' - QQ' = Q_{ro} - P_m \cos(\theta+\sigma_t)$$

FIG. 13. THE RECEIVING-END POWER-CIRCLE DIAGRAM

If now the scale of the diagram be altered once more, this time by multiplying each vector by E_r, then one obtains the receiving-end *power-circle diagram* of Fig. 13. In this diagram each circle expresses graphically a particular relation between the active power P_r and the reactive power Q_r in terms of the sending-end voltage E_s, the receiving-end voltage E_r, and the

constants of the transmission network. The nature of this relation is ascertainable from the constants of the power-circle diagram. For, comparing Figs. 12 and 13, it is seen that the radius of any power circle is $E_s E_r/B = E_s E_r/Z_t = P_m$, the maximum transfer power of the transmission system; while the co-ordinates of the power-circle centre (R in Fig. 13) are

$$P = -(AE_r^2/B) \cdot \cos(\beta - \alpha) = -(E_r^2/Z_r) \cdot \cos \rho_r = -P_{ro},$$

the receiving-end driving-point power, and

$$Q = (AE_r^2/B) \cdot \sin(\beta - \alpha) = (E_r^2/Z_r) \cdot \sin \rho_r = Q_{ro}.$$

A little consideration of the geometry of Fig. 13 will show that the co-ordinates (P, Q) of any point on a power circle must then satisfy the relation

$$(P + P_{ro})^2 + (Q - Q_{ro})^2 = P_m^2 \quad . \quad . \quad (45)$$

This is the so-called power-circle equation of a transmission network and is, in fact, the equation of a circle referred to a system of rectangular co-ordinates in which the abscissae represent active power (P) and the ordinates represent reactive power (Q). Moreover it is identical with equation (35*b*), which was derived analytically from a consideration of the vector power at the receiving end of the transmission system; whereas equation (45) has been derived graphically from a consideration of the receiving-end vector diagram. The equivalence of (35*b*) and (45) may be demonstrated by putting (35*b*) in the form of two equations—the active power equation of (37) and the corresponding reactive power equation: $Q_r = Q_{ro} - P_m \cos(\theta + \sigma_t)$—and then eliminating the sine and cosine factors by means of the relation $\cos^2 x + \sin^2 x = 1$.

From the point of view of setting up the power-circle diagram from the known network constants **A** and **B**, however, it is more convenient to express the power-circle centre in the polar co-ordinate form, viz.—

$$S_r \underline{|\psi_r} = -\mathbf{A}E_r^2/\mathbf{B} = -E_r^2/\mathbf{Z}_r = -(E_r^2/Z_r) \underline{|-\rho_r} = (E_r^2/Z_r) \underline{|\pi - \rho_r}$$

The distance to the centre from the origin of the diagram is then $S_r = E_r^2/Z_r$, while the angle which the vector radius to the centre makes with the reference axis is

$$\psi_r = (\pi - \rho_r) = (\pi/2 + \sigma_r) = (\pi + \alpha - \beta)$$

Hence $P_{ro} = S_r \sin \sigma_r$ and $Q_{ro} = S_r \cos \sigma_r$ are the rectangular co-ordinates of the receiving-end power-circle centre in the

second quadrant (see Fig. 13). Referring to equation (35*a*), it is seen that the second term is nothing other than $S_r \underline{|\psi_r}$, the position of the power-circle centre expressed in polar co-ordinates; while the first term similarly represents a circle of radius $P_m = E_s E_r / Z_t$, traced out by a vector whose zero position (given by $\theta = 0$) is an axis making an angle $-\rho_t = -\beta$ with the zero axis of vector reference. On comparing Figs. 8, 12, and 13 it is evident that this axis coincides with the receiving-end voltage. In other words, *equation* (35*a*) *is the equation of the receiving-end power circle expressed in polar co-ordinates* and, in particular, in terms of the angle θ between the sending-end and receiving-end voltages. ×

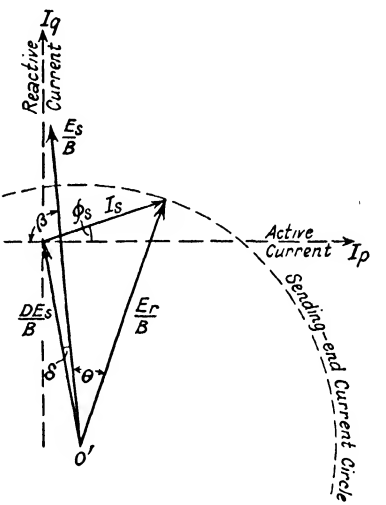

FIG. 14. THE SENDING-END CURRENT-CIRCLE DIAGRAM

The circle diagrams for the sending end are derived from the vector diagram of Fig. 9 in exactly the same way. Fig. 14 shows the sending-end current-circle diagram (obtained by dividing each vector in Fig. 9 by the impedance $\mathbf{B} = B \underline{|\beta}$*), in which the dotted circle has become the terminal locus of the current vector $\mathbf{I}_s$. In this case the radius of the current circle is proportional to the receiving-end voltage; at the same time the distance of the current-circle centre from the origin of the diagram is proportional to the sending-end voltage. For the radius of the circle is E_r/B, while its centre lies at the end of the vector $\mathbf{DE}_s/\mathbf{B} = (DE_s/B) \underline{|(\delta - \beta)}$ and thus has the co-ordinates

$$I_p = (DE_s/B) \cdot \cos(\beta - \delta) \text{ and } I_q = -(DE_s/B) \cdot \sin(\beta - \delta).$$

The corresponding power-circle diagram, obtained by multiplying each vector in Fig. 14 by the sending-end voltage E_s, is given in Fig. 15. The radius of any power circle is thus

* *N.B.* In this case, however, the angle $+\theta$ is measured in the opposite direction, so that rotation through $-\beta$ means an anti-clockwise rotation of the vector diagram.

again $E_s E_r/B = E_s E_r/Z_t = P_m$, that is, the maximum transfer power of the transmission system for any given values of E_s and E_r. The co-ordinates of the power-circle centre (S in Fig. 15) are in this case

$$P = (DE_s^2/B) \cdot \cos(\beta - \delta) = (E_s^2/Z_s) \cdot \cos \rho_s = P_{so},$$

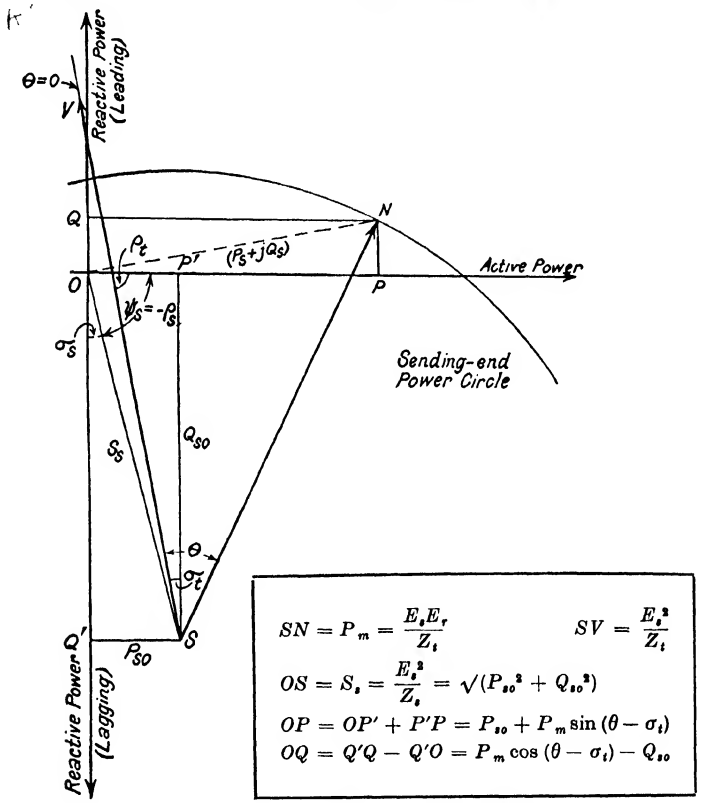

FIG. 15. THE SENDING-END POWER-CIRCLE DIAGRAM

the sending-end driving-point power, and

$$Q = -(DE_s^2/B) \cdot \sin(\beta - \delta) = -(E_s^2/Z_s) \cdot \sin \rho_s = -Q_{so}.$$

Here, again, it is seen that the co-ordinates (P, Q) of any point on a power circle must in consequence satisfy the relation

$$(P - P_{so})^2 + (Q + Q_{so})^2 = P_m^2 \quad . \quad . \quad (46)$$

which is identical with (36*b*).

In order to set up the sending-end power-circle diagram from the known network constants **D** and **B** it is in this case also more convenient to express the power-circle centre in the polar co-ordinate form, viz. $S_s \underline{|\psi_s} = \mathbf{D}E_s^2/\mathbf{B} = E_s^2/\mathbf{Z}_s = (E_s^2/Z_s) \underline{|-\rho_s}$. The distance to the centre from the origin of the diagram is then $S_s = E_s^2/Z_s$, while the angle which the vector radius to the centre makes with the reference axis is

$$\psi_s = -\rho_s = (\sigma_s - \pi/2) = (\delta - \beta).$$

Hence, and as may be seen at once from Fig. 15, $P_{so} = S_s \sin \sigma_s$ and $Q_{so} = S_s \cos \sigma_s$ are the rectangular co-ordinates of the sending-end power-circle centre in the fourth quadrant.

Again, referring to equation (36*a*), it will be observed that the first term is $S_s \underline{|\psi_s}$, the position of the power-circle centre expressed in polar co-ordinates; while the second term similarly represents a circle of radius $P_m = E_s E_r/Z_t$, traced out by a vector whose zero position (given by $\theta = 0$) is an axis making an angle $-\rho_t = -\beta$ with the zero axis of vector reference.* Hence equation (36*a*) is the polar equation of the sending-end power circle expressing the variation in sending-end vector power $(P_s + jQ_s)$ with the angle θ between the sending- and receiving-end voltages.

The power-circle diagrams of Figs. 13 and 15, then, furnish a graphical interpretation of the basic network power equations (35) and (36) and are thus of the utmost importance to an understanding of the electrical behaviour of synchronous transmission systems, quite apart from their utility in calculating the performance of an interconnector. For they show at a glance the alterations in terminal voltage necessary to permit system load changes to occur without altering the reactive power requirements at the termini and, conversely, they will indicate the variation in terminal power factor required in order that the system may accommodate itself to load changes without altering the sending- and receiving-end voltages. In addition, and as will be shown in the following chapters, they can be successfully used to determine the power limits of an interconnector, and to calculate the maximum load which a synchronous system can carry without loss of stability under normal conditions of operation.

The Loss- and Efficiency-circle Diagrams. The two circle diagrams described in the preceding section may conveniently

* This is the same angle as in the case of the receiving-end power-circle diagram. The zero-θ axes of the two diagrams are therefore always parallel.

be combined into a single chart, as shown in Fig. 16, having a common set of axes representing active and reactive power. It will be observed, however, that there is no single point on the combined chart which defines a particular operating condition in the transmission system. The reason for this is that the chart lacks a common voltage axis, besides which the two power circles are traversed in opposite directions.* Hence any operating point on the receiving-end chart, such as M, corresponding to a receiving-end power $P_r = OK$, is always associated with a corresponding operating point on the sending-end chart, such as N, for which the sending-end power is given by $P_s = OL$. The unique feature of the combined chart of Fig. 16 is that it at once enables one to find the operating point N corresponding to the point M (and vice versa) by virtue of the characteristic relationship between P_s and P_r, implicit in the fundamental power equations (35) and (36). For the angle URM in the receiving-end chart is the angle θ between the terminal voltages E_s and E_r, since the vectors RM and RU represent these voltages in magnitude and direction. But in the sending-end chart the vectors SV and SN also represent the terminal voltages E_s and E_r in magnitude and direction, so that the angle NSV is again identical with the angle θ between these two voltages. Hence if M is known, the corresponding value of θ can be read off from the receiving-end chart. The required operating point N is then readily found by entering the sending-end chart with this value of θ.

The combined chart of Fig. 16 thus fulfils the dual function of power chart and vector diagram. But it can do much more besides. A little consideration will show that it can be made to serve as a general performance chart from which the transmission losses, the transmission efficiency, and the net reactive power demand of the system may be readily obtained, in addition to the active power, reactive power, and power factor at the sending and receiving ends under load and no-load conditions. For the transmission losses are

$$P_l = (P_s - P_r) = (OL - OK) = KL$$

while the transmission efficiency is $\eta = P_r/P_s = OK/OL$. Furthermore, for the operating condition shown in Fig. 16 (viz. $\theta = 40°$), the vector power loss is

$$MN = \sqrt{[(P_s - P_r)^2 + (Q_s - Q_r)^2]} = \sqrt{(P_l^2 + Q_l^2)}$$

* *Cf.* footnote on p. 31.

where the co-ordinates of M and N are (P_r, Q_r) and (P_s, Q_s) respectively, so that the net reactive power demand is

$$Q_l = (Q_s - Q_r) = (LN - KM)$$

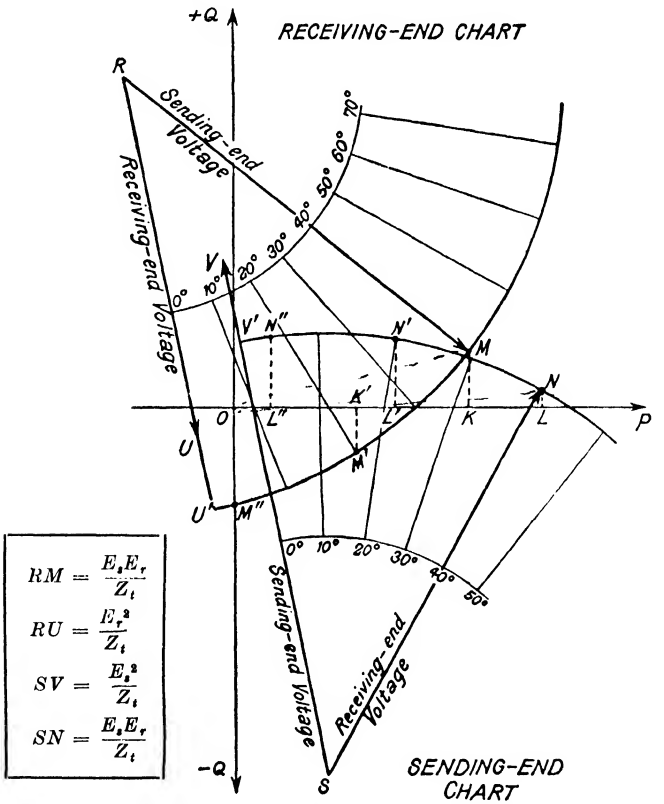

FIG. 16. COMBINED SENDING- AND RECEIVING-END CHART

If Q_l is negative—as in this case—the transmission system takes a net lagging reactive power; if Q_l is positive—as in the case where the operating points are M' and N'—the net reactive power taken by the system is leading.* The active power difference P_l is evidently always positive, R being in the second quadrant and S in the fourth quadrant, so that OL is of

* *Leading* reactive power is reckoned *positive*; *lagging* reactive power, *negative*.

necessity greater than OK, no matter what are the relative positions of the corresponding operating points M and N.

It is interesting to note that the special condition of no load at the receiving end can also be examined on the combined chart of Fig. 16. Here the operating point on the receiving-end chart is M'', corresponding to $P_r = 0$, so that an amount of lagging reactive power represented by OM'' is required at the receiving end if the sending-end voltage is to be maintained at the value E_s corresponding to the power circle $U'M''M'M$. The operating point on the sending-end chart for this condition is N'', where $\angle V'SN'' = \angle U'RM''$. Hence OL'' represents the power loss due to the charging current of the transmission system, while $L''M''$ represents the leading reactive power demand at the sending end. The net reactive power taken by the system is in this case

$$(L''N'' - OM'') = (L''N'' + M''O)$$

and is therefore leading, as is to be expected.

The use of the combined sending- and receiving-end chart in determining the transmission loss P_l, although simple and convenient, is not altogether satisfactory from the standpoint of accuracy in the results obtained. For the power loss P_l is read from the chart indirectly, as the difference of two powers individually many times larger than P_l. It is possible, of course, to overcome this difficulty by calculating P_s from P_r, making use of the real parts of equations (35*b*) and (36*b*). For the first enables θ to be found in terms of P_r, P_m, P_{ro}, and σ_t, which value, substituted in the second, then gives P_s in terms of P_{so}, P_m, σ_t, and θ. But this method of determining P_l is too laborious if more than one or two operating conditions are considered. An alternative method consists in performing the integration $\int \mathbf{i}^2 r dx$,* where $\mathbf{i}$ is the current at any point on the transmission system (regarded as an "equivalent transmission line" having distributed constants) and x is the distance of the point from the sending end.[11] This method is perhaps even more laborious, as it leads to an exceedingly cumbersome formula for P_l, unless resort is had to the "position angle" transformation developed by the author to facilitate the analysis of transmission-line performance.[12]

It will be appreciated, therefore, that any graphical method

* Strictly speaking, the total power loss is the sum of the leakage loss $\int \mathbf{v}^2 g dx$ and the resistance loss $\int \mathbf{i}^2 r dx$, but in practice the former component of P_l is negligible.

for determining P_l not indirectly, as the difference of P_s and P_r, but directly in terms of E_s and E_r, has a tremendous practical advantage over the analytical methods mentioned above. And it is most fortunate that the analysis underlying the power-circle diagram lends itself, by way of the combined loss- and efficiency-circle diagram, to an elegant modification which leads to a direct graphical determination not only of the transmission losses but of the transmission efficiency as well.

The derivation of the loss-circle diagram is as follows: Referring to the fundamental network equations (5) and (6), and taking $\mathbf{E}_r$ as vector datum, it is seen that the vector powers at the sending and receiving ends are given by

$$P_s + jQ_s = \mathbf{E}_s'\mathbf{I}_s = (\mathbf{A}'\mathbf{E}_r' + \mathbf{B}'\mathbf{I}_r')\,(\mathbf{C}\mathbf{E}_r + \mathbf{D}\mathbf{I}_r)$$
$$= [\mathbf{A}'E_r + \mathbf{B}'(I_p - jI_q)] \times [\mathbf{C}E_r + \mathbf{D}(I_p + jI_q)] \quad (47a)$$

and $$P_r + jQ_r = \mathbf{E}_r'\mathbf{I}_r = E_r\,(I_p + jI_q) \quad . \quad . \quad . \quad . \quad (47b)$$

respectively. The power loss P_l is then real part of the complex power representing the vector difference of equations (47a) and (47b). That is to say—

$$P_l = (P_s - P_r) = |\,E_s'I_s\,| - |\,E_r'I_r\,|$$
$$= \text{Real part of}\,[(A_1 - jA_2)\,E_r + (B_1 - jB_2)\,(I_p - jI_q)]$$
$$\times\,[(C_1 + jC_2)\,E_r + (D_1 + jD_2)\,(I_p + jI_q)] - E_rI_p$$

On multiplying out and collecting the real terms, one finds—

$$P_l = kE_r^2 + lE_rI_p + mE_rI_q + n\,(I_p^2 + I_q^2)$$
$$= kE_r^2 + lP_r + mQ_r + \frac{n}{E_r^2}\,(P_r^2 + Q_r^2) \quad . \quad (48)$$

where* $k = A_1C_1 + A_2C_2,$
$l = A_1D_1 + A_2D_2 + B_1C_1 + B_2C_2 - 1,$
$= 2\,(A_2D_2 + B_1C_1),$
$m = A_2D_1 - A_1D_2 + B_1C_2 - B_2C_1,$
$= 2\,(A_2D_1 - B_2C_1),$
$n = B_1D_1 + B_2D_2$

* The relation between the four network constants is $\mathbf{AD} - \mathbf{BC} = 1$, giving rise to the subsidiary relations

$$\left.\begin{aligned} A_1D_1 - A_2D_2 - B_1C_1 + B_2C_2 &= 1 \\ A_1D_2 + A_2D_1 - B_1C_2 - B_2C_1 &= 0 \end{aligned}\right\}$$

These in turn lead to the further relation

$$(l+1)^2 - (4kn - m^2) = 1 \quad . \quad . \quad . \quad (49)$$

which is of such vital importance in simplifying the structure of the loss-circle and efficiency-circle equations (see below). It will be observed that l and m are numerics; but that k is the sum of a conductance and a susceptance while n is the sum of a resistance and a reactance, so that the product kn is also a numeric.

Equation (48) may be rearranged to give*

$$\left(P_r+\frac{l}{2n}E_r^2\right)^2+\left(Q_r+\frac{m}{2n}E_r^2\right)^2=\frac{P_lE_r^2}{n}+(l^2+m^2-4kn)\frac{E_r^4}{4n^2}$$
$$=\frac{E_r^2}{n}\left(P_l-\frac{l}{2n}E_r^2\right) \quad . \quad (50)$$

It will be observed that this is the equation of a circle, referred to a system of P_r-Q_r co-ordinates, whose centre is fixed (for a given receiving-end voltage) and whose radius is a function of the power loss P_l. Equation (50) is the fundamental *loss-circle equation*, and may be written

$$(P+p)^2+(Q+q)^2=r^2 \quad . \quad . \quad (51)$$

in which $P=P_r$ is the transmitted power, $Q=Q_r$ is the reactive power at the receiving end, r is the radius of the loss circle corresponding to a given power loss P_l, and $-p$ and $-q$ are the co-ordinates of the common loss-circle centre. Equations (50) and (51) are equivalent, provided

$$p=\frac{l}{2n}E_r^2=\left(\frac{A_2D_2+B_1C_1}{B_1D_1+B_2D_2}\right)E_r^2 \quad . \quad . \quad (52a)$$

$$q=\frac{m}{2n}E_r^2=\left(\frac{A_2D_1-B_2C_1}{B_1D_1+B_2D_2}\right)E_r^2 \quad . \quad . \quad (52b)$$

$$r=E_r\cdot\sqrt{\left(\frac{P_l-p}{n}\right)} \quad . \quad . \quad . \quad . \quad (52c)$$

Equation (50) may thus be represented by a family of concentric circles whose common centre lies in the third quadrant of a system of rectangular P-Q co-ordinates.† The family constitutes the *loss-circle diagram* of the transmission system and may be included along with the power-circle diagram in a general receiving-end chart. The power loss associated with a particular value of transmitted power is then represented by the radius of the loss circle passing through the "operating point" on the power circle (e.g. M, M' and M'' in Fig. 16). In an actual loss-circle diagram a series of loss circles is usually calculated from equation (52c) for equal increments in P_l, and these circles are then drawn in and marked with their appropriate

* See footnote on previous page.

† It is interesting to note that in the case of a short transmission line, which may be represented by a simple series impedance, and for which in consequence $A_1=D_1=1$, A_2, D_2, C_1, and C_2 are all zero, $B_1=R$, and $B_2=X$, one finds from equations (52) that $p=0$, $q=0$, and $r=E_r\cdot\sqrt{(P_l/R)}$. Hence the loss-circle equation becomes $P^2+Q^2=E_r^2(P_l/R)$. This is evident from the fact that in this case $P_l=I_r^2R=(I_p^2+I_q^2)R$.

P_l values. As it is but seldom that any particular operating point in the power-circle diagram happens to fall on a loss circle, the distance of the operating point from the loss-circle centre will usually have to be measured, on the power scale of the diagram, and the corresponding value of P_l calculated from equation (52c). In order to avoid this calculation and, at the same time, the necessity for including loss circles

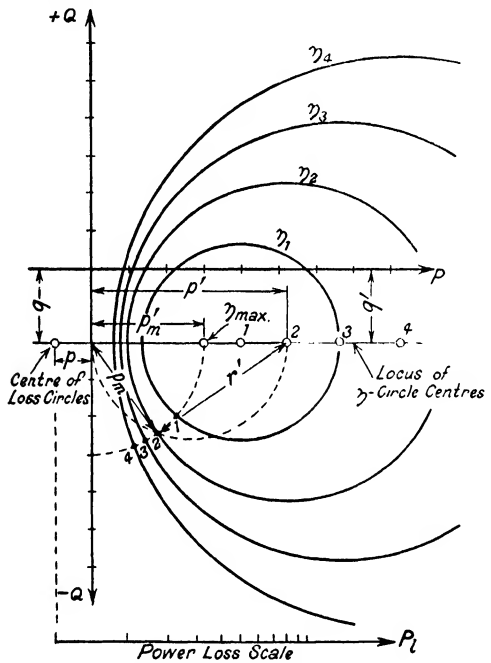

FIG. 17. LOSS- AND EFFICIENCY-CIRCLE DIAGRAM

on the receiving-end chart, it will be found more convenient to compute a separate power-loss scale from equation (52c) and to place this scale, graduated directly in terms of P_l, at the bottom of the diagram. The actual distance between the given operating point and the loss-circle centre can then be transferred to this scale so as to give the corresponding value of the power loss directly (*cf.* Fig. 17).

The practical value of such a general receiving-end chart is considerably enhanced by providing a means of determining from it not only the total power loss inherent in the transmission

of a given amount of power, with given sending-end and receiving-end voltages, but also the corresponding efficiency of the transmission system. The latter, being defined as the ratio of the receiving-end and sending-end powers, is given by $\eta = P_r/(P_r + P_l)$, so that $P_l = P_r\ (1/\eta - 1)$. On substituting this value of P_l, in equation (50) one obtains after some transformation the corresponding *efficiency-circle equation* which may be written in the standard form—

$$(P - p')^2 + (Q + q')^2 = (r')^2 \quad . \quad . \quad (53)$$

where $$p' = \frac{1/\eta - (l+1)}{2n} E_r^2 = p\left(\frac{1 - \eta - \eta l}{\eta l}\right) \quad . \quad (54a)$$

$$q' = \frac{m}{2n} E_r^2 = q \quad . \quad . \quad . \quad . \quad . \quad (54b)$$

and $$r' = \sqrt{\left[(p')^2 + \frac{m^2}{4n^2} E_r^4 - \frac{k}{n} E_r^4\right]}$$

$$= \sqrt{\left[(p')^2 - \frac{l^2 + 2l}{4n^2} E_r^4\right]} \quad . \quad . \quad . \quad (55a)$$

It will be observed that (53) is thus the equation of a circle whose radius depends upon the transmission efficiency η. It is to be noted, too, that the vertical displacement of the centre is fixed and equal to that of the loss-circle centre. Also, the horizontal displacement is a function of η, so that the efficiency circles are eccentric. Hence their centres lie on a straight line through the loss-circle centre and parallel to the P axis, in the fourth quadrant, as shown in Fig. 17.

An examination of equation (55*a*) reveals that the radius of the efficiency circle diminishes as the efficiency η increases. *The transmission efficiency is a maximum for that operating point on the chart which coincides with the particular point representing the efficiency circle of zero radius.* The value of this maximum efficiency is accordingly obtained by putting $r_t = 0$ in (55*a*). This gives

$$p_m' = \frac{\sqrt{(l^2 + 2l)}}{2n} E_r^2 = p\sqrt{(1 + 2/l)} \quad . \quad . \quad (56)$$

as the abscissa of the maximum efficiency point. On substituting this value of p' in equation (54*a*), one finds for the maximum transmission efficiency—

$$\eta_{max} = \frac{1}{(l+1) + \sqrt{[(l+1)^2 - 1]}} \quad . \quad . \quad (57)$$

A corresponding substitution in equation (55*a*) then gives for the efficiency-circle radius—

$$r' = \sqrt{[(p')^2 - (p_m')^2]} \quad . \quad . \quad . \quad (55b)$$

Equation (55*b*) at once leads to the simple geometrical construction of the efficiency circles shown in Fig. 17. The abscissa p_m' of the maximum-efficiency operating point η_{max} is first determined from equation (56), and a quadrant of a circle of radius p_m' is then drawn from this point to the Q axis as shown. The abscissae p' of the efficiency-circle centres are next determined from equation (54*a*) for a range of η values, and the centres marked on the locus parallel to the P axis, as indicated at 1, 2, 3, etc. If a semicircle be erected on this locus between the Q axis and the appropriate efficiency-circle centre, then the required efficiency circle must pass through the point of intersection of this semicircle and the quadrant drawn through η_{max}, because this point is the apex of a right-angled triangle having the abscissa p' as its hypotenuse, and p_m' and r' for the remaining two sides. And the three sides of such a triangle obey the relation expressed by (55*b*). By erecting a number of such semicircles a series of points of intersection, 1, 2, 3, etc., are found which determine the radii of the several efficiency circles.

The Straight-line Loss Diagram. The main drawback in the use of loss or efficiency circles is that their inclusion on the power-circle diagram is apt to make the chart as a whole confusing and thus awkward to read. This difficulty may be overcome by the use of the so-called *straight-line loss diagram*, in which the family of concentric loss circles is replaced by a single line corresponding to each power circle in the chart, i.e. to each value of sending-end voltage E_s for a given receiving-end voltage E_r. By the choice of a suitable loss scale the power loss corresponding to any particular operating point on the receiving-end chart is then represented simply by the perpendicular distance from the operating point to the appropriate loss line.

Reverting to the basic power equations (37) and (38), it is evident that the power loss is given by

$$\begin{aligned} P_l &= (P_s - P_r) = [P_{so} + P_m \sin(\theta - \sigma_t)] - [P_m \sin(\theta + \sigma_t) - P_{ro}] \\ &= (P_{so} + P_{ro}) - 2\,P_m \sin\sigma_t \cos\theta \quad . \quad . \quad . \quad . \quad (58) \end{aligned}$$

The power loss of the transmission system can thus be represented graphically as the difference between a length $(P_{so} + P_{ro})$ and the projection of a vector $2P_m \sin \sigma_t$ on an axis with which that vector makes an angle θ. This relationship is illustrated in Fig. 18, in which the *loss line* is the perpendicular to the zero θ axis passing through a point distant $(P_{so} + P_{ro})$ from the loss-circle centre.

It will be observed that the radius of the loss circle is 2 sin σ_t times that of the power circle, whereas the angular variable θ is the same for both. Hence by choosing a power-loss scale such that the radius of the loss circle, measured on that scale, is equal to the radius of the power circle, measured on the power scale of the receiving-end chart, it becomes possible to use the power circle itself in the manner shown in Fig. 18. A little consideration will show that under these circumstances the loss scale must be greater than the power scale in the ratio $1/2 \sin \sigma_t$,* while the zero-θ axis of Fig. 18 must coincide with the vector representing the receiving-end voltage in the power-circle diagram. The resulting dual diagram is shown in Fig. 19.

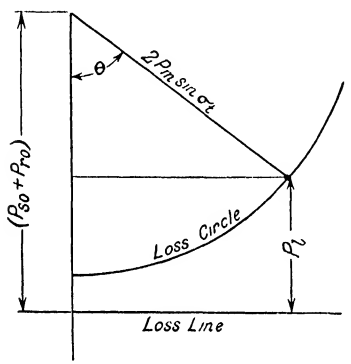

FIG. 18. THE STRAIGHT-LINE LOSS DIAGRAM

The distance RT, equal to $(P_{so} + P_{ro})$ units of the power-loss scale, or $\dfrac{P_{so} + P_{ro}}{2 \sin \sigma_t}$ units of the power scale, is measured off on the zero-θ axis of the power-circle diagram and a perpendicular erected at the point T. By drawing a parallel through the operating point M to meet RT at W, the power loss $P_l = TW$ can be read directly on the power-loss scale.

The Universal Power-Transmission Chart. The circle diagrams for active and reactive power transmitted, system power loss, and transmission efficiency that have been developed in the preceding sections, and which in practice are usually co-ordinated to form a comprehensive receiving-end chart, are

* It will be remembered that σ_t, being the complement of the transfer impedance angle $\rho_t = \beta$, is very small, of the order of a few degrees only, so that 2 sin σ_t will be much less than unity.

all premised on constant terminal voltages E_s and E_r. It is often necessary, however, to investigate the performance of a transmission system under conditions of varying sending-end or receiving-end voltage. In the former case, with E_r fixed, the effect of varying E_s can be studied without much difficulty on a single receiving-end chart, for the power-circle diagram then consists of a family of concentric circles each of which

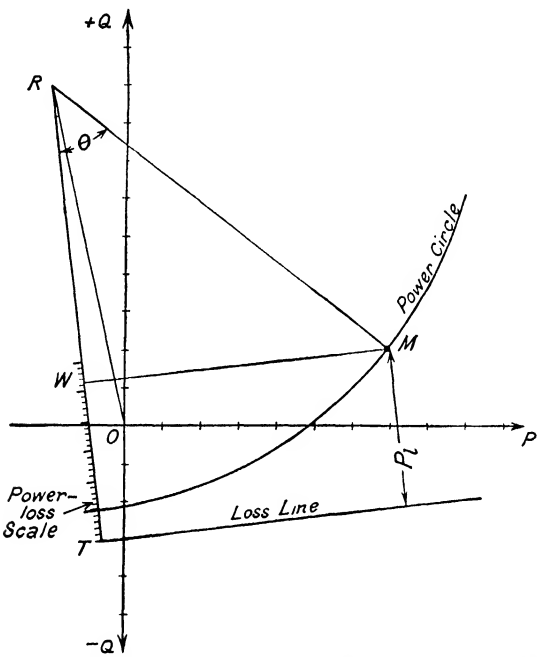

FIG. 19. THE COMBINED POWER-CIRCLE AND LOSS-LINE DIAGRAM

corresponds to one definite value of E_s, while the loss-circle diagram is in this case also a single family of concentric circles. Moreover, the efficiency circles are independent of E_s, both as regards magnitude and in respect of their location on the chart. Finally, the alternative straight-line loss diagram then consists of a series of parallel loss lines, each pertaining to a particular power circle, since the distance RT in Fig. 19 is a function of E_s as well as of E_r.

On the other hand, if the sending-end voltage is fixed and the receiving-end voltage is the variable, a number of charts

are required, one for each chosen value of E_r. For the co-ordinates of the power- and loss-circle centres are functions of E_r, so that the power-circle diagram consists of a family of eccentric circles* and the loss-circle diagram comprises several families of concentric circles, each family corresponding to a particular value of E_r. In fact, the several power-circle centres all lie at distances from the P-Q origin proportional to E_r^2 on an axis passing through it at an angle

$$\psi_r = (\pi/2 + \sigma_r) = \tan^{-1}\left(\frac{Q_{ro}}{-P_{ro}}\right) = \frac{A_2B_1 - A_1B_2}{A_1B_1 + A_2B_2}$$

while the several loss-circle centres lie in the same way on a similar axis at an angle

$$\psi_l = \tan^{-1}\left(\frac{-q}{-p}\right) = \frac{A_2D_1 - B_2C_1}{A_2D_2 + B_1C_1}$$

Furthermore, the co-ordinates of the efficiency-circle centres are also functions of E_r, so that the efficiency-circle diagram in this case consists of several families of eccentric circles, each family corresponding to a particular value of E_r.

To include all these diagrams on a single chart would lead to well-nigh hopeless confusion in obtaining practical results. And as the case of variable receiving-end voltage is often of considerable importance in transmission system studies—especially in the study of system stability, where the problems involve changes in the angle θ accompanied by changes in the magnitudes of both E_s and E_r—it becomes necessary, therefore, to compute a series of receiving-end charts, each chart relating to a specific value of the receiving-end voltage.†

The necessity for computing a series of charts to cover a given voltage range at the receiving end can be avoided, fortunately, by the use of a modified chart in which the positions of the several diagram centres are quite independent of the receiving-end voltage. This modified chart is, in effect, a *universal power-transmission chart*, and is applicable at any value of terminal voltage at the sending and the receiving ends of the transmission system.

* *Cf.* Chapter III

† The above arguments, of course, apply equally to the sending-end charts except that there each chart would relate to a specific value of E_s and would contain a power-circle diagram in which each of the concentric circles refers to one definite value of E_r. (*Cf.* Figs. 13 and 15.)

Referring to the fundamental power equations (35) and (36), it is seen that if these be divided throughout by E_r^2 and E_s^2 respectively, one obtains the modified power-circle equations—

$$[(P_r/E_r^2)^2 + a_r^2] + [(Q_r/E_r^2)^2 - b_r^2] = c^2\,(E_s/E_r)^2 \quad . \quad (59)$$

$$[(P_s/E_s^2)^2 - a_s^2] + [(Q_s/E_s)^2 + b_s^2] = c^2\,(E_r/E_s)^2 \quad . \quad (60)$$

where

$$a_r = \frac{\sin \sigma_r}{Z_r}; \quad b_r = \frac{\cos \sigma_r}{Z_r};$$

$$a_s = \frac{\sin \sigma_s}{Z_s}; \quad b_s = \frac{\cos \sigma_s}{Z_s}; \qquad c = \frac{1}{Z_t}.$$

Equations (59) and (60) are in each case those of a family of concentric admittance circles referred to a system of rectangular co-ordinates in which the abscissae represent conductance (P/E^2) and the ordinates susceptance (Q/E^2). Moreover, in this co-ordinate system the common centre of the admittance circles is fixed, for *its position is entirely independent of voltage* and is determined only by the network constants of the transmission system; and the circle radius depends on *the ratio of the terminal voltages* rather than on the actual magnitude of either. In the modified chart based on equation (59) or (60) therefore, the circle centre has the constant co-ordinates, $(-a_r, b_r)$ or $(a_s, -b_s)$, while the circle radius is given by the constant c multiplied or divided by the terminal voltage ratio E_s/E_r, depending upon whether the chart relates to conditions at the receiving or sending end of the transmission system.

Such a chart is consequently of universal application, as the active and reactive powers corresponding to any given operating point and voltage ratio may be obtained simply through multiplication of the co-ordinate readings by the appropriate value of E_s^2 or E_r^2. Furthermore, as the radii of the modified power circles are proportional to a voltage ratio, these circles will be evenly spaced, thus facilitating interpolation and in consequence making the chart easy to read. Two actual examples of this universal power transmission chart are given in Figs. 22 and 23.

Examples of Power Chart Construction and Utilization. All the charts discussed in the present chapter are premised on the transmission system being single-phase. That is to say, in a polyphase system E_s and E_r represent *line-to-neutral* voltages, while P_r, P_s and Q_r, Q_s represent active and reactive

powers respectively *per phase*. These charts remain applicable to three-phase transmission systems, however, provided certain precautions are observed in the choice of units. A little consideration will show that if in this case the symbols E_S and E_R denote *line voltages* expressed in *kilovolts*, while P_R, P_S and Q_R, Q_S similarly denote *three-phase powers* expressed in *megawatts* and *megavars* respectively, then, in spite of the change in units, equations (45) to (58) remain valid when the lower-case subscripts s and r are changed to the capital subscripts S and R. This fortuitous circumstance arises by virtue of the relations—

$$\left.\begin{aligned}\text{Single-phase power in VA.} &= \frac{(\text{Phase voltage in V.})^2}{\text{Impedance per phase in } \Omega}\\ \text{Three-phase power in MVA.} &= \frac{(\text{Line voltage in kV.})^2}{\text{Impedance per phase in } \Omega}\end{aligned}\right\}$$

For example, the universal charts of Figs. 22 and 23 will indicate MW. and MVAr. if the co-ordinates of any operating point are multiplied by the square of the appropriate terminal line voltage in kilovolts. Alternatively, they will equally well indicate watts and reactive volt-amperes per phase if the same co-ordinates are multiplied by the square of the corresponding terminal phase voltage expressed in volts. From the practical standpoint, however, it is more convenient to work in terms of MW., MVAr., and kV. when applying circle diagrams to the solution of power system problems.

Example 1. *A selected generating station supplies power over a single-circuit three-phase* 132 000 *V. transmission line of the British Grid system, having the following constants per mile—*

Resistance = 0·251 *ohm* *Conductance* = 0 *mho*

Reactance = 0·669 *ohm* *Susceptance* = 4·425 *micromhos*

If the length of the transmission line is 200 *miles and the voltage at each end is maintained constant at* 132 000 *V. by power-factor control, determine by means of a combined sending- and receiving-end chart* (a) *the line loss and transmission efficiency for a transmitted power of* 50 000 *kW.*, (b) *the reactive power requirements and the power factors at the two ends of the line for this value of receiving-end load, and* (c) *the charging current at the sending end and the power loss in the line due to this current when the receiving end is on no load.*

Solution.

$$\mathbf{Z} = (R + jX) = 200(0{\cdot}251 + j0{\cdot}669) = 142{\cdot}9\,\underline{|69{\cdot}4^\circ}$$

$$\mathbf{Y} = (G + jB) = 200(0 + j4{\cdot}425 \times 10^{-6}) = 0{\cdot}885 \times 10^{-3}\,\underline{|90^\circ}$$

$$\mathbf{ZY} = 142{\cdot}9 \times 0{\cdot}885 \times 10^{-3}\,\underline{|69{\cdot}4^\circ + 90^\circ} = 0{\cdot}1264\,\underline{|159{\cdot}4^\circ}$$

Entering Chart I with 0·1264 as the size of $\mathbf{ZY}$ and 159·4° as the angle of $\mathbf{ZY}$, one finds $\cosh \sqrt{\mathbf{ZY}} = 0{\cdot}942 \,\underline{|1{\cdot}3°}$. Similarly from Chart II one finds $(\sinh \sqrt{\mathbf{ZY}})/\sqrt{\mathbf{ZY}} = 0{\cdot}9804 \,\underline{|0{\cdot}4°}$. Hence the network constants of the transmission line are—

$$\mathbf{A} = \mathbf{D} = \cosh \sqrt{\mathbf{ZY}} = 0{\cdot}942 \,\underline{|1{\cdot}3°}$$

$$\mathbf{B} = \mathbf{Z}(\sinh \sqrt{\mathbf{ZY}})/\sqrt{\mathbf{ZY}} = 142{\cdot}9 \times 0{\cdot}9804 \,\underline{|69{\cdot}4° + 0{\cdot}4°}$$
$$= 140{\cdot}1 \,\underline{|69{\cdot}8°}$$

$$\mathbf{C} = \mathbf{Y}(\sinh \sqrt{\mathbf{ZY}})/\sqrt{\mathbf{ZY}} = 0{\cdot}885 \times 10^{-3} \times 0{\cdot}9804 \,\underline{|90° + 0{\cdot}4°}$$
$$= 0{\cdot}8676 \times 10^{-3} \,\underline{|90{\cdot}4°}$$

The transfer and driving-point impedances of the system are accordingly—

$$\mathbf{Z}_t = \mathbf{B} = 140{\cdot}1 \,\underline{|69{\cdot}8°} \text{ ohms}$$

$$\mathbf{Z}_r = \frac{\mathbf{B}}{\mathbf{A}} = \frac{140{\cdot}1 \,\underline{|69{\cdot}8°}}{0{\cdot}942 \,\underline{|1{\cdot}3°}} = 148{\cdot}7 \,\underline{|68{\cdot}5°} \text{ ohms}$$

$$\mathbf{Z}_s = \frac{\mathbf{B}}{\mathbf{D}} = \frac{140{\cdot}1 \,\underline{|69{\cdot}8°}}{0{\cdot}942 \,\underline{|1{\cdot}3°}} = 148{\cdot}7 \,\underline{|68{\cdot}5°} \text{ ohms}$$

The power-circle centres are then given by—

$$S_r = \frac{E_R^2}{Z_r} = \frac{132^2}{148{\cdot}7} = 117{\cdot}2 \text{ MVA.}; \; \psi_r = (\pi - \rho_r) = (180° - 68{\cdot}5°) = 111{\cdot}5°$$

$$S_s = \frac{E_S^2}{Z_s} = \frac{132^2}{148{\cdot}7} = 117{\cdot}2 \text{ MVA.}; \; \psi_s = -\rho_s = -68{\cdot}5°$$

Hence $+P_{ro} = 117{\cdot}2 \times \cos 111{\cdot}5° = -43$ MW. | $+Q_{ro} = 117{\cdot}2 \times \sin 111{\cdot}5° = 109$ MVAr.

and $+P_{so} = 117{\cdot}2 \times \cos(-68{\cdot}5°) = 43$ MW. | $-Q_{so} = 117{\cdot}2 \times \sin(-68{\cdot}5°) = -109$ MVAr.

Finally, $P_m = \dfrac{E_S E_R}{Z_t} = \dfrac{132 \times 132}{140{\cdot}1} = 124{\cdot}4$ MVA.

The receiving- and sending-end power circles based on the above constants are shown in Fig. 20.

(*a*) The receiving-end power circle gives $\theta = 28°$ for $P_R = 50$ MW. Transferring this value of θ to the sending-end power circle gives $P_S = 60$ MW. The power loss is thus—

$$P_L = (P_S - P_R) = (60 - 50) = 10 \text{ MW.} = \underline{10\,000 \text{ kW.}}$$

and the transmission efficiency is—

$$\eta = \frac{P_R}{P_S} = \frac{50}{60} = 0{\cdot}833 = \underline{83{\cdot}3 \text{ per cent}}$$

(*b*) The operating point on the receiving-end power circle for $P_h = 50$ MW. has the ordinate $Q_R = 25{\cdot}5$ MVAr., while that on the sending-end power circle for $P_S = 60$ MW. has the ordinate $Q_S = 14{\cdot}5$

MVAr. The reactive power requirements at the two ends of the line are accordingly—

Sending end: 14·5 MVAr. = 14 500 kVAr. leading

Receiving end: 25·5 MVAr. = 25 500 kVAr. leading

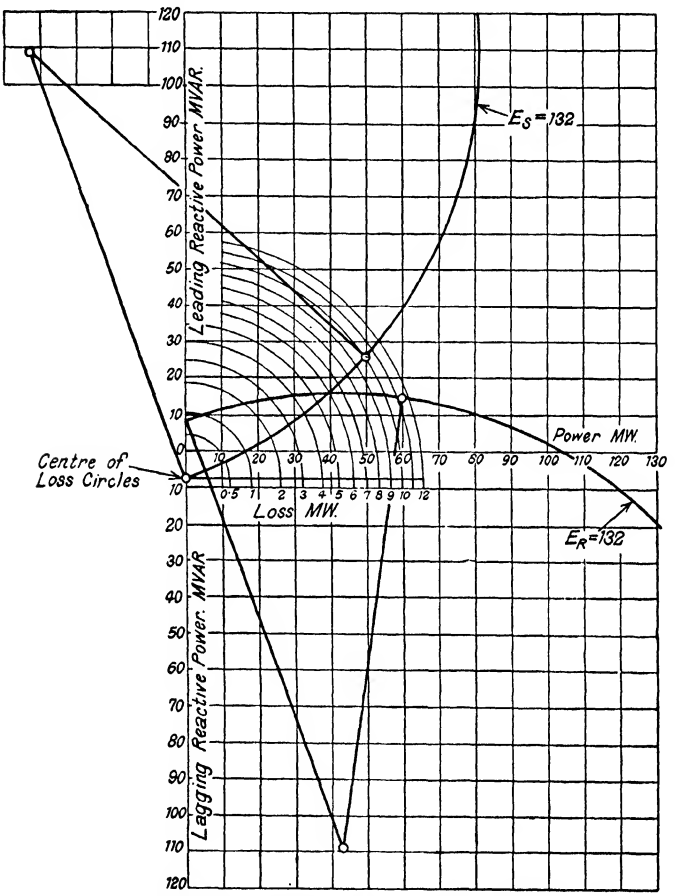

FIG. 20. COMBINED POWER CHART FOR 200-MILE 132 KV. TRANSMISSION LINE

The net reactive power taken by the transmission line is thus

$$Q_L = (Q_S - Q_R) = -11 \text{ MVAr.} = 11\,000 \text{ kVAr. lagging}$$

The receiving-end power-factor angle is—

$$\phi_r = \tan^{-1}(Q_R/P_R) = \tan^{-1}(25{\cdot}5/50) = \tan^{-1} 0{\cdot}51 = 27°$$

while the corresponding angle at the sending end is—

$$\phi_s = \tan^{-1}(Q_S/P_S) = \tan^{-1}(14{\cdot}5/60) = \tan^{-1} 0{\cdot}241 = 13{\cdot}5°$$

Hence the terminal power factors are—

Sending end: $\cos 13{\cdot}5° = \underline{0{\cdot}972 \text{ leading}}$

Receiving end: $\cos 27° = \underline{0{\cdot}891 \text{ leading}}$

(*c*) The receiving-end power circle gives $\theta = 0{\cdot}2°$ for $P_R = 0$. On transferring this value of θ to the sending-end power circle one finds $P_S = 0{\cdot}5$ and $Q_S = 8{\cdot}5$. The sending-end (charging) current is thus—

$$I_{So} = \frac{1\,000 Q_S}{\sqrt{3} E_S} = \frac{8\,500}{\sqrt{3} \times 132} = \underline{37 \text{ A. leading}}$$

and the power loss due to this current is—

$$P_S = 0{\cdot}5 \text{ MW.} = \underline{500 \text{ kW.}}$$

Incidentally, it will be seen from the receiving-end power circle when $P_R = 0$, $Q_R = -7{\cdot}5$. That is to say, in order to maintain 132 kV. under no-load conditions it is necessary to supply 7 500 kVAr. *lagging* at the receiving end.

Example 2. *Verify the figures for power loss and transmission efficiency obtained in the preceding example by means of* (a) *the loss-circle diagram,* (b) *the efficiency-circle diagram, and* (c) *the straight-line loss diagram.*

Solution. (*a*) Reverting to Example 1, the general network constants, expressed in the rectangular form, are—

$$A_1 + jA_2 = A\cos\alpha + jA\sin\alpha = 0{\cdot}942\cos 1{\cdot}3° + j0{\cdot}942\sin 1{\cdot}3° = 0{\cdot}9419 + j0{\cdot}02138$$

$$B_1 + jB_2 = B\cos\beta + jB\sin\beta = 48{\cdot}4 + j131{\cdot}6$$

$$C_1 + jC_2 = C\cos\gamma + jC\sin\gamma = (-0{\cdot}00606 + j0{\cdot}8676) \times 10^{-3}$$

$$D_1 + jD_2 = D\cos\delta + jD\sin\delta = 0{\cdot}9419 + j0{\cdot}02138$$

The auxiliary constants are thus—

$$k = A_1C_1 + A_2C_2 = (0{\cdot}9419 \times -0{\cdot}00606 \times 10^{-3}) + (0{\cdot}02138 \times 0{\cdot}8676 \times 10^{-3}) = (-5{\cdot}705 + 18{\cdot}545) \times 10^{-6} = \underline{12{\cdot}84 \times 10^{-6}}$$

$$l = 2(A_2D_2 + B_1C_1) = (2 \times 0{\cdot}02138 \times 0{\cdot}02138) + (2 \times 48{\cdot}4 \times -0{\cdot}00606 \times 10^{-3}) = (0{\cdot}9136 - 0{\cdot}5863) \times 10^{-3} = \underline{0{\cdot}3273 \times 10^{-3}}$$

$$m = 2(A_2D_1 - B_2C_1) = (2 \times 0{\cdot}02138 \times 0{\cdot}9419) - (2 \times 131{\cdot}6 \times -0{\cdot}00606 \times 10^{-3}) = 40{\cdot}27 + 1{\cdot}594 \times 10^{-3} = \underline{0{\cdot}04186}$$

$$n = B_1D_1 + B_2D_2 = (48{\cdot}4 \times 0{\cdot}9419) + (131{\cdot}6 \times 0{\cdot}02138) = 45{\cdot}56 + 2{\cdot}81 = \underline{48{\cdot}37}$$

The co-ordinates of the loss-circle centre are accordingly—

$$-p = -\frac{l}{2n}E_R^2 = -\frac{0{\cdot}3273 \times 10^{-3} \times (132)^2}{2 \times 48{\cdot}37} = -0{\cdot}06 \text{ MW.}$$

$$-q = -\frac{m}{2n}E_R^2 = -\frac{0{\cdot}04186 \times (132)^2}{2 \times 48{\cdot}37} = -7{\cdot}55 \text{ MVAr.}$$

The loss-circle radius is—

$$r = \frac{E_R}{\sqrt{n}} \cdot \sqrt{(P_L - p)} = \frac{132}{\sqrt{48{\cdot}37}} \cdot \sqrt{(P_L - 0{\cdot}06)}$$
$$= 18{\cdot}98\sqrt{(P_L - 0{\cdot}06)} \text{ MVA.}$$

Below are tabulated corresponding values of r and P_L.

P_L MW.. .	1	2	3	4	5	6	7	8	9	10	11	12
r MVA. . .	18·4	26·4	32·5	37·7	42·2	46·3	50·0	53·5	56·6	59·8	62·8	65·6

The loss-circle diagram is shown in Fig. 20. It is found that the loss circle for which $P_L = 10{\cdot}1$ MW. passes through the operating point on the receiving-end power circle for which $P_R = 50$ MW. This value of power loss agrees with that found under (*a*) in Example 1.

(*b*) The locus of the efficiency-circle centres is the horizontal axis $Q = -q' = -q = -7{\cdot}55$ MVAr. The maximum transmission efficiency as given by equation (57) is—

$$\eta_{max} = \frac{1}{1{\cdot}0003273 + \sqrt{[(1{\cdot}0003273)^2 - 1]}} = 99{\cdot}7 \text{ per cent}$$

and occurs at a load whose value is given by equation (56)—

$$p'_m = 0{\cdot}059\sqrt{(1 + 2/1{\cdot}000327)} = 0{\cdot}10 \text{ MW.} = 103 \text{ kW.}$$

The abscissae of the several efficiency-circle centres as given by equation (54*a*) are—

$$p' = \frac{132^2}{2 \times 48{\cdot}37}\left(\frac{1}{\eta} - 1{\cdot}000327\right) = 180\left(\frac{1}{\eta} - 1{\cdot}00033\right) \text{ MW.}$$

while the corresponding efficiency-circle radii as given by equation (55*b*) are—

$$r' = \sqrt{\left[32\,400\left(\frac{1}{\eta} - 1{\cdot}00033\right)^2 - 0{\cdot}01\right]} \text{ MVA.}$$

The receiving-end power- and efficiency-circle diagrams are shown in Fig. 21. It will be observed that the efficiency circle for which $\eta = 83$ per cent would pass through the operating point on the power circle corresponding to $P_R = 50$ MW. This value of efficiency is in close agreement with that found under (*a*) in Example 1.

(*c*) The distance of the loss line from the centre of the receiving-end power circle is $(P_{so} + P_{ro}) = (43 + 43) = 86$ MW. *in units of the loss scale.* The loss-scale unit is

$$\frac{1}{2 \sin \sigma_t} = \frac{1}{2 \times \sin 20{\cdot}2°} = \frac{1}{2 \times 0{\cdot}3453} = 1{\cdot}448$$

times the power-scale unit. The loss line is thus perpendicular to the

zero θ-axis at a point on it distant $1{\cdot}448 \times 86 = 124{\cdot}3$ MW., measured in units of the power scale.

The straight-line loss diagram based on the above data is shown in Fig. 21. It is seen that the parallel to the loss line passing through

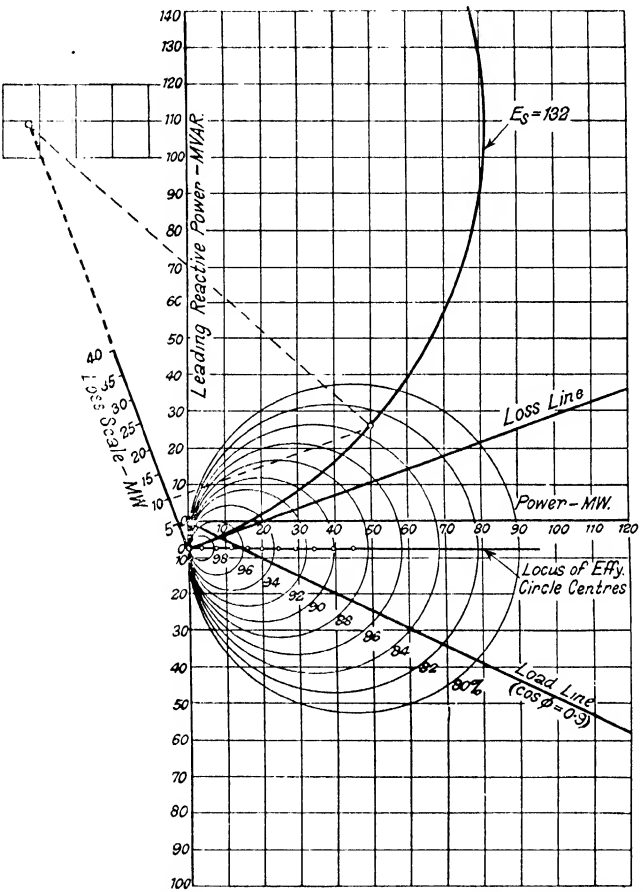

FIG. 21. RECEIVING-END POWER, LOSS, AND EFFICIENCY CHART FOR 200-MILE 132 KV. TRANSMISSION LINE

the operating point on the power circle for which $P_R = 50$ MW., meets the loss scale at $P_L = 10$ MW. This checks with the values for the power loss already obtained by alternative methods.

Example 3. *Find the value of transmitted power that will relieve the synchronous plant at the receiving end of the line in Example* 1 *of all reactive power loading if the load power factor is* (a) *unity, and* (b) 0·9

lagging. What would be the reactive power demand at the receiving end in the case of a load of 40 000 *kW. at* 0·9 *lagging power factor?*

Solution. A straight line in the fourth quadrant passing through the origin of the power-circle diagram and making an angle of $\cos^{-1}(0{\cdot}9) = 25{\cdot}8°$ with the power axis is the locus of all points representing loads at 0·9 lagging power factor. Similarly the power axis is the locus of all load points for which $\cos\phi = 1{\cdot}0$.

(*a*) The required power value is given by the abscissa of the point

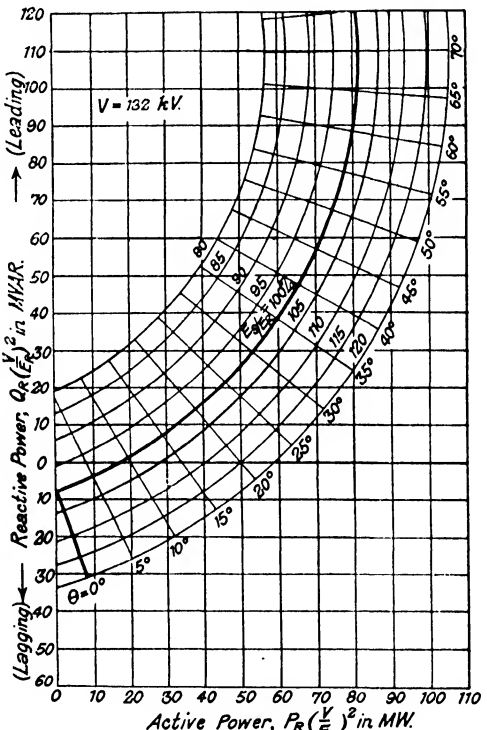

Fig. 22. Universal Receiving-end Chart for a 200-mile 132 kV. Transmission Line based on a Nominal Voltage of 132 kV.

where the power circle crosses the power axis of the diagram. As will be seen from either Fig. 20 or 21, this value is $P_R = 17$ MW. In other words, if the power transmitted to the receiving end be 17 000 kW. and $E_S = E_R = 132$ kV., then the receiving-end power factor will be unity.

(*b*) In this case the required value of P_R is given by the point of intersection of the power circle and the *load line* corresponding to a power factor of 0·9 lagging. From Fig. 21 it is seen that the co-ordinates

of this point are $P_R = 8{\cdot}5$ MW., $Q_R = -4{\cdot}5$ MVAr. In other words, with a load of 8 500 kW. the reactive power required by the line at the receiving end in order that $E_R = E_S = 132$ kV. is 4 500 kVAr. lagging, which amount is supplied by the reactive power component of the load kVA. The net reactive power taken is $(Q - P \tan \phi)$, where Q is the reactive power demand at unity power factor (i.e. the ordinate of the operating point on the power circle) and $P \tan \phi$ is the reactive power component of the load. With $P = 40$ MW., Fig. 21 gives $Q = 17$ MVAr. and $P \tan \phi = -20$ MVAr. The net reactive power demand is, therefore, 37 MVAr. leading.

Example 4. *Investigate the effect of varying the sending-end voltage within a range of* ± 20 *per cent upon the power loss, the transmission efficiency, and the net reactive power taken, for the transmission line of Example* 1, *assuming the power transmitted to be* 50 000 *kW. at unity power factor. Determine also the sending-end voltage which will give a terminal voltage at the receiving end of* 132 *kV. on open circuit.*

Solution. It is necessary to prepare two universal power transmission charts based on the modified power-circle equations (59) and (60). As explained in the preceding section, these charts are really admittance-circle diagrams and thus their scales require to be multiplied by either E_S^2 or E_R^2 in order that they may be used as power-circle diagrams. That is to say, *they are power-circle diagrams which are direct-reading at unity voltage* instead of at E_S or E_R volts. From a practical point of view, however, it is more convenient to make these charts direct-reading at some nominal terminal voltage, say V, rather than at unity voltage. To obtain correct power values from such charts it is then necessary to multiply the scale readings by $(E_S/V)^2$ in the case of the sending-end chart, and by $(E_R/V)^2$ in the case of the receiving-end chart.

In this present example evidently the best value to choose for the nominal voltage is $V = 132$ kV., for then the power scales will be the same as for Example 1, where $E_S = E_R = 132$ kV. Also, as will be seen from equations (59) and (60), the co-ordinates of the power-circle centres are in this case $(-a_r V^2, b_r V^2)$ and $(a_s V^2, -b_s V^2)$, and thus have the same values as in Example 1. The universal charts can therefore be set up directly from the data underlying Fig. 20.

Fig. 22 shows the receiving-end chart, and Fig. 23 the sending-end chart. Each power circle corresponds to a definite terminal voltage

E_S/E_R	P_R	R.E. Chart		Q_R	θ	E_R/E_S	S.E. Chart		P_S	Q_S	P_L	η	Q_L
%	MW.	P	Q	MVAr.	°	%	P	Q	MW.	MVAr.	MW.	%	MVAr.
120	50	50	− 8	− 8	18	83	39	− 5	56·2	− 7·2	6·2	89·0	0·8
115	50	50	0	0	20	87	42	− 0·5	55·5	− 0·7	5·5	90·0	− 0·7
110	50	50	8	8	22	91	46	4·5	55·8	5·5	5·8	89·6	− 2·5
105	50	50	17	17	25	95	53	9·5	58·4	10·4	8·4	85·7	− 6·6
100	50	50	25·5	25·5	28	100	60	14·5	60·0	14·5	10·0	83·3	− 11·0
95	50	50	35·5	35·5	31	105	67·5	20	61·7	18·2	11·7	81·1	− 17·3
90	50	50	46	46	35	111	78·5	25·5	63·6	20·6	13·6	78·5	− 25·4
85	50	50	58·5	58·5	41	118	95	28·5	68·6	20·6	18·6	73·0	− 37·9
80	50	50	74	74	48·5	125	117	28·5	74·9	18·2	24·9	66·8	− 55·8

ratio, the ratios being E_S/E_R in Fig. 22 and E_R/E_S in Fig. 23. The results of the investigation are given in the table on p. 53. The given value of P_R is first converted to its corresponding scale value, viz. $P = P_R(V/E_R)^2$, and the receiving-end chart is entered with this value. A succession of operating points is thus found corresponding to the series of E_S/E_R ratios chosen. For example, the value $E_S/E_R = 120$ per cent gives $Q = -8$ MVAr. and $\theta = 18°$. The reactive power

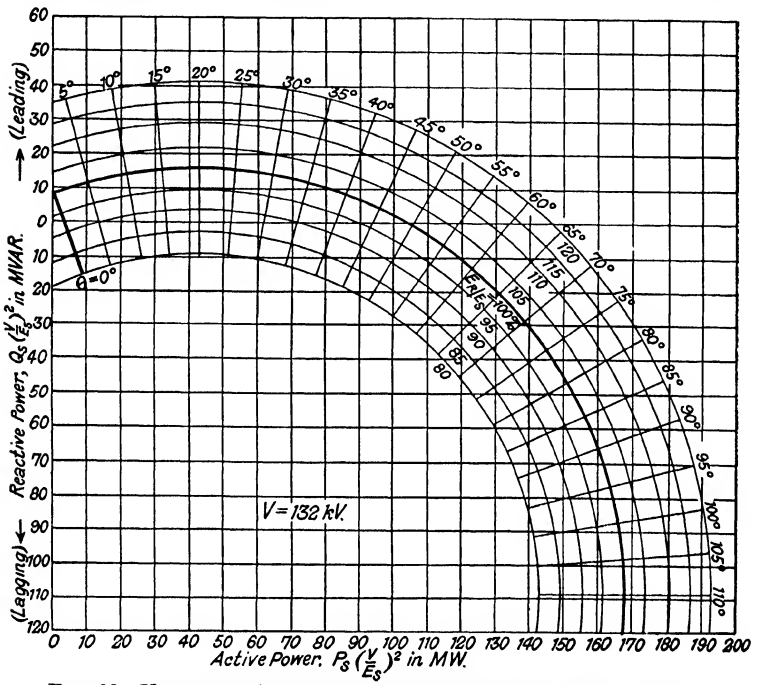

FIG. 23. UNIVERSAL SENDING-END CHART FOR A 200-MILE 132 KV. TRANSMISSION LINE BASED ON A NOMINAL VOLTAGE OF 132 KV.

required at the receiving end is then $Q_R = Q(E_R/V)^2$, which in this case is the same as Q, since $V = 132$ kV. $= E_R$.

For the sending-end chart the inverse voltage ratio is $E_R/E_S = 83$ per cent. Entering the chart along the angle line $\theta = 18°$, the required operating point is found where this line intersects the 83 per cent voltage-ratio circle. For this point one finds $P = 39$ MW. and $Q = -5$ MVAr. in terms of the scale values of the sending-end chart, based on the nominal voltage $V = 132$ kV. On multiplying these values by $(E_S/V)^2$, where E_S is here 120 per cent of E_R, i.e. 158 kV., one finally obtains $P_L = 56{\cdot}2$ MW. and $Q_S = -7{\cdot}2$ MVAr. Hence the power loss is $P_S = 6{\cdot}2$ MW. $= 6\,200$ kW., while the net reactive power taken is $Q_L = [-7{\cdot}2 - (-8)] = 0{\cdot}8$ MVAr. $= 800$ kVAr. lead-

ing. Finally, the transmission efficiency is $\eta = P_R/P_S = (50/56{\cdot}2) = 89$ per cent. The same procedure is followed for the remaining values of the terminal-voltage ratio E_S/E_R.

Referring to Fig. 22, it is seen that the voltage-ratio circle passing through the origin of the receiver chart—the operating point corresponding to open-circuit conditions—is that for $E_S/E_R = 94$ per cent. Hence the sending-end voltage giving 132 kV. on open circuit at the receiving end is $E_S = 0{\cdot}94 \times 132 = 124$ kV. There is thus a $6\frac{1}{2}$ per cent voltage rise along the line under open-circuit conditions—a characteristic transmission phenomenon known as the "Ferranti effect."

References

(1) R. A. Philip: "Economic Limitations to the Aggregation of Power Systems," *Trans. A.I.E.E.*, 1911, Vol. 30, pp. 596–636.

(2) H. B. Dwight: "The Calculation of Constant-voltage Transmission Lines," *Elec. Journal*, 1914, Vol. 11, p. 487.

(3) H. B. Dwight: "Electrical Characteristics of Transmission Systems," *Trans. A.I.E.E.*, 1922, Vol. 41, p. 781.

(4) R. D. Evans and H. K. Sels: "Transmission Line Circuit Constants and Resonance," *Elec. Journal*, 1921, Vol. 18, p. 306; "Transmission Lines and Transformers," *ibid.*, p. 356; "Circle Diagrams for Transmission Systems," *ibid.*, p. 530; and *ibid.*, 1922, Vol. 19, p. 53.

(5) L. Thielemans: "Calculs, diagrammes et régulation des lignes de transport d'énergie à longue distance," *Revue générale de l'électricité*, 1920, Vol. 7, pp. 403, 435, 475, and 515; and *ibid.*, 1921, Vol. 9, pp. 451, 599, 675, 878, and 929.

(6) C. L. Fortescue and C. F. Wagner: "Some Theoretical Considerations of Power Transmission," *Trans. A.I.E.E.*, 1924, Vol. 43, p. 16.

(7) F. E. Terman: "The Circle Diagram of a Transmission Network," *Trans. A.I.E.E.*, 1926, Vol. 45, pp. 1081–92.

(8) *Cf.* M. G. Say: *The Performance and Design of A.C. Machines*, Ch. XVII, Eqns. (158) and (159), p. 426 (Pitman, London, 1948).

(9) F. E. Terman: "The General Circle Diagram of Electrical Machinery," *Trans. A.I.E.E.*, 1930, Vol. 49, p. 376.

(10) For an excellent treatment of the orthodox method of establishing the power-circle diagram *vide* H. Waddicor: *The Principles of Electric Power Transmission* (4th Edn.), Ch. VIII, pp. 168–80 (Chapman & Hall, London, 1939).

(11) *Cf.* P. D. Morgan and S. Whitehead: "The Impedance and Power Losses of Overhead Lines," *Journ. I.E.E.*, 1930, Vol. 68, pp. 390–2 and 404–6.

(12) *Vide* H. Rissik: "Transmission Line Analysis," *Electrician*, 1938, Vol. 120, p. 539.

CHAPTER III

THE POWER LIMITS OF A SYNCHRONOUS INTERCONNECTOR

In the case of electrical machines and apparatus the criterion of limiting power is intimately bound up with mechanical and thermal considerations and, in general, is in no way determined by purely electrical, i.e. circuit, characteristics. On the other hand, in the case where a synchronous generator supplies power to, say, a static impedance load of variable magnitude, the criterion of limiting power is essentially of an electrical character. For, assuming the generator excitation and the load power factor both to be maintained constant, the power supplied to the load by the synchronous machine will be a function of its terminal voltage as well as of the load current. But the former depends upon the latter, in virtue of the finite impedance of the machine; so that the operative variable is the load current, which in turn depends on the machine voltage and the magnitude of the impedance load. Here the criterion of limiting power is a relatively simple one. In fact, and as is well known, it is that the load impedance should equal the internal impedance of the synchronous machine.[1] In the last analysis, therefore, although it is the load itself which determines the power supplied by the machine, the power limit is determined by the electrical characteristics of the machine.

It is clear that in the simple asynchronous power transmission system considered above the conception of maximum power, or a power limit, is not associated with a possible loss of synchronism. For there is obviously no question of synchronism being lost by a system containing only a single synchronous machine. On the other hand, when considering transmission systems of a synchronous character, in which the power transmitted is mainly a function of the angular displacement between two synchronous but otherwise independent voltages, the maximum value of transmitted power is reached with the final breakdown of the system, when the synchronous machines fall out of step. That is to say, the criterion of maximum or limiting power here is that synchronism should finally be lost

when the displacement angle between the terminal voltages of the system exceeds a certain critical value.*

The Maximum-power Concept. When considering power system interconnection in general, it is necessary to distinguish between three possible values of the maximum power transmitted (or *power limit*, as it is more commonly termed) namely—

1. The power limit of the interconnector alone, i.e. the steady-state stability limit of a transmission link between two infinite buses,† which is a function of the interconnector impedance. In practice this limit is applicable in the case of two metropolitan supply systems, each having a large installed capacity, connected by a tie line.

2. The power limit of the transmission system as a whole—that is, taking into account the limiting effect of the synchronous machines at each end of the interconnector—when the system load is increased very slowly, and the machine terminal voltages are maintained constant by regulator action. This is termed the *steady-state stability limit* of the transmission system, and is a function of the impedances of the synchronous machines as well as of the interconnector.

3. The power limit of the system during sudden changes in load or upon the incidence of a disturbance, when the air-gap voltages of the machines remain sensibly constant. This is known as the *transient stability limit*, and is a function of the machine inertias as well as of the system impedances.

In Case 1, with which the present chapter is concerned,‡ the existence of a power limit is most easily demonstrated by means of the fundamental power-circle diagram—in particular, the receiving-end power chart. Its construction is based on the equivalent network of the interconnector in its most general form, that is to say, including sending-end and receiving-end

* This particular criterion of limiting power is the so-called *steady-state stability* criterion, and is defined by $(dP/d\theta) = 0$, from which condition the critical value of θ, and thus the corresponding *power limit* P_M, may be determined. The general question of steady-state stability is discussed in Chapter IV.

† By the term "infinite bus" is understood a point at which the voltage is constant in magnitude, phase, and frequency and is independent of the active and reactive power flowing past the point. This condition is approached when the capacity of the synchronous plant connected to the point is extremely large in comparison with the power flow under consideration. From the point of view of power system stability an infinite bus may be represented by a synchronous machine of zero impedance and infinite inertia.

‡ Cases 2 and 3 are discussed in Chapters IV and V respectively.

terminal transformers. Equations (23) or (24) may be used to find the constants of this equivalent network. Considering the typical circle diagram of Fig. 24, for example, representing the relation between active power P and reactive power Q transmitted by an interconnector whose terminal voltages are E_S and E_R, the maximum value of transmitted power (P_M) is defined by the operating point M, i.e. the point lying on the appropriate power circle, farthest away from the Q-axis.*

In other words, *the power limit is represented in the circle diagram by the abscissa of the vertical tangent to the power circle,* because any power value greater than this, since it is represented by a point lying outside the power circle, does not correspond to a possible operating condition, based upon the given terminal voltages which determine the size of the power circle and its position in the P-Q diagram. However, as the power-circle radius is proportional to the product of these voltages, a little consideration will show that the power limit can be raised by increasing the sending-end voltage E_S or the receiving-end voltage E_R, or both.

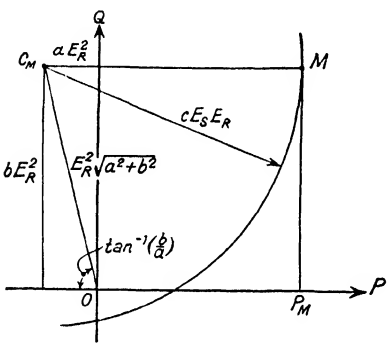

FIG. 24. THE CIRCLE DIAGRAM FOR TRANSMITTED POWER

Referring to the circle diagram in Fig. 24, the equation to the power circle is—

$$(P + aE_R^2)^2 + (Q - bE_R^2)^2 = (cE_SE_R)^2 \quad . \quad . \quad (61)$$

Here the co-ordinates of the centre are $-aE_R^2$ MW. and $+bE_R^2$ MVAr., and the circle radius is cE_SE_R MVA. where E_S and E_R are line pressures expressed in kV., and a, b, and c are circuit constants defined by—

* As mentioned in Chapter II, the term "transmitted power" is synonymous with "receiving-end power." The former term, however, is used throughout the present chapter as the sending end of the interconnector is of no particular interest where power limits are concerned. For the same reason the circle diagram is drawn, and referred, simply to $P - Q$, rather than to $P_R - Q_R$ co-ordinates.

$$-a + jb = -\frac{\mathbf{A}}{\mathbf{B}} = -\frac{A}{B}\underline{|(\alpha - \beta)} = \frac{A}{B}\underline{|(\pi + \alpha - \beta)}$$

$$= -\frac{A}{B}\cos(\beta - \alpha) + j\frac{A}{B}\sin(\beta - \alpha) \quad . \quad . \quad (62a)$$

$$= -\left(\frac{A_1B_1 + A_2B_2}{B_1^2 + B_2^2}\right) + j\left(\frac{A_1B_2 - A_2B_1}{B_1^2 + B_2^2}\right) \quad . \quad (62b)$$

and $$c = \frac{1}{B} = \frac{1}{\sqrt{(B_1^2 + B_2^2)}} \quad . \quad . \quad . \quad . \quad (63)$$

where $\mathbf{A} = A\,\underline{|\alpha} = A_1 + jA_2$ and $\mathbf{B} = B\,\underline{|\beta} = B_1 + jB_2$ are the appropriate constants of the equivalent network.

From the circle diagram it is seen by inspection that the maximum value of transmitted power, given by the abscissa of the vertical tangent at M is—

$$P_M = cE_SE_R - aE_R^2 \quad . \quad . \quad . \quad (64)$$

while the amount of reactive power which must be drawn over the interconnector in order that the transmitted power may reach this maximum value, under the given terminal voltage conditions, is similarly seen to be—

$$Q_M = bE_R^2 \quad . \quad . \quad . \quad . \quad . \quad (65)$$

The above relations may be established formally by considering the limiting power criterion—the transmitted power cannot exceed that value which corresponds to the operating point lying on the vertical tangent to the power circle. This point is defined by the condition $(dP/dQ) = 0$. Differentiation of equation (61) with respect to Q gives—

$$2(P + aE_R^2)\frac{dP}{dQ} + 2(Q - bE_R^2) = 0$$

which, with $dP/dQ = 0$, becomes $Q = bE_R^2$ as given by equation (65). Substitution of this limiting value of Q in equation (61) then gives $P = cE_SE_R - aE_R^2$ for the limiting power. As is to be expected, this is the relation of equation (64).

Equation (64) is thus the *power-limit equation* of the interconnector, expressing the relation between the limiting transmitted power, and the voltages at the sending and receiving ends. When determining the power limit of an interconnector this fundamental equation must be considered

in the light of three possible conditions of power transmission, viz. constant receiving-end voltage, equal sending- and receiving-end voltages, and constant sending-end voltage.

CASE 1 (E_R = constant). Here equation (64) becomes

$$P_M = k_1 E_S - k_2 \quad . \quad . \quad . \quad (66)$$

where k_1 and k_2 are constants. In this case, therefore, the limiting transmitted power is a linear function of the sending-end voltage E_S and is restricted only by the maximum possible value of this voltage. Moreover, the co-ordinates of the several

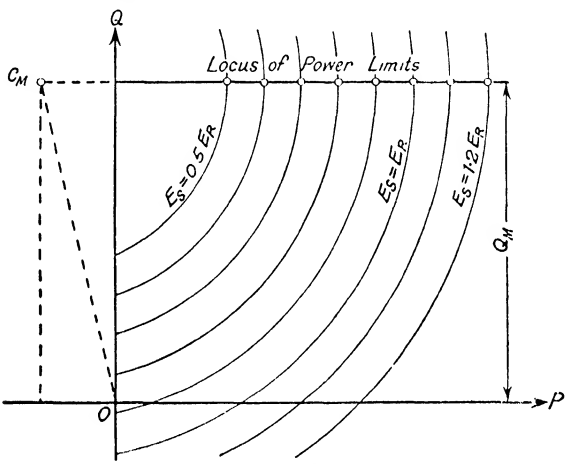

FIG. 25. POWER-CIRCLE DIAGRAM FOR CONSTANT E_R

power-circle centres are constant, so that the power circles are concentric, while their radii are directly proportional to E_S. Furthermore, it is seen from equation (65) that Q_M is constant. Hence the power-limit locus is the straight line passing through the common centre of the power circles and parallel to the P axis. The power-circle diagram for this condition of operation is shown in Fig. 25.

CASE 2 ($E_S = E_R = E$). Equation (64) becomes in this case

$$P_M = (c - a)\, E^2 \quad . \quad . \quad . \quad (67)$$

Hence with equal sending- and receiving-end voltages the power limit of an interconnector is directly proportional to the square of the transmission voltage. Also, the co-ordinates of the power-circle centres and the radii of the power circles both

vary as the square of the terminal voltage E. Hence the locus of the power-circle centres is the straight line making the angle $\tan^{-1}(b/a)$ with the negative P-axis and passing through the origin of the circle diagram, as shown in Fig. 26. The distance of any centre from the origin is then $E^2\sqrt{(a^2 + b^2)}$ MVA.

Referring to equation (65), it is seen that in this case

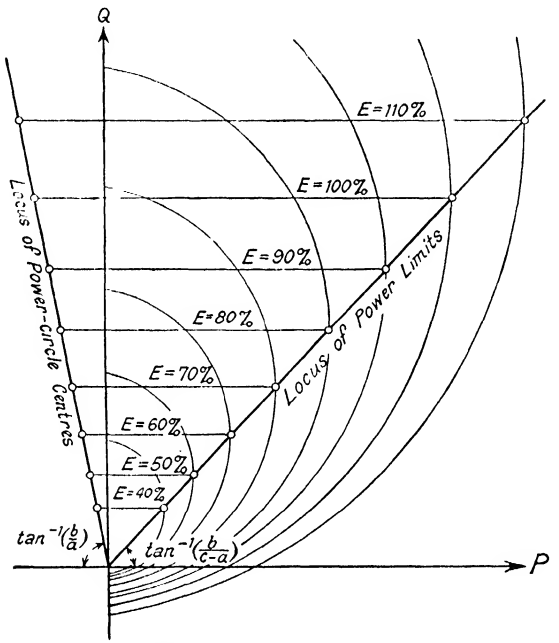

FIG. 26. POWER-CIRCLE DIAGRAM FOR $E_S = E_R = E$

$Q_M = bE^2$. This relation, in conjunction with equation (67), then gives

$$P_M = \frac{c - a}{b} Q_M \quad . \quad . \quad . \quad (68)$$

as the equation to the power-limit locus, i.e. the locus of the points on the several power circles corresponding to maximum transmitted power. Equation (68) represents a straight line in the first quadrant passing through the origin, as shown in Fig. 26.

CASE 3 (E_S = constant). In this case equation (64) becomes

$$P_M = a\,[k^2 - (k - E_R)^2] \quad . \quad . \quad . \quad (69)$$

where $k = (c/2a)\, E_S$. It is at once seen from this equation that P_M is zero when E_R is either zero or equal to $2k$. Hence there must be some value of E_R intermediate between 0 and $2k$ for which P_M reaches a finite maximum value. This unique value of E_R is thus determined by the condition that

$$dP_M/dE_R = -\,2a\,(k - E_R) = 0$$

which gives $E_R = k$. Denoting this critical value of receiving-end voltage by E_U, we have—

$$E_U = \frac{c}{2a}\, E_S \qquad . \qquad . \qquad . \qquad . \quad (70)$$

On substituting $E_R = k$ in equation (69), one finds for the maximum value of the power limit—

$$P_U = ak^2 = \frac{c^2}{4a}\, E_S \qquad . \qquad . \qquad . \quad (71a)$$

This is the so-called *ultimate power limit* of the interconnector. The corresponding value of reactive power, required in order that this limit may be reached, is found from equation (65) to be—

$$Q_U = bk^2 = \frac{bc^2}{4a^2}\, E_S{}^2 \qquad . \qquad . \qquad . \quad (71b)$$

The existence of an ultimate power limit, having a finite value given by equation (71*a*), is also clear from a consideration of the power-circle diagram for constant sending-end voltage, shown in Fig. 27. For the co-ordinates of the power-circle centres are proportional to $E_R{}^2$, while the radii are proportional to E_R. The power circles are thus eccentric, their centres lying on an axis through the origin, making the angle $\tan^{-1}(b/a)$ with the negative P-axis. Beyond a certain value of E_R—the critical value E_U—the abscissa of the power-circle centre ($-\,aE_R{}^2$) increases more rapidly than the circle radius (cE_SE_R), so that the value of P_M begins to decrease.

The Power-limit Parabola. In Cases 1 and 2, considered above, the locus of maximum power in the circle diagram is a straight line, either parallel to the P-axis or passing through the origin at an angle to that axis. On the other hand, in Case 3 the power-limit locus is a parabola lying in the first and second quadrants of the power-circle diagram.

The equation to this parabolic locus is found by eliminating E_R between equations (65) and (69), which gives—

$$(bP_M + aQ_M)^2 = bc^2E_S^2Q_M \quad . \quad . \quad . \quad (72)$$

The above equation may be put in the form

$$(P_M \sin \psi + Q_M \cos \psi)^2 = 2R \sin \psi \, . \, Q_M, \quad . \quad (72a)$$

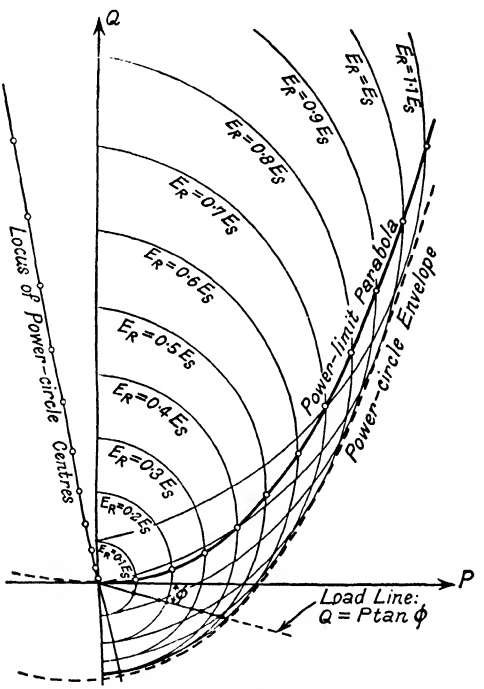

FIG. 27. POWER-CIRCLE DIAGRAM FOR CONSTANT E_S

where $\tan \psi = b/a$ and $R = c^2E_S^2/2\sqrt{(a^2 + b^2)}$. Equation (72*a*) represents a parabola whose axis is inclined at an angle ψ to the negative P-axis, i.e. is parallel to the line of power-circle centres, and crosses the Q-axis at the point $Q = R \sin \psi$. Fig. 28 shows this power-limit locus to scale, the extent of the usual power-circle diagram being indicated by the dotted rectangle. A typical power circle is that for $E_R = E_S$, whose centre is shown at C_M. As may be seen from the diagram, for this circle P_M is given by OL, and Q_M by LM.

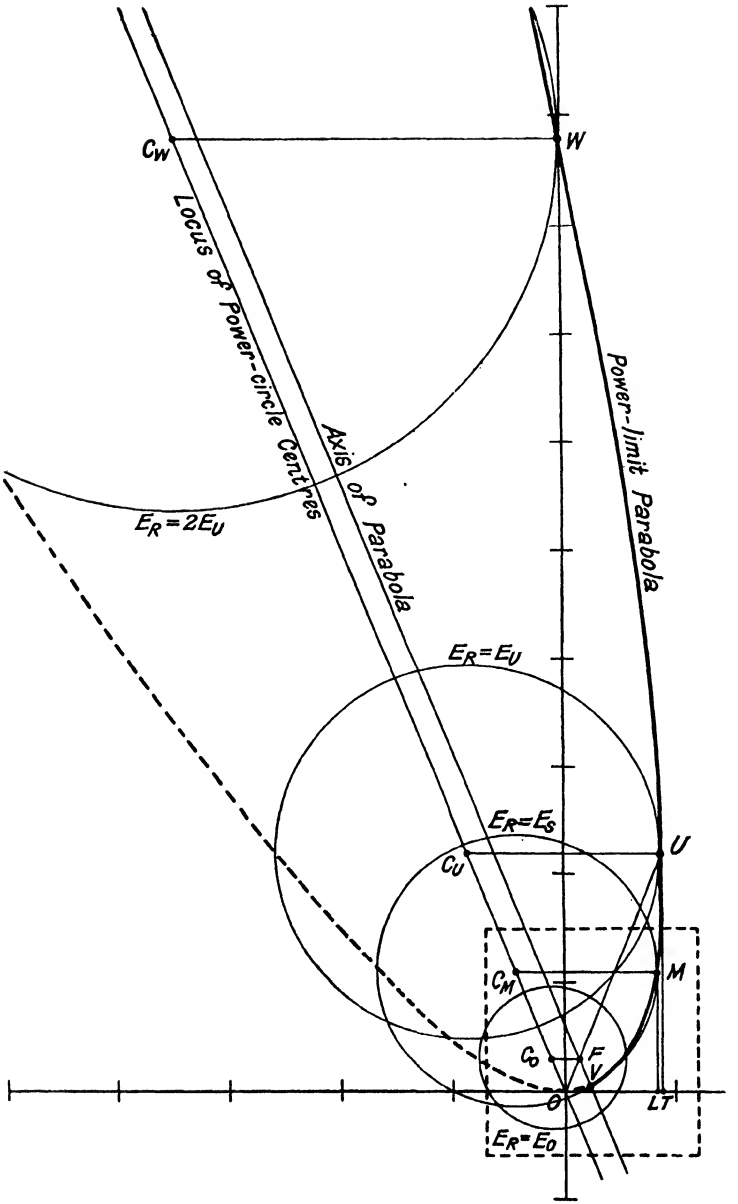

FIG. 28. THE PARABOLIC LOCUS OF MAXIMUM POWER

The power circle corresponding to the critical value of receiving-end voltage, $E_R = E_U$, is shown with centre at C_U, U being the operating point corresponding to the ultimate power limit. Hence $P_U = OT = \frac{1}{2}C_U U$, since $C_U U = cE_S E_U = (c^2 E_S^2/2a)$; also $Q_U = TU$. The power-limit parabola touches the P-axis at the origin and crosses the Q-axis at the point W, where $OW = 4Q_U$. This value of the ordinate at W is at once obtained by putting $P_M = 0$ in equation (72), for this gives either $Q_M = 0$ or $Q_M = (bc^2 E_S^2/a^2)$. The power circle passing through W must consequently be that for $E_R = 2E_U$, in order that its radius $C_W W$ may be $4(\frac{1}{2}C_U U) = 4P_U = 2cE_S E_U$.

The form of locus equation given by equation (72a) is, however, more convenient to use in practice in that it leads at once to a relatively simple geometrical construction of the parabolic power-limit locus. This construction makes use of two well-known properties of the parabola, viz. that the length of the subnormal is constant and equal to half the latus rectum, and that the two ends of the normal to the parabola at any point are equidistant from the focus. Referring to Fig. 29, OC_U is the line of power-circle centres, making the angle $\psi = \tan^{-1}(b/a)$ with the negative P-axis. Make $OC = R$, and draw CD parallel to the P-axis meeting the Q-axis at D. Then $OD = R \sin \psi$, so that the axis of the parabola is the parallel to OCC_U passing through D. At E, where $OD = DE$, draw EY parallel to the P-axis and intersecting OY, perpendicular to the line of centres, at Y. Through Y draw WZ parallel to the line of centres, meeting the Q-axis at W and the P-axis at Z. Then, since $OE = 2R \sin \psi$, we have $OY = 2R \tan \psi$ and thus—

$$OW = \frac{2R \tan \psi}{\cos \psi} = \frac{c^2 E_S^2}{\sqrt{(a^2 + b^2)}} \cdot \frac{b}{a} \cdot \frac{\sqrt{(a^2 + b^2)}}{a} = \frac{bc^2 E_S^2}{a^2} = 4Q_U$$

Hence W is the point where the parabola crosses the Q-axis (see Fig. 28).

To find the point U of Fig. 28, bisect WZ at X and join OX. Then U is the mid-point of OX. For the ordinate TU is one-quarter of OW, and is thus equal to Q_U. Similarly, the abscissa OT is one-quarter of OZ, and is hence equal to P_U, since

$$OZ = \frac{2R \tan \psi}{\sin \psi} = \frac{2R}{\cos \psi} = \frac{c^2 E_S^2}{\sqrt{(a^2 + b^2)}} \cdot \frac{\sqrt{(a^2 + b^2)}}{a} = \frac{c^2 E_S^2}{a} = 4P_U$$

To construct the parabola it is first of all necessary to locate the focus. Its position is given by F, the point where OX intersects the axis of the parabola. For F is the mid point of DG, since DG and WZ are parallel, and hence ODG and OWZ are similar triangles. Consequently $OF = DF = \frac{1}{2}R$, since

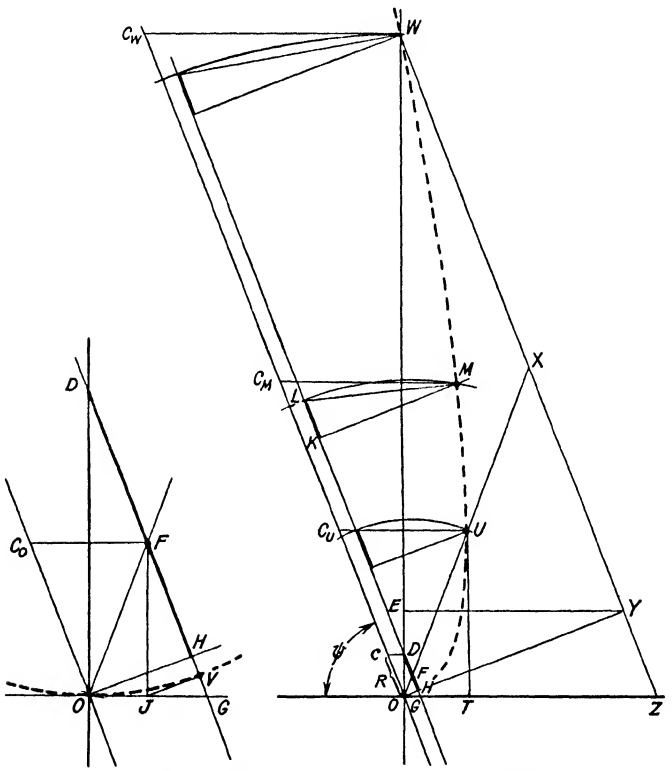

FIG. 29. GEOMETRY OF THE POWER-LIMIT PARABOLA

$DG = CO = R$. But DO is the normal to the parabola at the point O. Hence F must be the focus. The subnormal at O is $DH = (DO) \times \sin\psi = R\sin^2\psi$, and for all other points on the parabola it has this same value. Hence a point M, say, on the parabola may be found by taking any point K on the axis, making the intercept KL equal to DH, and drawing an arc with centre at F and radius FL to meet the perpendicular at K in the point M. Then LM is the normal to the parabola at

M, while $C_M M$, drawn parallel to the P-axis, is the radius of the power circle for which M is the "limiting" operating point.

The vertex of the power-limit parabola is located at V where $FV = \frac{1}{2}R \sin^2 \psi$.* Referring to the inset diagram of Fig. 29 it is seen that V must then be the mid point of HG. For

$$FJ = \tfrac{1}{2}(DO) = \tfrac{1}{2}R \sin \psi,$$

so that

$$FV = (FJ) \times \sin \psi = \tfrac{1}{2}R \sin^2 \psi.$$

But FJ bisects OG at J, since F is the mid point of DG. Similarly, JV must bisect HG at V.

The parallel to the P-axis through F meets the line of centres in C_0, where $OC_0 = \frac{1}{2}(OC) = \frac{1}{2}R$. The point C_0 is consequently the centre of the particular power circle whose radius is equal to R. That this must be so is clear from consideration of the relation between the radius of any power circle and the distance of its centre from the origin. If E_R be the receiving-end voltage corresponding to the power circle in Fig. 29 having C_M for its centre, then $OC_M = E_R{}^2\sqrt{(a^2 + b^2)}$ and $C_M M = cE_S E_R$. Hence

$$OC_M = (CM_M)^2 \times \frac{\sqrt{(a^2 + b^2)}}{c^2 E_S{}^2} = (C_M M)^2 \times \frac{1}{2R}$$

Thus the radius of the power circle whose centre is C_0 must be $\sqrt{(2R \times OC_0)} = \sqrt{(2R \times \frac{1}{2}R)} = R$. If E_0 be the value of the receiving-end voltage to which this power circle relates, then $cE_S E_0 = R$, so that

$$E_0 = \frac{R}{cE_S} = \frac{cE_S}{2\sqrt{(a^2 + b^2)}} = E_U \cos \psi \,. \qquad (73)$$

This particular power circle also is shown in Fig. 28.

Regulated and Unregulated Interconnectors. The power-circle diagram of Fig. 27 clearly shows that a given amount of power P can be transmitted over an interconnector under different receiving-end conditions. The ordinate for a given P cuts many power circles, each of which corresponds to a particular value of E_R, and becomes a tangent to the one circle for which $E_R = \sqrt{(P/a)}$, when P represents the maximum power (P_M) that can be transmitted at that voltage.† These

* In the parabola $y^2 = 4ax$ the latus rectum is $4a$, the subnormal is $2a$, and the distance from the focus to the vertex is a.

† It should be noted here that each power circle, except the limiting one for which $P = P_M$, is intersected twice by the ordinate at P. As explained in Chapter IV, however, the upper point of intersection (i.e. that for which $Q > Q_M$) corresponds to an unstable operating condition and in consequence need not be considered.

several points of intersection are characterized by differing values of the reactive power demand Q.

In the same way the amount of power P that can be transmitted at a given value of E_R depends on the reactive power Q available at the receiving-end, since the operating point (P, Q) must lie on the power circle. This property of the power circle is made use of in so-called regulated systems of power transmission by power-factor control of the receiving-end voltage under conditions of varying system load. The almost universal form in which this method of voltage control occurs in practice is that where synchronous phase modifiers at the receiving end are used to adjust Q in accordance with P so that the operating point (P, Q) remains on the power circle defined by the given values of E_S and E_R.[2] It will be observed from the power-circle diagram that this method of voltage control necessitates a very rapid increase in synchronous phase-modifier capacity when the transmitted power approaches the limiting value for the given voltage conditions. For one finds from the power-circle equation (61) that

$$\frac{dQ}{dP} = \frac{P + aE_R^2}{\sqrt{[c^2E_S^2E_R^2 - (P + aE_R^2)^2]}}$$

which becomes infinite when $P = (cE_SE_R - aE_R^2) = P_M$.

As for the power limit of such a regulated transmission system, it is implicit in the criterion of limiting power established in the preceding section that sufficient reactive power be available at the receiving end to enable the power limit P_M to be reached. In other words, *the power-limit parabola is based on the assumption of virtually unlimited synchronous phase-modifier capacity at the receiving end* and represents, in effect, one extreme condition of operation—the regime of "regulated interconnection." The other extreme is represented by the converse regime of "unregulated interconnection," which is based on the assumption that the reactive power available at the receiving end is determined solely by the power factor of the load.[3]

In the case of an unregulated interconnector, therefore, the power locus is perforce represented in the circle diagram of Fig. 27 by the "load line" whose equation is $Q = P \tan \phi$, where ϕ is the power-factor angle of the load.* On substituting

* Following the usual convention, ϕ is negative for lagging and positive for leading power factors. The load line of Fig. 27 thus represents a varying load of constant lagging power factor equal to $\cos \phi$.

this value of Q in the power-circle equation (61) one obtains for the basic power relation of the unregulated interconnector—

$$(P + aE_R^2)^2 + (P \tan \phi - bE_R^2)^2 = c^2E_S^2E_R^2$$

which, after some transformation, reduces to—

$$[P \sec \phi + (a \cos \phi - b \sin \phi) E_R^2]^2 + (a \sin \phi + b \cos \phi)^2E_R^2 = c^2E_S^2E_R^2 \quad . \quad (74)$$

The condition for maximum transmitted power may be found by differentiating equation (74) with respect to E_R and putting $dP/dE_R = 0$ in the derived equation, which gives—

$$P \sec \phi + (a \cos \phi - b \sin \phi)E_R^2 = \frac{c^2E_S^2 - 2\,(a \sin \phi + b \cos \phi)^2E_R^2}{2\,(a \cos \phi - b \sin \phi)} \quad . \quad (75)$$

Eliminating P between equations (74) and (75) then gives the particular value of E_R corresponding to the power limit of the unregulated interconnector. Denoting this limiting value by E_E, one obtains—

$$E_E = \sqrt{\left[\frac{\sqrt{(a^2 + b^2)} - a \cos \phi + b \sin \phi)}{2\sqrt{(a^2 + b^2)} \,.\, (a \sin \phi + b \cos \phi)^2}\right]} \,.\, cE_S \quad . \quad (76)$$

which, on substitution in either equations (74) or (75), finally gives the power limit of the unregulated interconnector as—

$$P_E = \frac{\cos \phi\,(\sqrt{(a^2 + b^2)} - a \cos \phi + b \sin \phi)}{2\,(a \sin \phi + b \cos \phi)^2} c^2E_S^2 \quad . \quad (77)$$

$$= E_E^2\sqrt{(a^2 + b^2)} \,.\, \cos \phi \quad . \quad . \quad . \quad . \quad . \quad (77a)$$

In the special case of a unity power factor load, for which $\phi = 0$, equations (77) and (77a) become—

$$P_E = \frac{\sqrt{(a^2 + b^2)} - a}{2b^2} c^2E_S^2 \quad . \quad . \quad . \quad . \quad . \quad (78)$$

$$= E_E^2\sqrt{(a^2 + b^2)} \quad . \quad . \quad . \quad . \quad . \quad . \quad (78a)$$

Another special case of interest is that for which $\phi = \tan^{-1}(b/a)$, when equation (76) becomes—

$$E_E = \frac{c}{2a} E_S = E_U \quad . \quad . \quad . \quad . \quad . \quad . \quad . \quad (79)$$

and equation (77*a*) consequently gives for the power limit—

$$P_R = aE_U^2 = P_U \quad . \quad . \quad . \quad (80)$$

This result is to be expected, since the load line which passes through the operating point corresponding to the ultimate power limit of the interconnector must have the slope—

$$\tan \phi = \frac{Q_U}{P_U} = \frac{bE_U^2}{aE_U^2} = \frac{b}{a}$$

The Power-circle Envelope. It will be observed from Fig. 27, relating to the case of constant sending-end voltage, that a curve can be drawn which is a tangent to all the power circles. This curve, known as the *power-circle envelope*, actually represents the boundary of the power-circle diagram. A power P, transmitted over the interconnector to a load of power factor $\cos \phi$, is represented in the diagram by a point whose co-ordinates are $(P, P \tan \phi)$. If this point falls inside the envelope, then two power circles can be drawn which will intersect at that point. In other words, for any operating point within the power-circle envelope there are two values of E_R which will satisfy the given conditions of transmitted power P, load power factor $\cos \phi$, and sending-end voltage E_S, i.e. which will satisfy equation (74). For an operating point on the envelope, only one value of E_R will satisfy the given conditions, namely, that corresponding to the power circle to which the envelope is a tangent at that point. Finally, in the case of a point lying outside the envelope, there is no value of E_R, which will satisfy the given conditions of power transmission. That is to say, such a point represents an imaginary operating condition.

For an unregulated interconnector, therefore, the limiting transmitted power is evidently the abscissa of the point of intersection of the load line and the power-circle envelope, because there is no value of receiving-end voltage that will yield an operating point lying on the load line and, at the same time, corresponding to a transmitted power in excess of this limiting value. Hence the value of E_R corresponding to the *envelope power limit*—as the above limiting value of transmitted power is termed—is determined by the radius of the power circle to which the envelope is a tangent at the point where it is intersected by the load line.

To find the equation of the power-circle envelope, resort

must be had to the following well-known theorem in the differential calculus: If a series of curves represents the loci of a function having a certain parameter which determines the consecutive loci, then the envelope of the curves represents a derived function whose equation is obtained by differentiating the equation of the original function with respect to that parameter, and eliminating the parameter between the resulting and original equations. In the present case, therefore, it is necessary to differentiate the fundamental power-circle equation with respect to the parameter E_R, and then to eliminate E_R between this derived equation and the original power-circle equation. The resulting equation, expressing the relation between P and Q in terms of E_S and the auxiliary network constants a, b, and c, is then the equation of the power-circle envelope.

The fundamental power-circle relation expressed by equation (61) may be put in the more convenient form—

$$P^2 + Q^2 + (a^2 + b^2)\,E_R^4 = 2\sqrt{(a^2 + b^2)}\,.\,(R - P\cos\psi + Q\sin\psi)\,E_R^2 \quad . \quad (81)$$

where, as before, $R = c^2E_S^2/2\sqrt{(a^2 + b^2)}$ and $\tan\psi = b/a$. Differentiation of equation (81) with respect to E_R gives—

$$4\,(a^2 + b^2)\,E_R^3 = 4\,\sqrt{(a^2 + b^2)}\,.\,(R - P\cos\psi + Q\sin\psi)\,E_R$$

i.e.
$$R - P\cos\psi + Q\sin\psi = E_R^2\,\sqrt{(a^2 + b^2)} \quad . \quad (82)$$

On eliminating E_R between (81) and (82) one then obtains—

$$P^2 + Q^2 = (R - P\cos\psi + Q\sin\psi)^2 \quad . \quad . \quad (83)$$

as the equation of the power-circle envelope. Equation (83) represents a parabola whose focus is the origin of the power-circle diagram, whose axis is the line of power-circle centres (making the angle ψ with the negative P-axis), and whose vertex is distant $\frac{1}{2}R$ from the focus.* Furthermore, the value of E_R determining the power circle to which the envelope is a tangent at any given point (P, Q) is given by equation (82) or,

* If $\psi = 0$, for example, the envelope equation becomes simply—

$$P^2 + Q^2 = (R - P)^2$$

i.e.
$$Q^2 = 4(\tfrac{1}{2}R)(\tfrac{1}{2}R - P)$$

which is of the form $y^2 = 4a(a - x)$. This latter equation represents a parabola about the x-axis whose focus coincides with the origin of co-ordinates and whose vertex coincides with the point on the x-axis for which $x = a$.

more conveniently, by eliminating R between equations (82) and (83), which gives—

$$E_R = \sqrt[4]{\frac{P^2 + Q^2}{a^2 + b^2}} \quad . \quad . \quad . \quad . \quad (84)$$

In the case of a regulated interconnector, where unlimited synchronous phase-modifier capacity is assumed, the operative power limit is the *ultimate power limit* (P_U) of the interconnector. A little consideration will show that it is represented on the power-circle envelope by the point where it is met by the tangent parallel to the Q-axis, its value being given by the abscissa of this point, defined by the condition $(dP/dQ) = 0$. Differentiation of equation (83) with respect to Q gives—

$$2P\frac{dP}{dQ} + 2Q = 2\,(R - P\cos\psi + Q\sin\psi)\left(\sin\psi - \cos\psi\frac{dP}{dQ}\right)$$

On putting $\dfrac{dP}{dQ} = 0$ in the above expression, one obtains—

$$Q = \sin\psi\,(R - P\cos\psi + Q\sin\psi) = \sqrt{(P^2 + Q^2)}\sin\psi$$
$$= P\tan\psi \text{ which reduces to } Q.$$

Hence $Q_U = P_U\tan\psi$ is a condition determining the ultimate power limit. In other words, the operating point in the power-circle diagram corresponding to this limit lies on the load line whose slope is $\tan\psi = (b/a)$. On substituting $P_U\tan\psi$ for Q_U in the power-circle envelope equation (83), one obtains, finally—

$$P_U\sec\psi = R - P_U\cos\psi + P_U\sin\psi\tan\psi$$

i.e. $$P_U\,(1 + \cos^2\psi - \sin^2\psi) = R\cos\psi$$

or $$P_U = \frac{R}{2\cos\psi} = \frac{c^2E_s^2}{2\sqrt{(a^2 + b^2)}}\cdot\frac{\sqrt{(a^2 + b^2)}}{2a} = \frac{c^2}{4a}E_s^2$$

as the ultimate value of the limiting transmitted power under conditions of varying E_R and constant E_s. As is to be expected, the above result is identical with equation (71a). The critical value of receiving-end voltage E_U corresponding to this ultimate power limit is found from equation (84) to be—

$$E_U = \sqrt[4]{\frac{P_U^2\,(1 + \tan^2\psi)}{a^2 + b^2}} = \sqrt[4]{\left(\frac{P_U^2}{a^2 + b^2}\cdot\frac{a^2 + b^2}{a^2}\right)} = \sqrt{\frac{P_U}{a}}$$
$$= \sqrt{\left(\frac{c^2}{4a^2}E_s^2\right)} = \frac{c}{2a}E_s$$

a result which, in turn, is identical with equation (70).

In the case of the unregulated interconnector, where the reactive power available at the receiving end is determined by the load power factor $\cos\phi$, the operative power limit is the *envelope power limit* (P_E), already defined as the value of transmitted power given by the abscissa of the point where the load line intersects the power-circle envelope. This limit is accordingly to be evaluated by putting $Q_E = P_E \tan\phi$ in the equation of the power-circle envelope (83). The substitution gives—

$$P_E \sec\phi = R - P_E \cos\psi + P_E \tan\phi \sin\psi$$

i.e. $$P_E (1 + \cos\psi \cos\phi - \sin\psi \sin\phi) = R \cos\phi$$

from which

$$P_E = \frac{R\cos\phi}{1 + \cos(\psi + \phi)} \qquad . \quad . \quad . \quad . \quad . \quad (85)$$

$$= \frac{c^2 E_S^2}{2\sqrt{(a^2 + b^2)}} \cdot \frac{\cos\phi \sqrt{(a^2 + b^2)}}{\sqrt{(a^2 + b^2)} + a\cos\phi - b\sin\phi}$$

$$= \frac{\cos\phi (\sqrt{(a^2 + b^2)} - a\cos\phi + b\sin\phi)}{2(a\sin\phi + b\cos\phi)^2} c^2 E_S^2 \quad (85a)$$

Here again, this result is the same as (77), which was obtained from the basic power relation (74) of the unregulated interconnector.

Referring to the envelope equation (83), the point where the power-circle envelope crosses the P-axis may be found by putting $Q = 0$ in the equation. The abscissa of this point is accordingly given by the relation $P = (R - P\cos\psi)$, from which—

$$P = \frac{R}{1 + \cos\psi} \qquad . \quad . \quad . \quad . \quad . \quad (86)$$

$$= \frac{c^2 E_S^2}{2\sqrt{(a^2 + b^2)}} \cdot \frac{\sqrt{(a^2 + b^2)}}{\sqrt{(a^2 + b^2)} + a}$$

$$= \frac{\sqrt{(a^2 + b^2)} - a}{2b^2} c^2 E_S^2 \qquad . \quad . \quad . \quad (86a)$$

This value of P is the same as that given by equation (78), the reason being that the P-axis is the load line for $\cos\phi = 1$. Similarly, by putting $P = 0$ in equation (83), one finds for the

ordinate of the point where the power-circle envelope crosses the Q-axis—

$$Q = -\frac{R}{1+\sin\psi} \quad . \quad . \quad . \quad . \quad . \quad (87)$$

$$= -\frac{c^2E_s^2}{2\sqrt{(a^2+b^2)}} \cdot \frac{\sqrt{(a^2+b^2)}}{\sqrt{(a^2+b^2)}+b}$$

$$= \frac{b-\sqrt{(a^2+b^2)}}{2a^2}c^2E_s^2 \, . \quad . \quad . \quad . \quad (87a)$$

Finally, the co-ordinates of the vertex, whose distance from the origin is $\frac{1}{2}R$, are given by—

$$P_v = \tfrac{1}{2}R\cos\psi = P_v\cos^2\psi \quad . \quad . \quad (88a)$$

and

$$Q_v = \tfrac{1}{2}R\sin\psi = Q_v\cos^2\psi \quad . \quad . \quad (88b)$$

The locus of the envelope function expressed by equation (83) leads to the same general method of geometrical construction for the power-circle envelope as was developed for the power-limit parabola. The construction of the envelope parabola is shown in Fig. 30 and, like that of Fig. 29, is based on the constants $R = c^2E_s^2/2\sqrt{(a^2+b^2)}$ and $\psi = \tan^{-1}(b/a)$. The procedure is as follows: Take any point C_M on the line of power-circle centres, and from it lay off the distance $C_MN = R$ in the direction C_MO. At N erect a perpendicular to the line of centres. With O as centre and OC_M as radius draw an arc to meet this perpendicular at M. Then M is a point on the power-circle envelope. In fact, it is the point where the envelope is a tangent to the power circle whose centre is C_M and whose radius is consequently C_MM.

As before, the construction is based on the property of the parabola that the subnormal (C_MN) is constant and equal to the semi-latus rectum (R). Its validity may be shown by considering the projections on the line of centres of the co-ordinates of the point M. It is seen from Fig. 30 that the projection of the abscissa P is $P\cos\psi$, while the corresponding projection of the ordinate Q is $Q\sin\psi$. Hence

$$ON = VN - VO = (Q\sin\psi - P\cos\psi)$$

and, since $NC_M = R$, and $OC_M = (ON + NC_M)$,

$$OC_M = (R + Q\sin\psi - P\cos\psi).$$

Also $OM = \sqrt{(P^2 + Q^2)}$. But, by construction, $OM = OC_M$, so that $\sqrt{(P^2 + Q^2)} = R + Q \sin \psi - P \cos \psi$, which is the envelope equation of (83). Again, $C_M M$ is the

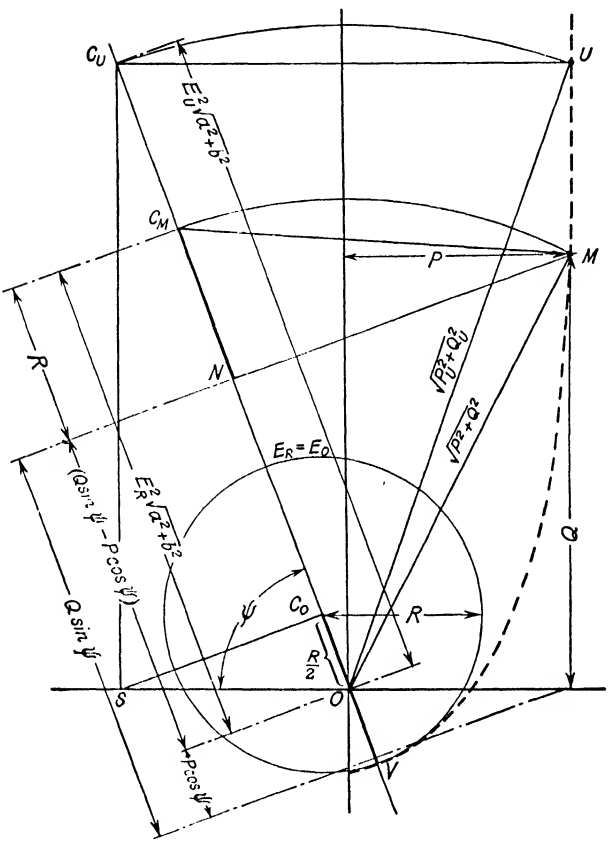

FIG. 30. GEOMETRY OF THE POWER-CIRCLE ENVELOPE

normal to the parabola at the point M, since $OC_M = OM$ and O is the focus. Hence C_M is the centre of the circle to which the parabola is a tangent at M, i.e. of the power-circle whose radius is $C_M M$. If E_R be the value of the receiving-end voltage to which this power circle corresponds, then $OC_M = E_R^2\sqrt{(a^2 + b^2)}$.

Consequently

$$\sqrt{(P^2 + Q^2)} = E_R{}^2\sqrt{(a^2 + b^2)} = R - P\cos\psi + Q\sin\psi$$

as given by (82), (83), and (84) conjointly.

C_0 is then the centre of the power circle to which the envelope is a tangent at the vertex V, for $OC_0 = OV = \frac{1}{2}R$. The corresponding value of receiving-end voltage is found from equation (84) to be—

$$E_0 = \sqrt[4]{\frac{P_V{}^2 + Q_V{}^2}{a^2 + b^2}} = \sqrt[4]{\frac{\frac{1}{4}R^2}{a^2 + b^2}}$$

$$= \frac{cE_S}{2\sqrt{a^2 + b^2}} = E_U\cos\psi.$$

This result agrees with equation (73), established by an alternative method. This particular power circle is, incidentally, the smallest circle which touches the envelope.

It is evident, too, from Figs. 29 and 30, that the power-circle envelope, the power-limit parabola, and the limiting power circle for which $E_R = E_U$ all meet at a common point of tangency, namely, the operating point in the power-circle diagram corresponding to the ultimate power limit of the interconnector.

The Universal Power-limit Chart. It will be observed from equations (72*a*) and (83) that the maximum-power locus and the power-circle envelope both have $R = c^2E_S{}^2/2\sqrt{(a^2 + b^2)}$ as parameter. The equations thus represent two families of parabolas, each parabola in either family corresponding to a particular value of sending-end voltage. To determine the power limits of an interconnector for several values of E_S thus entails a considerable amount of labour in constructing the appropriate families of parabolas.

The necessity for drawing a number of these parabolic loci to cover a given range of sending-end voltage is avoided, however, by the use of a modified chart in which the co-ordinates are conductance and susceptance instead of active and reactive power. If equations (72*a*) and (83) are divided throughout by $E_S{}^4$, one obtains the modified power-limit locus—

$$\left(\frac{P_M}{E_S{}^2}\sin\psi + \frac{Q_M}{E_S{}^2}\cos\psi\right)^2 = \frac{bc^2}{a^2 + b^2}\cdot\left(\frac{Q_M}{E_S{}^2}\right) \quad . \quad (89)$$

and the corresponding modified power-circle envelope—

$$\left(\frac{P}{E_S{}^2}\right)^2 + \left(\frac{Q}{E_S{}^2}\right)^2 = \left(\frac{c^2}{2\sqrt{(a^2 + b^2)}} - \frac{P}{E_S{}^2}\cos\psi + \frac{Q}{E_S{}^2}\sin\psi\right)^2 \quad (90)$$

Equation (89) represents a parabolic admittance locus whose latus rectum is $b^2c^2/(a^2 + b^2)^{\frac{1}{2}}$, while equation (90) represents a similar locus whose latus rectum is $c^2/\sqrt{(a^2 + b^2)}$, both being referred to a co-ordinate system in which the abscissae represent conductance (P/E_s^2) and the ordinates susceptance (Q/E_s^2). These two loci thus together constitute a *universal power-limit chart*, as the active and reactive powers corresponding to a given power limit under conditions of constant sending-end voltage and variable receiving-end voltage may be obtained simply through multiplication of the co-ordinate readings by the appropriate value of E_s^2.

Under these circumstances the power-circle radii will be proportional to the voltage ratio E_R/E_S, the circle radius at the ultimate power limit being simply $c^2/2a$ and the limiting voltage ratio $(E_U/E_S) = c/2a$. The co-ordinates of this limiting point in the chart are then $(P_U/E_s^2) = c^2/4a$ and $(Q_U/E_s^2) = bc^2/4a^2$. Similarly, the co-ordinates of any point on the power-limit parabola become $(P_M/E_s^2) = c\,(E_R/E_S) - a\,(E_R/E_S)^2$ and $(Q_M/E_s^2) = b\,(E_R/E_S)^2$, while the power circle to which the envelope is a tangent at any given point becomes that for which the voltage ratio is—

$$\frac{E_R}{E_S} = \sqrt[4]{\left[\frac{(P/E_s^2)^2 + (Q/E_s^2)^2}{a^2 + b^2}\right]}$$

Finally, the construction of the two universal power-limit loci will remain unchanged except that the starting-point is no longer the parameter R but the constant $c^2/2\sqrt{(a^2 + b^2)}$.

Examples on the Use of Power Limit Charts. The following examples on power limits refer to an interconnector consisting of a single-circuit three-phase transmission line of the British Grid system having a length of 150 miles and terminating at each end in a 60 000 kVA. three-phase transformer whose characteristics* are as follows:—

	Per cent
Reactance	9·5
Full-load I^2R loss	0·63
Magnetizing current	3·81
No-load core loss	0·27

* *Vide* Table 3 on p. 717 of the *Journ. I.E.E.*, 1929, Vol. 67.

The sending-end and receiving-end voltages of this interconnector are considered as referring to the low-tension sides of the terminal transformers.

Considering Example 1 of Chapter II, it is seen that for the 150-mile line $\mathbf{ZY} = 0{\cdot}0711\,|159{\cdot}4°$. Charts I and II (between pp. 8 and 9) then give $\cosh\sqrt{\mathbf{ZY}} = 0{\cdot}967\,|0{\cdot}7°$ and $(\sinh\sqrt{\mathbf{ZY}})/\sqrt{\mathbf{ZY}} = 0{\cdot}989\,|0{\cdot}25°$.

Hence the network constants of the transmission line are—

$$\mathbf{A}_L = \mathbf{D}_L = 0{\cdot}967\,|0{\cdot}7° = 0{\cdot}967 + j0{\cdot}0118$$

$$\mathbf{B}_L = 107{\cdot}2\,|69{\cdot}4° \times 0{\cdot}989\,|0{\cdot}25° = 36 + j99{\cdot}4$$

$$\mathbf{C}_L = 0{\cdot}664 \times 10^{-3}\,|90° \times 0{\cdot}989\,|0{\cdot}25° = (-0{\cdot}0028 + j0{\cdot}656) \times 10^{-3}$$

Referred to a base voltage of 132 kV. the transformer constants become—

$$R_T = \frac{10 \times 0{\cdot}63 \times (132)^2}{60\,000} = 1{\cdot}83 \text{ ohms}$$

$$X_T = \frac{10 \times 9{\cdot}5 \times (132)^2}{60\,000} = 27{\cdot}59 \text{ ohms}$$

$$G_T = \frac{0{\cdot}27 \times 60\,000}{132^2 \times 10^5} = 9{\cdot}15 \times 10^{-6} \text{ mho}$$

$$B_T = \frac{3{\cdot}81 \times 6\,000}{132^2 \times 10^5} = 131{\cdot}2 \times 10^{-6} \text{ mho}$$

and hence $\mathbf{Z}_T = 1{\cdot}83 + j27{\cdot}59$ and $\mathbf{Y}_T = (9{\cdot}15 - j131{\cdot}2) \times 10^{-6}$.

The network constants of the interconnector are then found from equations (24) to be—

$$\mathbf{A} = \mathbf{D} = 0{\cdot}969 + j0{\cdot}00923 = 0{\cdot}969\,|0{\cdot}5°$$

$$\mathbf{B} = 38{\cdot}83 + j152{\cdot}22 = 157\,|75{\cdot}7°$$

$$\mathbf{C} = (4{\cdot}24 + j405{\cdot}45) \times 10^{-6} = 405{\cdot}45 \times 10^{-6}\,|89{\cdot}4°$$

[**Check**:— $\mathbf{AD} = 0{\cdot}9388\,|1° = 0{\cdot}9385 + j0{\cdot}0164$;
$\mathbf{BC} = 0{\cdot}06366\,|165{\cdot}1° = -0{\cdot}0615 + j0{\cdot}0164$;
$\therefore \mathbf{AD} - \mathbf{BC} = 1 + j0$.]

Example 1. *Construct the universal power-limit chart for the above interconnector and determine the ultimate power limits for sending-end voltages of* 132 *kV. and* 120 *kV. Determine also the corresponding values of receiving-end voltage and reactive power demand.*

Solution. Referring to equations (62) and (63), the auxiliary constants are—

$$\begin{cases} a = \dfrac{A}{B}\cos(\beta - \alpha) = \dfrac{0{\cdot}969}{157}\cos 75{\cdot}2^\circ = \underline{0{\cdot}001576 \text{ mho}} \\ b = \dfrac{A}{B}\sin(\beta - \alpha) = \dfrac{0{\cdot}969}{157}\sin 75{\cdot}2^\circ = \underline{0{\cdot}005967 \text{ mho}} \\ c = \dfrac{1}{B} = \underline{0{\cdot}00637 \text{ mho}} \end{cases}$$

Also $\sqrt{(a^2 + b^2)} = 0{\cdot}969/157 = 0{\cdot}006172$ mho and $\psi = \tan^{-1}(b/a) = 75{\cdot}2^\circ$. Hence the fundamental constant of the universal power-limit chart has the value—

$$\frac{c^2}{2\sqrt{(a^2 + b^2)}} = \frac{0{\cdot}00637^2}{2 \times 0{\cdot}006172} = 0{\cdot}003287 \text{ mho}$$

As in the case of the universal power transmission charts of Figs. 22 and 23, it is more convenient to make the power-limit chart direct-reading at some nominal voltage V rather than at one volt. The power limits for any given value of sending-end voltage are then found from the chart by multiplying the scale readings by $(E_S/V)^2$. Choosing $V = 132$ kV., we have—

$$R = c^2V^2/2\sqrt{(a^2 + b^2)} = 0{\cdot}003287 \times 132^2 = 57{\cdot}3 \text{ MVA.}$$

The construction of the power-limit parabola and the power-circle envelope then proceeds as previously described (see Figs. 29 and 30). The resulting power-limit chart is shown in Fig. 31.

From the chart we find for the operating point U—

$$P_U(V/E_S)^2 = 112{\cdot}5 \text{ MW.}; \qquad Q_U(V/E_S)^2 = 425 \text{ MVAr.}$$

Hence with $E_S = 132$ kV. the ultimate power limit is $\underline{112{\cdot}5 \text{ MW.}}$ and the corresponding reaction power demand is $\underline{425 \text{ MVAr.}}$ Also we have

$$E_U = \sqrt{\frac{P_U}{a}} = \sqrt{\frac{112{\cdot}5}{0{\cdot}001576}} = \underline{267 \text{ kV.}}$$

[**Check.** $P_U = R/2 \cos\psi$ and $Q_U = P_U \tan\psi$. Hence with $E_S = V$ we have—

$$P_U = 57{\cdot}3/2 \cos 75{\cdot}2^\circ = 112{\cdot}2 \text{ MW.}$$

and $$Q_U = 112{\cdot}2 \times \tan 75{\cdot}2^\circ = 424{\cdot}5 \text{ MVAr.}]$$

Again, with $E_S = 120$ kV., the ultimate power limit is—

$$P_U = 112{\cdot}5(132/120)^2 = \underline{136 \text{ MW.}}$$

while the corresponding reactive power demand is—

$$Q_U = 425(132/120)^2 = 514 \text{ MVAr.}$$

the receiving-end voltage under these conditions is then—

$$E_U = 267(132/120) = \underline{294 \text{ kV.}}$$

Example 2. *Determine from the chart of the previous example the power limit of the interconnector under the following operating conditions;* (a) *Sending-end voltage* = 132 *k V.*; *receiving-end voltage* = 120 *k V.* (b) *Sending-end voltage* = 120 *k V.*; *receiving-end voltage* = 132 *k V.*

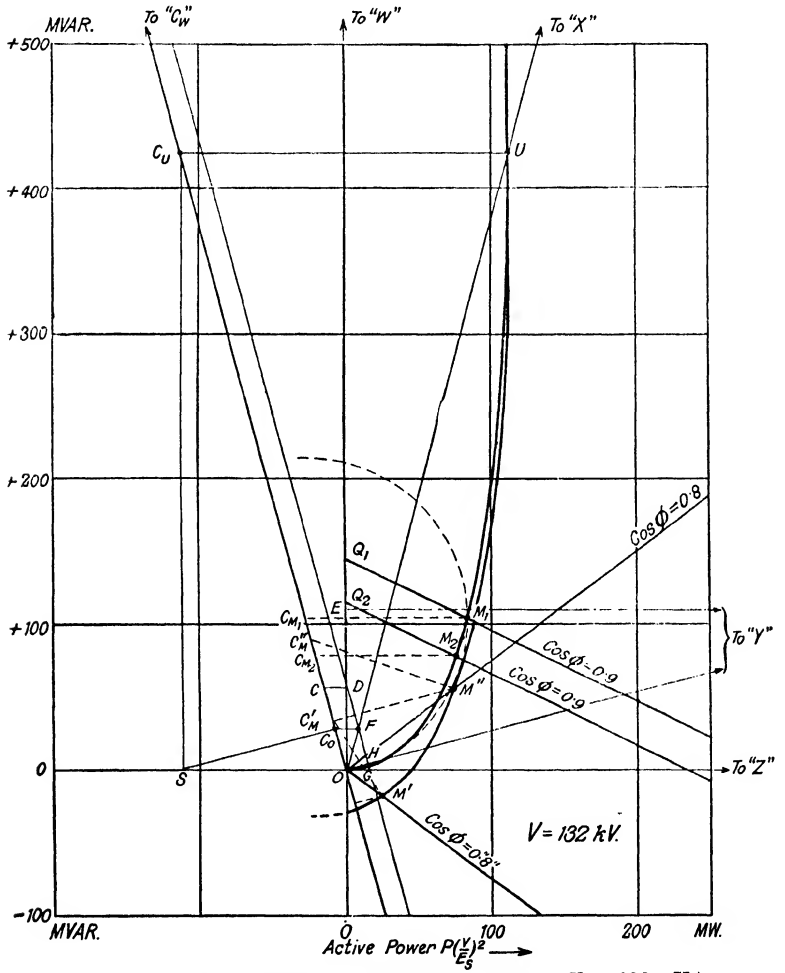

FIG. 31. THE UNIVERSAL POWER-LIMIT CHART (V = 132 kV.)

If in each case the load power factor is 0·9 lagging, what amount of reactive power must be supplied by synchronous phase modifiers at the receiving end in order that this power limit may actually be reached?

Solution. (*a*) The centre of the appropriate power circle is located at C_{M2} where—

$$OC_{M2} = E_R^2\sqrt{(a^2 + b^2)} \,.\, (V/E_S)^2 = 120^2 \times 0{\cdot}006172(V/E_S)^2$$
$$= 88{\cdot}9(V/E_S)^2 \text{ MVA.}$$

Draw $C_{M2}M_2$ parallel to the P-axis to meet the power-limit parabola at M_2. Then M_2 is the operating point corresponding to the required power limit. From the chart we find for the point M_2—

$$P_M(V/E_S)^2 = 76 \text{ MW.}$$

so that with $E_S = 132$ kV. the power limit of the interconnector is 76 MW. Through M_2 draw the load line M_2Q_2, making an angle $\phi = \cos^{-1}(0{\cdot}9)$ with the P-axis to meet the Q-axis at Q_2. Then the ordinate OQ_2 represents the required synchronous phase modifier capacity, for—

$$Q_2 = Q_{M2} + P_{M2} \tan \phi$$

where Q_{M2} is the reactive power demand at M_2, and $P_{M2} \tan \phi$ is the reactive power component of the apparent load Q_2M_2. The chart gives—

$$Q_2(V/E_S)^2 = 113{\cdot}5 \text{ MVAr.}$$

so that with $E_S = 132$ kV. the required synchronous phase modifier output is 113·5 MVAr. leading.

(*b*) In this case the centre of the limiting power circle is at C_{M1} where

$$OC_{M1} = 132^2 \times 0{\cdot}006172(V/E_S)^2 = 107{\cdot}5(V/E_S)^2 \text{ MVA.}$$

The operating point is then at M_1, where the abscissa is

$$P_M(V/E_S)^2 = 83{\cdot}5 \text{ MW.}$$

Hence with $E_S = 120$ kV. the power limit of the interconnector is $83{\cdot}5 \times (132/120)^2 = 101$ MW. The load line M_1Q_1 for $\cos \phi = 0{\cdot}9$ meets the Q-axis at Q_1 where the reactive power is $Q_1(V/E_S)^2 = 145$ MVAr. With $E_S = 120$ kV. the required synchronous phase modifier capacity at the receiving end of the interconnector is consequently $145 \times (132/120)^2 = 175{\cdot}5$ MVAr. leading.

Example 3. *If the power transmitted over the interconnector is* 40 000 *kW. at* 0·8 *lagging power factor, find the optimum sending-end voltage when no synchronous phase modifiers are installed at the receiving end. What is then the value of the receiving-end voltage? What would be the corresponding voltages if the load power factor were* 0·8 *leading?*

Solution. The optimum sending-end voltage is that for which the given power represents the envelope power limit.

(*a*) The load line for $\phi = -\cos^{-1}(0{\cdot}8) = -36{\cdot}9°$ meets the envelope at the point M' whose abscissa is $P(V/E_S)^2 = 25$ MW. The required sending-end voltage is thus—

$$E_S = V\sqrt{\frac{P}{25}} = 132\sqrt{\frac{40}{25}} = 132 \times 1{\cdot}265 = 167 \text{ kV.}$$

Also, $\sqrt{(P^2 + Q^2)} = P \sec \phi = (40/0{\cdot}8) = 50$ MVA. The corresponding receiving-end voltage is then given by equation (84) as—

$$E_R = \sqrt{\frac{50}{0{\cdot}006172}} = \underline{90 \text{ kV.}}$$

[**Check.** Equation (85) gives for the envelope power limit

$$P_E(V/E_S)^2 = \frac{57{\cdot}3 \times 0{\cdot}8}{1 + \cos(75{\cdot}2° - 36{\cdot}9°)} = \frac{45{\cdot}84}{1{\cdot}8808} = 24{\cdot}4 \text{ MW.}]$$

(*b*) The load line for $\phi = +\cos^{-1}(0{\cdot}8) = +36{\cdot}9°$ meets the envelope in Fig. 31 at the point M'' whose abscissa is $P(V/E_S)^2 = 74$ MW. The required sending-end voltage in this case is accordingly—

$$E_S = V\sqrt{\frac{P}{74}} = 132 \times \sqrt{\frac{40}{74}} = 132 \times 0{\cdot}727 = \underline{96 \text{ kV.}}$$

Here again $\sqrt{(P^2 + Q^2)} = P \sec \phi = (40/0{\cdot}8) = 50$ MVA., so that the receiving-end voltage in this case is also $E_R = \underline{90 \text{ kV.}}$*

[**Check.** Equation (85) gives for the envelope power limit

$$P_E(V/E_S)^2 = \frac{57{\cdot}3 \times 0{\cdot}8}{1 + \cos(75{\cdot}2° + 36{\cdot}9°)} = \frac{45{\cdot}84}{0{\cdot}6243} = 73{\cdot}4 \text{ MW.}]$$

It may be mentioned here that the British "grid" lines are designed for a working current density of 1 250 A. per square inch for the equivalent copper section, corresponding to a full-load current of 220 A., i.e. a transmitted power per circuit of 40 000 kW. at 0·8 power factor. At 132 kV. the ultimate power limit of 112 500 kW. thus represents an overload of some 180 per cent and is never likely to be reached in practice.

* That this must necessarily be so is at once clear from equation (77*a*), for the power factor is here the same in both cases, viz. $\cos \phi = 0{\cdot}8$.

References

(1) *Cf.* H. Rissik: "Transmission Systems," *Electrician*, 1939, Vol. 122, p. 138.

(2) *Vide* Chapter VIII of H. Waddicor's *Principles of Electric Power Transmission* (fourth edition) (Chapman & Hall, London, 1939).

(3) For a discussion of the general case of limited synchronous phase-modifier capacity, corresponding to a condition of operation intermediate between these two extremes, see Appendix III of the author's paper in the *Journ. I.E.E.*, 1940.

CHAPTER IV

STEADY-STATE STABILITY

THE stability of a power system is defined as the ability of the system to operate intact both under steady load conditions and during disturbances—that is, to remain in synchronous equilibrium in the steady state and to regain that equilibrium after a disturbance to the system has taken place. What is known as the *steady-state stability limit* of a transmission system is thus the maximum value of transmitted power when the load is increased very slowly. The *transient stability limit*, on the other hand, is the maximum power the system can carry when it is subjected to a transient disturbance such as a sudden change in load, a system fault, or a switching operation.

The investigations of Chapter III were concerned with the power limitations of the interconnector alone, i.e. considered as a power-transmitting link between two infinite buses. In an actual transmission system, however, the interconnector cannot be regarded in isolation but must be considered in association with the synchronous machines between which it serves as an electrical power-transmitting link. That is to say, the size and characteristics of the machines as well as the nature of the loads supplied by them must be taken into account in determining the maximum amount of power which can be transmitted by the interconnector under stable operating conditions.

This question of system stability is, in fact, of vital importance even in the case of power systems or generating stations interconnected by tie lines which, having regard to their economic purpose, would otherwise be electrically weak. In the past such interconnectors were designed to ensure a maximum operating economy for the systems or stations concerned and, as under normal conditions of power interchange the amount of power to be transferred was never very large, they were as often as not of a relatively light character. As the result, the limit of stable operation could be, and sometimes was, exceeded when load fluctuations occurred on the interconnected systems. In fact, instances are known of steady-state instability having arisen with interconnectors of this type. It has been realized in recent years, however, that in order to prevent loss of

synchronism during unforeseen load fluctuations or system disturbances an interconnector must be designed to permit the transfer of adequate synchronizing power. In other words, it is the stability of the transmission system, of which the interconnector forms the principal part, rather than the economics of the interconnection, which will constitute the basis for design in the majority of cases.

Synchronizing Power. Mention has already been made of the fact that power transmission by means of alternating current can take place in one or other of two fundamental ways. The almost universal way is that based on synchronous operation, in which the machines at the two ends of the transmission system run at fixed speeds corresponding to a definite system frequency and independently of the power interchanged between them. The synchronous tie, whether embodied in an underground cable or overhead line, may suddenly break asunder if called upon to carry an excessive amount of power.

Asynchronous operation, on the other hand, is obtained when neither or only one end of the transmission system has synchronous machines connected to it. Here the speed relation between the machines at the two ends of the interconnector is no longer fixed but depends upon the power transmitted. The asynchronous tie between generator and load is inherently flexible, and it is capable of transmitting power to an extent limited solely by the capacity of the machines. This inestimable advantage of asynchronous power transmission systems is a noticeable counterweight to the technical disadvantages of induction generators, and explains why consideration has recently been given to the possibility of employing such a system for long-distance power transmission.[1]

Although the property of electrical rigidity is inherent in and fundamental to the operation of present-day power systems, a quantitative, and even a qualitative analysis of *synchronism*—as this vital property is termed—often eludes the grasp of the power system engineer, who inclines to the view that this question is the concern of the machine designer. And so it is, up to a point. Beyond that point, however, the essentials of synchronous operation become bound up with the phenomenon of *synchronizing power*, and it is this particular kind of power with which the system engineer is primarily concerned. For it is upon the ability of his power system interconnectors to transmit this power under all possible conditions of operation,

both normal and abnormal, that the commercial utility of that system ultimately depends.

To appreciate the true significance of synchronizing power it is necessary to bear in mind that the concept of a perfectly rigid electrical tie implicit in the synchronous interconnection of machines, generating stations, or power systems as described above is not quite accurate. For synchronism is strictly maintained only in the narrow sense that there is no *continuous* slip between the rotating magnetic field due to the excitation of the rotor, and the revolving magnetic field set up by the polyphase currents flowing in the stator windings of a synchronous machine. Although these fields are in synchronism, the link between them is not absolutely rigid, but elastic; and it is the elasticity of this invisible link which is the basis of synchronous operation *per se*. The torque exerted by or on the rotor shaft of a synchronous machine depends directly upon the amount of stretch of this elastic link. The one is a measure of the other. In fact, the existence of such a torque is the physical manifestation of the forces brought into play by the mutual displacement of these two synchronous magnetic fields.

The field due to the rotor excitation is set up in a direction along the rotor-pole axis. The corresponding field flux then produces a voltage at right angles to this axis* which is, in effect, the no-load e.m.f. or *excitation voltage* of the machine. The field set up by the stator current, however, and the armature flux to which it gives rise, will have a direction depending on the machine load. For the direction as well as the magnitude of this field depends partly upon the phase displacement between the stator current and the voltage to which it is due, and which appears at the machine terminals; and partly upon the further phase displacement between this terminal voltage and the induced e.m.f. or *air-gap voltage* to which it corresponds. It is this latter voltage which is generated by the resultant field of the machine, i.e. the vector difference of the rotor and stator fields.[2]

In a synchronous machine under load conditions, then, the reaction of the stator field upon the rotor field—known as armature reaction—causes the rotor-pole axis to be displaced from its no-load position by an angular amount depending on the magnitude and power factor of the load current. This angle is termed the torque angle and is represented in the vector

* I.e. when employing the usual vector-diagram convention.

diagram (Fig. 32) by the angle λ between the excitation voltage E and the air-gap voltage E'. The voltage drop subtended by this angle is always at right angles to the load current[3] and is consequently regarded as being due to a fictitious reactance known as the armature-reaction reactance X_a of the machine. Also, as mentioned above, a further angular displacement arises between the air-gap voltage E' and the terminal voltage V, this angle in turn being subtended by the aggregate voltage drop in the armature

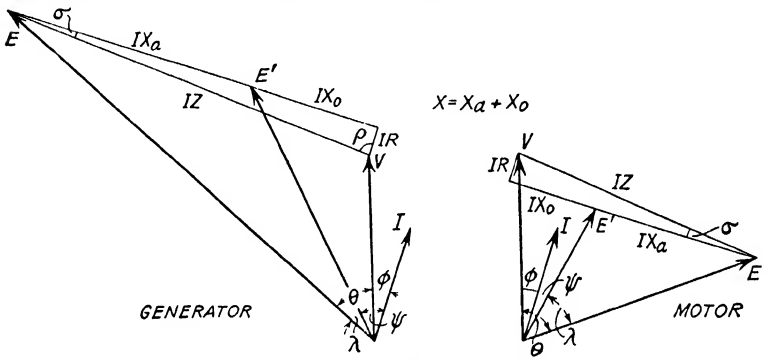

FIG. 32. VECTOR DIAGRAM OF A SYNCHRONOUS MACHINE

E = Excitation voltage.
E' = Air-gap voltage.
V = Terminal voltage.
λ = Torque angle.
θ = Load angle.
I = Load current.
ψ = Internal p.f. angle.
ϕ = External p.f. angle.
IR = Armature resistance drop.
IX_o = Leakage reactance drop.
IX_a = Armature-reaction reactance drop.
IX = Synchronous reactance drop.
IZ = Synchronous impedance drop.
ρ = Synchronous impedance angle.
$\sigma = \pi/2 - \rho$.

resistance R and leakage reactance X_o. The overall displacement angle θ between the excitation and terminal voltages—termed the load angle of the machine—is then subtended by the impedance drop IZ, where Z is the *synchronous impedance* defined by—

$$Z = \sqrt{R^2 + X^2} = \sqrt{R^2 + (X_o + X_a)^2}.$$

The reactance $X = (X_o + X_a)$ is known as the *synchronous reactance.*

Referring to Fig. 32, it is seen that the electrical equivalent of the power at the shaft of the machine is

$$\begin{aligned} P_g &= EI \cos(\theta \pm \phi) = I(V \cos \phi + IR) \\ &= VI \cos \phi + I^2R \\ &= \text{Terminal output} + \text{load loss} \end{aligned}$$

in the case of a generator, and

$$\begin{aligned} P_M &= EI \cos(\theta \mp \phi) = I(V \cos \phi - IR) \\ &= VI \cos \phi - I^2R \\ &= \text{Terminal input} - \text{load loss} \end{aligned}$$

in the case of a motor. By considering the projections of the several voltages of Fig. 32 on an axis making the angle $\rho = \tan^{-1}(X/R)$ with the terminal voltage V one finds,[4] after some transformation, for the electrical output of the generator

$$\begin{aligned} P_G &= \frac{E^2}{Z} \cos \rho - \frac{EV}{Z} \cos(\theta + \rho) \\ &= \frac{E^2}{Z} \sin \sigma + \frac{EV}{Z} \sin(\theta - \sigma) \\ &= P_{Go} + P_m \sin(\theta - \sigma) \quad . \quad . \quad . \quad . \quad (91) \end{aligned}$$

and for the electrical input to the motor

$$\begin{aligned} P_M &= \frac{EV}{Z} \cos(\rho - \theta) - \frac{E^2}{Z} \cos \rho \\ &= \frac{EV}{Z} \sin(\theta + \sigma) - \frac{E^2}{Z} \sin \sigma \\ &= P_m \sin(\theta + \sigma) - P_{Mo} \quad . \quad . \quad . \quad . \quad (92) \end{aligned}$$

where $\sigma = (\pi/2 - \rho) = \tan^{-1}(R/X)$. If the armature resistance is neglected, so that $\sigma = 0$, the above two equations reduce to

$$P_G = P_M = \frac{EV}{X} \sin \theta = P_m \sin \theta \quad . \quad . \quad . \quad (93)$$

The analysis above refers to machines with *non-salient-pole* rotors, and assumes the *synchronous reactance* to be *constant*.

It will be observed that equations (91) and (92) are of the same form as the general network power equations (37) and (38) and, in fact, may be derived from them directly by considering the equivalent network of a synchronous machine, in which $\mathbf{A} = \mathbf{D} = 1$, $\mathbf{B} = \mathbf{Z} = Z \angle \rho = (R + jX)$, and $\mathbf{C} = 0$*; while equation (93) is but a special case of equation (42) which indicated that, if all resistance be neglected, the power transferred between any two points on an a.c. system is a simple function of the difference in phase angle of the voltages at those two points.

* See page 10.

Now let us consider a synchronous machine connected to an infinite bus, i.e. to an ideal machine of zero impedance and infinite inertia, so that the terminal voltage V in Fig. 32 is rigidly fixed in magnitude and in phase. The interchange of electrical power between the machine and the infinite bus may then be followed with reference to Fig. 33, in which I_1 is the initial load current and E_1 the corresponding excitation voltage. The vector E_1 may also be regarded as indicating the direction of the rotor-pole axis, when the vector V will similarly coincide with the corresponding axis of the ideal machine representing the infinite bus.* Suppose now the shaft power be increased slightly. The increment of torque momentarily

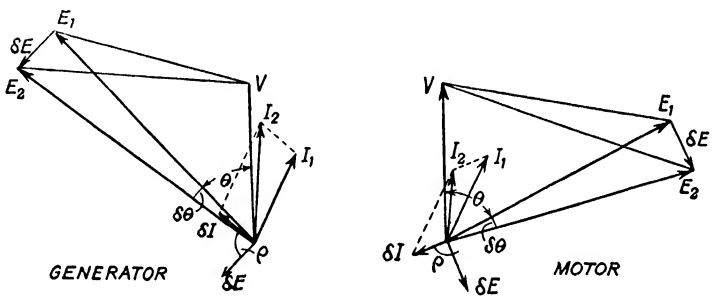

FIG. 33. SYNCHRONOUS MACHINE ON INFINITE BUS

destroys the synchronism between the machine and the infinite bus, and will accelerate the rotor if the machine is a generator, but will retard it in the case of a motor. As a result, the rotor-pole axis will come to occupy a new position, for which the corresponding excitation voltage vector is E_2. This change in position is accompanied by a change in the impedance drop between E and V, indicated by the difference vector δE in Fig. 33. This latter change is in turn accompanied by a change in load current indicated by the vector δI, lagging behind δE by the impedance angle ρ. As the machine impedance is predominantly reactive, and thus $\rho \approx 90°$, the current increment δI is very nearly either in phase or in anti-phase with E_1 and E_2, so that the change in electrical power is $\delta P = \pm E \,.\, \delta I$. In the case of a generator the power increment δP is positive, i.e.

* Actually the motor-pole axes lie 90° ahead of the voltages E_1 and V. It is their relative position, however, rather than their absolute positions with which we are concerned in stability studies, so that this angular difference is of no moment.

generated, and slows up the machine, pulling it back into synchronism with the infinite bus. In the case of a motor the power increment is negative, i.e. *supplied*, and speeds up the machine, urging it forward into synchronism again. In both cases synchronism is restored when the electrical power corresponding to the new load current I_2 (i.e. $E_2 I_2 \cos \psi_2$) balances the increased power at the shaft of the machine.

It is clear from the foregoing considerations that the increment δP is essentially one of *synchronizing power*, and that the development of this power is entirely dependent on the fact that the synchronous impedance of the machine is preponderatingly reactive. In other words, *the interchange of power between synchronous machines takes place by virtue of a process tending normally to keep the machines in synchronism and depending for its action upon the existence of reactance between them.* Furthermore, the concept of synchronizing power is intimately bound up with the angle separating the excitation voltages of the machines or, what amounts to the same thing, the angle between the machine rotors, for they are actually the physical elements of the power-transmission system between which synchronism is maintained. In fact, the synchronizing power of a machine may be defined as that portion of its internal electrical power which varies with the load angle. Referring to equations (91) and (92), it is seen that in the case of a generator the synchronizing power is $P_m \sin (\theta - \sigma)$, while in the case of a motor it is $P_m \sin (\theta + \sigma)$. Also, the invariable element of the electrical power is seen to be

$$\frac{E^2}{Z} \sin \sigma = \frac{E^2}{Z} \cdot \frac{R}{Z} = \left(\frac{E}{Z}\right)^2 R = I_{so}^2 R \quad . \quad . \quad (94)$$

that is, the power lost in the machine due to the short-circuit current obtained with the same field excitation as that giving the excitation voltage E on open circuit.*

The Power/Angle Diagram. Equations (91) and (92) at once lead to the so-called *power/angle diagram* of a synchronous machine, expressing the relation between its internal electrical power, i.e. the electrical equivalent of the mechanical power exerted at the shaft of the machine rotor, and the load angle θ. The diagrams for both generator and motor are shown in

* The synchronous impedance of a machine is defined as the ratio of open-circuit terminal voltage to short-circuit current, for the same value of field excitation.

Fig. 34, and it is seen that actually they are displaced sinusoids, the axes of symmetry being defined by $P = P_{Go}$ and $P = -P_{Mo}$ respectively. The significance of the power/angle diagram as a power characteristic is that it provides a graphical illustration of the all-important phenomenon of synchronism. Consider, for example, the upper curve of Fig. 34, relating to a synchronous generator connected to an infinite bus. Assuming the mechanical power exerted at the rotor shaft to be such that the corresponding electrical power developed is, say, P_{G1}, then the

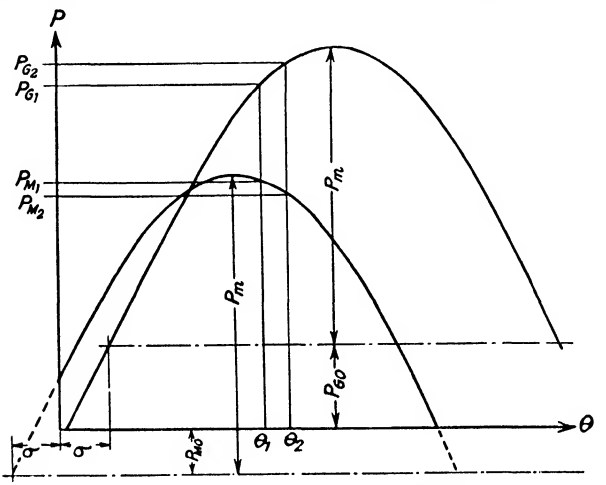

FIG. 34. POWER/ANGLE DIAGRAMS OF A SYNCHRONOUS GENERATOR AND MOTOR

load angle will be θ_1 under equilibrium or steady-state conditions. Suppose now the prime mover gradually supplies a small increase in shaft power. Under the influence of the increased mechanical torque the machine rotor will forge ahead out of synchronism with the infinite bus, and consequently (see Fig. 32) the excitation voltage E will gain on the isynchronous busbar voltage V. As the result, the load angle will increase by an amount $\delta\theta$, say, from θ_1 to θ_2. The power/angle diagram of Fig. 34 indicates that this increase in load angle is accompanied by an increase in electrical power developed, the increment being $\delta P = (P_{G2} - P_{G1})$. This increase in electrical power delivered to the infinite bus in turn causes the machine to slow up and regain synchronism at a new load angle θ_2, for which the electrical power P_{G2} is equal to the

increased shaft power. Conversely, if the initial load angle had been θ_2, then a gradual reduction in mechanical power supplied by the prime mover would cause the generator to slow up slightly, allowing the busbar voltage V to overtake the machine excitation voltage E and so reduce the load angle from θ_2 to θ_1. In this case the negative increment $-\delta\theta$ produces a drop in synchronizing power, and thus in the electrical power developed by the machine, so that equilibrium is once more established and synchronism regained at a smaller load angle θ_1, where the new value of electrical power balances the reduced shaft power.

Consider, now, the lower curve of Fig. 34, relating to a synchronous motor connected to an infinite bus. Assuming, as before, equilibrium to be initially established at the same load angle θ_1, for which the electrical power developed is P_{M1}, a value in this case beyond the point of maximum power: suppose the shaft load of the motor to increase by a small amount. Under the influence of the increased mechanical torque the machine rotor will drop back out of synchronism with the infinite bus, and consequently (see Fig. 32) the excitation voltage E will lose on the isynchronous busbar voltage V. The load angle will again increase by an amount $\delta\theta$, say, from θ_1 to θ_2. In this case, however, the power/angle diagram indicates that the increase in load angle is accompanied by a drop in synchronizing power and thus a decrease in electrical power developed, the increment being $-\delta P = (P_{M2} - P_{M1})$ numerically. This reduction in electrical power implies a still greater discrepancy between the electrical and mechanical torques applied to the rotor shaft, so that the rotor continues to drop back out of synchronism. It will be seen from Fig. 34 that the process is cumulative and that the machine inevitably falls out of synchronism altogether. In fact, the initial assumption of equilibrium at the load angle θ_1 is in this case false for the conditions illustrated by the lower characteristic of Fig. 34. This particular angle does not represent a stable operating condition.

We therefore arrive at the conclusion that the condition for steady-state stability—the maintenance of synchronism during gradual load changes, that is—is simply that the increment of synchronizing power δP, and the incremental change $\delta\theta$ to which it is due, should both have the same algebraic sign. In other words, *the synchronizing power coefficient $dP/d\theta$ must be*

positive. Referring to the basic power equations (91) and (92), it is seen that in the case of a generator this coefficient has the value $P_m \cos(\theta - \sigma) = P_m \sin(\theta + \rho)$, which is positive for $0 < \theta < (\pi - \rho)$; while for a motor its value is $P_m \cos(\theta + \sigma) = P_m \sin(\rho - \theta)$, which is positive for $0 < \theta < \rho$.

The *steady-state stability limit* is then reached when $dP/d\theta = 0$, which occurs when $\theta = (\pi - \rho)$ and $\theta = \rho$ for generator and motor respectively. Reference to Fig. 34 shows that this limit is nothing other than the maximum power as given by the power/angle diagram.* The limiting power at which a machine will still remain in synchronism is therefore determined by the synchronous impedance angle $\rho = \tan^{-1}(X/R)$.

Transmission Stability. Having discussed the behaviour of synchronous machines from the aspect of steady-state stability, it is necessary to examine, finally, the general problem of transmission stability under normal, steady-state conditions of system operation. In the case of present-day a.c. power systems the fundamental power limit is that at which one or more synchronous machines, or machine groups, fall out of step when the power interchanged is increased so slowly that any transient phenomena may be neglected. It is this fundamental power limit which is termed the steady-state stability limit, and, in a complex power system, it will be different for each of the several synchronous ties that link up the various machine groups throughout the system. The determination of these several power limits is thus intimately bound up with the resolution of the power network into a number of interconnected transmission systems, each comprising two groups of synchronous machines (together with their connected loads) electrically coupled by an interconnector.

On reducing each such group to an "equivalent" machine, i.e. one whose electrical and mechanical characteristics are sensibly the same as those of the machine group considered as a whole, and on replacing each interconnector (including any terminal transformers) by an equivalent electrical network, the problem resolves itself into the determination of the

* It is evident that this limit is identical with the power limit as given by the power-circle diagrams of Figs. 13 and 15. For the power/angle diagram is based on the same equations, and is thus merely a specialized form of the circle diagram. The counterpart to the power/angle diagram is then the reactive power/angle diagram, but this is of no great practical interest. It is worth noting, however, that power/angle diagrams can be derived from power-circle diagrams merely by plotting corresponding values of active power P and transmission or load angle θ.

steady-state stability limits of a number of simple two-machine systems.

The existence of a power limit in the case of a synchronous machine connected to an infinite bus, established in the preceding section, is reflected in the behaviour of an elementary two-machine system such as that of Fig. 35 (*a*), in which G represents a synchronous generator supplying power to a synchronous motor M over an interconnector. E_S and E_R are the sending- and receiving-end voltages of the interconnector,

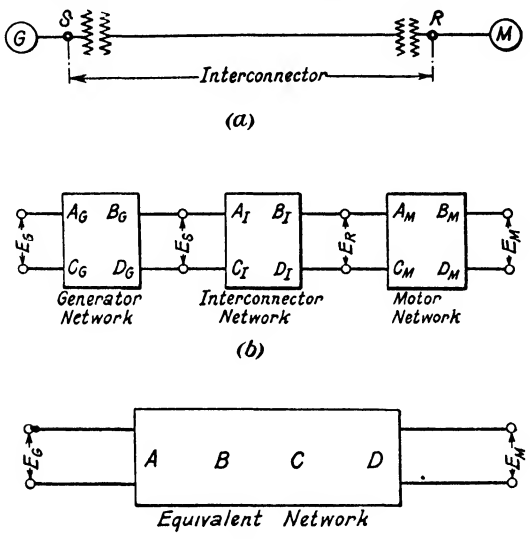

FIG. 35. THE GENERAL TWO-MACHINE SYSTEM

and E_G and E_M the excitation voltages of the machines, i.e. the voltages behind their synchronous impedances.

Neglecting for the moment all shunt admittances, then at no load E_G, E_S, E_R, and E_M are all in phase. On the application of a load to the shaft of the synchronous motor the excitation voltage E_M drops back in phase with respect to the terminal E_R by a certain angle θ_M. The vector difference between these two voltages causes a load current to flow in the impedance of the machine, and the latter thus draws electrical power from the generator equal to the product of E_R and the component of the load current in phase with it. This load current, in traversing the impedance of the interconnector, requires a further

angular displacement θ_I between the terminal voltages E_S and E_R. Moreover, before the generator can supply the electrical power required, its mechanical input must be increased. This increase is manifested by the rotor forging ahead of its no-load position, so that the excitation voltage E_G is made to lead the terminal voltage E_S by an angle θ_G, which continues to increase until the vector difference between E_G and E_S becomes sufficient to drive the load current through the synchronous impedance of the machine. Under load conditions, then, the excitation voltages of the two synchronous machines are displaced by an aggregate angle $\theta = (\theta_G + \theta_I + \theta_M)$. The interchange of power between the machines, that is to say, the transmission of power over the interconnector, accordingly takes place by virtue of an angular displacement between the excitation voltages E_G and E_M or, more fundamentally, between the machine rotors which are the physical elements that are, in actuality, synchronously tied.

The interchange of power between generator and motor may be followed with reference to the system vector diagram of Fig. 36, in which I_1 is the initial load current and E_{G1}, E_{M1} are the initial machine excitation voltages, θ_1 being the corresponding system angle. An increase in the motor load will cause the motor excitation voltage to assume a new position E_{M2}, calling for an increment in current equal to $\delta E_M/Z_M$ and lagging behind the voltage difference δE_M by the impedance angle ρ_M. This current is approximately in anti-phase with E_M, and thus makes the motor draw power from the generator over the interconnector. The corresponding increment in generated power can only be obtained by the prime mover accelerating the generator rotor through a small angle, so that its excitation voltage changes from E_{G1} to E_{G2}. The voltage difference δE_G produces an increment in current which is approximately in phase with E_G, being equal to $\delta E_G/Z_G$ and lagging by the impedance angle ρ_G. Hence the generator will supply the power increment required by the motor. The aggregate increment in current δI causes the load current to reach a new value I_2 such that the transfer impedance drop I_2Z is equal to the difference voltage between E_{G2} and E_{M2}. The new load angle of the system is then θ_2.

Here, also, the interchange of power is bound up with the concepts of synchronizing power and steady-state stability. The analysis in this case proceeds from a consideration of the

basic network equations of the transmission system. Fig. 35 (*b*) shows the three networks, connected in series, representing the three components of the two-machine system. The network constants of the generator and motor are given by equations (18) and (19) respectively, while those of the interconnector are given by equations (23) or (24). As explained in Chapter I,

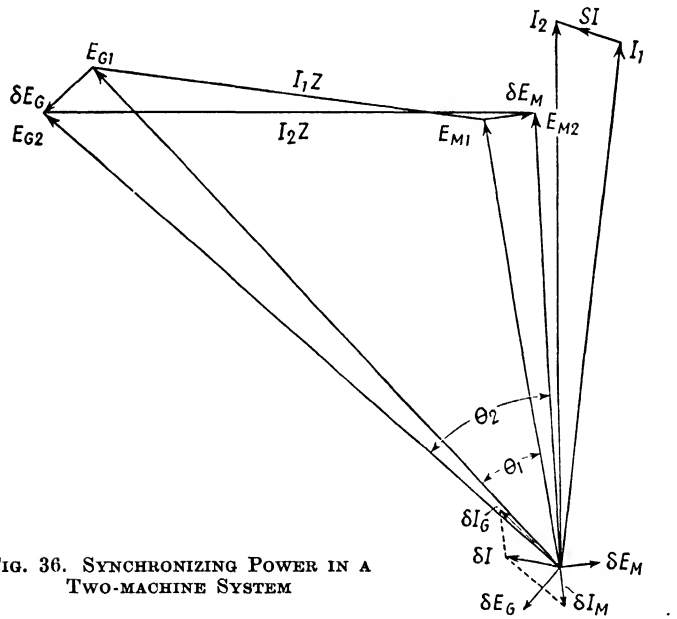

FIG. 36. SYNCHRONIZING POWER IN A TWO-MACHINE SYSTEM

these three networks may be replaced by a single equivalent network, indicated in Fig. 35 (*c*), having constants **A**, **B**, **C**, and **D** which are functions of the twelve subsidiary network constants. For example, the transfer impedance of the two-machine system is—

$$\mathbf{B} = \mathbf{A}_G (\mathbf{A}_I\mathbf{B}_M + \mathbf{B}_I\mathbf{D}_M) + \mathbf{B}_G (\mathbf{C}_I\mathbf{B}_M + \mathbf{D}_I\mathbf{D}_M)$$

as given by the second of the four network equations (22).

The fundamental power equations of the system of Fig. 35 are then—

$$P_G = \frac{E_G^2}{Z_G} \sin \sigma_G + \frac{E_G E_M}{Z} \sin (\theta - \sigma). \quad . \quad (95)$$

and

$$P_M = \frac{E_M^2}{Z_M} \sin \sigma_M - \frac{E_G E_M}{Z} \sin (\theta + \sigma) . \quad . \quad (96)$$

where P_G is the electrical power *output* of the generator, and is *positive*; while P_M is the electrical *input* to the motor and is *negative*.* Here $Z_G|\underline{\rho_G} = \mathbf{B/D}$, the generator driving-point impedance, and $Z_M|\underline{\rho_M} = \mathbf{B/A}$, the motor driving-point impedance; while $Z|\underline{\rho} = \mathbf{B}$, the transfer impedance between the machine excitation voltages E_G and E_M. Also, the angles σ_G, σ_M, and σ as usual denote the complements of the several impedance angles ρ_G, ρ_M, and ρ. Equations (95) and (96) may be written in the more convenient form—

$$P_G = P_{Go} + P_m \sin(\theta - \sigma) \quad . \quad . \quad . \quad (99)$$

and

$$P_M = P_{Mo} - P_m \sin(\theta + \sigma) \quad . \quad . \quad . \quad (100)$$

where P_{Go} and P_{Mo} are the driving-point powers of the generator and motor respectively, and P_m is the maximum transfer power. In the special case where all series resistance and shunt admittance is neglected, so that only reactance is considered as being in circuit between the machine voltages, both the above equations reduce to the simple form—

$$P_G = -P_M = \frac{E_G E_M}{X_G + X_I + X_M} \sin\theta = P_m \sin\theta \quad . \quad . \quad . \quad (101)$$

as then $\sigma_G = \sigma_M = \sigma = 0$, and $Z_G = X_G$, $Z_M = X_M$, and $Z_I = X_I$.

It will be observed that equations (99) and (100) again represent displaced sinusoids in a diagram where electrical power is plotted against the angle θ. The power/angle diagram of the two-machine system is accordingly as shown in Fig. 37. The axes of symmetry are defined by the driving-point powers

* This is the usual convention for the algebraic sign of the electrical power of a synchronous machine. In the general case, where two generators supplying their own load networks are interconnected, their power outputs may be expressed in the form—

$$P_1 = \frac{E_1^2}{Z_{11}} \sin\sigma_{11} + \frac{E_1 E_2}{Z_{12}} \sin(\theta_{12} - \sigma_{12}) \quad . \quad . \quad (97)$$

and

$$P_2 = \frac{E_2^2}{Z_{22}} \sin\sigma_{22} + \frac{E_1 E_2}{Z_{21}} \sin(\theta_{21} - \sigma_{21}) \quad . \quad . \quad (98a)$$

$$= \frac{E_2^2}{Z_{22}} \sin\sigma_{22} - \frac{E_1 E_2}{Z_{12}} \sin(\theta_{12} + \sigma_{12}) \quad . \quad . \quad (98b)$$

where $Z_{11}|\underline{(\pi/2-\sigma_{11})}$ and $Z_{22}|\underline{(\pi/2-\sigma_{22})}$ are the driving-point impedances, and E_1 and E_2 the excitation voltages of the two machines. $Z_{12}|\underline{(\pi/2-\sigma_{12})} = Z_{21}|\underline{(\pi/2-\sigma_{21})}$ is the transfer impedance between the machines and θ_{12} is the angle by which E_1 is ahead of E_2 (so that $\theta_{21} = -\theta_{12}$), on the assumption that machine 1 is transmitting power to machine 2.

$P = P_{Go}$ and $P = P_{Mo}$ (the invariable parts of the electrical powers of the two machines) while the symmetrical sinusoid representing the synchronizing power of the machines (that part of the electrical power which varies with the angle θ) is defined by $P = P_m \sin(\theta - \sigma)$ for the generator and $P = P_m \sin(\theta + \sigma)$ for the motor.* The *average synchronizing power* transmitted

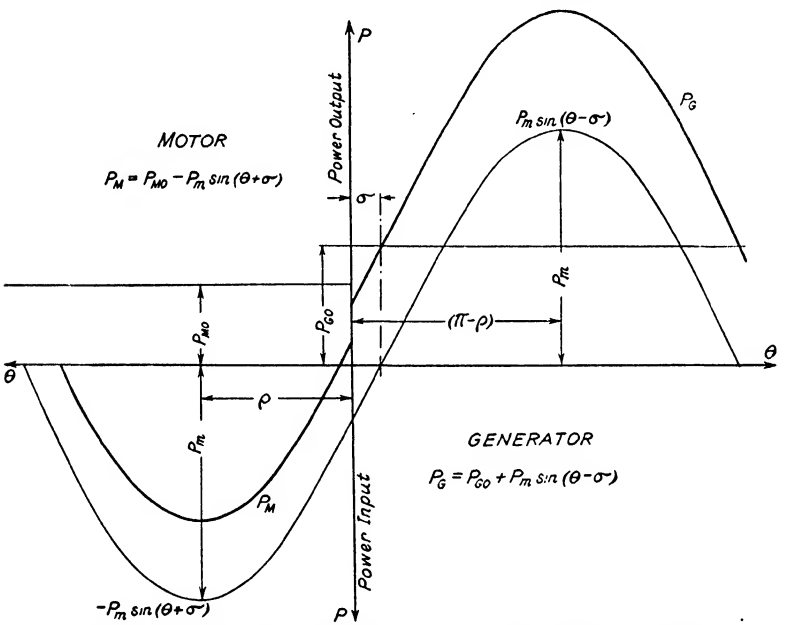

FIG. 37. POWER/ANGLE DIAGRAM OF THE TWO-MACHINE SYSTEM

by the interconnector is thus numerically equal to—

$$P = \tfrac{1}{2}[P_m \sin(\theta - \sigma) + P_m \sin(\theta + \sigma)]$$

$$= P_m \cos\sigma \sin\theta = \frac{E_G E_M}{Z} \cos\sigma \sin\theta$$

$$= \frac{E_G E_M \sin\theta}{X(1 + R^2/X^2)} \quad . \quad . \quad . \quad . \quad . \quad (102)$$

where the transfer impedance is expressed in the form $\mathbf{Z} = (R + jX)$. The above result is basically the same as

* The motor power/angle diagram has actually been drawn in the opposite sense to the generator diagram, so that for the motor $P = P_m \sin[(-\theta) - \sigma]$ in Fig. 37.

equation (40), expressing the average electrical power transmitted by an interconnector in terms of the sending- and receiving-end voltages.

On applying the stability criterion developed in the preceding section, it will be observed that there are two limiting conditions for which the transmission system can become unstable and synchronism be lost, corresponding to maximum power at the motor and generator respectively. The lower of these two limits of steady-state stability is given by $dP_M/d\theta = 0$ when $\theta = \rho$; the upper limit is defined by $dP_G/d\theta = 0$, and is reached when $\theta = (\pi - \rho)$. Also, in the particular case where only system reactance is considered, and hence equation (101) applies, these two limits coincide as both are reached when $\theta = \pi/2$. In practice, *the steady-state stability limit of the system is reached when the electrical power input to the motor attains its maximum value*, that is, when the angle between the machine excitation voltages becomes equal to the impedance angle of the system: because under practical conditions of system operation the power transmitted must correspond to the load at the motor end, for it is only at that end that variations in system load can occur. In other words, the power limit of the system is defined by the maximum load which the motor can carry without being pulled out of synchronism.

Under such conditions of system operation the upper limit of stability, corresponding to maximum power developed by the generator, is of theoretical interest only. For, although in the region $\rho < \theta < (\pi - \rho)$ the synchronizing power coefficient $dP/d\theta$ is positive for the generator, it is negative for the motor (see Fig. 37). This region is thus one in which the motor power is decreasing with θ, but the generator power is still increasing. It is therefore essentially one of transmission instability under normal operating conditions in which the increase in angle takes place by virtue of a gradually increasing load on the motor. Assuming, however, an operating condition in which the motor were prevented from falling out of synchronism at $\theta = \rho$, then the system would eventually break down at $\theta = (\pi - \rho)$, when the generator would be driven out of synchronism by its prime mover.

The Dynamic Stability Criterion. The criterion of stability established earlier in this chapter inevitably implies a dynamic concept of transmission stability. For, although the general problem of steady-state stability is concerned with equilibrium

conditions, the successive steady states of system operation are necessarily reached as the result of equilibrating processes which, in turn, arise through momentary differences between the mechanical power exerted at the shaft of a machine and the electrical power developed by it. No matter how small these differences are, or how slowly they are adjusted, the fact remains that the electrical transmission of varying amounts of power can only take place by reason of their finite existence. In other words, machine inertia is a factor which, strictly speaking, enters into the problem of steady-state stability as well as that of transient stability. But whereas in the latter case it plays an important, if not the leading part, in the former case its role is a minor one.

To appreciate the significance of machine inertia as a determining factor in problems of transmission stability it is necessary to consider the motion of a body rotating under the influence of differentially applied torques. In the first place, the fundamental equation of motion of such a body is—

$$\text{Angular acceleration} = \frac{\text{net accelerating torque}}{\text{moment of inertia}}$$

i.e.
$$\frac{d^2\theta}{dt^2} = \frac{\Delta T}{J} \quad . \quad . \quad . \quad . \quad (103)$$

This equation may be put in the alternative form—

$$\text{Angular acceleration} = \frac{\text{angular velocity} \times \text{net accelerating power}}{2 \times \text{stored kinetic energy}}$$

i.e.
$$\frac{d^2\theta}{dt^2} = \frac{\omega \times (\omega \,.\, \Delta T)}{2 \times (\frac{1}{2} J\omega^2)} = \frac{\omega \,.\, \Delta P}{2W} \quad . \quad . \quad (104)$$

In the case of an electrical machine, if θ is expressed in electrical radians, then $\omega = 2\pi f$, so that equation (104) becomes—

$$\frac{d^2\theta}{dt^2} = \frac{\pi f}{W} \cdot \Delta P \quad . \quad . \quad . \quad . \quad . \quad (105)$$

where f is the electrical frequency, W is the kinetic energy stored in the rotor of the machine at synchronous speed, and ΔP is the power differential acting in the direction of rotation. Hence—

$$\frac{W}{\pi f} \cdot \frac{d^2\theta}{dt^2} = \Delta P = \text{(mechanical power)} - \text{(electrical power)} \quad (106)$$

Referring to equations (99) and (100), and denoting the mechanical powers exerted on the machine rotors by P_{GM} and P_{MM}, and the corresponding electrical powers developed in the air-gap by P_{GE} and P_{ME}, then under steady-state conditions

$$\left.\begin{aligned} P_{GM} &= P_{GE} = P_{Go} + P_m \sin(\theta - \sigma) \\ P_{MM} &= P_{ME} = P_{Mo} - P_m \sin(\theta + \sigma) \end{aligned}\right\}$$

Suppose now that, as the result of some change in circuit conditions, the steady-state angle θ between the excitation voltages E_G and E_M increases by the small amount Δ. Under these circumstances the electrical powers developed by the machines change to the new values—

$$\left.\begin{aligned} P'_{GE} &= P_{Go} + P_m \sin(\theta + \Delta - \sigma) \\ P'_{ME} &= P_{Mo} - P_m \sin(\theta + \Delta + \sigma) \end{aligned}\right\}$$

The steady-state balance between electrical and mechanical power is thereby destroyed, and the machine rotors in consequence experience the power differentials—

$$\begin{aligned} \Delta P_G &= P_{GM} - P'_{GE} = P_m[\sin(\theta - \sigma) - \sin(\theta + \Delta - \sigma)] \\ &= P_m[\sin(\theta - \sigma) \,.\, (1 - \cos\Delta) - \cos(\theta - \sigma) \,.\, \sin\Delta] \\ &= -P_m \cos(\theta - \sigma) \,.\, \Delta \\ \Delta P_M &= P_{MM} - P'_{ME} = P_m[\sin(\theta + \Delta + \sigma) - \sin(\theta + \sigma)] \\ &= P_m[\cos(\theta + \sigma) \,.\, \sin\Delta - \sin(\theta + \sigma) \,.\, (1 - \cos\Delta)] \\ &= P_m \cos(\theta + \sigma) \,.\, \Delta \end{aligned}$$

since for small angles $\cos\Delta = 1$ and $\sin\Delta = \tan\Delta = \Delta$.

Moreover, if θ_G and θ_M are the angular positions of the excitation voltages with reference to some voltage vector rotating at synchronous speed, then the angle between the machine rotors is initially $\theta = (\theta_G - \theta_M)$, but subsequently becomes $(\theta - \Delta) = (\theta_G - \Delta_G) - (\theta_M - \Delta_M)$, where Δ_G and Δ_M are the absolute changes in angular position of E_G and E_M. The relative change in angle is thus $\Delta = (\Delta_G - \Delta_M)$. The relative acceleration of the machine rotors is then—

$$\frac{d^2\Delta}{dt^2} = \frac{d^2\Delta_G}{dt^2} - \frac{d^2\Delta_M}{dt^2} = \pi f\left(\frac{\Delta P_G}{W_G} - \frac{\Delta P_M}{W_M}\right)$$

as given by equation (106), where W_G and W_M are their stored energies at synchronous speed.

Hence—

$$\frac{d^2\Delta}{dt^2} = -\pi f P_m \left[\frac{\cos(\theta-\sigma)}{W_G} + \frac{\cos(\theta+\sigma)}{W_M}\right]\cdot\Delta$$

$$= -\pi f P_m \left[\left(\frac{1}{W_G}+\frac{1}{W_M}\right)\cos\theta\cos\sigma + \left(\frac{1}{W_G}-\frac{1}{W_M}\right)\sin\theta\sin\sigma\right]\cdot\Delta \quad . \quad (107)$$

This equation is of the form $d^2\Delta/dt^2 = -k\Delta$, which is the equation of simple harmonic motion provided the constant coefficient k is positive. The condition that the relative motion of the machine rotors be oscillatory, i.e. that any small change Δ in their relative position will bring into play forces tending to restore them to their initial relative position, is therefore that the expression in square brackets in equation (107) be positive, since the remaining factor $\pi f P_m$ is always positive. In other words, the criterion of steady-state stability is defined by the relation—

$$\left(\frac{1}{W_G}+\frac{1}{W_M}\right)\cos\theta\cos\sigma + \left(\frac{1}{W_G}-\frac{1}{W_M}\right)\sin\theta\sin\sigma > 0$$

i.e.
$$\frac{W_G+W_M}{W_G-W_M} > \tan\theta\tan\sigma$$

or
$$\tan\theta < \left(\frac{W_G+W_M}{W_G-W_M}\right)\tan\rho \quad . \quad . \quad (108)$$

The steady-state stability limit of the transmission system is thus reached at a critical value of θ defined by

$$\tan\theta = \left(\frac{W_G+W_M}{W_G-W_M}\right)\frac{X}{R} \quad . \quad . \quad . \quad (109)$$

where X and R are the reactance and resistance components respectively of the transfer impedance $\mathbf{Z}$ and $\rho = \tan^{-1}(X/R)$ is the impedance angle.

Equation (108) expresses the so-called dynamic stability criterion established originally by Wagner and Evans,[5] and subsequently by Dahl [6] in a somewhat different manner. The resulting stability limit, defined by equation (109), is then the maximum power which can be interchanged between the two machines without loss of synchronism, when the angle between

the machine rotors is increased slowly. Equation (109) leads to the following conclusions regarding the critical angle for stability:—

1. If the inertia of the generator is very large compared to that of the motor, so that W_M is negligible in comparison with W_G, then $\theta = \rho$.
2. If the inertia of the motor is very large compared to that of the generator, so that W_G is negligible in comparison with W_M, then $\theta = (\pi - \rho)$.
3. If the machine inertias are equal, so that $W_G = W_M$, then $\theta = \pi/2$.
4. If $W_G > W_M$, then $\rho < \theta < \pi/2$.
5. If $W_G < W_M$, then $\pi/2 < \theta < (\pi - \rho)$.
6. If the transfer impedance of the system has negligible resistance, so that $R = 0$, then $\theta = \pi/2$ and is independent of the machine inertias.

Condition 1 clearly corresponds to the case of a synchronous motor connected to an infinite bus, where synchronism is lost when the pull-out angle, defined by $dP/d\theta = 0$ in conjunction with equation (92), is reached. Similarly, condition 2 represents the converse case of a generator connected to an infinite bus, where the system breaks down due to the machine being driven out of synchronism as soon as the load angle attains the critical value defined by $dP/d\theta = 0$ in conjunction with equation (91). Condition 6 in turn corresponds to the special case of a transmission system whose power/angle equation is given by equation (93), for which $dP/d\theta = 0$ gives $\theta = \pi/2$ as the limiting angle consistent with transmission stability. The intermediate conditions, for which the critical angle lies between ρ and $(\pi - \rho)$, are to be interpreted as follows:—

The relative acceleration of the machines, that is to say, the rate of change of the relative speed of generator and motor, is the resultant of their absolute accelerations; in other words, of the rate of change of their individual speeds from those corresponding to the system frequency. The individual accelerations $d^2\theta_G/dt^2$ and $d^2\theta_M/dt^2$ depend on the machine inertias as well as upon the power differentials tending to accelerate the machine rotors. For values of $\theta < \rho$ these accelerations are of opposite sign, and the relative acceleration of the machines is negative. Or, to put the matter in another way, up to this point any increase in θ produces acceleration of the motor and retardation of the generator, both effects

acting to prevent any further increase in the angle θ. For values of θ lying between ρ and $(\pi - \rho)$ the individual accelerations $d^2\theta_G/dt^2$ and $d^2\theta_M/dt^2$ are both negative, that is to say, in this region any increase in θ produces retardation of the motor as well as of the generator. Provided the resultant rate of change of the individual machine speeds is such as to produce a net acceleration of the motor relative to the generator, the system will remain stable. It is clear that this resultant acceleration depends on the relative inertias of generator and motor, and a little consideration will show that it is possible for stability to be retained up to a value of $\theta = (\pi - \rho)$ so long as the generator retards more rapidly than the motor, provided the system as a whole can drop somewhat below normal synchronous speed. Finally, for values of $\theta > (\pi - \rho)$ the absolute accelerations of the machines again become of opposite sign, but their relative acceleration is now positive. Hence any increase in θ beyond this point produces acceleration of the generator together with retardation of the motor, so that the angle θ will continue to increase and synchronism will be lost.

In considering the possibility of stable operation with values of θ beyond ρ, the pull-out angle of the motor, it must be borne in mind that such operation can only arise under circumstances in which the increase in angular displacement is brought about by a change in the constants of the system under conditions of constant load, the inertias of the machines being such that stability can be regained. These circumstances, however, never arise under practical conditions of system operation, so that this regime of operation can be demonstrated only in the laboratory. In practice the increase in angular displacement arises, under steady-state conditions at least, from an increment of load, so that the system cannot regain stability once the angular displacement has exceeded the pull-out angle of the motor, defined by $\theta = \rho$.

The Calculation of Steady-state Stability. In determining the steady-state stability limit of a transmission system consisting of equivalent generator, interconnector, and equivalent motor, the given conditions of operation are generally those of constant voltage at the ends of the interconnector, i.e. at the terminals of the synchronous machines. The machine excitation voltages are then assumed to vary in accordance with the requirements of system angle and synchronous impedance drop, the adjustment being effected by either manual or automatic field

regulation. Under these circumstances the excitation voltages are functions of the system load, so that the power/angle equations (99) and (100) are not applicable directly to any simple construction or calculation of the appropriate power/angle curves.

Generally speaking, there are four main methods by which the steady-state power limit may be evaluated:—

1. By actual construction of the system power/angle diagram, involving step-by-step calculation.
2. By trigonometrical analysis of the voltage vector diagram.
3. By the construction of the power-circle diagrams for the interconnector, the equivalent generator, and the equivalent motor networks.
4. By means of a mechanical model which is an exact mechanical analogue of the electrical transmission system.

Method 1 is instructive, but the actual computation of the power/angle diagram is laborious. Briefly, the procedure is as follows: For a chosen value of receiving-end power the corresponding load current is calculated from the given sending- and receiving-end voltages and the several component impedances of the transmission system. By a converse method the machine excitation voltage values corresponding to this load current are then calculated. These values are then substituted in the power/angle equation, and the system angle found corresponding to the chosen power value. In this way a point on the power/angle characteristic is determined. By choosing a succession of receiving-end power values and repeating the above procedure, the complete power/angle characteristic can be plotted. The steady-state stability limit is then given by the maximum receiving-end power, corresponding to the peak of the power/angle characteristic.

Method 2 is useful only in the special case where all series resistance as well as shunt admittance is neglected, that is to say, where the transmission system as a whole is considered as having reactance only. Method 3 is generally applicable and may in fact be used to plot the system power/angle diagram. The alternative semi-graphical methods due to Edith Clarke [7] and to Dwight,[8] and based on the system vector diagram, as well as the corresponding approximate method developed by Rissik,[9] are also generally applicable, but as these are not so convenient to use as method 3 they will not be considered here. Method 4 is of considerable interest in that it affords a striking

illustration of the close analogy which often obtains between mechanical and electrical engineering problems. These last three methods of evaluating the steady-state stability limit of a transmission system are considered in detail below.

(*a*) *Analytical Method based on the System Vector Diagram.* In the particular case where the transmission system contains reactance only, the system vector diagram is as shown by Fig. 38. Here E_G and E_M are the machine excitation voltages, E_S and E_R the corresponding terminal voltages, and X_G, X_I, X_M the several reactances acting between these voltages. θ_G and θ_M are the machine load angles and θ_I is the transmission angle, subtended by the reactance drop IX_I of the interconnector.

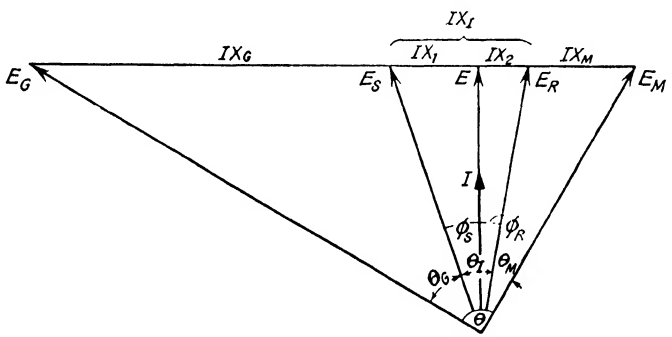

FIG. 38. STABILITY-LIMIT VECTOR DIAGRAM FOR A TRANSMISSION SYSTEM CONTAINING REACTANCE ONLY

The system angle is then the sum total of the machine load angles and the transmission angle, viz. $\theta = (\theta_G + \theta_I + \theta_M)$, and the steady-state stability limit is defined by $\theta = \pi/2$. The vector diagram of Fig. 38 has actually been drawn to illustrate this condition. In the majority of power-transmission systems the terminal voltages E_S and E_R (referred to the low-tension sides of the transformers at either end of the interconnector) will be more or less equal, so that the receiving end will operate at leading power factor and the sending end at lagging power factor. Consequently at some point on the interconnector the voltage will be in phase with the load current I. In Fig. 38 this voltage is indicated as E. The interconnector reactances considered as acting between the voltage E and the terminal voltages E_S and E_R are denoted by X_1 and X_2, where $(X_1 + X_2) = X_I$.

Under these circumstances the power interchanged between the machines* is given by—

$$P = \frac{E_G E_M}{X_G + X_I + X_M} \sin\theta \quad . \quad . \quad . \quad . \quad (110)$$

$$= \frac{E_S E_R}{X_I} \sin\theta_I = \frac{E_G E_S}{X_G} \sin\theta_G = \frac{E_R E_M}{X_M} \sin\theta_M.$$

The above alternative forms of equation (101) respectively express the power transmitted by the interconnector as given by equation (42), and the electrical powers of the generator and motor as given by equation (93). In the absence of all resistance there can be no power lost in transmission, so that from energy considerations alone all three powers must be equal. The identity between the four equations for the system power is but an expression of the following axiom, whose validity can be established from the trigonometry of the vector diagram :—

In a transmission system containing reactance only, the power transmitted is given by the product of the voltages at any two points on the system divided by the intervening reactance and multiplied by the sine of the angle between the two voltages.

The maximum power occurs when $\theta = \pi/2$ and is equal to—

$$P_m = \frac{E_G E_M}{X_G + X_I + X_M} \quad . \quad . \quad . \quad (111)$$

Denoting by $X_a = X_G + X_1$ the reactance acting between E_G and E, and by $X_b = X_2 + X_M$ the reactance acting between E and E_M, Fig. 38 then gives—

$$E^2 = (IX_a) \times (IX_b) = I^2 \,.\, X_a X_b$$

so that $E/I = \sqrt{(X_a X_b)}$.

Furthermore, $E_G^2 = (E^2 + I^2 X_a^2)$ and $E_M^2 = (E^2 + I^2 X_b^2)$ from which—

$$E_G = I\sqrt{X_a X_b + X_a^2} = I\sqrt{X_a\,(X_a + X_b)},$$

and $$E_M = I\sqrt{X_a X_b + X_b^2} = I\sqrt{X_b\,(X_a + X_b)}.$$

Hence the maximum power as given by equation (111) becomes

$$P_m = \frac{E_G E_M}{X_a + X_b} = \frac{I^2 \,.\, (X_a + X_b)\sqrt{(X_a X_b)}}{X_a + X_b}$$

$$= I^2 \,.\, \sqrt{(X_a X_b)} = I^2 \,.\, \frac{E}{I} = EI \quad . \quad (112)$$

* *Cf.* Equation (101).

which is a result only to be expected, since E and I are in phase.

Again, Fig. 38 gives $E_S^2 = E^2 + I^2X_1^2$ and $E_R^2 = E^2 + I^2X_2^2$, from which—

$$\cos\phi_S = \frac{E}{E_S} = \sqrt{\frac{X_aX_b}{X_1^2 + X_aX_b}}$$

$$\text{and} \quad \cos\phi_R = \frac{E}{E_R} = \sqrt{\frac{X_aX_b}{X_2^2 + X_aX_b}},$$

where ϕ_S and ϕ_R are the sending- and receiving-end power-factor angles. Also $\cos^2\phi + \sin^2\phi = 1$, so that

$$\sin\phi_S = \sqrt{(1 - \cos^2\phi_S)} = \frac{X_1}{\sqrt{(X_1^2 + X_aX_b)}}$$

$$\text{and} \quad \sin\phi_R = \sqrt{(1 - \cos^2\phi_R)} = \frac{X_2}{\sqrt{(X_2^2 + X_aX_b)}}$$

Finally, $\theta_I = \phi_S + \phi_R$, so that—

$$\begin{aligned}\sin\theta_I &= \sin(\phi_S + \phi_R) = \sin\phi_S\cos\phi_R + \cos\phi_S\sin\phi_R \\ &= \frac{X_1\sqrt{(X_aX_b)} + X_2\sqrt{(X_aX_b)}}{\sqrt{[(X_1^2 + X_aX_b)(X_2^2 + X_aX_b)]}} \\ &= \frac{X_I\sqrt{(X_aX_b)}}{\sqrt{(X_1^2 + X_aX_b)}\cdot\sqrt{(X_2^2 + X_aX_b)}}\end{aligned}$$

The power transmitted by the interconnector is consequently

$$\begin{aligned}\frac{E_SE_R}{X_I}\sin\theta_I &= \frac{E\sqrt{(X_1^2 + X_aX_b)}}{\sqrt{(X_aX_b)}}\cdot\frac{E\sqrt{(X_2^2 + X_aX_b)}}{\sqrt{(X_aX_b)}} \\ &\qquad \cdot\frac{1}{X_I}\cdot\frac{X_I\sqrt{(X_aX_b)}}{\sqrt{(X_1^2 + X_aX_b)}\cdot\sqrt{(X_2^2 + X_aX_b)}} \\ &= \frac{E^2}{\sqrt{(X_aX_b)}} = E^2\cdot\frac{I}{E} = EI\end{aligned}$$

which is the same result as equation (112), thus establishing the validity of the axiom on p. 106 for the special case in which $\theta = \pi/2$.*

* The general validity of this axiom can be established in a similar manner, but this will not be gone into here.

The maximum power is found from equation (112) to be

$$P_m = EI = E^2 \cdot \frac{I}{E}$$
$$= \frac{E_R^2 \cdot X_a X_b}{X_2^2 + X_a X_b} \cdot \frac{1}{\sqrt{(X_a X_b)}} = \frac{E_R^2 \sqrt{(X_a X_b)}}{X_2^2 + X_a X_b}$$
$$= \frac{E_R^2 \sqrt{[(X_G + X_1)(X_2 + X_M)]}}{X_2^2 + (X_G + X_1)(X_2 + X_M)} \quad . \quad . \quad (113)$$

In the particular case where the transmission system operates with equal sending- and receiving-end voltages so that $E_S = E_R$ and thus $X_1 = X_2 = \frac{1}{2}X_I$, the above equation becomes—

$$P_m = \frac{E_R^2 \sqrt{[(X_G + \frac{1}{2}X_I)(X_M + \frac{1}{2}X_I)]}}{(\frac{1}{2}X_I)^2 + (X_G + \frac{1}{2}X_I)(X_M + \frac{1}{2}X_I)} \quad . \quad (114)$$

a well-known result already established by Nickle, Edith Clarke, and others.[10] Again, when the system operates with unity power factor at the receiving end, so that $E_R = E$ and thus $X_2 = 0$, and $X_1 = X_I$, equation (113) reduces to—

$$P_m = \frac{E_R^2}{\sqrt{[X_M (X_G + X_I)]}} \quad . \quad . \quad . \quad . \quad . \quad (115)$$

another well-known result.[11]

As only the terminal voltages E_S and E_R and the system reactances X_G, X_I, and X_M are known, it is necessary to evaluate X_1 and X_2 in terms of these five constants. Denoting the terminal-voltage ratio E_S/E_R by r, then—

$$r^2 = \frac{E_S^2}{E_R^2} = \frac{E^2 + I^2 X_1^2}{E^2 + I^2 X_2^2} = \frac{X_a X_b + X_1^2}{X_a X_b + X_2^2}$$

from which, with $(X_1 + X_2) = X_I$, one obtains the relation—

$$\frac{X_1}{X_2} = \frac{r^2 X_I^2 + (r^2 - 1) \cdot X_G (X_I + X_M)}{X_I^2 - (r^2 - 1) \cdot X_M (X_I + X_G)} \quad . \quad (116)$$

Assuming $X_1 > X_2$, one may write—

$$\left.\begin{aligned} X_1 &= \tfrac{1}{2}X_I + x \\ X_2 &= \tfrac{1}{2}X_I - x \end{aligned}\right\}$$

where $x = \frac{1}{2}(X_1 - X_2)$. After some transformation one finds—

$$x = \frac{(X_G + \frac{1}{2}X_I)(X_M + \frac{1}{2}X_I) + (\frac{1}{2}X_I)^2}{\left(\frac{r^2 + 1}{r^2 - 1}\right)X_I + X_G - X_M} \quad . \quad (117)$$

Equation (113) then gives, finally, for the maximum power—

$$P_m = \frac{(r^2-1)\,E_R^2}{2X_I} \cdot \sqrt{\left[\frac{1}{x^2}\,(X_G + \tfrac{1}{2}X_I)\,(X_M + \tfrac{1}{2}X_I) - \left(1 + \frac{X_G - X_M}{x}\right)\right]}. \quad (118)$$

It is sometimes required to know also the angle between E_S and E_R when this power limit is reached. It has already been demonstrated that—

$$P_m = EI = \frac{E_S E_R}{X_I} \sin \theta_I.$$

The required angle is thus given by—

$$\sin \theta_I = \frac{P_m X_I}{E_S E_R} = \frac{P_m X_I}{r E_R^2} = \frac{r^2-1}{2r} \cdot \sqrt{\left[\frac{1}{x^2}\,(X_G + \tfrac{1}{2}X_I)\,(X_M + \tfrac{1}{2}X_I) - \left(1 + \frac{X_G - X_M}{x}\right)\right]}. \quad (119)$$

(*b*) *Semi-graphical Method based on System Power-circle Diagrams.* The following method of determining the steady-state stability limit of a transmission system, due to Wagner and Evans,[12] furnishes an apt illustration of the value of power-circle diagrams as a means of attacking power transmission problems. As in the previous case, the method assumes E_S and E_R to be known, as also the circuit constants of the transmission network as a whole.

Referring to Fig. 39, the combined sending- and receiving-end power-circle diagram of the interconnector is first constructed as described in Chapter II. The centre of the receiving-end power circle is defined by—

$$S_R \,\underline{|\psi_R} = -\,(\mathbf{A}_I/\mathbf{B}_I)E_R^2 = (A_I E_R^2/B_I)\,\underline{|(\pi + \alpha_I - \beta_I)}$$

and thus has the co-ordinates—

$$\left.\begin{aligned} S_R \cos \psi_R &= -\frac{A_I E_R^2}{B_I} \cos (\beta_I - \alpha_I) \\ S_R \sin \psi_R &= +\frac{A_I E_R^2}{B_I} \sin (\beta_I - \alpha_I) \end{aligned}\right\} \quad . \quad . \quad (120)$$

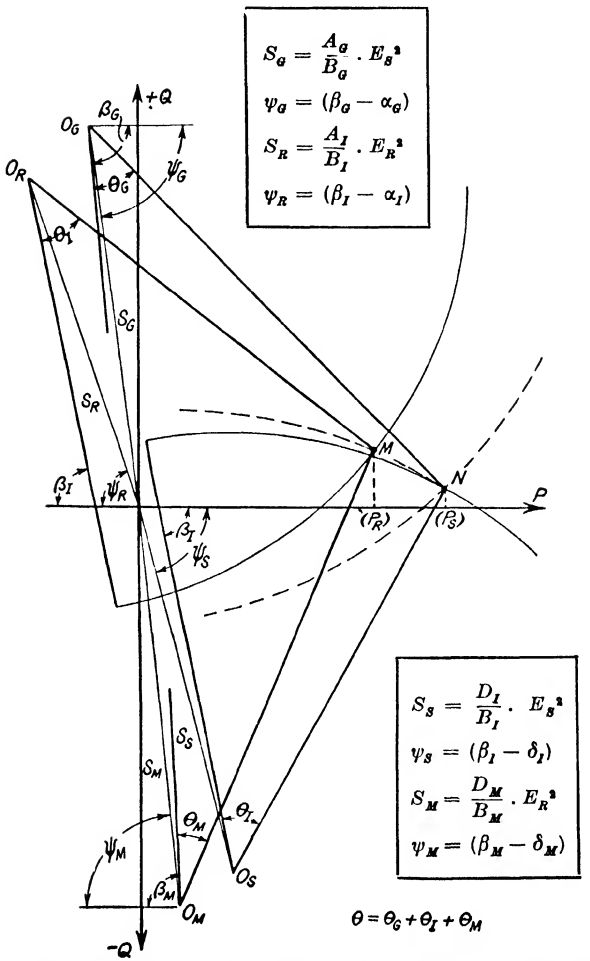

FIG. 39. POWER-CIRCLE DIAGRAMS OF A TRANSMISSION SYSTEM

while the centre of the sending-end power circle is similarly defined by $S_S \angle \psi_S = (\mathbf{D_I/B_I})\, E_S^2 = (D_I E_S^2/B_I) \angle (\delta_I - \beta_I)$, and thus has the co-ordinates—

$$\left.\begin{aligned} S_S \cos \psi_S &= + \frac{D_I E_S^2}{B_I} \cos (\beta_I - \delta_I) \\ S_S \sin \psi_S &= - \frac{D_I E_S^2}{B_I} \sin (\beta_I - \delta_I) \end{aligned}\right\} \quad . \quad . \quad (121)$$

where $\mathbf{A}_I$, $\mathbf{B}_I$, and $\mathbf{D}_I$ are the interconnector network constants as found from equations (23) or (24). The radii of the two power circles are both equal to $E_S E_R/B_I$. The combined circle diagram is shown by the full lines in Fig. 39. The zero-θ_I reference axis is in each case a line passing through the centre of the power circle (O_R and O_S in the diagram) and making the angle β_I with the power axis.

For a given value of transmitted power (i.e. receiving-end power), the angle between E_S and E_R will be θ_I and the operating points will be M and N on the receiving- and sending-end power circles respectively, as shown in Fig. 39. Considering the equivalent network of the "generator," the point N must lie also on the receiving-end power circle for that network, as the sending end of the interconnector is at once the receiving end of the generator. Now, the centre of this receiving-end power circle (shown dotted in Fig. 39) is defined by—

$$S_G \underline{|\psi_G} = -(\mathbf{A}_G/\mathbf{B}_G)E_S^2 = (A_G E_S^2/B_G)\underline{|(\pi + \alpha_G - \beta_G)}$$

and thus has co-ordinates—

$$\left.\begin{aligned} S_G \cos \psi_G &= -\frac{A_G E_S^2}{B_G} \cos (\beta_G - \alpha_G) \\ S_G \sin \psi_G &= +\frac{A_G E_S^2}{B_G} \sin (\beta_G - \alpha_G) \end{aligned}\right\} \quad . \quad . \quad (122)$$

where $\mathbf{A}_G$ and $\mathbf{B}_G$ are network constants of the equivalent generator. The zero-θ_G axis is in this case a line passing through the power-circle centre (O_G in Fig. 39) and making the angle β_G with the power axis. The load angle θ_G of the equivalent generator, corresponding to the angle θ_I between E_S and E_R, is then the angle between this axis and the radius vector $O_G N$.

In the same way, considering the equivalent network of the "motor," the operating point M on the receiving-end power circle of the interconnector must lie also on the sending-end power circle for the motor network. The centre of this power circle (shown dotted in Fig. 39) is in turn defined by—

$$S_M \underline{|\psi_M} = (\mathbf{D}_M/\mathbf{B}_M)E_R^2 = (D_M E_R^2/B_M)\underline{|(\delta_M - \beta_M)}$$

and thus has co-ordinates—

$$\left.\begin{aligned} S_M \cos \psi_M &= +\frac{D_M E_R^2}{B_M} \cos (\beta_M - \delta_M) \\ S_M \sin \psi_M &= -\frac{D_M E_R^2}{B_M} \sin (\beta_M - \delta_M) \end{aligned}\right\} . \quad . \quad (123)$$

where $\mathbf{D}_M$ and $\mathbf{B}_M$ are network constants of the equivalent motor. Here the zero-θ_M axis is a line passing through the power-circle centre (O_M in Fig. 39) and making the angle β_M with the power axis. The load angle θ_M of the equivalent motor is then the angle between this axis and the radius vector $O_M M$.

The system angle θ corresponding to the given value of transmitted power is then simply—

$$\theta = \theta_G + \theta_I + \theta_M \quad . \quad . \quad . \quad (124)$$

the individual angles being obtained directly from the diagram. By choosing a number of power values, a succession of operating points such as M and N are located in the diagram, and the corresponding values of θ_G, θ_I, and θ_M are then read off. A curve is then plotted showing the relation between transmitted power P and system angle θ. The steady-state power limit is then given by the value of P for which $\theta = \beta$, where β is the angle of the transfer impedance $\mathbf{B}$ of the transmission system as a whole, which may be found from the relation—

$$B\,|\underline{\beta} = \mathbf{B} = \mathbf{A}_G(\mathbf{A}_I\mathbf{B}_M + \mathbf{B}_I\mathbf{D}_M) + \mathbf{B}_G(\mathbf{C}_I\mathbf{B}_M + \mathbf{D}_I\mathbf{D}_M) \quad . \quad (125)$$

as given by equation (22).

It will be observed that this method does not require a knowledge of E_G and E_M. These excitation voltages can, however, be obtained subsequently from the composite power-circle diagram. For, referring to Fig. 39, the radius of the generator power circle is $O_G N = E_G E_S / B_G$, from which—

$$E_G = \frac{B_G}{E_S} \times (O_G N) \quad . \quad . \quad . \quad (126)$$

Similarly, the radius of the motor power circle is $S_M M = E_R E_M / B_M$, from which—

$$E_M = \frac{B_M}{E_R} \times (O_M M) \quad . \quad . \quad . \quad (127)$$

It is then possible to check the accuracy of the construction, for the transmitted power P, given by the abscissa of the operating point M, is also the power input to the equivalent motor and thus has the value—

$$P = \frac{D_M E_R^2}{B_M} \cos(\beta_M - \delta_M) - \frac{E_R E_M}{B_M} \cos(\theta_M + \beta_M)$$

$$= S_M \cos\psi_M + (O_M M) \,.\, \sin(\theta_M + \beta_M - \pi/2)$$

$$= (\text{abscissa of centre } O_M) + (\text{projection of radius } O_M M \text{ on power axis}).$$

By inserting the appropriate values of the vector radius $O_M M$ and the load angle θ_M in the above expression, values of P should be obtained which check with those given by the abscissae of the several operating points such as M.

Again, knowing E_G and E_M, it is possible to construct the power angle diagram of the transmission system from the fundamental power equation (96) or (98*b*). It will be found that the peak value of motor power is reached at the pull-out angle $\theta = \beta = \rho$, the transfer impedance angle.

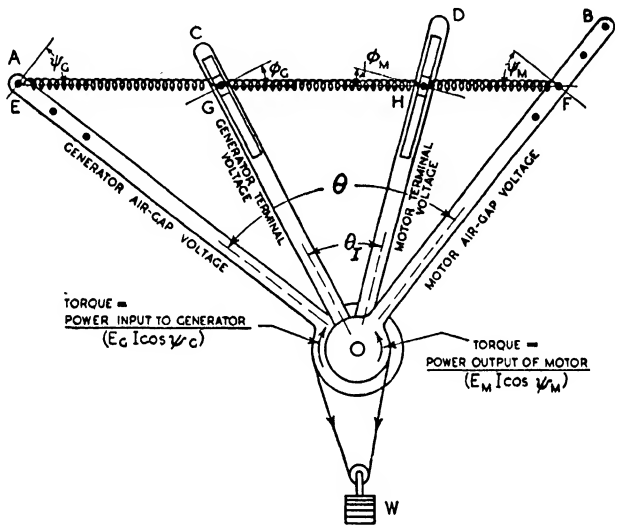

FIG. 40. MECHANICAL ANALOGUE OF AN ELECTRICAL TRANSMISSION SYSTEM

(*c*) *Method based on the Use of a Mechanical Model.* This interesting and instructive method makes use of a model which is, in effect, a mechanical transmission system that simulates very closely the action of a synchronous system of electric power transmission. The idea of a mechanical analogue is due to Griscom,[12] and the model illustrated diagrammatically in Fig. 40 is strictly analogous to the equivalent two-machine system represented by the vector diagram of Fig. 38.

The mechanical model consists essentially of four arms, *A*, *B*, *C*, and *D*, pivoted independently on a common axis *O*. Arms *A* and *B* have large hubs in which are pulley grooves,

these being spanned by a loop of cord which also passes round a small jockey pulley to which a variety of weights can be attached. The arms are linked by three springs at E, F, G, and H. The spring ends at E and F are fixed while those at G and H are free to slide in radial slots. If the arm lengths OE and OF are adjusted in proportion to the motor air-gap voltages,* E_G and E_M, then the spring extensions EG, GH, and HF will equal, to the same scale, the several reactance drops IX_G, IX_I, and IX_M of Fig. 38. Similarly, the distances of the sliding pivots G and H from the axis O will represent the terminal voltages E_S and E_R. The spring tension acting between E and F is then equivalent to the load current I, while the torque exerted by either arm A or B, being equal to the product of the arm length and the component of spring tension perpendicular to the arm, thus represents the electrical power ($P = EI \cos \psi$) at the air gap of the machine.

If now the system be gradually loaded by adding weights W to the jockey pulley, all four arms will swing stably farther and farther apart, the relative separations depending on the strengths of the several springs, until the net restoring torque due to the spring tension (i.e. the synchronizing power of the system) begins to diminish with increasing angle θ between arms A and B. A little consideration will show that this must occur when $\theta = 90°$. For, although the spring tension (load current) increases with increasing system angle up to $\theta = 180°$, the torque (electrical power) corresponding to the product of arm length and the component of spring tension at right angles to the arm increases up to $\theta = 90°$ only, beyond which angle it commences to decrease again. In fact, if the load W is raised slightly above the value required to produce a displacement angle of $\theta = 90°$ the system at once becomes unstable; the springs then suddenly go on stretching under the influence of this fixed load, and the whole system of levers falls out of balance. In other words, synchronism is lost.

The power limit of such a mechanical system can be raised by employing stronger springs, corresponding to deceased reactances X_G, X_I, and X_M in the electrical system; and by increasing the lengths of the arms, corresponding to higher

* I.e. the voltages behind the transient reactances of the machines, these being the constant elements in the majority of stability studies. In the case of steady-state stability as considered in the present chapter, OE and OF represent the excitation voltages, i.e. the voltages behind the synchronous reactances of the machines.

transmission voltages. An alternative way of increasing the power limit is to insert a rigid mechanical prop between G and H, corresponding in the electrical system to the provision of an intermediate synchronous condensor station on a long transmission line. Transient effects due to suddenly applied loads may be studied by adding increments of weight W suddenly, but without impact, while line faults may be simulated by deflecting the middle spring towards the axis O. Mechanical models of the type installed in Fig. 40 have, in fact, been successfully used to obtain quantitative as well as qualitative solutions to a number of power transmission problems.[13]

Examples of System Stability Studies. The methods of determining the steady-state stability limit of a transmission system described above relate to relatively simple systems which can be represented by an equivalent generator, an interconnector, and an equivalent motor. In many cases it is not possible to reduce a given system to such a simple equivalent. In fact, it is more than likely that the transmission system will reduce instead to an interconnector linking two equivalent generators, each with its own load. In that case it is necessary to take into account the characteristics of these loads as well as of the machines themselves. To do so, however, would be exceeding the scope of the present work. Two approximate methods of dealing with such loads are, however, given in the examples at the end of Chapter V.

Moreover, the assumption has been made that the machine reactances (i.e. $X = X_a + X_o$ in Fig. 32) are circuit constants, like the interconnector reactance, and are thus independent of the system load. That is to say, synchronous reactance has been taken as the power-limiting factor in the case of the machines; and synchronous reactance takes no account of saturation. In actual fact, however, when considering the steady-state stability limit, the inevitable saturation of the machines produces a stiffening effect equivalent to the action of a machine reactance considerably lower in value than the true synchronous reactance. This reactance is usually referred to as the "saturated synchronous reactance." Various empirical methods have been proposed for adjusting the synchronous reactance to a value commensurate with the saturation of the machine under load.[14] Here, again, it is beyond the scope of the present volume to enlarge upon these methods. Suffice it to

say that the saturated value in practice varies roughly from 60 to 80 per cent of the unsaturated value.

Example 1. *The interconnector considered in the three examples at the end of Chapter III serves to link a station containing a 60 000 kVA. generator with another station which may be regarded as being equivalent to two 25 000 kW. motors designed for full-load operation at 0·8 p.f. The generator has a synchronous reactance of 110 per cent; that of the motors is 90 per cent. Assuming 132 kV. to be maintained at the two ends of the interconnector (referred to the low-tension sides of the terminal transformers), determine the steady-state stability limit of the system. By how much would this limit be increased if all series resistance and shunt admittance were neglected?*

Solution. Referring to p. 78, the network constants of the interconnector are—

$$\mathbf{A}_I = \mathbf{D}_I = 0{\cdot}969 + j0{\cdot}00923 = 0{\cdot}969\,\underline{|0{\cdot}5^\circ}$$
$$\mathbf{B}_I = 38{\cdot}83 + j152{\cdot}22 = 157{\cdot}0\,\underline{|75{\cdot}7^\circ}$$
$$\mathbf{C}_I = (4{\cdot}24 + j405{\cdot}45) \times 10^{-6} = 405{\cdot}5 \times 10^{-6}\,\underline{|89{\cdot}4^\circ}$$

As the interconnector is symmetrical about its mid point (indicated by the fact that $\mathbf{A}_I = \mathbf{D}_I$), the auxiliary constants a and b evaluated on p. 79 apply to both sending- and receiving-end power circles. The co-ordinates of their respective centres are thus—

$$P_{S0} - jQ_{S0} = (a - jb)E_S^2 = (1{\cdot}576 - j5{\cdot}967) \times 10^{-3} \times 132^2$$
$$= \underline{27{\cdot}5 - j104{\cdot}0}\ \text{MVA.}$$

or
$$S_S\,\underline{|\psi_S} = E_S^2\sqrt{(a^2 + b^2)}\,\underline{|\tan^{-1}(-b/a)}$$
$$= 107{\cdot}5\,\underline{|-75{\cdot}2^\circ}\ \text{MVA.}$$

and
$$-P_{R0} + jQ_{R0} = (-a + jb)E_R^2 = (-1{\cdot}576 + j5{\cdot}967) \times 10^{-3} \times 132^2$$
$$= \underline{-27{\cdot}5 + j104{\cdot}0}\ \text{MVA.}$$

or
$$S_R\,\underline{|\psi_R} = E_R^2\sqrt{(a^2 + b^2)}\,\underline{|\tan^{-1}(b/-a)}$$
$$= 107{\cdot}5\,\underline{|104{\cdot}8^\circ}\ \text{MVA.}$$

The power-circle radius is in each case—

$$cE_SE_R = 0{\cdot}00637 \times 132 \times 132 = 114{\cdot}5\ \text{MVA.}$$

Fig. 41 shows the power-circle diagram in which the receiving- and sending-end circle centres are O_R and O_S respectively.

To locate the centres of the equivalent generator and motor power circles in the diagram it is first of all necessary to evaluate the appropriate network constants. Assuming a saturated reactance value equal to 70 per cent of the synchronous reactance proper, the generator reactance is—

$$X_G = \frac{0{\cdot}7 \times 1{\cdot}1 \times 132^2}{60} = 223{\cdot}6\ \text{ohms}$$

while the equivalent motor reactance is—

$$X_M = \frac{0{\cdot}7 \times 90 \times 132^2}{2 \times (25/0{\cdot}8)} = 175{\cdot}65\ \text{ohms}$$

As the machine networks in this case are simple reactances, we have—

$$\mathbf{A}_G = \mathbf{D}_G = 1;\ \mathbf{C}_G = 0;\ \mathbf{B}_G = R_G + jX_G = 0 + j223{\cdot}6$$
$$\mathbf{A}_M = \mathbf{D}_M = 1;\ \mathbf{C}_M = 0;\ \mathbf{B}_M = R_M + jX_M = 0 + j175{\cdot}65$$

The centre of the generator output circle O_G thus has co-ordinates—

$$-P_{G0} + jQ_{G0} = 0 + j\frac{E_S^2}{X_G} = 0 + j\frac{132^2}{223{\cdot}6} = \underline{0 + j77{\cdot}9}\ \text{MVAr.}$$

while the corresponding centre O_M has co-ordinates—

$$P_{M0} - jQ_{M0} = 0 - j\frac{E_R^2}{X_M} = 0 - j\frac{132^2}{175{\cdot}65} = \underline{0 - j99{\cdot}2}\ \text{MVAr.}$$

The zero-θ reference axes for the generator output and motor input power circles are thus the same, namely, the Q-axis of the diagram. In the case of the sending-end and receiving-end power circles they are the axes passing through the centres O_S and O_R and inclined to the P-axis at the transfer impedance angle $\beta_I = 75{\cdot}2°$, as shown in Fig. 41.

By choosing successive values of θ_I at 5° intervals a series of operating points is obtained, such as M and N. On joining the former to O_M and the latter to O_G the corresponding values of θ_M and θ_G may be read off directly from the diagram. For example, with $\theta_I = 30°$, as shown in Fig. 41, the vector radius O_MM gives $\theta_M = 23{\cdot}75°$, while O_GN gives $\theta_G = 39{\cdot}75°$. The system angle is thus—

$$\theta = 39{\cdot}75° + 30° + 23{\cdot}75° = 93{\cdot}5°$$

corresponding to a transmitted power $P_R = 52{\cdot}5$ MW. as given by the abscissa of the operating point M. The results are tabulated below, and the relation between P_R and θ is shown plotted in Fig. 42.

P_R	1·0	10·5	20·0	29·0	37·3	45·4	52·5	59·8	66·0	71·3	76·0	80·0	83·2	85·2	86·7	87·0	86·9
θ_I	0	5	10	15	20	25	30	35	40	45	50	55	60	65	70	75·7	80
θ_G	−0·5	7·5	16·0	23·5	30·5	36·0	39·8	43·0	45·0	46·5	47·0	47·5	47·5	47·0	46·5	45·5	45·0
θ_M	0·5	6·5	11·5	15·5	19·0	21·5	23·8	25·0	26·0	26·5	26·5	26·3	25·8	25·3	24·5	23·5	22·5
θ	0	19·0	37·5	54·0	69·5	82·5	93·5	103·0	111·0	118·0	123·5	128·8	133·3	137·3	141·0	144·7	147·5

The value of θ corresponding to the steady-state stability limit of the system is $\theta = \beta$, where β is the angle of the system transfer impedance $\mathbf{B}$. As only X_G and X_M occur in the equivalent machine networks, it is more convenient in this case to evaluate $\mathbf{B}$ by transforming the interconnector network into its equivalent $\mathbf{T}$ and then adding the machine reactances to the two arms to give an overall $\mathbf{T}$, than to use equation (125). Referring to equation (25), we have, since $\mathbf{A}_I = \mathbf{D}_I$—

$$\mathbf{Z}_1 = \mathbf{Z}_2 = \frac{\mathbf{A}_I - 1}{\mathbf{C}_I} = \frac{\mathbf{B}_I}{\mathbf{A}_I + 1}$$
$$= \frac{38{\cdot}83 + j152{\cdot}22}{1{\cdot}969 + j0{\cdot}00923} = 19{\cdot}72 + j77{\cdot}2\ \text{ohms},$$

and $$\mathbf{Y} = \mathbf{C}_I = (4{\cdot}24 + j405{\cdot}4) \times 10^{-6}\ \text{mhos}.$$

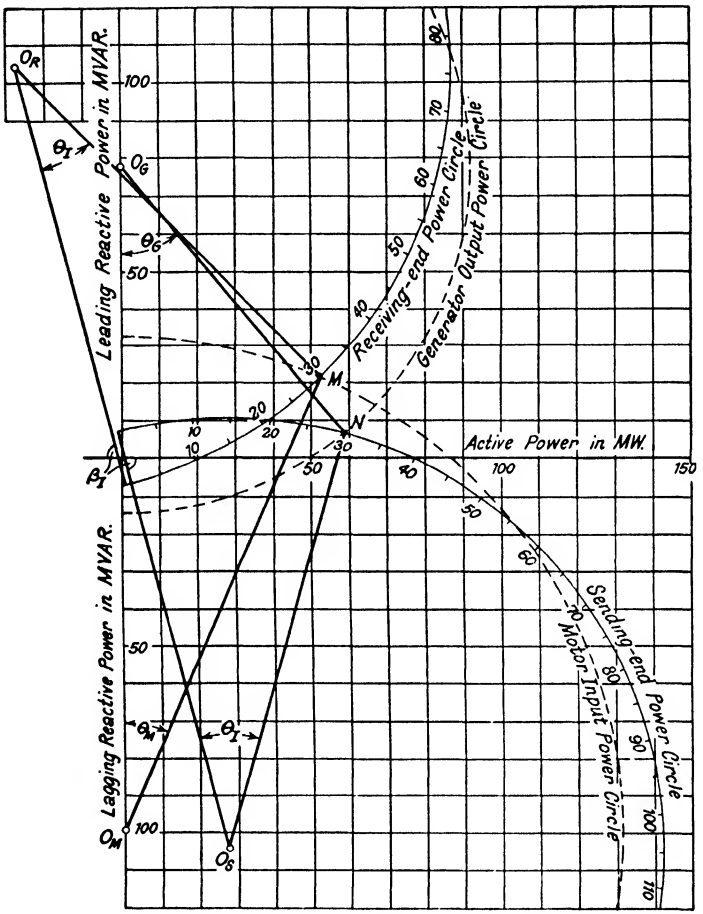

FIG. 41. POWER-CIRCLE DIAGRAM OF EXAMPLE 1

Equations (14) then give for the transfer impedance of the overall equivalent **T**-circuit—

$$\begin{aligned}\mathbf{B} &= (jX_G + \mathbf{Z}_1) + (\mathbf{Z}_2 + jX_M) + (jX_G + \mathbf{Z}_1)(\mathbf{Z}_2 + jX_M)\mathbf{Y} \\ &= (19{\cdot}72 + j300{\cdot}8) + (19{\cdot}72 + j252{\cdot}85) \\ &\quad + (19{\cdot}72 + j300{\cdot}8)(19{\cdot}72 + j252{\cdot}85)(4{\cdot}24 + j405{\cdot}4) \times 10^{-6} \\ &= (39{\cdot}43 + j553{\cdot}65) - (4{\cdot}62 + j26{\cdot}00) \\ &= 34{\cdot}81 + j527{\cdot}65 \text{ ohms.}\end{aligned}$$

Hence the pull-out angle of the system is—

$$\beta = \tan^{-1}(527{\cdot}65/34{\cdot}81) = \tan^{-1}(15{\cdot}16) = 86{\cdot}25°$$

Fig. 42 then gives $P_m = \underline{48{\cdot}25 \text{ MW.}}$ as the limiting power for steady-state stability.

If all series resistance and shunt admittance be neglected, then the interconnector may be replaced by a lumped reactance $X_I = (X_{TS} + X_L + X_{TR})$. Referring to Example 1 on p. 78, it is seen that—

$$X_{TR} = 27{\cdot}59 + (150 \times 0{\cdot}669) + 27{\cdot}59 = 155{\cdot}54 \text{ ohms}$$

Equation (114) then gives for the steady-state power limit—

$$P_m = \frac{132^2\sqrt{[(223{\cdot}6 + 77{\cdot}77)\,(175{\cdot}65 + 77{\cdot}77)]}}{77{\cdot}77^2 + (301{\cdot}37 \times 253{\cdot}42)}$$

$$= \frac{132^2 \times \sqrt{76\,385}}{82\,434} = \underline{58{\cdot}43 \text{ MW.}}$$

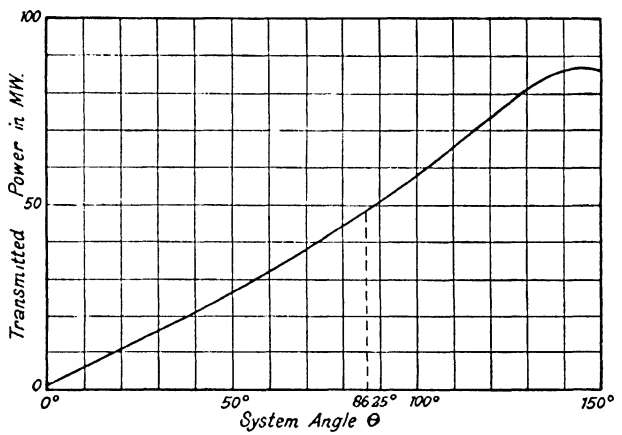

FIG. 42. RELATION BETWEEN TRANSMITTED POWER AND SYSTEM ANGLE

By considering reactance only, therefore, the maximum transmitted power consonant with steady-state stability appears 21 per cent greater than is actually the case.

Example 2. *Plot power/angle diagrams for the case of the previous example,* (a) *for the interconnector alone, and* (b) *for the transmission system as a whole. Hence determine the power limits of the interconnector and the system, and the corresponding pull-out angles.*

Solution. (*a*) The interconnector power/angle diagram may be plotted directly from the tabulated data of the previous example, for the transmitted power is—

$$P_R = \frac{E_S E_R}{B_I}\cos(\theta_I - \beta_I) - \frac{A_I E_R^2}{B_I}\cos(\alpha_I - \beta_I)$$

$$= \frac{132 \times 132}{157}\cos(\theta_I - 75{\cdot}7°) - \frac{0{\cdot}969 \times 132^2}{157}\cos(0{\cdot}5° - 75{\cdot}7°)$$

$$= 114{\cdot}5 \sin(\theta_I + 14{\cdot}3°) - 27{\cdot}5$$

which is the equation of the receiving-end power circle of Fig. 41. The power/angle diagram is shown in Fig. 43, from which $P_{max} = 87$MW. and $\theta_1 = 75{\cdot}7°$.

(*b*) Here it is necessary to find E_G and E_M, for the equivalent motor power output is given by—

$$P_M = \frac{E_G E_M}{B}\cos(\theta - \beta) - \frac{AE_M^2}{B}\cos(\alpha - \beta)$$

$$= \frac{E_G E_M}{528{\cdot}5}\cos(\theta - 86{\cdot}25°) - \frac{0{\cdot}878E_M^2}{528{\cdot}5}\cos(0{\cdot}65° - 86{\cdot}25°)^*$$

$$= \frac{E_G E_M}{528{\cdot}5}\sin(\theta + 3{\cdot}75°) - \frac{E_M^2}{15\,685} \quad . \quad . \quad . \quad . \quad (128)$$

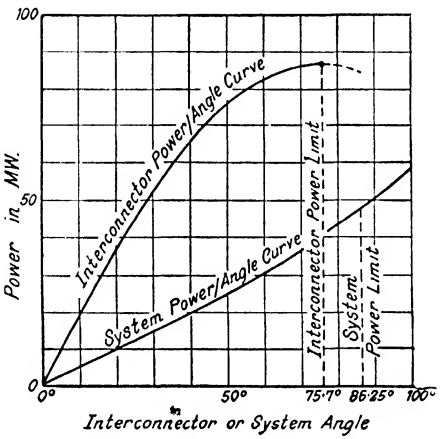

FIG. 43. POWER/ANGLE DIAGRAMS FOR SYSTEM AND INTERCONNECTOR

The pull-out angle is here clearly $\theta = 86{\cdot}25°$, but this angle does not necessarily correspond to any maximum value of P_M. For, with conditions of constant E_S and E_R, the excitation voltages E_G and E_M are variable, i.e. are themselves functions of the power transmitted. The appropriate values of E_G and E_M can be obtained from the power-circle diagram of Fig. 41 and equations (126) and (127), the latter giving—

$$E_G = \frac{223{\cdot}6}{132} \times O_G N = 1{\cdot}694 \times O_G N$$

and

$$E_M = \frac{175{\cdot}65}{132} \times O_M M = 1{\cdot}393 \times O_M M$$

The results are tabulated below and shown plotted in Fig. 43. With $\theta = 86{\cdot}25°$ one finds $P_M = 48$ MW., which is in close agreement with

* The network constant $\mathbf{A} = A\underline{|\alpha}$ is found from equations (22) to be $\mathbf{A} = \mathbf{A}_1 + jX_G\mathbf{C}_1 = 0{\cdot}878 + j0{\cdot}0102 = 0{\cdot}878\,\underline{|0°{\cdot}65}$.

the value obtained previously. Actually, in this particular case, $P_G = P_S$ and $P_M = P_R$, because the machines have been assumed to have no losses, so that this power/angle curve should be identical with that of Fig. 42, which gives $P_{max} = 87$ MW.

$\delta°$	0	19·0	37·5	54·0	69·5	82·5	93·5	103·0
E_G kV	120	116	118	123	132	143	156	180
E_M kV	128	132	139	149	160	173	184	197
P_m MW	0·9	9·2	18·9	28·0	36·6	44·9	51·9	64·3

References

(1) See, for example, A. Leonhard: "Stability Conditions in the Operation of Asynchronous Machines over Long Transmission Lines," *Elektrotechnik und Maschinenbau*, 1938, Vol. 56, p. 405; and *ibid.*, 1939, Vol. 57, p. 77.

(2) *Vide* H. Rissik: "Alternator Performance," *Electrical Review*, 1938, Vol. 122, p. 243.

(3) *Cf.* M. G. Say: *The Performance and Design of Alternating Current Machines*, p. 421 (Pitman, London, 1948).

(4) *Op. cit.*, Fig. 271.

(5) *Vide* C. F. Wagner and R. D. Evans: "Static Stability Limits and the Intermediate Condenser Station," *Trans. A.I.E.E.*, 1928, Vol. 47, p. 94.

(6) O. G. C. Dahl: *Electric Power Circuits*, Vol. 2, pp. 71–5 (McGraw Hill Publishing Co., London, 1938).

(7) *Cf.* Edith Clarke: "Steady-state Stability in Transmission Systems," *Trans. A.I.E.E.*, 1926, Vol. 45, p. 22.

(8) *Cf.* H. B. Dwight: "A Graphical Solution of Steady-state Stability," *Electrical Engineering*, 1934, Vol. 53, p. 566.

(9) *Cf.* H. Rissik: "Transmission Systems," *Electrician*, 1939, Vol. 122, p. 138.

(10) C. A. Nickle, *Trans. A.I.E.E.*, 1926, Vol. 45, p. 1; Edith Clarke, *ibid.*, p. 22; W. W. Lewis, *Transmission Line Engineering* (McGraw Hill Book Co., New York, 1928).

(11) *Vide* Reference (6), p. 60.

(12) *Vide* Reference (5).

(13) *Vide* S. B. Griscom: "A Mechanical Analogy to the Problem of Transmission Stability," *Elec. Journal*, 1926, Vol. 23, p. 230; also R. C. Bergvall and P. H. Robinson: "Quantitative Analysis of Power System Disturbances," *Trans. A.I.E.E.*, 1928, Vol. 47, p. 915.

(14) *Cf.* C. Kingsley, Jr.: "Saturated Synchronous Reactance," *Trans. A.I.E.E.*, 1935, Vol. 54, p. 300.

CHAPTER V

TRANSIENT STABILITY

THE problem of transient stability is concerned with the behaviour of a transmission system during disturbances or under abnormal conditions of operation. What is termed the transient stability limit is simply the maximum power that can be transmitted without loss of synchronism when a sudden change occurs that radically alters the transmission system in some way. The distinction between the concepts of steady-state and transient stability is thus nothing other than that between continuity and discontinuity in the process of power interchange. Under steady-state conditions synchronism may be lost as the result of a continuous change in the direction of increasing system load. Whereas under transient conditions loss of synchronism may, and not infrequently does, occur as the result either of a discontinuous change in the amount of power transmitted, or else of a change in value of the electrical constants of the transmission system which, in the last analysis, determine the power transmitting capacity of the system.

Discontinuous changes making for transient instability may thus be grouped in three categories—

1. Sudden changes in load, i.e. load switching or loss of a synchronous machine.
2. Circuit operations, e.g. switching out a section of a multi-circuit transmission line.
3. System faults, i.e. the incidence and subsequent clearing of a short circuit, whether occurring directly, or indirectly as the result of a lightning stroke.

The limit of transient stability during such system changes may in certain circumstances coincide with the steady-state stability limit although in general it will be much less. For example, if the circuit arrangements of an interconnected system are such that the continued loss of any synchronous tie can be tolerated, then the maximum power that can be transmitted over the interconnector is limited only by considerations of steady-state stability. This situation has arisen in many instances in America where "synchronizing at the load" has been applied to metropolitan power systems. With this

particular method of interconnection there are no direct ties between the synchronous machines of the system, but only indirect ties through a multiplicity of connections at substation or utilization voltages. The same principle has been considered in connection with long-distance transmission projects, when it involves bussing of the system on the low-voltage side only at the receiving end. Since the operation of such a system contemplates the disconnection of an entire unit, comprising generator and interconnector (including terminal transformers), on the occurrence of any fault, it is evident that transient instability need scarcely be considered and that each unit may be operated close to its steady-state stability limit.

In the vast majority of power systems, however, the limit of steady-state stability can serve only as a guide to the power limit that may actually be approached by improvements in apparatus and in the circuit and operating arrangements of the transmission system. Past experience has gone to show that the maximum power that can be transmitted without loss of synchronism throughout the incidence and subsequent clearing of a severe fault on the system, such as a line-to-line or a double line-to-ground fault near the generators, is seldom more than about 70 per cent of that determined from considerations of steady-state stability. In other words, when the change in power transmitted—whether direct; or indirect, as the result of an alteration in the transfer impedance of the system—is of a transient nature, the limit of stability for the transmission system is of necessity lower than the steady-state stability limit. And it is not too much to say that the intensity of research devoted in recent years to the study of transient stability problems has been inspired by the thought of closing the gap between these two power limits.[1]

Fundamental Conceptions. In general, system stability, under fault conditions, or any other conditions which alter the system network, depends upon—

1. The ability of the system circuits to transmit adequate synchronizing power, and
2. The inertias of the various machines.

When a fault occurs on the system, the short-circuit currents flowing into the fault are predominantly reactive, so that the generator outputs suddenly change from active to reactive power. The abrupt fall in synchronizing power output causes a momentary acceleration of each machine whose magnitude

is determined by the rotor inertia. The net result is an increase in system angle which may or may not be checked. If it is checked by the flow of sufficient synchronizing power, the system angle will oscillate about its future normal position, corresponding to the new circuit conditions obtaining when the fault is cleared, and the system will remain stable. On the other hand, if the increase in system angle continues unchecked, then synchronism will ultimately be lost as the result of system instability.

Under transient conditions of this kind, as contrasted with conditions of steady-state operation, the incremental changes in machine speed are so rapid that the field flux-linkages remain sensibly constant. Hence the air-gap voltage, i.e. the voltage behind the so-called transient reactance of the machine, is virtually fixed in magnitude during a disturbance; only its phase relationship to some arbitrary reference vector is susceptible of change. In considering abrupt changes in this phase relationship the effect of machine inertia is paramount. For, during the period under investigation, the governor of the prime mover has not sufficient time to alter the mechanical input to the generator, while the effect of asynchronous damping torques may be neglected. It is not often realized that the moments of inertia involved in transient stability problems are of very considerable magnitude. For example, the kinetic energy stored in a 50 000 kVA. turbo-alternator running at 1 500 r.p.m. is about the same as that of a train weighing 300 tons and travelling at a mile a minute, viz. of the order of 350 000 kW.-sec. And it would take some 14 seconds for such a machine to come to rest under the influence of an opposing torque equal to that developed at full load.

The concept of transient stability, then, is bound up with the storage and release of kinetic energy during the very brief interval of time in which a system disturbance occurs, and is thus primarily concerned with the behaviour of rotating masses as influenced by sudden changes in applied torque. As explained in Chapter IV, when discussing the dynamic criterion of steady-state stability, the equation of motion of a machine rotor is—

$$\frac{d^2\theta}{dt^2} = \frac{\omega \,.\, \Delta P}{2W} \quad . \quad . \quad . \quad . \quad (129a)$$

$$= (180 f/HP_n)\, \Delta P \quad . \quad . \quad (129b)$$

$$= \Delta P/M \quad . \quad . \quad . \quad . \quad (129c)$$

where ΔP is the instantaneous power differential causing acceleration, W is the kinetic energy stored in the rotor at synchronous speed, P_n is the machine rating, H is the energy stored per unit of machine rating, and M is the so-called *inertia constant* of the machine. The angular acceleration $d^2\theta/dt^2$ is expressed in electrical degrees per second per second* and the machine rating in kVA., so that the inertia constant has the dimensions kW./deg./sec.^{2} It is, in fact, the power differential that will give unit acceleration to the machine rotor. A little consideration will show that M is equal to the angular momentum of the rotor at synchronous speed; while $2H$ is nothing other than the time taken for the rotor to come to rest from synchronous speed under the influence of an opposing torque equal to that developed at full load.† The stored energy W is expressed in kilowatt-seconds, and is given by—

$$W = 0{\cdot}231\, J\, (N/1\,000)^2 \text{ kW.-sec.}$$

where J is the moment of inertia of the rotor in lb.-ft.^{2}, and N is the synchronous speed of the machine in r.p.m.

The power differential ΔP is, by definition, the instantaneous difference between the mechanical power exerted at the rotor shaft and the electrical power developed in the air gap, that is—

$$\Delta P = P_M - P_E \quad . \quad . \quad . \quad (130)$$

As mechanical power (input) and electrical power (output) are both reckoned positive, in the case of a generator an excess of P_M over P_E will make ΔP *positive*, and hence will give rise to *acceleration* of the rotor. Conversely, in the case of a motor, for which mechanical power (output) and electrical power (input) are both negative, if P_M is numerically greater than P_E, then ΔP will be *negative*, resulting in *retardation* of the machine rotor. Substitution of equation (130) in equation (129*c*) gives—

$$M\frac{d^2\theta}{dt^2} = P_M - P_E \quad . \quad . \quad . \quad (131)$$

as the fundamental equation of motion of a synchronous machine. Solution of this equation enables the angle θ between the air-gap voltage and some arbitrary reference voltage to be

* This is the most practical form of expression. If θ is in radians instead of in degrees, then the factor 180 in equation (129*b*) must be replaced by π. (See also footnote on p. 158.)

† For $M = \frac{2W}{\omega} = \frac{2(\frac{1}{2}J\omega^2)}{\omega} = J\omega$. Similarly, $2H = \frac{2W}{P_n} = \frac{J\omega^2}{\omega T_n} = \frac{J\omega}{T_n}$.

evaluated in terms of time t. As already mentioned, the relation between θ and t is of paramount importance to the transient stability of a synchronous system. In fact, *the ultimate criterion of system stability is that θ should be a periodic function of t for all machines in the system.*

As a rule, an interconnected system will contain a number of machines (or machine groups that can be replaced by equivalent machines), in which case the complexity of the transient stability problem increases with the number of actual or equivalent machines being considered as separate entities. For one thing, the electrical output P_E of any given machine is a function of the phase position of its air-gap voltage relative to the air-gap voltages of *all* the other machines: while it also depends upon the magnitudes of these voltages, as well as upon the transfer impedances between them and the air-gap voltage of the machine considered. As the result, the establishing of a transient stability criterion for a multi-machine system is fraught with immense practical difficulties, and the problem is virtually insoluble if the number of machines exceeds four. Equations have been developed for the power output of a generator in the multi-machine case,[2] and examples of their application to the three-machine and four-machine problems have been published.[3] In all such cases, however, a solution of equation (131) is only possible by step-by-step methods involving the expenditure of a great deal of time and labour, even when certain simplifying assumptions are made. Hence when considering the transient stability of an interconnected system the endeavour should always be made to reduce the problem to that of a two-machine system. For then, and only then, is it possible to establish a simplified stability criterion based on the power/angle diagram.

When discussing this simple transmission system in the preceding chapter it was assumed throughout that the receiving-end machine was an equivalent motor. In the transient analysis which follows, this assumption will be abandoned, and the general case will be considered where two generators, supplying their own load networks, are free to interchange power over a general impedance network representing the synchronous interconnector between them. Corresponding quantities appropriate to the two machines will be denoted by the subscripts 1 and 2, and it will furthermore be assumed that the air-gap voltage of machine 1 leads that of machine 2,

i.e. that machine 1 sends power over the interconnector to machine 2. The fundamental machine equations are then—

$$\left.\begin{aligned} M_1\,(d^2\theta_1/dt^2) &= P_{M_1} - P_{E_1} = \Delta P_1 \\ M_2\,(d^2\theta_2/dt^2) &= P_{M_2} - P_{E_2} = \Delta P_2 \end{aligned}\right\} \quad . \quad . \quad (132)$$

The angle between the air-gap voltages of the machines—in other words, between the machine rotors—is $\theta = (\theta_1 - \theta_2)$. The relative acceleration of the machine rotors is thus given by—

$$\frac{d^2\theta}{dt^2} = \frac{d^2\theta_1}{dt^2} - \frac{d^2\theta_2}{dt^2} = \frac{\Delta P_1}{M_1} - \frac{\Delta P_2}{M_2} \quad . \quad . \quad (133)$$

which gives—

$$\frac{d}{dt}\cdot\left(\frac{d\theta}{dt}\right)^2 = 2\,\frac{d\theta}{dt}\cdot\frac{d^2\theta}{dt^2} = 2\left(\frac{\Delta P_1}{M_1} - \frac{\Delta P_2}{M_2}\right)\frac{d\theta}{dt}.$$

Integrating both sides, one obtains—

$$\left(\frac{d\theta}{dt}\right)^2 = 2\int_{\theta_0}^{\theta}\left(\frac{\Delta P_1}{M_1} - \frac{\Delta P_2}{M_2}\right)d\theta$$

where θ_0 is the steady-state system angle at time $t = 0$. The angular velocity with which the machines swing apart as the result of their relative acceleration is consequently—

$$\frac{d\theta}{dt} = \sqrt{\left[2\int_{\theta_0}^{\theta}\left(\frac{\Delta P_1}{M_1} - \frac{\Delta P_2}{M_2}\right)d\theta\right]}.$$

The machines will continue to swing apart, i.e. the angular separation θ between their air-gap voltages will go on increasing, unless and until their relative velocity $d\theta/dt$ becomes zero. Hence the machines will come to rest with respect to each other if and when:

$$\int_{\theta_0}^{\theta}\left(\frac{\Delta P_1}{M_1} - \frac{\Delta P_2}{M_2}\right)d\theta = 0 \quad . \quad . \quad (134)$$

Equation (134) expresses the fundamental criterion of transient stability in a two-machine system, established originally by Park and Bancker in their classic paper [4] entitled "System Stability as a Design Problem," for it specifies the condition that must be satisfied if the system angle is to be a periodic function of time. This simplified stability criterion may be stated as follows—

If, as the result of a discontinuous change in the system transfer power, the machines of a two-machine system swing apart, then

*the system will remain stable, provided the machines come to rest with respect to each other.**

The stability criterion expressed by equation (134) is applicable to any two-machine system. We shall first of all consider its application in the ideal case where the system contains reactance only, deferring consideration of the general two-machine system to a later section of the present chapter. Equations (95) and (96) then give for the power outputs of the two machines—

$$P_{E_1} = \frac{E_1 E_2}{X} \sin\theta = P_m \sin\theta \quad . \quad . \quad (135)$$

$$P_{E_2} = -\frac{E_1 E_2}{X} \sin\theta = -P_m \sin\theta \quad . \quad (136)$$

where E_1 and E_2 are the air-gap voltages of the machines, θ is the angle between them, X is the total system reactance, and P_m is the maximum transfer power. Also, as under steady-state conditions $P_{M1} = P_{E1}$ and $P_{M2} = P_{E2}$, equations (135) and (136) lead to the further relation $P_{M1} = -P_{M2} = P_M$ (say). Hence

$$\Delta P_1 = -\Delta P_2 = P_M - P_m \sin\theta \quad . \quad . \quad (137)$$

The equation of motion of the system is then—

$$\frac{d^2\theta}{dt^2} = \frac{\Delta P_1}{M_1} - \frac{\Delta P_2}{M_2} = \left(\frac{1}{M_1} + \frac{1}{M_2}\right)(P_M - P_m \sin\theta)$$

$$= \frac{1}{M}(P_M - P_m \sin\theta)$$

$$\text{or} \quad M\frac{d^2\theta}{dt^2} = P_M - P_m \sin\theta \quad . \quad . \quad . \quad . \quad . \quad (138)$$

$$\text{where} \quad M = \frac{M_1 M_2}{M_1 + M_2} \quad . \quad . \quad . \quad . \quad . \quad . \quad (139)$$

Equation (138) is at once recognized as the equation of motion of a synchronous machine, whose inertia constant is defined by equation (139) and whose air-gap voltage is separated by the

* The implication here is that they come to rest at the end of the first swing of the damped oscillation which, under conditions of transient stability, characterizes the change in system angle from the initial to the future steady-state value. Or, to put the matter in another way, the above stability criterion is based on the assumption that, if the system disturbance does result in instability, then synchronism will be lost during the attempted first swing. Experience goes to show that, in the majority of cases, this assumption is justifiably made.

system angle θ from the arbitrary reference voltage.* In other words, it is the equation of motion of a synchronous generator located at the sending end of the system and supplying power to an infinite bus at the receiving end. This fictitious or "equivalent" machine has the same mechanical input and electrical output as the actual machines, and differs from them only in its inertia constant, which has a value obtained by "paralleling" the inertia constants of the actual machines. The absolute acceleration of this fictitious machine is then the same as the relative acceleration of the actual machines.

Thus a two-machine system containing reactance only can be replaced by an *equivalent system having a single generator at the sending end and an infinite bus at the receiving end.* This equivalence theorem† is of immense practical importance, for it leads at once to a graphical expression of the stability criterion defined by equation (134), based on the power/angle diagram of a synchronous machine connected to an infinite bus.

The "Equal Area" Stability Criterion. In general, if we put $\Delta P_1 = -\Delta P_2 = \Delta P$, where ΔP is defined by equation (138), the equation of motion of the equivalent machine replacing the two machines in an ideal transmission system containing reactance only becomes simply—

$$\frac{d^2\theta}{dt^2} = \frac{\Delta P}{M} \quad . \quad . \quad . \quad . \quad (140)$$

where M is the equivalent inertia constant defined by equation (139). The angular velocity with which the actual machines swing apart then becomes the angular velocity with which this equivalent machine separates from an idealized machine of infinite inertia and zero impedance which is the physical representation of an infinite bus. Or, putting the matter somewhat differently, the rate of separation of the machine air-gap voltages E_1 and E_2 is unaffected by considering E_1 as the air-gap voltage of the equivalent machine and E_2 as the voltage of the infinite bus. This velocity of separation is defined by the relation—

$$\left(\frac{d\theta}{dt}\right)^2 = \frac{2}{M}\int_{\theta_0}^{\theta} \Delta P \, . \, d\theta \quad . \quad . \quad . \quad (141)$$

* *Cf.* Equation (131).

† As will be shown later, this theorem also holds in the case of the general two-machine system, for which the machine inputs and outputs at the two ends of the system are no longer the same.

The integral in equation (141) represents an area, namely, the area under the differential power/angle curve $\Delta P = F(\theta)$ between the limits θ_0 and θ. The physical meaning to be attached to this representation is not far to seek. For the inertia constant M is nothing other than the angular momentum of the equivalent machine rotor at the synchronous speed $\omega = 360f$, and is thus equal to $J\omega$, where J is its moment of inertia. Equation (141) may thus be put in the form—

$$\tfrac{1}{2}J\left(\frac{d\theta}{dt}\right)^2 = \frac{1}{\omega}\int_{\theta_0}^{\theta} \Delta P \,.\, d\theta = \int_{\theta_0}^{\theta} \Delta T \,.\, d\theta \qquad . \quad (142)$$

It is at once seen that the left-hand side of this equation is the gain in kinetic energy of the machine rotor due to the acceleration $d^2\theta/dt^2$; while the right-hand side is the area under the differential torque/angle curve $\Delta T = (1/\omega)\, F(\theta)$ between the limits θ_0 and θ, and is thus the work done on the machine rotor in accelerating it from its initial angle θ_0 to the new angle θ.

The fundamental stability criterion expressed by equation (134), when applied to the ideal two-machine system, i.e. a transmission system containing reactance only, thus reduces to the simple form—

$$\int_{\theta_0}^{\theta} \Delta P \,.\, d\theta = 0 \qquad . \quad . \quad . \quad (143)$$

This is, however, still an implicit criterion, for the angle of separation reached by the two machines when they come to rest with respect to each other at the end of their first swing apart—the upper limit of integration θ in equation (143), that is—still remains to be defined. An explicit criterion of transient stability is accordingly to be obtained only by introducing a further condition, defining the specific angle θ at which the machines come to rest with respect to each other. A little consideration will show that this condition is simply that *the power differential ΔP be negative or, in the limit, zero.* Because if ΔP is still positive when the machines have come to rest with respect to each other, they will commence to swing apart once more, eventually falling out of synchronism. On the other hand, if ΔP is negative, then relative retardation will occur after the machines have come to rest with respect to each other, with the result that they will swing together and the system will remain stable; while if ΔP is zero the stability will

be critical, for the oscillation of the machines will have died out completely at the end of their first swing apart, i.e. it is aperiodic.

(*a*) *Transient Stability with Increased System Load.* The conditions necessary for transient stability according to the criterion expressed by equation (143) in conjunction with $\Delta P \gtrless 0$, are most easily studied by considering the case where the steady-state equilibrium of the system is disturbed by a sudden increase in the steam supply to the prime mover of the

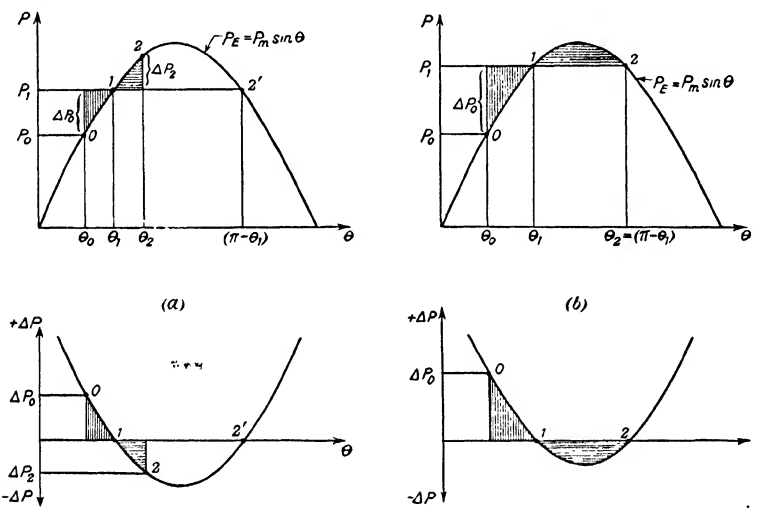

FIG. 44. TRANSIENT STABILITY DURING SUDDEN INCREASE IN SYSTEM LOAD

equivalent generator. Referring to the upper diagram of Fig. 44 (*a*), the undisplaced sinusoid $P_E = P_m \sin\theta$ represents the power/angle curve of the equivalent generator, with $P_m = E_1E_2/X$ where E_1 and E_2 are the air-gap voltages of the sending- and receiving-end machines and X is the aggregate system reactance acting between them. Under steady-state operating conditions the system angle is θ_0 and the power input to the generator is $P_0 = P_m \sin\theta_0$,* represented by the operating point 0 in the power/angle diagram. Suppose now the mechanical input be suddenly increased from P_0 to P_1, for

* In the ideal system here considered, where $P_{E_1} = -P_{E_2}$ and $P_{M_1} = -P_{M_2}$, all these four quantities are numerically equal to P_0, since initially $\Delta P_0 = 0$.

which the new steady-state angle is θ_1. This condition is represented in the power/angle diagram by the point 1, and is defined by $P_1 = P_m \sin \theta_1$. The instantaneous power differential producing acceleration of the machines is thus—

$$\Delta P = P_1 - P_E = P_m (\sin \theta_1 - \sin \theta) \quad . \quad (144)$$

The differential power/angle curve represented by equation (144) is shown plotted in the lower diagram of Fig. 44 (*a*).

Assuming the machines to come to rest with respect to each other when $\theta = \theta_2$, represented by the operating point 2 in the power/angle diagram of Fig. 44 (*a*), equation (143) gives as the criterion of transient stability—

$$\int_{\theta_0}^{\theta_2} \Delta P \, . \, d\theta = \int_{\theta_0}^{\theta_2} P_m (\sin \theta_1 - \sin \theta) \, d\theta = 0$$

i.e. $$(\theta_2 - \theta_0) \sin \theta_1 + \cos \theta_2 - \cos \theta_0 = 0$$

or $$\cos \theta_2 + \theta_2 \sin \theta_1 = \cos \theta_0 + \theta_0 \sin \theta_1 \quad . \quad . \quad (145)$$

The angle θ_2 at which the machines finally come to rest during their first swing apart is then defined by the condition that $\Delta P \gtrless 0$ when $\theta = \theta_2$, i.e. that $\sin \theta_1 \gtrless \sin \theta_2$ or $\theta_1 \gtrless (\pi - \theta_2)$. The limit of transient stability is reached (see Fig. 44 (*b*)) when θ_2 attains the critical value $(\pi - \theta_1)$. The stability limit is thus explicitly defined by equation (145) with $\theta_2 = (\pi - \theta_1)$, giving—

$$(\pi - \theta_1 - \theta_0) \sin \theta_1 = \cos \theta_1 + \cos \theta_0 \quad . \quad (146)$$

or, approximately—

$$\sin \theta_1 = 0{\cdot}724 + 0{\cdot}276 \sin \theta_0 \quad . \quad . \quad (146a)$$

For any given value of θ_0, corresponding to a given input P_0, there is thus a limiting value of P_1 which, if exceeded, results in loss of synchronism through transient instability. Or, to put the matter in another way, if the system is initially transmitting a certain power $P_0 = P_m \sin \theta_0$, the limiting value to which the power transmitted can be suddenly raised without the shock causing synchronism to be subsequently lost is—

$$P_1 = P_m \sin \theta_1 = 0{\cdot}724 \, P_m + 0{\cdot}276 \, P_0$$

$$= \left(0{\cdot}276 + \frac{0{\cdot}724}{\sin \theta_0} \right) P_0 \, . \quad . \quad . \quad . \quad (147)$$

This critical relation between P_1 and P_0 is shown by Fig. 45.

The physical significance of the explicit stability criterion expressed by equation (146) will be understood by considering

the mechanism of the disturbance to the system caused by the sudden increment in power input $\Delta P = (P_1 - P_0)$. As the result of the excess* of power input P_1 over the initial steady-state power output $P_0 = P_m \sin \theta_0$, the rotor of the equivalent generator will accelerate and thus advance in phase (relative to the infinite bus) towards some new equilibrium position for which $P_1 = P_m \sin \theta_1$, where θ_1 is the new steady-state system

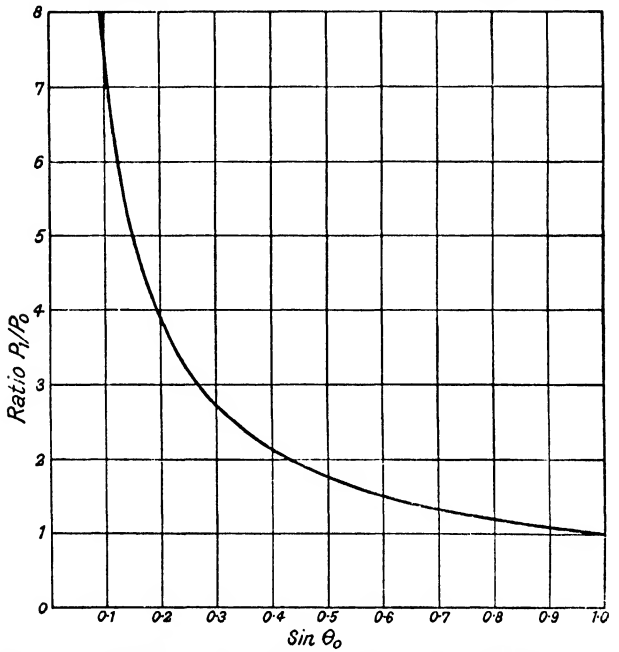

FIG. 45. RELATION BETWEEN SUDDENLY APPLIED AND INITIAL LOADS FOR SYSTEM STABILITY

angle. Now, the acceleration of the machine rotor from θ_0 to θ_1 occupies a finite time, during which the rotor gains in kinetic energy. The amount of gain is—

$$\int_{t_0}^{t_1} \Delta P \,.\, dt = \frac{1}{\omega}\int_{\omega t_0}^{\omega t_1} \Delta P \,.\, d(\omega t) = \frac{1}{\omega}\int_{\theta_0}^{\theta_1} \Delta P \,.\, d\theta$$

$$= \frac{1}{\omega}\int_{\theta_0}^{\theta_1} (P_1 - P_m \sin \theta)\, d\theta$$

* Due to an assumed increase in the steam supply to the prime mover of the equivalent generator.

which is proportional to the area between the input line $P = P_1$ and the power/angle curve $P = P_m \sin \theta$ between the limits θ_0 and θ_1, shown vertically shaded in Fig. 44 (*a*). This gain in kinetic energy is manifested by a corresponding increase in speed, so that by the time the rotor reaches its future equilibrium position it will be revolving at something more than synchronous speed. The rotor consequently overshoots this position and tends to reach a still further advanced position *which may lie beyond the limiting angle for steady-state stability*, $\theta = 90°$. However, during this part of the swing the power differential ΔP is negative,* as may be seen by reference to the lower diagram of Fig. 44 (*a*), so that the rotor is being retarded. Retardation continues, becoming more and more rapid as θ increases, as the result of which the rotor slows down and eventually regains the original synchronous speed. By this time the rotor has advanced to some angle θ_2. During its advance from θ_1 to θ_2 the deficiency of mechanical input to the machine rotor was being made good by the release of the kinetic energy stored during the preceding interval. The loss of kinetic energy is—

$$\int_{t_1}^{t_2} \Delta P \, . \, dt = \frac{1}{\omega}\int_{\omega t_1}^{\omega t_2} \Delta P \, . \, d(\omega t) = \frac{1}{\omega}\int_{\theta_1}^{\theta_2} \Delta P \, . \, d\theta$$

$$= \frac{1}{\omega}\int_{\theta_1}^{\theta_2} (P_1 - P_m \sin \theta) \, d\theta$$

which is proportional to the area between the input line $P = P_1$ and the power/angle curve $P = P_m \sin \theta$ between the limits θ_1 and θ_2, shown horizontally shaded in Fig. 44 (*a*). In the absence of rotor damping, all the kinetic energy stored during the interval from θ_0 to θ_1 is released during the subsequent interval from θ_1 to θ_2. The net gain in kinetic energy between the instants when the rotor was initially revolving at synchronous speed (at $\theta = \theta_0$) and when it has subsequently regained synchronous speed (at $\theta = \theta_2$) is therefore nil. Hence—

$$\frac{1}{\omega}\int_{\theta_0}^{\theta_1} (P_1 - P_m \sin \theta) \, d\theta + \frac{1}{\omega}\int_{\theta_1}^{\theta_2} (P_1 - P_m \sin \theta) \, d\theta = 0$$

or

$$\int_{\theta_0}^{\theta_2} (P_1 - P_m \sin \theta) \, d\theta = \int_{\theta_0}^{\theta_2} \Delta P \, . \, d\theta = 0$$

which is the fundamental stability criterion of equation (143).

* i.e. the electrical output of the machine $P_E = P_m \sin \theta$ is greater than its mechanical input $P_M = P_1$.

The amount of overshoot from θ_1 to θ_2, before the rotor of the equivalent machine returns to synchronous speed—that is, before the actual machines have come to rest with respect to each other—is thus determined by the condition that the two shaded areas in Fig. 44 (*a*) be equal or, what amounts to the same thing, that the input line $P = P_1$ should be the mean ordinate to the power/angle curve $P = P_m \sin \theta$ between the limits $\theta = \theta_0$ and $\theta = \theta_2$. Hence—

$$P_1 (\theta_2 - \theta_0) = \int_{\theta_0}^{\theta_2} P_m \sin \theta \, . \, d\theta = P_m (\cos \theta_0 - \cos \theta_2)$$

which, with $P_1 = P_m \sin \theta_1$, is the same result as equation (145). Furthermore, it will be observed from Fig. 44 (*a*) that the machine rotor, having reached the end of its first swing at $\theta = \theta_2$, will only seek to return to its future equilibrium position provided that at that instant it is still undergoing retardation, i.e. that the operating point 2 on the power/angle curve is still above the input line ($\Delta P < 0$). The limiting position of the operating point in Fig. 44 (*a*) is thus 2′, where the power differential producing retardation becomes zero. Hence transient stability is only assured provided *the area under the power/angle curve and above the input line is greater than or, in the limit, equal to the area between the power/angle curve, the input line, and the ordinate through the initial operating point.* This is the so-called "equal area" criterion of transient stability. Expressed in another way, it states that the limit of transient stability is reached when the input line is the mean ordinate to the power/angle curve between the ordinate $\theta = \theta_0$ and the ordinate through their point of intersection, where $\theta_2 = (\pi - \theta_1)$. This means that—

$$P_1 (\pi - \theta_1 - \theta_0) = \int_{\theta_0}^{(\pi - \theta_1)} P_m \sin \theta \, . \, d\theta = P_m (\cos \theta_1 + \cos \theta_0)$$

which is the same result as equation (146), as is to be expected.

Under transient conditions, then, the maximum swing of the machines consistent with stability is not limited to the peak of the power/angle curve as is the case under steady-state conditions. At the same time the extreme angle of separation may not exceed the value $(\pi - \theta_1)$, where θ_1 is defined by equation (146).

(*b*) *Transient Stability with Circuit Switching.* Having discussed the "equal area" criterion of transient stability in the

elementary case of a transmission system subjected to a sudden increase in load,* let us next apply this criterion to the important practical case of a disturbance to the system brought about by a switching operation. The fact that a transmission system including a double-circuit interconnector may become unstable when one of the parallel circuits is switched out, even though the system load may be less than the steady-state power limit of the system under the new circuit conditions, is illustrated by Fig. 46. The upper power/angle curve $P_E = P_m \sin\theta$ shows the initial relation between transmitted power and system angle. The lower curve $P_E' = P_m' \sin\theta$

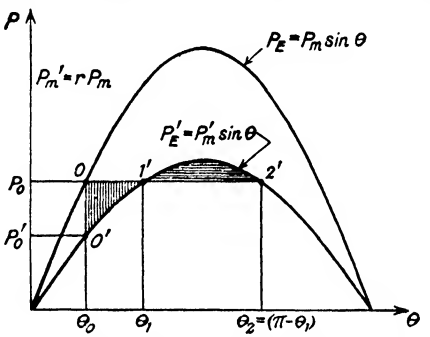

FIG. 46. TRANSIENT STABILITY DURING SWITCHING OF A PARALLEL TRANSMISSION CIRCUIT

shows the relation between the two after the transmission system has been changed by switching out one interconnector circuit. Here $P_m = E_1E_2/X$ is the maximum transfer power before switching, while $P'_m = E_1E_2/X'$ is the lower value attained by it after switching. For the result of the switching operation is to increase the system transfer reactance from its initial value X to some new value X' which is considerably greater.

In the power/angle diagram of Fig. 46 the initial equilibrium position is represented by the operating point 0, for which the mechanical power input to the equivalent generator P_0 is balanced by the electrical power output $P_m \sin\theta_0$. After

* The two-machine system considered above may equally well be represented by an equivalent motor at the receiving end and an infinite bus at the sending end, when an increase in mechanical power from P_0 to P_1 corresponds to a direct increase in the system load. In that case the power/angle diagrams of Fig. 44 are reversed with respect to the θ-axis, since both P_M and P_E are negative for a motor. The analysis is the same in either case.

switching (assumed to occur instantaneously) the operating point becomes 0′, corresponding to the lower value of transfer power $P_m' \sin \theta_0$. The effect on the system is the same as if the initial equilibrium position had been at 0′, for which $P_0' = P_m' \sin \theta_0$, and the generator input had suddenly been increased by the amount $\Delta P_0 = (P_0 - P_0')$. The stability limit is thus given by equator (146) when referred to the lower power/angle curve. If r denote the peak transfer-power ratio P_m'/P_m, that is—

$$r = \frac{\text{transfer reactance before switching}}{\text{transfer reactance after switching}}$$

then the maximum load P_0 which the system can carry throughout the switching operation, without loss of synchronism occurring as the result, is—

$$\begin{aligned} P_0 &= P_m' \sin \theta_1 = rP_m \sin \theta_1 \\ &= rP_m (0{\cdot}724 + 0{\cdot}276 \sin \theta_0) \end{aligned}$$

as given by equation (146*a*). Hence—

$$\sin \theta_0 = P_0/P_m = r (0{\cdot}724 + 0{\cdot}276 \sin \theta_0)$$

from which
$$\sin \theta_0 = \frac{0{\cdot}724r}{1 - 0{\cdot}276r} \quad . \quad . \quad . \quad . \quad (148)$$

giving
$$P_0 = \frac{0{\cdot}724rE_1E_2}{(1 - 0{\cdot}276r)X} \quad . \quad . \quad . \quad . \quad (149)$$

as the transient stability limit. The relation expressed by equations (148) and (149) is shown in Fig. 47. It is evident that for $0 < r < 1$ the transient stability limit is always less than the steady-state stability limit.

(*c*) *Transient Stability with System Faults.* Probably the most important type of transient disturbance to which a transmission system may be subjected is the discontinuous change in power transfer brought about by a fault on the system. From the point of view of applying the "equal area" stability criterion to this type of disturbance it is necessary to distinguish between a fault on a feeder and a fault on one of two or more parallel transmission circuits. In the former case the transmission system reverts to its initial steady-state condition upon the clearing of the fault. In the latter case it operates under a new steady-state condition brought about by the switching out of the faulty circuit.

The transient conditions obtaining throughout the incidence and subsequent clearing of a fault on a feeder, whether at the

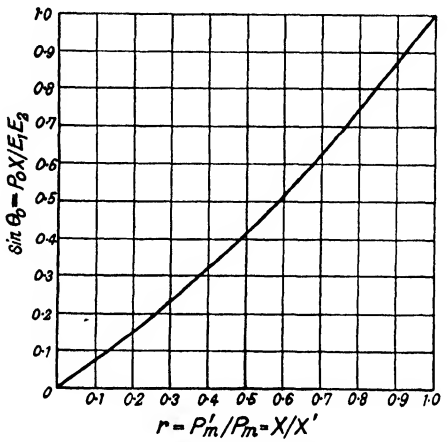

FIG. 47. TRANSIENT STABILITY CHARACTERISTIC FOR A DISCONTINUOUS CHANGE IN SYSTEM TRANSFER REACTANCE

sending or receiving end of the system, are shown by the power/angle diagram of Fig. 48. As before, the operating point 0 corresponds to the initial steady-state condition for which

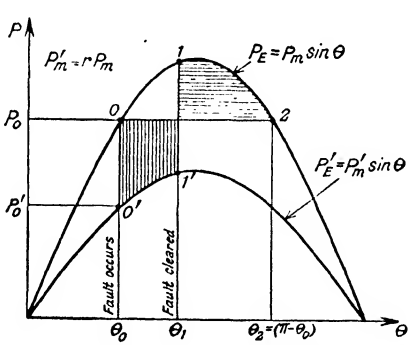

FIG. 48. TRANSIENT STABILITY WITH FAULT ON A FEEDER

$P_0 = P_m \sin \theta_0$. Upon the occurrence of the fault the transfer reactance of the system increases from X to X', so that the operating point becomes 0′, for which the available synchronizing power is only $P_0' = P_m' \sin \theta_0 = rP_m \sin \theta_0$, where $r = P_m'/P_m = X/X'$ as before. The instantaneous power

differential $\Delta P = (P_0 - P_m' \sin\theta)$ then causes a relative acceleration of the machines at the two ends of the system, the aggregate kinetic energy gained being represented by the area between the "separating-power line" $P = P_0$ and the "synchronizing power/angle curve" $P = P_m' \sin\theta$. Assuming the fault to be cleared at the instant when the angle separating the machines has reached the value $\theta = \theta_1$, corresponding to the operating point 1′ in Fig. 48, the transfer reactance at once reverts to its initial value, so that the operating point suddenly changes to 1. As the result, the power differential becomes $\Delta P = (P_0 - P_m \sin\theta)$, which in this case is negative, causing a relative retardation of the machines. This retardation continues until the machines reach the end of their first swing apart, represented by the operating point 2, when they finally come to rest with respect to each other. The system will be stable if the kinetic energy released during the interval from $\theta = \theta_1$ to $\theta = \theta_2$ is greater than the kinetic energy gained during the preceding interval from $\theta = \theta_0$ to $\theta = \theta_1$. The stability limit is reached with that value of θ_1 which makes the net gain of kinetic energy during the first swing zero, i.e. which makes the vertically and horizontally shaded areas of Fig. 48 equal.

The "equal area" stability criterion in this case implies that the separating-power line $P = P_0$ should be the mean ordinate to the operative portions of the two power/angle curves, $P_E' = P_m' \sin\theta$ and $P_E = P_m \sin\theta$. Hence—

$$P_0(\theta_2 - \theta_0) = \int_{\theta_0}^{\theta_1} P_m' \sin\theta \,.\, d\theta + \int_{\theta_1}^{\theta_2} P_m \sin\theta \,.\, d\theta$$

$$\text{i.e. } (\pi - 2\theta_0)\, P_m \sin\theta_0 = P_m \left[r \int_{\theta_0}^{\theta_1} \sin\theta \,.\, d\theta + \int_{\theta_1}^{\pi - \theta_0} \sin\theta \,.\, d\theta \right]$$

$$\text{or} \qquad (\pi - 2\theta_0) \sin\theta_0 = r(\cos\theta_0 - \cos\theta_1) + \cos\theta_0 + \cos\theta_1$$
$$= (1 + r)\cos\theta_0 + (1 - r)\cos\theta_1$$

The limiting value of θ_1, the angle of separation reached by the machines when the fault is cleared, is thus given by—

$$\cos\theta_1 = \frac{(\pi - 2\theta_0)\sin\theta_0 - (1 + r)\cos\theta_0}{(1 - r)} \quad . \quad (150)$$

This is termed the *critical clearing angle* for transient stability.

It is evident that if the fault is sustained, so that $\theta_1 > \theta_2$, there is only one discontinuity (viz. at $\theta = \theta_0$), and the conditions illustrated in Fig. 46 then apply. The value of P_0 is then determinate. But in the general case illustrated in

Fig. 48, P_0 is a function of θ_1. Clearly if P_0 is increased, then θ_1 must be decreased if the two shaded areas in Fig. 48 are to remain equal, that is to say, *the greater the system load, the quicker must the fault be cleared if the system is to remain stable.* This is perhaps self-evident; but it cannot be definitively proved except by transient stability analysis. Curves relating the limiting system load P_0 to the critical clearing angle θ_1 or, more precisely, to the time interval between $\theta = \theta_0$ and $\theta = \theta_1$, are known as "stability curves" and are of great importance in the practical study of interconnected systems under transient conditions.

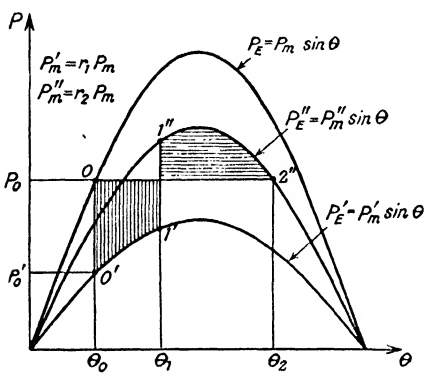

FIG. 49. TRANSIENT STABILITY WITH FAULT ON A TRANSMISSION CIRCUIT

The most general case to which the "equal area" stability criterion can be applied is, however, that of a fault occurring on one circuit of a double-circuit interconnector. Here the clearing of the fault results in one of the two circuits being isolated, so that a new condition of steady-state operation thereafter obtains. This case is illustrated in Fig. 49. As before, the initial steady-state condition is represented by the operating point 0 in the power/angle diagram, for which $P_0 = P_m \sin \theta_0$. The occurrence of the fault brings about the first discontinuity in power transfer, as the result of which the operating point becomes 0', for which $P_0' = P_m' \sin \theta_0 = r_1 P_0$, where $r_1 = P_m'/P_m = X/X'$ or—

$$r_1 = \frac{\text{transfer reactance before the fault}}{\text{transfer reactance during the fault}}$$

The power differential $\Delta P = (P_0 - r_1 P_m \sin \theta)$ then produces relative acceleration of the machines so that they swing apart to some angle $\theta = \theta_1$, when the fault is cleared by the opening of the circuit-breakers at the two ends of the circuit (i.e. a transmission line, or a section thereof if the line is sectionalized). The clearing of the fault brings about a second discontinuity in power transfer, namely, the sudden increase in available

synchronizing power from the value $r_1P_m \sin \theta_1$ to a new value $r_2P_m \sin \theta_1$, where $r_2 = P_m''/P_m = X/X''$ or—

$$r_2 = \frac{\text{transfer reactance before the fault}}{\text{transfer reactance after the fault}}$$

The operating point in the power/angle diagram thus changes from 1′ to 1″, the latter point lying not on the initial power/angle curve as in Fig. 48, but upon the curve $P_E'' = P_m'' \sin \theta$, corresponding to a value of system reactance X'' intermediate between the faulted value X' and the pre-fault value X. The synchronizing power demand is henceforward greater than the power input to the system, resulting in a relative retardation of the machines, which finally come to rest with respect to each other at a maximum angle of separation θ_2 defined by $P_0 = P_m'' \sin \theta_2$, corresponding to the operating point 2″ in the power/angle diagram.

The angular separation of the machines at the end of their first swing apart is thus given by—

$$\sin \theta_0 = \frac{P_0}{P_m''} = \frac{P_m \sin \theta_0}{r_2 P_m} = \frac{1}{r_2} \sin \theta_0$$

i.e.
$$\theta_2 = \pi - \sin^{-1}\left(\frac{\sin \theta_0}{r_2}\right) \quad . \quad . \quad . \quad (151)$$

which reduces to $\theta_2 = (\pi - \theta_0)$ when $r_2 = 1$, as in the preceding case where $X'' = X$. The "equal area" stability criterion is then that—

$$\int_{\theta_0}^{\theta_1} (P_0 - P_m' \sin \theta) d\theta + \int_{\theta_1}^{\theta_2} (P_0 - P_m'' \sin \theta) d\theta = 0$$

i.e.
$$P_0 (\theta_1 - \theta_0) - r_1 P_m (\cos \theta_0 - \cos \theta_1) + P_0 (\theta_2 - \theta_1) - r_2 P_m (\cos \theta_1 - \cos \theta_2) = 0$$

which, with $P_0 = P_m \sin \theta_0$, gives—

$$\cos \theta_1 = \frac{(\theta_2 - \theta_0) \sin \theta_0 - r_1 \cos \theta_0 + r_2 \cos \theta_2}{r_2 - r_1} \quad . \quad . \quad (152)$$

$$= \frac{\sin \theta_0 [\pi - \theta_0 - \sin^{-1}(\sin \theta_0 / r_2)] - r_1 \cos \theta_0 - \sqrt{(r_2^2 - \sin^2 \theta_0)}}{r_2 - r_1} \quad (152a)$$

an expression which reduces to the form given by equation (150) when $r_2 = 1$.

The stability criterion established by equation (152) or (152*a*) defines the critical clearing angle θ_1 as that particular value

of θ at the second discontinuity which makes the horizontally shaded area in Fig. 49, representing the kinetic energy of the system released during the retardation interval, equal to the vertically shaded area representing the kinetic energy acquired by the system during the preceding acceleration interval, which followed upon the incidence of the fault. In other words, the critical angle θ_1 must be such that the separating power line $P = P_0$ is the mean ordinate to the operative portions of the power/angle curves $P_E' = P_m' \sin \theta$ and $P_E'' = P_m'' \sin \theta$. If the mean ordinate lies above the separating power line, the system will be stable; if it lies below this line, the system will be unstable. This is tantamount to expressing the transient stability criterion as equality between the fixed separating power P_0 and the *average* synchronizing power $(1/\Delta\theta) \int P d\theta$ throughout the interval represented by the increase in angular separation $\Delta\theta$ during the first swing apart of the machines. The "equal area" stability criterion may accordingly be stated thus:—

A transmission system can only regain synchronism after a disturbance provided the average synchronizing power during the first swing of the machines exceeds the separating power during the same period.*

For then, and only then, will the machines oscillate about their future relative position in the steady state.

A special case which is of considerable importance is that of a three-phase busbar fault at either the sending or receiving end of the transmission system. In that case all flow of power past the fault is cut off, for the fault reactance is zero and the transfer reactance of the system X' is in consequence infinite.† Hence P_m' and $r_1 = P_m'/P_m$ are both zero. When the fault is cleared, by switching out of the appropriate bus section and the interconnector circuit connected to it, the transfer reactance again falls to some value X'' intermediate between X' $(= \infty)$, and X. This case is illustrated by Fig. 50.

The critical clearing angle is given by equation (152) with $r_1 = 0$, which becomes—

$$\cos \theta_1 = \frac{(\theta_2 - \theta_0) \sin \theta_0 + r_2 \cos \theta_2}{r_2} \quad . \quad . \quad (153)$$

* Strictly speaking, the *average* separating power. For it is only in the ideal case here considered, in which the transmission system contains reactance only, that the separating power remains constant. (*Cf.* Figs. 49 and 55.)

† See p. 173, equation (204), in which X_e becomes zero.

or $$\cos \theta_1 = (\theta_2 - \theta_0) \sin \theta_2 + \cos \theta_2 \quad . \quad . \quad (154)$$

where θ_2 is given by equation (151).

The General Two-machine System. As already mentioned, the fundamental stability criterion expressed by equation (134) is applicable to any two-machine system. In the ideal case so far considered, the series reactance of the system alone has been taken into account, an assumption which can only give an approximation to the actual conditions obtaining in practice but which, nevertheless, is very frequently made in stability studies by reason of the simplicity of the resulting transient analysis. Where greater accuracy is required, the series resistance as well as the shunt admittances of the system must also be taken into account, in which case the "equal area"

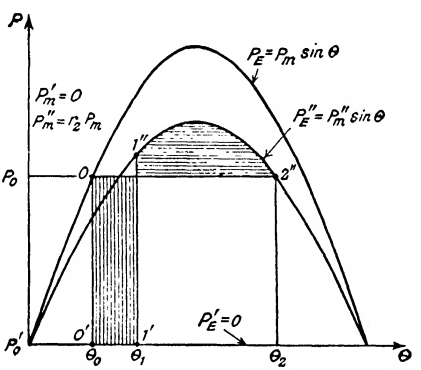

FIG. 50. TRANSIENT STABILITY WITH THREE-PHASE BUSBAR FAULT

criterion of limiting transient stability at first sight does not appear to be directly applicable as such. For equation (137), upon which is based the reduction of the actual two-machine system to an equivalent machine connected to an infinite bus, is then no longer valid. As the result, it would seem necessary to establish a simplified stability criterion from equation (134), making use of two actual power/angle diagrams in place of the one equivalent diagram.

As will be shown later, however, it is still possible to establish an equivalence that makes it possible in turn to apply the "equal area" stability criterion directly to the general two-machine case. Consequently the earlier method, based upon an analysis which treats the two machines separately, may now be regarded as having been superseded by a later and much

less laborious method based upon a generalized equivalent machine connected to an infinite bus through an impedance network of a quite general character. The earlier method of transient analysis is, nevertheless, of importance in that it brings home more clearly the essentials of the problem involved in the determination of transient stability, namely, the joint action of the two machines in the storage and release of kinetic energy and the dependence of synchronizing power on the characteristics of both machines as well as of the interconnector between them. A brief discussion of this fundamental method of analysis is thus not out of place here, if only as an introduction to the more practical method making use of an equivalent single-machine system.

In the general case of a two-machine system the electrical outputs of the two machines are no longer given by equations (135) and (136), but become*—

$$P_{E_1} = \frac{E_1^2}{Z_1}\sin\sigma_1 + \frac{E_1E_2}{Z}\sin(\theta-\sigma)$$
$$= P_{D1} + P_m\sin(\theta-\sigma) \quad . \quad . \quad . \quad (155)$$

and
$$P_{E_2} = \frac{E_2^2}{Z_2}\sin\sigma_2 - \frac{E_1E_2}{Z}\sin(\theta+\sigma)$$
$$= P_{D2} - P_m\sin(\theta+\sigma) \quad . \quad . \quad . \quad (156)$$

Here P_{D1} and P_{D2} are the driving-point power outputs of the two machines and P_m is the maximum transfer power between them, i.e. the *maximum synchronizing power* of the system. If P_{M_1} and P_{M_2} denote the mechanical inputs to the machines, then—

$$\Delta P_1 = (P_{M_1} - P_{D1}) - P_m\sin(\theta-\sigma)$$
$$= P_{0_1} - P_m\sin(\theta-\sigma) \quad . \quad . \quad . \quad (157)$$

and
$$\Delta P_2 = (P_{M_2} - P_{D2}) + P_m\sin(\theta+\sigma)$$
$$= P_{0_2} + P_m\sin(\theta+\sigma) \quad . \quad . \quad . \quad (158)$$

where P_{01} and P_{02} are the so-called *separating powers* of the two machines. Hence equation (134) becomes—

$$\int_{\theta_0}^{\theta}\left[\frac{P_{01} - P_m\sin(\theta-\sigma)}{M_1} - \frac{P_{02} + P_m\sin(\theta+\sigma)}{M_2}\right]d\theta = 0 \quad (159)$$

To apply the "equal area" stability criterion it is first of all necessary to plot the power/angle curves for the conditions obtaining (*a*) before the fault, (*b*) during the fault, and (*c*) after

* *Cf.* Chapter IV, equations (95) to (100) inclusive.

the fault, from equations (155) and (156). By including the input lines $P = P_{M1}$ and $P = P_{M2}$ on the resulting power/angle diagram (see Fig. 51) the power differentials $\Delta P_1 = (P_{M1} - P_{E1})$ and $\Delta P_2 = (P_{M2} - P_{E2})$ can be read off for successive values of system angle θ, and hence curves of $\left(\frac{\Delta P_1}{M_1} - \frac{\Delta P_2}{M_2}\right)$ can be plotted

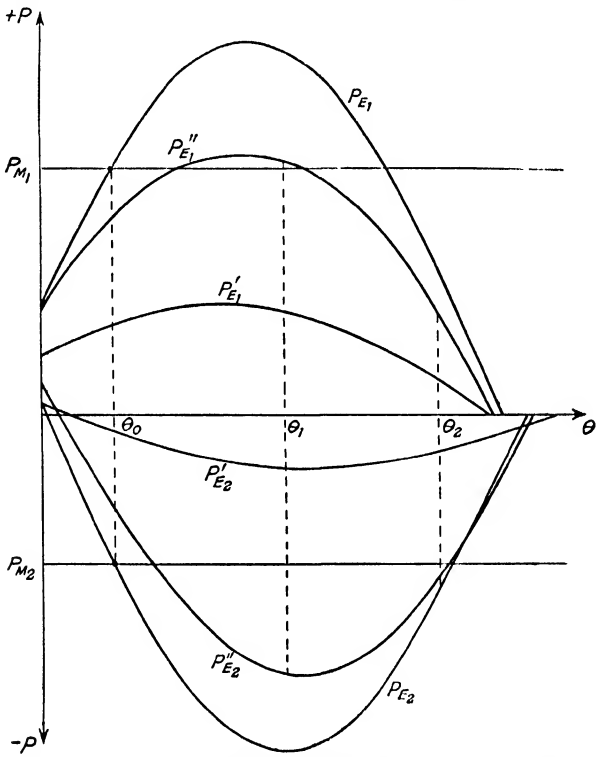

FIG. 51. POWER/ANGLE DIAGRAM FOR THE GENERAL TWO-MACHINE SYSTEM

in terms of θ. The actual curves required depend on the nature of the problem. Taking the case illustrated in Fig. 49 for the ideal two-machine system, one curve is required for condition (*b*) above and one for condition (*c*). These two curves are shown in Fig. 52. The second curve intersects the zero axis at $\theta = \theta_2$ in accordance with the requirement that, for critical stability, the relative acceleration as given by equation (133)

should be zero at the end of the first swing. The critical clearing angle θ_1 is then that particular value of θ, lying between θ_0 and θ_2, which makes the vertically and horizontally shaded areas in Fig. 52 equal.

It is seen that this indirect method of applying the "equal area" stability criterion is essentially a graphical method, requiring the plotting of eight separate curves. The time and labour involved in determining the critical clearing angle are accordingly considerable, even when the power/angle diagram is plotted from three power-circle diagrams, corresponding to the three conditions enumerated above, instead of from three

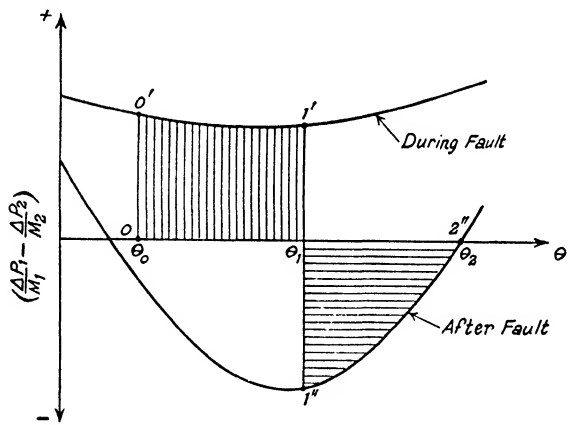

FIG. 52. THE "EQUAL AREA" STABILITY CRITERION APPLIED TO THE GENERAL TWO-MACHINE SYSTEM

sets of equations such as (155) and (156). The only possibility of calculating the critical angle θ_1 directly is that the bracketed expression in equation (159) be reducible to the elementary form $\Delta P/M$, where ΔP is some simple function of the actual machine inputs and outputs and M is a function of the actual machine inertias. In that case the stability criterion would refer to an equivalent single machine, as in the ideal two-machine system considered in the preceding section.

It will be remembered that the reduction of the ideal two-machine system to an equivalent single-machine system, comprising a generator at the sending end and an infinite bus at the receiving end (or vice versa), was rendered possible by the fact that, when the transmission system contains reactance

only, the sending-end machine operates as a generator and the receiving-end machine as a motor.* As the result, the equivalent machine must have the same mechanical input as the actual machine which it replaces; and the electrical characteristics of the equivalent circuit are the same as those of the actual transmission circuit linking the two machines. As was first shown by Dahl,[5] it is possible to establish a similar equivalence in the case of the general two-machine system. In other words, the solution of any two-machine stability problem can be based on a single power/angle curve, but with the distinction that in the general case the input to the equivalent machine is a function of the inputs to the two actual machines, and that the power/angle curve relates to a modified transmission circuit whose characteristics depend on the machine inertias as well as upon the electrical characteristics of the actual transmission system. This general equivalence, then, makes it possible to apply the "equal area" stability criterion directly to any two-machine system.

The acceleration of the equivalent generator is in this general case obtained by putting equation (133) in the form—

$$\frac{d^2\theta}{dt^2} = \frac{\Delta P_1}{M_1} - \frac{\Delta P_2}{M_2} = \frac{M_2 \,.\, \Delta P_1 - M_1 \,.\, \Delta P_2}{M_1 M_2} = \frac{\Delta P}{M} \quad . \quad (160)$$

where $M = M_1 M_2/(M_1 + M_2)$ is the inertia constant of the equivalent machine, as before, and ΔP is the *equivalent power differential* defined by—

$$\begin{aligned}
\Delta P &= \frac{M_2 \,.\, \Delta P_1 - M_1 \,.\, \Delta P_2}{M_1 + M_2} \\
&= \frac{M_2}{M_1 + M_2}[P_{M1} - P_{D1} - P_m \sin(\theta - \sigma)] \\
&\qquad - \frac{M_1}{M_1 + M_2}[P_{M2} - P_{D2} + P_m \sin(\theta + \sigma)] \\
&= \frac{M_2 P_{M1} - M_1 P_{M2}}{M_1 + M_2} - \frac{M_2 P_{D1} - M_1 P_{D2}}{M_1 + M_2} \\
&\quad - \frac{P_m}{M_1 + M_2}[M_2 \sin(\theta - \sigma) + M_1 \sin(\theta + \sigma)] \quad . \quad (161)
\end{aligned}$$

* That this must be so is evident from energy considerations alone. For other loads, represented by shunt impedances at the two ends of the system, are by hypothesis excluded from a system containing reactance only.

The first term in equation (161) is the *equivalent mechanical input*—

$$P_M = \frac{M_2 P_{M1} - M_1 P_{M2}}{M_1 + M_2} \quad . \quad . \quad . \quad . \quad . \quad (162)$$

while the second term is the *equivalent driving-point power*—

$$P_D = \frac{M_2 P_{D1} - M_1 P_{D2}}{M_1 + M_2}$$

$$= \frac{M_2 \frac{E_1^2}{Z_1} \sin \sigma_1 - M_1 \frac{E_2^2}{Z_2} \sin \sigma_2}{M_1 + M_2} \quad . \quad . \quad . \quad (163)$$

The third term in (161) is the *equivalent synchronizing power*—

$$P_S = P_m \left(\sin \theta \cos \sigma + \frac{M_1 - M_2}{M_1 + M_2} \cos \theta \sin \sigma \right)$$

$$= P_\mu \sin (\theta + \mu) \quad . \quad . \quad . \quad . \quad . \quad (164)$$

where $$P_\mu = \frac{P_m}{M_1 + M_2} \sqrt{(M_1^2 + M_2^2 + 2M_1 M_2 \cos 2\sigma)}$$

$$= P_m \sqrt{(1 - \frac{4M^2}{M_1 M_2} \sin^2 \sigma)} \quad . \quad . \quad . \quad (165)$$

and $$\tan \mu = \left(\frac{M_1 - M_2}{M_1 + M_2} \right) \tan \sigma \quad . \quad . \quad . \quad . \quad (166)$$

The equation of motion of the equivalent generator is thus—

$$M \frac{d^2\theta}{dt^2} = \Delta P = P_M - P_D - P_\mu \sin (\theta + \mu)$$

$$= P_0 - P_\mu \sin (\theta + \mu) \quad . \quad . \quad . \quad . \quad (167)$$

where $$P_0 = P_M - P_D = \frac{M_2 P_{o1} - M_1 P_{o2}}{M_1 + M_2} \quad . \quad . \quad (168)$$

is the *equivalent separating power*. Fig. 53 shows the power/angle diagram of the actual two-machine system, based on equations (155) to (158). The corresponding diagram for the equivalent generator, based on equations (162) to (167), is shown in Fig. 54.

Equations (161), (163) and (164) give for the *equivalent electrical output*—

$$P_E = P_D + P_\mu \sin (\theta + \mu) \quad . \quad . \quad (169)$$

which is the usual form of power/angle equation for a generator supplying power to an infinite bus. The steady-state power

limit of the equivalent system is attained when the equivalent synchronizing power reaches its maximum value, which occurs when $\theta = (\pi/2 - \mu)$, i.e. when—

$$\tan\theta = \cot\mu = \left(\frac{M_1 + M_2}{M_1 - M_2}\right)\cot\sigma$$
$$= \left(\frac{M_1 + M_2}{M_1 - M_2}\right)\frac{X}{R}. \quad . \quad . \quad . \quad (170)$$

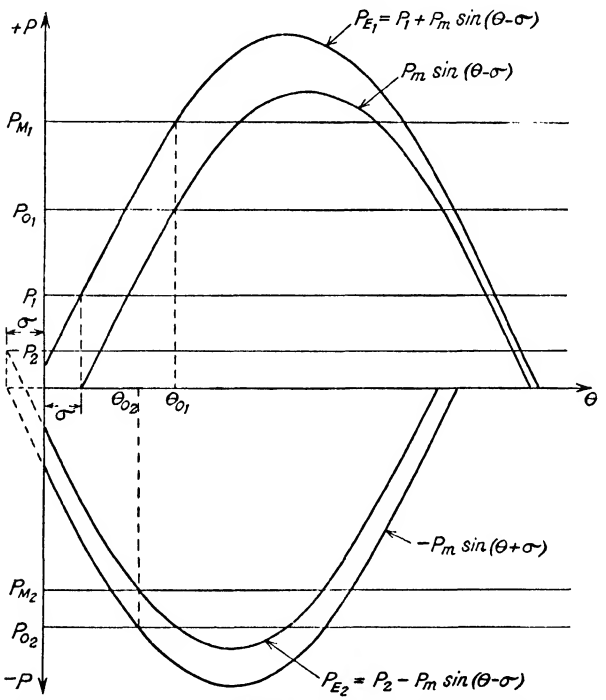

FIG. 53. POWER/ANGLE DIAGRAM OF THE GENERAL TWO-MACHINE SYSTEM

where X and R are the reactance and resistance components of the transfer impedance of the system, $\mathbf{Z} = Z \angle \rho$. This steady-state stability criterion is nothing other than the dynamic criterion established in Chapter IV, for equation (170) is identical with equation (109).*

* Except that equation (109) is stated in terms of stored energy $W = \frac{1}{2}\omega M$ instead of M.

It will be observed that in the special case where $M_1 = M_2$ $(= \frac{1}{2}M)$, the equivalent input becomes $P_M = \frac{1}{2}(P_{M1} - P_{M2})$, the equivalent driving-point power becomes $P_D = \frac{1}{2}(P_{D1} - P_{D2})$, and the equivalent synchronizing power becomes—

$$P_s = P_m \cos\sigma \sin\theta = \frac{E_1 E_2}{X\left(1 + \frac{R^2}{X^2}\right)} \sin\theta \quad . \quad (171)$$

which is the average synchronizing power of the system as given by equation (102).

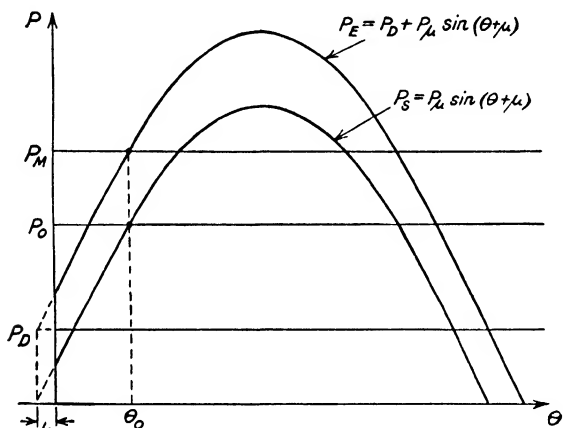

FIG. 54. POWER/ANGLE DIAGRAM OF THE EQUIVALENT SYSTEM

In order to apply the "equal area" criterion of stability on the basis of equation (167) it is first of all necessary to evaluate the equivalent separating power as given by equation (168) for the three system conditions governed by the transfer impedances **Z**, **Z**′, and **Z**″ and the corresponding driving-point impedances $\mathbf{Z}_1$, $\mathbf{Z}_1'$ and $\mathbf{Z}_1''$, and $\mathbf{Z}_2$, $\mathbf{Z}_2'$, and $\mathbf{Z}_2''$. Under pre-fault conditions the separating power is—

$$P_0 = \frac{1}{M_1 + M_2}\left[M_2\left(P_{M1} - \frac{E_1^2}{Z_1}\sin\sigma_1\right) - M_1\left(P_{M2} - \frac{E_2^2}{Z_2}\sin\sigma_2\right)\right]$$

$$= \frac{1}{M_1 + M_2}\left[M_2(P_{M1} - Y_1 E_1^2) - M_2\,(P_{M2} - Y_2 E_2^2)\right] \quad (172)$$

where $Y_1 = \sin \sigma_1 / Z_1$ and $Y_2 = \sin \sigma_2 / Z_2$. Under fault conditions the separating power changes to the value—

$$P_0' = P_M - P_D' = (P_M - P_D) + (P_D - P_D')$$
$$= P_0 + \frac{M_2 E_1^2 (Y_1 - Y_1') - M_1 E_2^2 (Y_2 - Y_2')}{M_1 + M_2} \quad . \quad (173)$$

Similarly, the separating power after the fault has been cleared becomes—

$$P_0'' = P_0 + \frac{M_2 E_1^2 (Y_1 - Y_1'') - M_1 E_2^2 (Y_2 - Y_2'')}{M_1 + M_2} \quad . \quad (174)$$

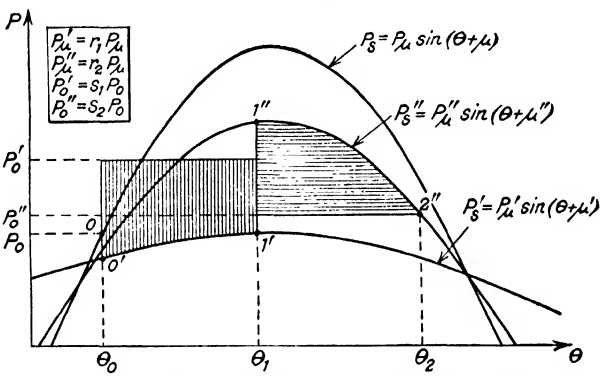

FIG. 55. TRANSIENT STABILITY WITH SYSTEM FAULT (EQUIVALENT SYSTEM)

Here Y_1' and Y_2', and Y_1'' and Y_2'', are respectively the values of Y_1 and Y_2 while the fault is on the system and after the fault is cleared.

Referring to Fig. 55, the accelerating power differential while the fault is on is—

$$\Delta P' = P_0' - P_\mu' \sin(\theta + \mu')$$
$$= s_1 P_0 - r_1 P_\mu \sin(\theta + \mu')$$

where $r_1 = \dfrac{\text{maximum synchronizing power during the fault}}{\text{maximum synchronizing power before the fault}}$

and $s_1 = \dfrac{\text{separating power during the fault}}{\text{separating power before the fault}}$

while μ' is the displacement angle of the synchronizing-power sinusoid during the fault.

Similarly, the retarding power differential after the fault is cleared is—

$$\begin{aligned}\Delta P'' &= P_0'' - P_\mu'' \sin(\theta + \mu'') \\ &= s_2 P_0 - r_2 P_\mu \sin(\theta + \mu''),\end{aligned}$$

where $r_2 = \dfrac{\text{maximum synchronizing power after the fault}}{\text{maximum synchronizing power before the fault}}$

and $s_2 = \dfrac{\text{separating power after the fault}}{\text{separating power before the fault}}$,

while μ'' is the displacement angle of the synchronizing-power sinusoid after the fault. The initial system angle θ_0 is given by the steady-state condition $\Delta P_0 = 0$, i.e $P_0 = P_\mu \sin(\theta_0 + \mu)$, from which—

$$\theta_0 = \sin^{-1}(P_0/P_\mu) - \mu \quad . \quad . \quad . \quad (175)$$

The system angle θ_2 at the end of the first swing is similarly given by the condition that $\Delta P_2 < 0$ or, in the limit, $\Delta P_2 = 0$. This limiting condition leads to the relation

$$s_2 P_0 = r_2 P_\mu \sin(\theta + \mu'')$$

from which—

$$\theta_2 = \pi - \mu'' - \sin^{-1}\left[\frac{s_2}{r_2}\sin(\theta_0 + \mu)\right] \quad . \quad (176)$$

The "equal area" conception of the transient stability limit then defines the critical clearing angle θ_1 by the relation—

$$\int_{\theta_0}^{\theta_1} \Delta P' \, . \, d\theta + \int_{\theta_1}^{\theta_2} \Delta P'' \, . \, d\theta = 0$$

The first integral is the area between the "faulted" separating-power line $P = P_0'$ and the "faulted" power/angle curve $P = P' \sin(\theta_\mu - \mu')$, representing the kinetic energy gained by the system during the acceleration interval from $\theta = \theta_0$ to $\theta = \theta_1$, and shown vertically shaded in Fig. 55. The second integral in turn is the area between the "cleared" separating-power line $P = P_0''$ and the "cleared" power/angle curve

$P = P_0'' \sin(\theta - \mu'')$, representing the kinetic energy withdrawn from the system during the subsequent retardation interval from $\theta = \theta_1$ to $\theta = \theta_2$, and shown horizontally shaded in Fig. 55. Evaluation of the integrals gives as the criterion of limiting transient stability—

$$P_0'(\theta_1 - \theta_0) - P_\mu'[\cos(\theta_0 + \mu') - \cos(\theta_1 + \mu')] + P_0''(\theta_2 - \theta_1) - P_\mu''[\cos(\theta_1 + \mu'') - \cos(\theta_2 + \mu'')] = 0$$

which, after some transformation, reduces to—

$$\cos\theta_1(r_2\cos\mu'' - r_1\cos\mu') - \sin\theta_1(r_2\sin\mu'' - r_1\sin\mu') = [s_2\theta_2 + (s_1 - s_2)\theta_1 - s_1\theta_0]\sin(\theta_0 + \mu) - r_1\cos(\theta_0 + \mu') + r_2\cos(\theta_2 + \mu'').$$

On putting $$\tan\gamma = \frac{r_2\sin\mu'' - r_1\sin\mu'}{r_2\cos\mu'' - r_1\cos\mu'}$$

one obtains, finally—

$$\cos(\theta_1 + \gamma) = \frac{[s_2\theta_2 - s_1\theta_0 + (s_1 - s_2)\theta_1]\sin(\theta_0 + \mu) - r_1\cos(\theta_0 + \mu') + r_2\cos(\theta_2 + \mu'')}{\sqrt{[r_1^2 + r_2^2 - 2r_1r_2\cos(\mu'' - \mu')]}} \quad (177)$$

Equation (177) expresses the critical clearing angle θ_1 in its most general form, corresponding to equation (152) in the ideal case where reactance only is considered. A simplified form of the above general expression results from an approximation which neglects the displacement angles of the synchronizing power sinusoids, μ, μ', and μ''. These angles are, in general, small, so that their sines may be taken as being zero and their cosines as unity. This approximation then gives the critical clearing angle in the form—

$$\cos\theta_1 \simeq \frac{[s_2\theta_2 + s_1\theta_0 - (s_1 - s_2)\theta_1]\sin\theta_0 - r_1\cos\theta_0 + r_2\cos\theta_2}{r_2 - r_1} \quad (178)$$

where $\theta_0 = \sin^{-1}(P_0/P_\mu)$ and $\theta_2 = \pi - \sin^{-1}(s_2P_0/r_2P_\mu)$. This approximate expression is the same as that established in a somewhat different manner by Kroneberg and Macferran.[6]

The approximation is generally justified in practice, for the error involved is small.[7]

Angle/Time or "Swing" Curves. The problem of transient stability very often presents itself in the following form: If a fault occurs at a certain point on an interconnected system and the fault is cleared by circuit-breaker action in a certain time, will the system remain stable? The solution of this problem is significant, for it has actually influenced the trend of high-voltage circuit-breaker design. The Boulder Dam transmission system may be cited as an example. This system, which went into service towards the end of 1936, was in the nature of a vast experiment, without precedent in the sphere of interconnection, for it was designed to operate at 287 kV. and the interconnector has a length of no less than 280 miles. The transient stability requirements of the system called for the interruption, under the worst possible fault conditions, of some 2 million kVA. in not more than 5 or 6 cycles, a condition which, with carrier current relaying, implied a maximum allowable operating time of 3 to 4 cycles for the circuit-breakers. The development of the so-called "Boulder Dam" type of impulse circuit-breaker is directly attributable to this fundamental requirement.

The above problem is clearly bound up with a determination of the time elapsing between the incidence of the fault and its subsequent clearing, i.e. the duration of the acceleration interval from $\theta = \theta_0$ to $\theta = \theta_1$, where θ_0 is the initial system angle under steady-state conditions and θ_1 is the increased angle reached at the instant the fault is cleared. In other words, this important transient stability problem involves the relation between time t and system angle θ—a relation usually expressed in the form of an angle/time or so-called "swing" curve. The equation of this curve is nothing other than the formal solution of the fundamental equation of motion—

$$M \frac{d^2\theta}{dt^2} = P_M - P_E = \Delta P \quad . \quad . \quad (179)$$

which may apply either to the individual machines of a multi-machine system, or to the equivalent machine in the case of the simplified two-machine system discussed in the preceding sections of this chapter. Such swing curves express the angular displacements of the machine rotors as a function of time, and their inspection will indicate whether synchronism will be lost

or whether the oscillations in angle brought about by the discontinuities in power interchange will ultimately die away and so lead to a new position of equilibrium.

In general, a formal mathematical solution of the swing equation expressed by (179) is not possible, so that a step-by-step method of solution must be resorted to. Probably the simplest and most widely used method of this kind is that which assumes the power differential ΔP to remain constant throughout successive small intervals of time Δt. For each such interval, then, equation (179) may be integrated twice, giving—

$$\theta = \theta_0 + \omega_0 t + \frac{\Delta P}{2M} t^2 \quad . \quad . \quad . \quad (180)$$

As at time $t = 0$, corresponding to the initial angle of displacement $\theta = \theta_0$, the machine is running at synchronous speed, its relative angular velocity is zero, so that $\omega_0 = 0$. Hence equation (180) becomes simply—

$$\theta = \theta_0 + \frac{\Delta P}{2M} t^2 \quad . \quad . \quad . \quad . \quad (181)$$

Assuming successive time intervals Δt, $2\Delta t$, $3\Delta t$, . . . $n\Delta t$ equation (181) may be written in the form—

$$\Delta\theta_n = \Delta\theta_{n-1} + k\,(\Delta P_{n-1} + \Delta P_{n-2}) \quad . \quad (182)$$

where

$$k = \frac{(\Delta t)^2}{2M} \quad . \quad . \quad . \quad . \quad (183)$$

is the so-called *acceleration constant* and the subscripts refer to the *end* of each interval considered. Equation (182) at once leads to the following method of tabulation, enabling a rapid

(1) Interval Number	(2) t	(3) P_M	(4) P_E	(5) ΔP	(6) $k \cdot \Delta P$	(7) $\Delta\theta$	(8) θ
0	0				$k \cdot \Delta P_0$	0	θ_0
1	Δt				$k \cdot \Delta P_1$	$\Delta\theta_1$	θ_1
2	$2\Delta t$				$k \cdot \Delta P_2$	$\Delta\theta_2$	θ_2
3	$3\Delta t$					$\Delta\theta_3$	θ_3
etc.	etc.					(*a*)	(*b*)

Note. (*a*) Col. $(7)_n$ = Col. $(7)_{n-1}$ + Col. $(6)_{n-1}$ + Col. $(6)_{n-2}$
(*b*) Col. $(8)_n$ = Col. $(7)_n$ + Col. $(8)_{n-1}$

step-by-step solution of the swing equation to be made. In order to avoid a cumulative error the time interval Δt should not exceed 0·05 sec., a value which gives on the average some 10 to 15 points on the curve throughout the first swing. The stepped line indicates a discontinuity occurring at the commencement of the fourth interval, due to a sudden change in output P_E. Quantities below this line hold *only* after (or *just* after) the occurrence of the discontinuity. Stability is assured if at some time $t = n\Delta t$, $\theta_n < \theta_{n-1}$; for this indicates that the extreme angle of swing has been reached.

Fig. 56 shows three typical swing curves relating to the case

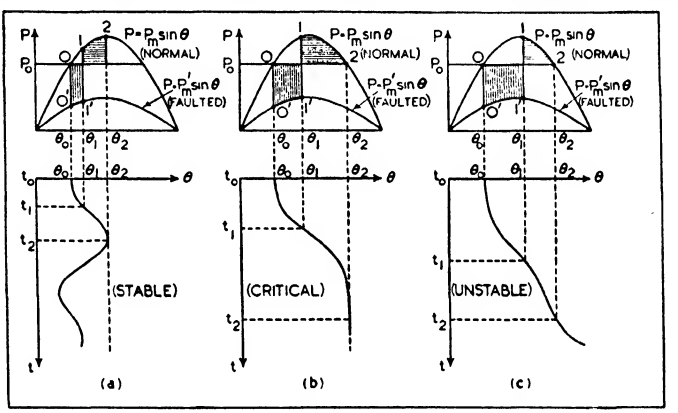

FIG. 56. POWER/ANGLE AND ANGLE/TIME CURVES RELATING TO A FAULT ON A FEEDER

of a transient disturbance due to the incidence of a feeder fault (*cf.* Fig. 48) at time $t_0 = 0$, corresponding to an initial system angle $\theta = \theta_0$, and its subsequent clearing at some specified time $t = t_1$, by which time the system angle has increased to a value $\theta = \theta_1$ as the result of the relative acceleration—

$$\frac{d^2\theta}{dt^2} = \frac{1}{M}(P_0 - P_m' \sin\theta)$$

Diagram (*a*) shows the oscillatory condition for the case of stability with an ample margin, consequent upon a rapid clearing of the fault. Here the "equal area" stability criterion gives a maximum angle (at the end of the first swing) θ_2, which is less than the critical value $(\pi - \theta_0)$ so that the power

differential $\Delta P = (P_0 - P_m \sin \theta)$ after the fault is cleared is still negative. Diagram (*b*) shows the aperiodic condition for the limiting case where the critical angle is reached just as the fault is cleared. Here $\theta_2 = (\pi - \theta_0)$ and the power differential ΔP is thus zero at the end of the first swing, so that the system will attempt to remain in equilibrium at this new angle* instead of returning to the original steady-state angle θ_0. Finally, diagram (*c*) shows the unstable condition in which the net gain in kinetic energy, represented by the difference between the vertically and horizontally shaded areas, is positive. In this case the fault is cleared too late to prevent the machines from continuing to swing apart after reaching the relative angle $\theta_2 = (\pi - \theta_0)$, so that synchronism is inevitably lost.

An important solution of the swing equation expressed by (179) arises in cases where P_E varies sinusoidally with θ, while P_M remains constant. Consider, for example, the case of the ideal two-machine system where $P_E = P_m \sin \theta$ is the electrical output of the equivalent machine, $P_0 = P_m \sin \theta_0$ is the initial mechanical input, and $P_1 = P_m \sin \theta_1$ is the final mechanical input, θ_0 and θ_1 being the corresponding system angles under steady-state conditions. Equation (179) then becomes—

$$M \frac{d^2\theta}{dt^2} = P_1 - P_m \sin \theta = P_m (\sin \theta_1 - \sin \theta) \quad . \quad (184)$$

Introducing a generalized time τ related to actual time t by—

$$\tau = t\sqrt{\frac{P_m}{M}} = t\sqrt{\left(\frac{180f}{H} \cdot \frac{P_m}{P_n}\right)} \quad . \quad . \quad (185)$$

where P_n is the machine rating and H is the kinetic energy stored in its rotor at synchronous speed in per unit† of the machine rating, equation (184) reduces to the general form—

$$\frac{d^2\theta}{d\tau^2} + \sin \theta = T \quad . \quad . \quad . \quad (186)$$

in which the constant T is here equal to $P_1/P_m = \sin \theta_1$. It will be observed that this generalized swing equation is independent of the inertia of the machine and of the electrical

* Evidently if $\theta_2 > (\pi/2) - \mu$ in the case of a general two-machine system *steady-state* instability will then result.

† The term *per unit* signifies a fraction having unity in the denominator. Thus x per unit is the same as $100x$ per cent or $1\,000x$ per thousand.

characteristics of the transmission system. Its solution, giving θ in terms of generalized time τ, is governed only by the power ratio T and, of course, by the initial angle θ_0. On separating the variables and integrating both sides one finds—

$$\frac{d\theta}{d\tau} = \sqrt{\left[2\int_{\theta_0}^{\theta} (T - \sin\theta)\, d\theta\right]}$$

$$= \sqrt{[2T\,(\theta - \theta_0 + 2\,(\cos\theta - \cos\theta_0)]}$$

$$\text{which gives } \tau = \int_{\theta_0}^{\theta} \frac{d\theta}{\sqrt{[2T\,(\theta - \theta_0) + 2\,(\cos\theta - \cos\theta_0)]}} \qquad (187)$$

as the general solution of equation (186).

The solution of equations of this type may be obtained directly on the integraph[8] or differential analyser, and appears in the form of families of curves representing the function $\tau = F\,(\theta, T, \sin\theta_0)$, known as *pre-calculated angle/time curves*. The standard curves obtained by Summers and McClure[9] on the integraph at the Massachusetts Institute of Technology comprise ten families for values of $\sin\theta_0$ from 0 to 0·9 at intervals of 0·1, each family consisting of a number of $\tau' - \theta$ curves (all radiating from the initial point $\tau' = 0$, $\theta = \theta_0$) for values of T ranging from 0·05 to 3·00. For given values of T and $\sin\theta_0$ the time taken for a machine rotor to accelerate from $\theta = \theta_0$ to $\theta = \theta_1$, say, is then obtained by multiplying the modified generalized time τ_1', corresponding to the angle θ_1 and found from the appropriate curve, by the modified constant $\sqrt{(M'/P_m)}$.* Fig. 57 shows the family of curves for $\sin\theta_0 = 0{\cdot}7$ corresponding to the initial angle $\theta_0 = 44{\cdot}5°$.

The most important use of these generalized swing curves is in connection with transient analyses based on the "equal

* Here M' is the inertia constant expressed in kW. per *radian* per sec.^{2}, so that $\pi M' = 180M = HP_n/f$. The introduction of the factor π in place of 180 in the fundamental relation between actual and generalized time thus leads to a modified time—

$$\tau' = \sqrt{(\pi/180)}.\tau = 0{\cdot}132\tau$$

where τ is defined by equation (187). This relation underlies the precalculated angle/time curves published by Summers and McClure, in spite of the fact that these curves show θ in electrical degrees and not radians. However, this modification has the advantage that it makes for a convenient generalized time scale, as will be seen from Fig. 57. The same remark applies to Figs. 58 to 74 inclusive, discussed in the following section.

area" stability criterion. In the case of a system fault the power ratio T is given by—

$$T = \frac{P_0}{P_m'} = \frac{\sin \theta_0}{r_1} \quad . \quad . \quad . \quad (188)$$

while the generalized time τ' is given by—

$$\tau' = t\sqrt{\frac{P_m'}{M'}} = t\sqrt{\left(\frac{\pi f}{H} \cdot \frac{r_1 P_m}{P_n}\right)} \quad . \quad . \quad (189)$$

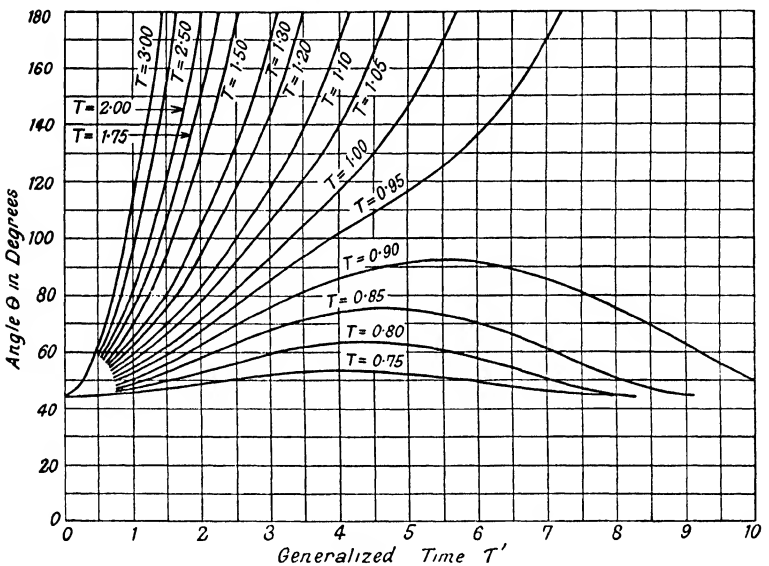

FIG. 57. FAMILY OF PRE-CALCULATED ANGLE/TIME CURVES FOR SIN $\theta_0 = 0{\cdot}7$ (SUMMERS AND MCCLURE)

These curves are applicable also to the general two-machine case, for which the swing equation is no longer given by (184), but by—

$$M\frac{d^2\theta}{dt^2} = P_0' - P_\mu' \sin(\theta + \mu')$$
$$= s_1 P_0 - r_1 P_\mu \sin(\theta + \mu') \quad . \quad . \quad (190)$$

which may be put in the modified generalized form—

$$\frac{d^2\theta'}{d\tau'^2} + \sin\theta' = T \quad . \quad . \quad . \quad (191)$$

where $\theta' = (\theta + \mu')$, and

$$T = \frac{s_1 P_0}{r_1 P_\mu} = \frac{s_1}{r_1} \sin (\theta_0 + \mu) \quad . \quad . \quad (192)$$

while the modified time is here—

$$\tau' = t \sqrt{\frac{P_\mu'}{M'}} = t \sqrt{\left(\frac{\pi f}{H} \cdot \frac{r_1 P_\mu}{P_n} \right)} \quad . \quad . \quad (193)$$

In the special case of a three-phase busbar fault, for which $r_1 = 0$, the time t as given by equations (189) and (193) is indeterminate. Under these circumstances the swing equation becomes simply

$$M \frac{d^2\theta}{dt^2} = P_0 \quad . \quad . \quad . \quad . \quad (194)$$

since the flow of all synchronizing power is cut off as long as the fault persists. The corresponding generalized swing equation is—

$$\frac{d^2\theta}{d\rho^2} = \sin \theta_0 \quad . \quad . \quad . \quad . \quad (195)$$

whose solution is—

$$\rho = \sqrt{\frac{2 (\theta - \theta_0)}{\sin \theta_0}} \quad . \quad . \quad . \quad (196)$$

where the generalized time ρ is in this case given by—

$$\rho = t \sqrt{\frac{P_m}{M}} = t \sqrt{\left(\frac{180 f}{H} \cdot \frac{P_m}{P_n} \right)} \quad . \quad . \quad (197)$$

The result expressed by these last two equations may, of course, be obtained directly from the swing equation which in this particular case admits of a formal mathematical solution. By direct integration of equation (194) one obtains—

$$\theta = \theta_0 + \omega_0 t + \frac{P_0}{2M} t^2 \quad . \quad . \quad . \quad (198)$$

As ω_0 ($= d\theta/dt$ at time $t = 0$) is zero, for the machines then have zero relative angular velocity, equation (198) gives—

$$t = \sqrt{\left(\frac{2M (\theta - \theta_0)}{P_0} \right)} = \sqrt{\left[\frac{2M}{P_m} \left(\frac{\theta - \theta_0}{\sin \theta_0} \right) \right]} \quad . \quad (199)$$

where θ and θ_0 are expressed in *degrees*, as in equations (187) and (196).

By means of the pre-calculated angle/time curves and equation (189), (193) or (199), therefore, the latest time of clearing a fault that will allow the system to regain stability may be found when the critical clearing angle θ_1 is known. This angle is given by equation (150), (152), (154), (177), or (178), as the case may be, derived from a consideration of the "equal area" stability criterion.

Switching Time or "Stability" Curves. Probably the most convenient form in which the results of transient stability studies may be presented is the family of switching time or so-called "stability" curves whose abscissae are the times of fault clearance, and whose ordinates are the maximum powers that can be carried by the system prior to the incidence of the fault without instability arising therefrom, assuming the fault to be cleared not later than the time indicated by the abscissa. This mode of presenting the results of system studies arises naturally from the methods of calculation involved in transient analysis. Each curve of the family is, in effect, a graphical representation of the function $P_0 = F(t_1)$ for a particular type or location of fault, where t_1 is the time of fault clearance corresponding to the critical clearing angle θ_1.

In the ordinary way the computing of such curves involves the repeated determination, either graphically or by direct calculation from the appropriate equations, of the critical clearing angle θ_1 in accordance with the "equal area" concept, each determination being based on a different value of initial system load P_0, and thus of initial system angle θ_0. It further involves the determination of the corresponding times of fault clearance t_1, either from pre-calculated angle/time curves or else by step-by-step methods. This process of computation is clearly laborious, especially where a number of different fault or system conditions are to be compared.

An alternative method of determining t_1 due to Byrd and Pritchard[10] avoids the necessity of having first to evaluate the critical clearing angle, and gives the generalized time τ' directly in terms of r_1, r_2, and $\sin \theta_0$. The function

$$\tau' = F(r_1, r_2, \sin \theta_0)$$

is shown in Figs. 58 to 73* in the form of seventeen families of

* The author is indebted to the editor of the *General Electric Review* for permission to reproduce these curves from the article by Messrs. Byrd and Pritchard.

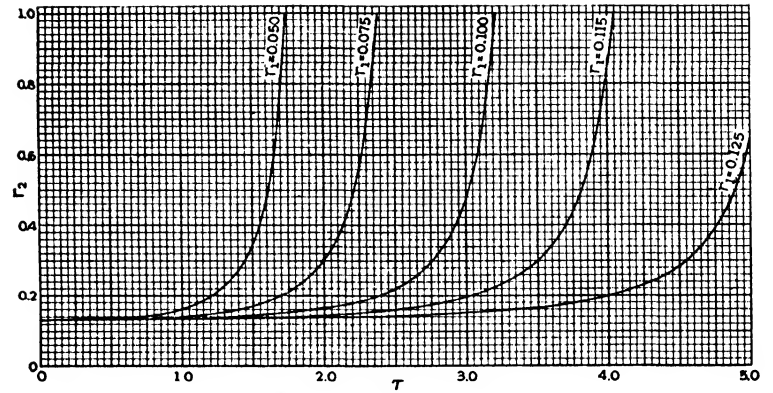

FIG. 58. SIN $\theta_0 = 0{\cdot}10$

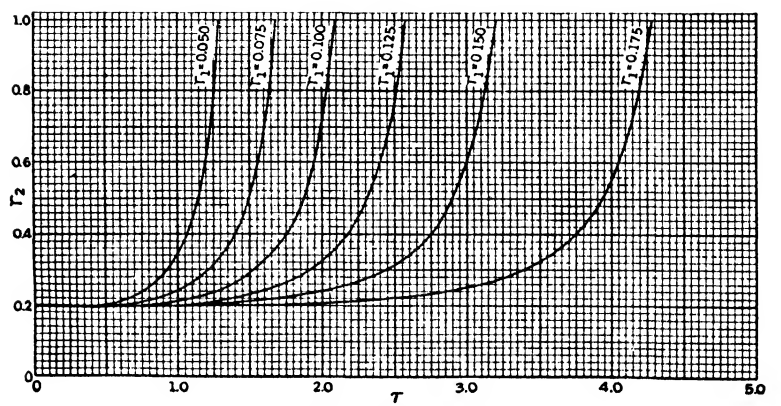

FIG. 59. SIN $\theta_0 = 0{\cdot}15$

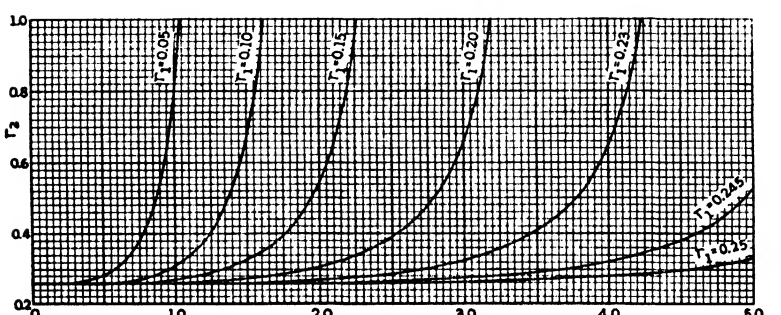

FIG. 60. SIN $\theta_0 = 0{\cdot}20$

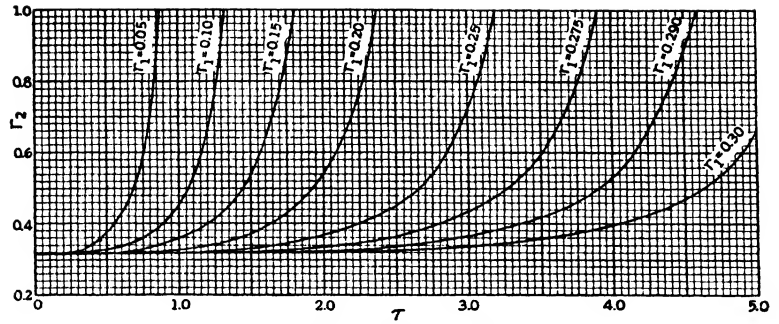

FIG. 61. SIN $\theta_0 = 0{\cdot}25$

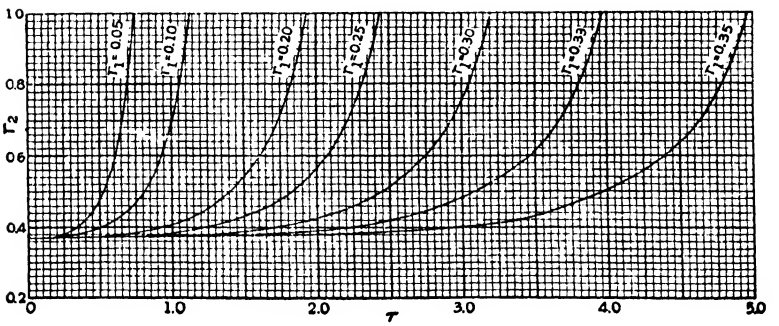

FIG. 62. SIN $\theta_0 = 0{\cdot}30$

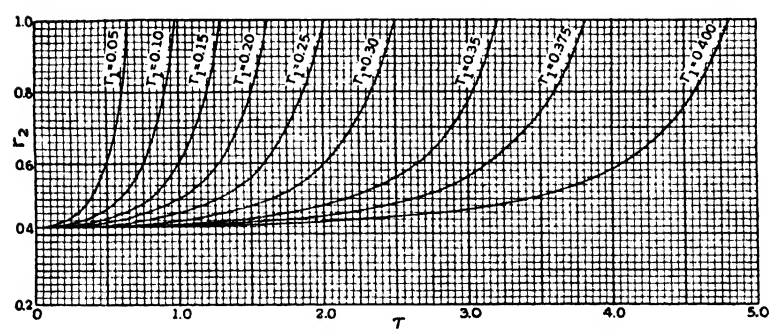

FIG. 63. SIN $\theta_0 = 0{\cdot}35$

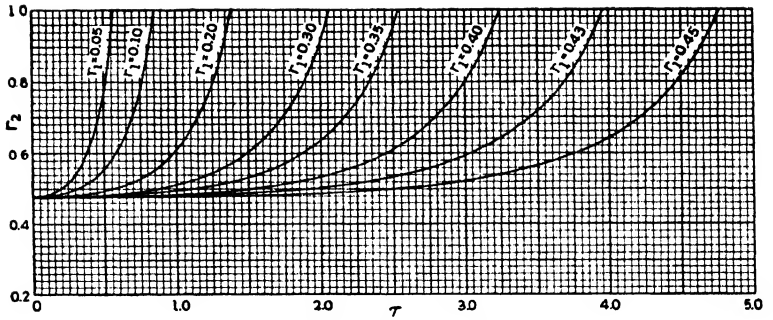

FIG. 64. SIN $\theta_0 = 0{\cdot}40$

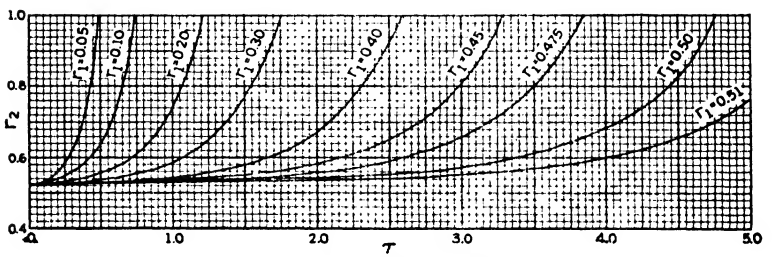

FIG. 65. SIN $\theta_0 = 0{\cdot}45$

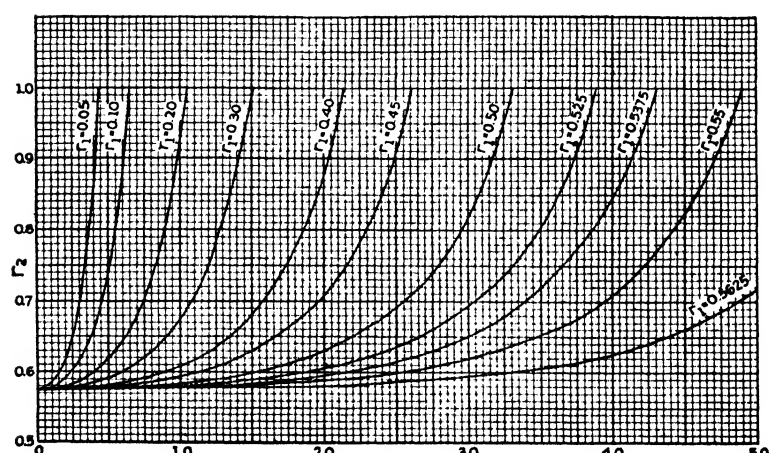

FIG. 66. SIN $\theta_0 = 0{\cdot}50$

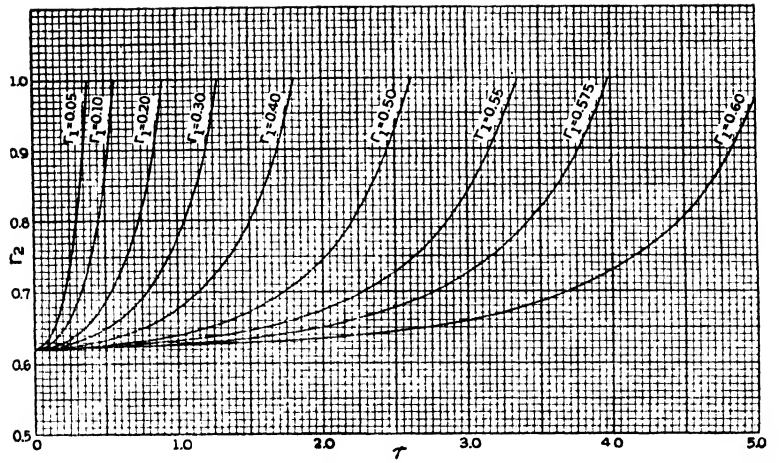

FIG. 67. SIN $\theta_0 = 0{\cdot}55$

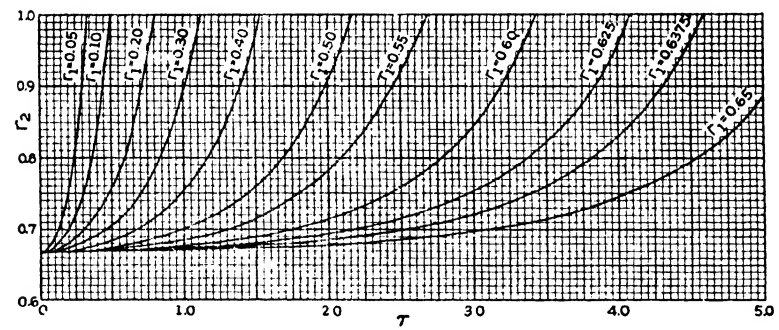

FIG. 68. SIN $\theta_0 = 0{\cdot}60$

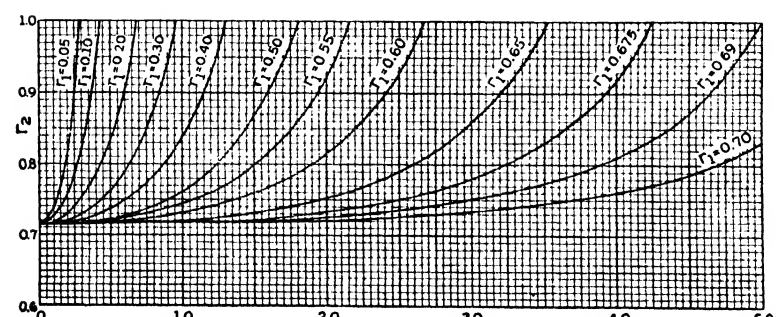

FIG. 69. SIN $\theta_0 = 0{\cdot}65$

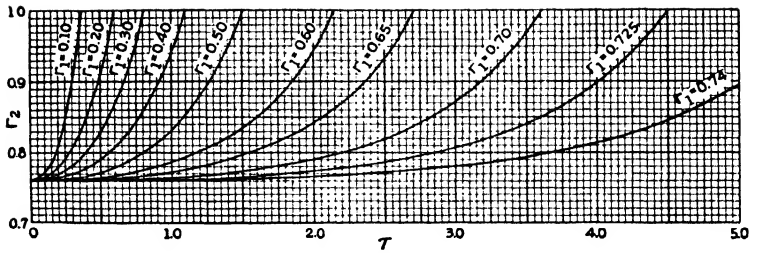

FIG. 70. SIN $\theta_0 = 0{\cdot}70$

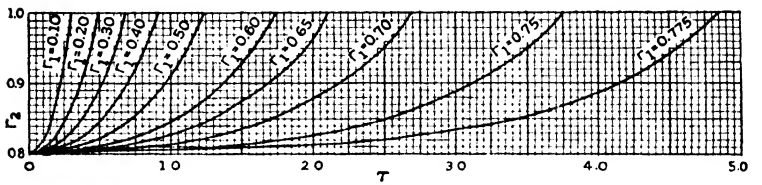

FIG. 71. SIN $\theta_0 = 0{\cdot}75$

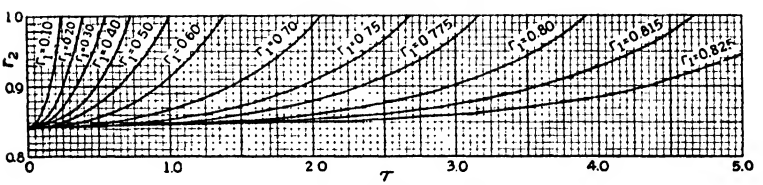

FIG. 72. SIN $\theta_0 = 0{\cdot}80$

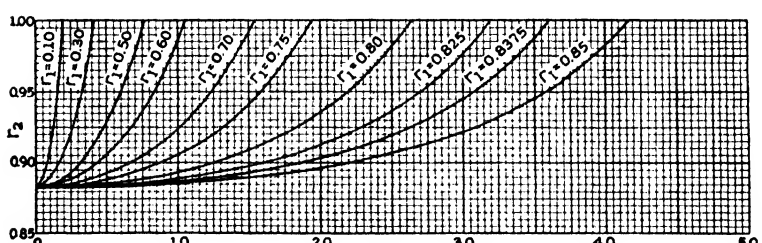

FIG. 73. SIN $\theta_0 = 0{\cdot}85$

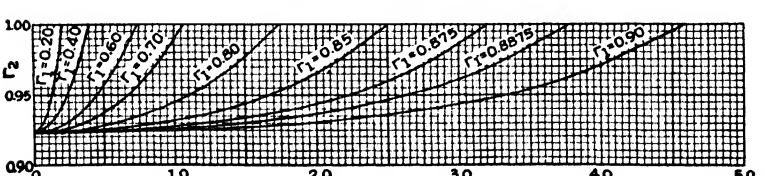

FIG. 74. SIN $\theta_0 = 0{\cdot}90$

generalized switching-time curves for values of sin θ_0 from 0·1 to 0·9 at intervals of 0·05. The τ'-r_2 curves of each family are arranged in a series of increasing r_1 values, ranging from 0·05 to 0·9, all the curves radiating from the point—

$$\tau' = 0, \quad r_2 = \frac{\sin \theta_0}{0{\cdot}724 + 0{\cdot}276 \sin \theta_0}.$$

These master curves enable the maximum initial system load, $P_0 = P_m \sin \theta_0$, consonant with transient stability, to be rapidly determined for any value of switching time t between zero and infinity, according to the relation—

$$\tau' = t\sqrt{\frac{P_m'}{M'}} = t\sqrt{\left(\frac{\pi f}{H} \cdot \frac{r_1 P_m}{P_n}\right)} \quad . \quad . \quad (200)$$

between modified generalized time and actual time, where M' is the inertia constant expressed in kW. per radian per sec.^{2}, as before.

Fig. 75 shows the characteristic relation between r and sin θ_0 given by equation (148). With $r = r_1$, Fig. 75 gives the sine of the maximum initial angle at which the machines could have been operating if the fault were not cleared during the first swing of the machines, from which the corresponding maximum system load can be found. This value of P_0 is that for $t = \infty$ and thus gives the asymptote to the stability curve. Similarly, with $r = r_2$, Fig. 75 gives the sine of the maximum initial angle at which the machines could have been operating if the switching operation necessary to clear the fault were made simultaneously with the incidence of the fault, from which the corresponding maximum system load can again be found. This value of P_0 in turn gives the point where the stability curve meets the axis $t = 0$.

Finally, Fig. 76 shows a family of curves expressing the function $\rho' = F(r_2, \sin \theta_0)$ applicable to the special case of a three-phase busbar fault, for which $r_1 = 0$. The relation between modified time and actual time is in this case—

$$\rho' = t\sqrt{\frac{P_m}{M'}} = t\sqrt{\left(\frac{\pi f}{H} \cdot \frac{P_m}{P_n}\right)} \quad . \quad . \quad (201)$$

The master curves of Fig. 76 enable the switching time to be found for a given value of system load in the same way as for the curves given in Figs. 58 to 74.

The Calculation of Transient Stability. The first step in the

study of any interconnected system is its simplification to an equivalent system that will substantially represent the actual one, particularly as to reactance and flywheel effect. In general, the process of simplification involves replacing parts of the system, e.g. a load or a generating station, by equivalent

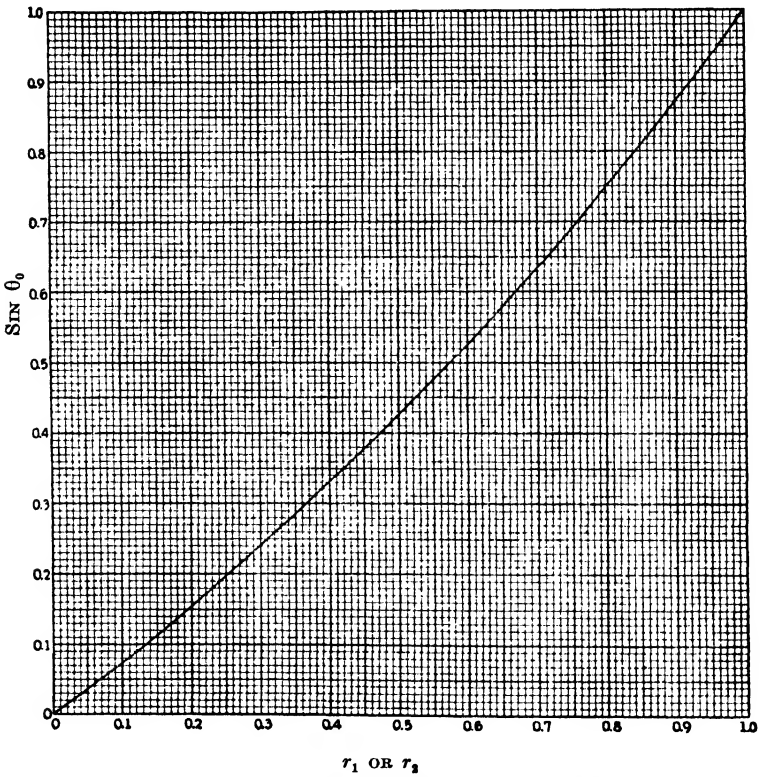

FIG. 75. CHARACTERISTIC RELATION BETWEEN r_1 OR r_2 AND SIN θ_0 FOR CRITICAL STABILITY

machines, and reducing the interconnecting network to a number of synchronous ties between these machines. It is often permissible to reduce a group of machines to a single equivalent machine, for the individual machines of a group may be so closely coupled as to make any local oscillations between them insufficient to influence the inter-group oscillations of the system as a whole. The selection of the machines

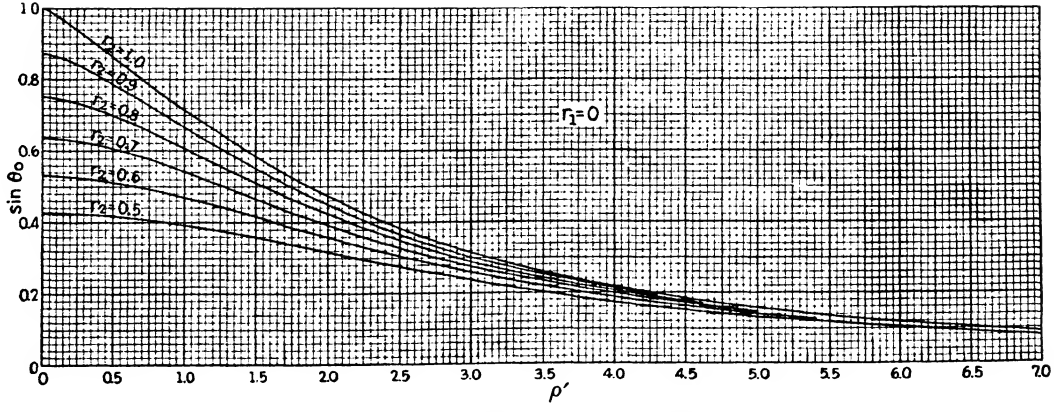

FIG. 76. GENERALIZED SWITCHING-TIME CURVES FOR THREE-PHASE BUSBAR FAULT
ρ' *versus* Sin θ_0

in a given system which may be grouped into an equivalent machine is largely a matter of applied logic, and cannot be subjected to hard-and-fast rules. For a given system, however, the location of the fault with respect to the group to be combined plays a very important part in determining how closely the machines of that group swing together. Bearing this consideration in mind, it will in many cases prove possible to reduce the actual system to an equivalent two-machine system whose behaviour can be studied according to the methods already described, with results which, although con-

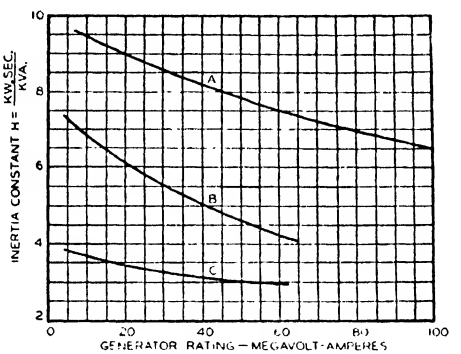

FIG. 77. INERTIA CONSTANTS OF LARGE TURBO-GENERATORS, TURBINE INCLUDED

A = 1 800 r.p.m. condensing. B = 3 600 r.p.m. condensing. C = 3 600 r.p.m. non-condensing.

stituting only a first approximation, will give a fair idea as to the correct solutions to the transient stability problems involved in the system study.

(*a*) *System Inertia.* To represent the real system, the equivalent machines in the first place should have the same flywheel effect as the machine groups which they severally represent. If H is the stored energy of the equivalent machine expressed in per unit of some arbitrarily chosen kVA. base (e.g. the short-circuit kVA. of the system at some important point, or the steady-state power limit of the system) and H_a, H_b, H_c, etc., are the corresponding stored energies of the actual machines in per unit *of the same base power*, then—

$$H = H_a + H_b + H_c + \ldots \text{ etc.} \quad . \quad . \quad (202)$$

As the H value of a machine is always expressed in kilowatt-seconds per kVA., i.e. in per unit of the machine rating, the

H values to be inserted in equation (202) must be found from the relation—

$$H_a = H_{m_a} \times \frac{\text{machine rating}}{\text{base power}} \quad . \quad . \quad (203)$$

where H_m is the stored energy in per unit *of machine kVA*. Figs. 77 and 78 enable appropriate values of H_m to be obtained for turbo-alternators and water-wheel alternators respectively.* Average values for other machines are given in Table I.

TABLE I

Type of Machine		H sec.
Synchronous condensers	large	1·25
	small	1·0
Synchronous motors	large	2·25
	small	2·0
Rotary converters		2·0
Induction motors.		0·5

(*b*) *System Reactance.*† One of the essential elements in the calculation of transient stability is the determination of the

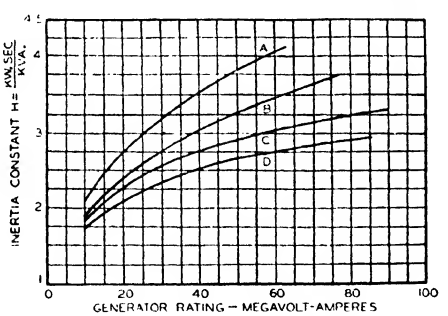

FIG. 78. INERTIA CONSTANTS OF LARGE VERTICAL-TYPE WATER-WHEEL GENERATORS, INCLUDING ALLOWANCE OF 15 PER CENT FOR WATER-WHEELS

A = 450–514 r.p.m. *C* = 138–180 r.p.m.
B = 200–400 r.p.m. *D* = 80–120 r.p.m.

electrical outputs of the synchronous machines involved. This implies that the impedances of the network to which the

* Taken from the A.I.E.E. First Report on Power System Stability (see Reference (1)).

† *Vide* H. Rissik: "The Calculation of Unsymmetrical Short Circuits," *BEAMA Journ.*, April-August, 1940.

machines are connected must be found for each of three conditions, viz. before the fault occurs, while the fault is on the system, and after the fault is cleared. (As a general rule, it is necessary to take into account only the reactance of the network, resistance playing a minor role in transient phenomena of the type here considered. It is permissible to assume, also, that the resistance of the fault itself is zero.) The value of transfer impedance Z or reactance X in the first and last cases is to be found by "solving" the network as for symmetrical three-phase short-circuit calculations.[11] In the second case, when the fault is not symmetrical, the network currents and voltages become unbalanced and symmetrical component theory must be employed in the solution of the network.[12] The problem of determining the maximum synchronizing power, $P_m = E_1E_2/Z \simeq E_1E_2/X$, in these three cases thus resolves itself into establishing and solving not only the normal, positive-sequence network but also the negative-sequence and zero-sequence networks. This in turn requires a knowledge of the negative- and zero-sequence reactances of the machines, transformers, and transmission lines or cables which make up the system network.

A simplified reactance diagram of the system should thus first be drawn up, the machines themselves being represented by their transient reactances, and all transient reactance values being calculated in per unit on the chosen kVA. base. In this case the relations that apply are—

$$x = X\% \times \frac{\text{base kVA.}}{100 \times \text{machine kVA.}} \text{ per unit}$$

or

$$x = X \text{ ohms} \times \frac{\text{kV.}^2}{\text{base MVA.}} \text{ per unit}$$

The simplified reactance network must then be reduced by repeated star/delta and delta/star transformations* to a simple reactive tie between the two equivalent machines of the system, this tie constituting the initial transfer reactance X under steady-state conditions.

Next, the negative and zero phase-sequence reactance diagrams must be drawn up and each reduced to a single reactance, *when viewed from the point of fault.* As is well known, a system fault may be represented by an *equivalent fault reactance* X_f connected as a shunt in the positive-sequence

* See Chapter I.

network at the point of fault. The value of X_F depends upon the nature of the fault, and is a simple function of the negative-sequence and zero-sequences reactances of the network, X_2 and X_0, viewed from the point of fault. The several values of X_F are tabulated below. This reactance is then included in the

Type of Fault	X_F
Single line-to-ground	$X_2 + X_0$
Double line-to-ground	$\frac{X_2 X_0}{X_2 + X_0}$
Line-to-line	X_2
Three-phase short circuit	0

original positive-sequence reactance diagram of the system network, which is finally reduced by a corresponding series of transformations to a simple **T** network. The top or bar of this **T** is thus connected between the air-gap voltages of the two equivalent machines of the simplified two-machine system, while the leg or staff of the **T** includes the equivalent fault reactance X_F, as shown in Fig. 79.

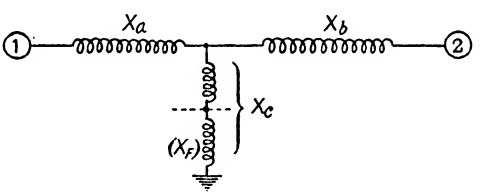

FIG. 79. EQUIVALENT **T** NETWORK OF SYSTEM UNDER FAULT CONDITIONS

If X_a and X_b denote the reactances forming the arms of the **T**, and X_c the reactance forming the staff of the **T**, then the transfer reactance of the system under fault conditions is—

$$X' = X_a + X_b + \frac{X_a X_b}{X_c} \quad . \quad . \quad (204)$$

If the transfer reactance after the fault is cleared is different from the corresponding reactance before the occurrence of the fault, so that, due to the disconnection of part of the system when the fault is cleared the transfer reactance does not fall from its "faulted" value X' to the pre-fault value X, but to some intermediate value X'', then this final value of transfer reactance must also be determined from the appropriate positive-sequence diagram. In this way the factors $r_1 = X/X'$ and $r_2 = X/X''$ may be found.

(c) *Transient Reactance Values.** In the foregoing calculations

* *Vide* H. Rissik: *loc. cit.*

it is the transient reactance of the synchronous machines which must be taken into consideration. This has a lower value than the synchronous reactance employed in steady-state analysis and in the determination of sustained short-circuit currents under fault conditions. Table II gives representative per unit values for the transient reactances of synchronous machines to positive-sequence currents (x'), negative-sequence currents (x_2), and zero-sequence currents (x_0). The table also gives some typical values which may be taken in the absence of further information.

In the case of transmission lines and cables, the negative-sequence reactances is the same as the positive-sequence reactance. The calculation of the zero-sequence reactance is a matter of some complexity and has been treated very fully by Monseth and Robinson.[13] It is customary, however, to take it as being 3·5 times the positive-sequence reactance, the effect of mutual reactance between the two circuits of a double-circuit line being negligible.*

So far as two-winding transformers are concerned, the positive- and negative-sequence reactances are also the same. The zero-sequence reactance, on the other hand, is either infinite or the same also depending on the connection of the transformer windings and whether or not there is a grounded neutral anywhere on the system.* Summers and McClure [14] have published simplified zero-sequence diagrams for several combinations of transformers and transmission lines. Some are reproduced in Table III. Three-winding transformers may be treated by the method developed by Boyajian,[15] while auto-transformers have been dealt with by Summers and McClure.[16] Monseth and Robinson have given numerous examples of zero-sequence circuits for three-winding transformers [17] and auto-transformers.[18]

(*d*) *Maximum Synchronizing Power.* Having determined r_1 and r_2, it is necessary to evaluate the maximum synchronizing power P_m corresponding to the initial steady-state condition for which the system load is given by $P_0 = P_m \sin \theta_0$. In general, the sending- and receiving-end busbar voltages E_S and E_R are held constant. Hence the air-gap voltages of the equivalent machines at the two ends of the system, E_1 and E_2, will vary† with the system load P_0 and thus with the initial steady-state

* *Vide* H. Rissik: *loc. cit.*

† Under *steady-state* conditions, that is to say. Under *transient* conditions E_1 and E_2 are assumed to remain constant.

TABLE II. PER UNIT REACTANCES OF SYNCHRONOUS MACHINES

Type of Synchronous Machine	Synchronous† Reactance (x_d)		Transient† Reactance (x'_d)		Negative Seq. Reactance (x_2)		Zero Seq. Reactance (x_0)	
	Range	Typical	Range	Typical	Range	Typical	Range	Typical
Turbo-alternators—								
Two-pole (3 000 r.p.m.)	0·95–1·45	1·10	0·12–0·21	0·15	0·07–0·14	0·09	0·01–0·08	*
Four-pole (1 500 r.p.m.)	1·00–1·45	1·15	0·20–0·28	0·23	0·12–0·17	0·14	0·02–0·14	*
Salient-pole alternators—								
With amortisseur	0·60–1·45	1·00	0·20–0·50	0·37	0·13–0·35	0·24	0·02–0·20	*
Without amortisseur	0·60–1·45	1·00	0·20–0·45	0·35	0·30–0·70	0·55	0·04–0·25	*
Synchronous condensers	1·45–1·95	1·60	0·30–0·60	0·40	0·17–0·37	0·24	0·02–0·15	*
Synchronous motors—								
High-speed	0·65–0·90	0·80	0·15–0·35	0·25	0·11–0·25	0·19	0·02–0·15	*
Low-speed	0·80–1·50	1·10	0·40–0·70	0·50	0·25–0·50	0·35	0·04–0·27	*

* x_0 varies so widely with the winding pitch that no average figure can be given.
† The suffix d indicates direct-axis values in the case of salient-pole machines.

TABLE III. ZERO-SEQUENCE IMPEDANCES OF INTERCONNECTORS

Case No.	Apparatus Connections in Single-line Diagram	Simplified Zero Phase-sequence Reactance Diagram	Zero Phase-sequence Reactance viewed from the Point of Fault
1	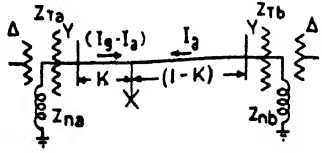	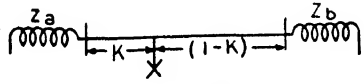 $Z_a = Z_{ta} + 3Z_{na}$ $Z_b = Z_{tb} + 3Z_{nb}$	$Z_o = \frac{AB}{A+B}$, where— $A = Z_a + KZ_{aa}$ $B = Z_b + (1-K)Z_{aa}$
2	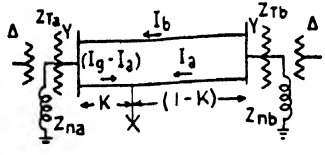	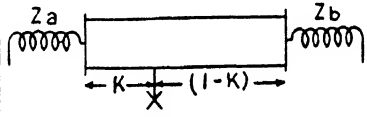 $Z_a = Z_{Ta} + 3Z_{na}$; $Z_{aa} = Z_{bb}$ $Z_b = T_{Tb} + 3Z_{nb}$; $Z_{ab} = Z_{ba}$	$Z_o = \frac{CF - DE}{C - E}$, where— $C = -[2Z_a + K(Z_{aa} + Z_{ab})]$ $D = (1+K)Z_a + K(Z_{aa} + KZ_{ab})$ $E = (2Z_b + (1-K)(Z_{aa} + Z_{ab}))$ $F = -[KZ_b + (1-K)KZ_{ab}]$
3	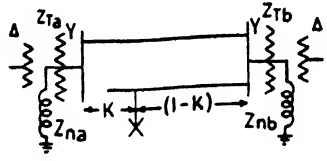	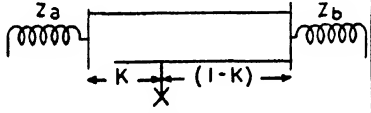 $Z_a = Z_{Ta} + 3Z_{na}$; $Z_{aa} = Z_{bb}$ $Z_b = Z_{Tb} + 3Z_{nb}$; $Z_{ab} = Z_{ba}$	$Z_o = \frac{GJ - HI}{G - I}$, where— $G = Z_b + (1-K)Z_{ab}$ $H = Z_b + (1-K)Z_{aa}$ $I = -[Z_a + Z_{aa} - (1-K)Z_{ab}]$ $J = (1-K)(Z_{aa} - Z_{ab})$

4	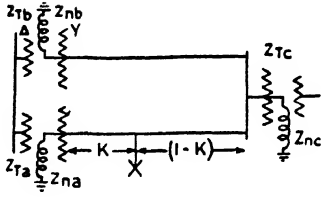	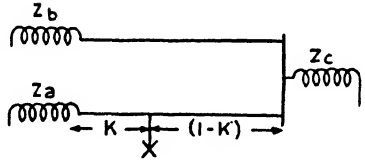 $Z_a = Z_{Ta} + 3Z_{na};\ Z_{aa} = Z_{bb}$ $Z_b = Z_{Tb} + 3Z_{nb};\ Z_{ab} = Z_{ba}$ $Z_c = Z_{Tc} + 3Z_{nc}$	$Z_o = \dfrac{QN - LM}{Q - M}$, where— $Q = Z_a + K(Z_{aa} - PZ_{ab})$ $L = Z_a + K(Z_{aa} - OZ_{ab})$ $M = (1-K)(Z_{aa} - PZ_{ab}) + (1-P)Z_c$ $N = (1-K)OZ_{ab} + OZ_c$ $O = \dfrac{K(Z_{ab} - Z_{aa}) - Z_a}{Z_b + Z_{aa} - Z_{ab}}$ $P = \dfrac{Z_{ab} - Z_{aa} - Z_a}{Z_b + Z_{aa} - Z_{ab}}$
5	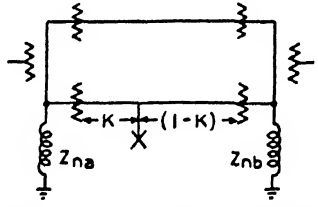 *Note.* Resolve double-winding transformers into— 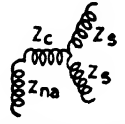 where Z_c is usually negative.	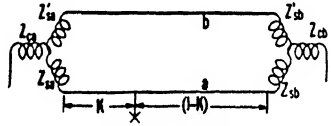 $Z_{ca} = Z_c + 3Z_{na};\ Z_{aa} = Z_{bb}$ $Z_{cb} = Z_c + 3Z_{nb};\ Z_{ab} = Z_{ba}$ Z_{sa}' is distinguished from Z_{sa} to allow for any lumped constants which might exist and destroy the symmetry.	$Z_o = \dfrac{RU - ST}{R - T}$, where— $R = -[Z_{ca} + Z_{sa} + K(Z_{aa} + WZ_{ab}) + WZ_{ca}]$ $S = Z_{ca} + Z_{sa} + K(Z_{aa} + YZ_{ab}) + YZ_{ca}$ $T = Z_{cb} + Z_{sb} + (1-K)(Z_{aa} + WZ_{ab}) + WZ_{cb}$ $U = -[YZ_{cb} + (1-K)YZ_{ab}]$ $V = Z_{sb}' + Z_{aa} + Z_{sa}' - Z_{ab}$ $W = (Z_{sb} + Z_{aa} + Z_{sa} - Z_{ab})/V$ $Y = (Z_{sa} + K(Z_{aa} - Z_{ab}))/V$

system angle θ_0. As the result, P_m will also be a function of θ_0. If the transient stability of the system is to be studied under different conditions of initial steady-state load, it will therefore be necessary to determine P_m and θ_0 for each value of P_0. In most cases it will be desirable to plot P_m and sin θ_0 (rather than θ_0) in terms of P_0 for values ranging from, say, 25 to 200 per cent of the normal system load. Here also it is convenient to specify both P_m and P_0 in per unit of the chosen base power. Similarly, E_1 and E_2 may conveniently be expressed in per unit of some arbitrary base voltage, e.g. the nominal transmission pressure.

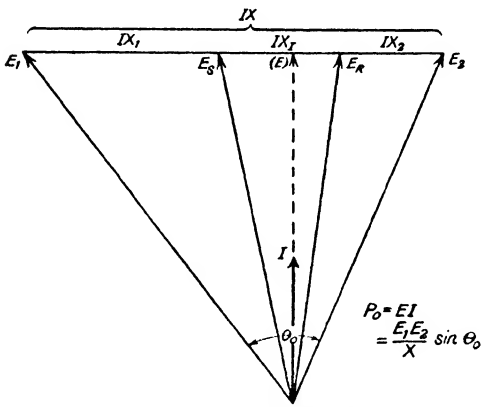

FIG. 80. SYSTEM VECTOR DIAGRAM FOR INITIAL STEADY-STATE CONDITION ($P_0 = P_m$ SIN θ_0)

Referring to the system vector diagram shown in Fig. 80, we have—

$$\sin \theta_0 = \frac{P_0}{P_m} = \frac{P_0 X}{E_1 E_2} \quad . \quad . \quad . \quad (205)$$

where X is the system transfer reactance, made up of X_1 and X_2, the transient reactances of machines 1 and 2, and X_I, the reactance of the interconnector between them. Also—

$$\begin{aligned}(IX)^2 &= E_1^2 + E_2^2 - 2E_1E_2 \cos \theta_0 \\ &= E_1^2 + E_2^2 - 2\sqrt{(E_1^2E_2^2 - P_0^2X^2)} \quad . \quad (206)\end{aligned}$$

Similarly, one finds

$$(IX_I)^2 = E_s^2 + E_R^2 - 2\sqrt{(E_s^2E_R^2 - P_0^2X_I^2)} \quad . \quad (207)$$

$$(IX_1)^2 = E_1^2 + E_s^2 - 2\sqrt{(E_1^2E_s^2 - P_0^2X_1^2)} \quad . \quad (208)$$

$$(IX_2)^2 = E_R^2 + E_2^2 - 2\sqrt{(E_R^2E_2^2 - P_0^2X_2^2)} \quad . \quad (209)$$

The per unit load current I can thus be found from equation (207), since E_s and E_R are given, as are also P_0 and X_I. This value of I when substituted in equations (208) and (209) then enables E_1 and E_2 to be found. Then, finally, $P_m = E_1E_2/X$,

while $\sin\theta_0 = P_0/P_m$. Alternatively, with I known from equation (207), the vector diagram of Fig. 80 can be drawn to scale, thus enabling E_1, E_2, and θ_0 to be obtained directly.

Two curves should then be plotted of P_m and $\sin\theta_0$ in terms of P_0, covering the range of system loads required. These curves form the starting-point in the computation of switching-time curves in accordance with the methods described in the preceding section. Taking successive values of $\sin\theta_0$ which are multiples of 0·05 (corresponding to the several families of generalized switching-time curves given in Figs. 58 to 74), the corresponding values of P_0 and P_m are tabulated along with the values of modified time τ' found from the appropriate generalized switching-time curves, with r_2 and r_1 as determined under (*b*) above. Values of $P_m' = r_1 P_m$ and of the factor $c\sqrt{(r_1 P_m)}$, where $c = \sqrt{(\pi f/HP_n)}$, $H = H_1H_2/(H_1 + H_2)$, and P_n is the base power,* are also tabulated. Multiplication of τ' by this factor then gives the critical switching time $t = t_1$ in seconds.

(*e*) *Inclusion of Resistance.* The foregoing method of procedure assumes that the system contains reactance only. The effect of series resistance and shunt admittance, including loads represented by constant shunt impedances instead of by equivalent synchronous machines,† may be taken into account by adopting the general method of equivalence established earlier in this chapter for the two-machine system. The impedance network of the system under fault conditions may be reduced to an equivalent **T** circuit having impedances $\mathbf{Z}_a'$ and $\mathbf{Z}_b'$ in the two arms and an impedance $\mathbf{Z}_c'$ in the staff, where $\mathbf{Z}_c'$ includes the equivalent fault impedance $\mathbf{Z}_F$. Then the driving-point impedances of the system are given by—

$$\mathbf{Z}_1' = \mathbf{Z}_a' + \frac{\mathbf{Z}_b'\mathbf{Z}_c'}{\mathbf{Z}_b' + \mathbf{Z}_c'} \quad . \quad . \quad . \quad (210)$$

$$\mathbf{Z}_2' = \mathbf{Z}_b' + \frac{\mathbf{Z}_a'\mathbf{Z}_c'}{\mathbf{Z}_a' + \mathbf{Z}_c'} \quad . \quad . \quad . \quad (211)$$

while the transfer impedance of the system is—

$$\mathbf{Z}' = \mathbf{Z}_a' + \mathbf{Z}_b' + \frac{\mathbf{Z}_a'\mathbf{Z}_b'}{\mathbf{Z}_c'} \quad . \quad . \quad (212)$$

* Taken as unity, if all other power values are expressed in per unit of P_n.

† This latter method, due to Park and Bancker,[19] is assumed to underly the process of network simplification outlined under (*a*) and (*b*) above. The figures usually taken for a composite load are $H = 1{\cdot}95$ kW.-sec. per kVA. and $x = 0{\cdot}5$ per unit of kW. rating, i.e. $(0{\cdot}5/\cos\phi)$ per unit of load kVA.

Under the initial and final steady-state conditions, on the other hand, the impedance network is defined by its general network constants, so that—

$$Z_1 = \frac{B}{D}; \quad Z_2 = \frac{B}{A}; \quad Z = B \quad . \quad . \quad (213)$$

and

$$Z_1'' = \frac{B''}{D''}; \quad Z_2'' = \frac{B''}{A''}; \quad Z'' = B'' \quad . \quad . \quad (214)$$

Equations (210) to (214) enable the several separating powers P_0, P_0', and P_0'' to be calculated. E_1 and E_2, as well as P_μ and sin $(\theta_0 + \mu)$, are then found as before.

Examples of System Stability Studies. The following three examples may be taken as typical of the more elementary stability problems that can be solved by the several methods of analysis outlined in the present chapter. Consideration of the more complex problems, such as those involving three or four machine-groups or equivalent machines, or those in which Blondel's two-reaction theory of synchronous machines has to be applied in evaluating the effective machine reactances, are beyond the scope of this volume.

Example 1. *A three-phase interconnector having a reactance of* 0·67 *ohm per mile and operating at a nominal voltage of* 132 *kV. between lines normally transmits* 30 000 *kW. at* 0·95 *p.f. lagging from a steam power station to a transforming station* 300 *miles distant. The generating station may be represented by a* 60 000 *kVA. turbo-alternator set running at* 1 500 *r.p.m., while the distant load may be considered as two synchronous motors designed for a full-load output of* 25 000 *kW. at* 0·8 *p.f. The step-up and step-down transformers at the two ends of the interconnector are each rated at* 60 000 *kVA. with a reactance of* 9½ *per cent. They are connected in delta/star, and the neutral points on the h.t. sides are directly earthed.*

Assuming the voltage to be held constant at the terminals of the equivalent synchronous motor load, determine the relation between the power transmitted and the latest time of fault clearance consistent with transient stability for (a) *a single line-to-earth fault, and* (b) *a double line-to-earth fault, at a point distant* 200 *miles from the generating station.*

Solution. From Table II the per unit positive-sequence and negative-sequence reactances of the generator and equivalent motor are taken to be 0·23 and 0·14, and 0·5 and 0·4 respectively; while Fig. 77 and Table I give $H_G = 7{\cdot}5$ and $H_M = 3{\cdot}5$ kW.-sec./kVA. Fig. 81 (*a*) shows the transient reactance diagram with all reactance values in per unit referred to a 60 000 kVA. base. The per unit reactance of the transmission line, for example, is here—

$$X_L = \frac{300 \times 0{\cdot}67 \times 60}{132^2} = 0{\cdot}692$$

The per unit stored energies at the two ends of the system are—

$$H_1 = 7{\cdot}5, \text{ and } H_2 = 3{\cdot}5 \times \frac{50\,000/0{\cdot}8}{60\,000} = 3{\cdot}64$$

so that the energy constant of the "equivalent" generator is

$$H = \frac{H_1 H_2}{H_1 + H_2} = \frac{7{\cdot}5 \times 3{\cdot}64}{11{\cdot}14} = \underline{2{\cdot}46}$$

To find the air-gap voltages E_G and E_M and the steady-state system angle θ_0 between them we can take the receiving-end terminal voltage, $E_R = 132$ kV. $= 1{\cdot}0$ per unit, as our axis of vector reference, *i.e.* $\mathbf{E}_R = 1{\cdot}0\,|\underline{0°} = 1{\cdot}0 + j0$. At full load and $\cos\phi = 0{\cdot}95$ lagging, we

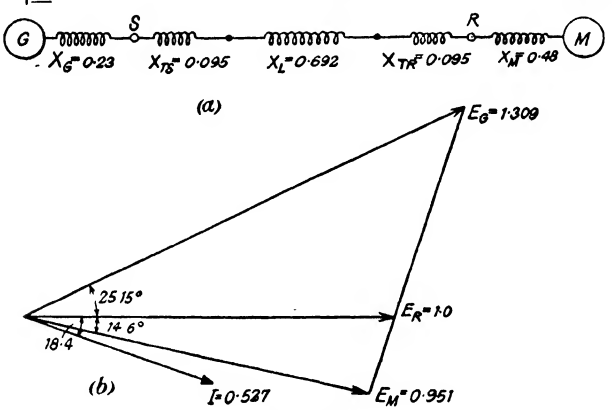

FIG. 81

have $P_R = 30\,000$ kW. and $Q_R = -P_R \tan\phi = -10\,000$ kVAr., so that—

$$P_R + jQ_R = \frac{30\,000 - j10\,000}{60\,000} = 0{\cdot}5 - j0{\cdot}167 \text{ per unit.}$$

Hence the full-load current is—

$$\mathbf{I} = I\,|\underline{\phi} = \frac{P_R + jQ_R}{E_R} = 0{\cdot}527\,|\underline{-18{\cdot}4°} \text{ per unit*.}$$

Denoting by X_N the total reactance between the points G and R in Fig. 81 (*a*), we have—

$$X_N = X_G + X_{TS} + X_L + X_{TR} = 1{\cdot}112 \text{ per unit}$$

and thus—

$$\mathbf{E}_G = \mathbf{E}_R + \mathbf{I}\mathbf{X}_N = 1{\cdot}0 + j1{\cdot}112(0{\cdot}5 - j0{\cdot}167) = 1{\cdot}309\,|\underline{25{\cdot}15°}$$

Similarly—

$$\mathbf{E}_M = \mathbf{E}_R - \mathbf{I}\mathbf{X}_M = 1{\cdot}0 - j0{\cdot}48(0{\cdot}5 - j0{\cdot}167) = 0{\cdot}951\,|\underline{-14{\cdot}6°}$$

* The use of per unit current values eliminates the phase factor $\sqrt{3}$ in three-phase calculations.

The initial system angle is thus $\theta_0 = 25{\cdot}15° + 14{\cdot}6° = 39{\cdot}75°$, giving $\sin \theta_0 = 0{\cdot}6395$. The maximum transfer power is

$$P_m = \frac{E_G E_M}{X} = \frac{1{\cdot}309 \times 0{\cdot}951}{1{\cdot}112 + 0{\cdot}48} = 0{\cdot}782 \text{ per unit}$$

The full-load vector diagram is shown in Fig. 81 (*b*).

[**Check.** $P_0 = P_m \sin \theta_0 = 0{\cdot}782 \times 0{\cdot}6395 = 0{\cdot}5$ per unit = 30 000 kW.]

By taking several values of I ranging from, say, one-quarter to twice full load ($P_0 = 0{\cdot}125$ to $1{\cdot}0$ per unit), and determining the corresponding values of $\sin \theta_0$ and P_m, the fundamental transfer-power curves of Fig. 82 are then plotted. The data for these two curves are tabulated below.

P_0	E_G	E_M	θ_0	$\sin \theta_0$	P_m
0·125	1·068	0·982	11·0	0·1897	0·659
0·250	1·128	0·968	21·5	0·3649	0·685
0·375	1·213	0·957	31·0	0·5143	0·729
0·500	1·309	0·951	39·8	0·6395	0·782
0·625	1·414	0·949	47·9	0·7417	0·843
0·750	1·526	0·951	55·3	0·8234	0·911
0·875	1·645	0·957	62·2	0·8847	0·989
1·000	1·765	0·968	68·8	0·9323	1·073

The next step in the calculation is to determine the transfer reactance of the system under fault conditions. As already explained, the fault can be represented by an appropriate reactance X_F, connected as a shunt at the point of fault, whose value is a simple function of the negative- and zero-sequence reactances of the system (X_2 and X_0) viewed from the point of fault. Fig. 83 (*a*) shows the negative-sequence reactance diagram of the system, all reactance values being calculated in per unit on a 60 000 kVA. base, as before. Denoting reactances between G and the point of fault by the subscript a, and reactances between M and the point of fault by the subscript b, we have—

$$X_{a_2} = 0{\cdot}14 + 0{\cdot}095 + 0{\cdot}461 = 0{\cdot}696$$

$$X_{b_2} = 0{\cdot}384 + 0{\cdot}095 + 0{\cdot}231 = 0{\cdot}710$$

and hence, since X_{a_2} and X_{b_2} are in parallel when viewed from the point of fault—

$$X_2 = \frac{X_{a_2} X_{b_2}}{X_{a_2} + X_{b_2}} = \frac{0{\cdot}696 \times 0{\cdot}710}{1{\cdot}406} = 0{\cdot}352$$

The corresponding zero-sequence reactance diagram is shown in Fig. 83 (*b*). The reactance of the transmission line to zero phase-sequence currents is taken as 3·5 times the positive phase-sequence value. As the neutral points of the transformers are earthed and

their l.t. windings are delta-connected, they both provide paths for the zero phase-sequence currents. Hence in this case we have—

$$X_{a_0} = 0{\cdot}095 + 1{\cdot}615 = 1{\cdot}710$$

$$X_{b_0} = 0{\cdot}095 + 0{\cdot}807 = 0{\cdot}902$$

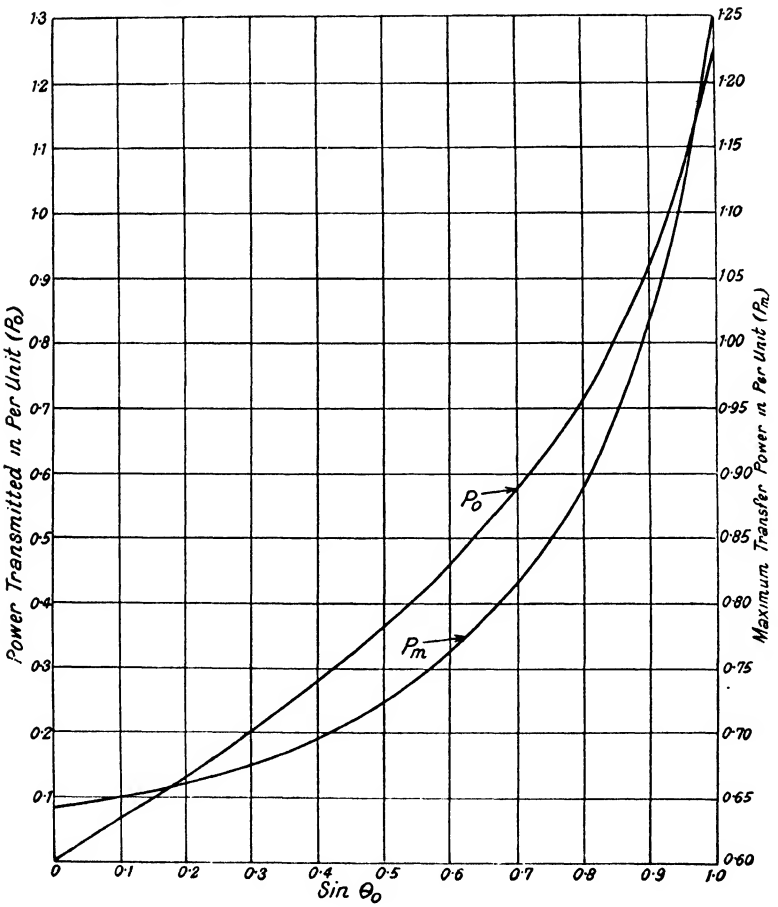

FIG. 82

so that, since these are in parallel as viewed from the fault,

$$X_0 = \frac{X_{a_0} X_{b_0}}{X_{a_0} + X_{b_0}} = \frac{1{\cdot}71 \times 0{\cdot}902}{2{\cdot}612} = 0{\cdot}590$$

For a single line-to-earth fault the equivalent fault reactance is—

$$X_F = X_2 + X_0 = 0{\cdot}352 + 0{\cdot}590 = \underline{0{\cdot}942}$$

while for a double line-to-earth fault—

$$X_F = \frac{X_2 X_0}{X_2 + X_0} = \frac{0{\cdot}352 \times 0{\cdot}590}{0{\cdot}942} = \underline{0{\cdot}220}$$

In the former case the negative- and zero-sequence networks are connected in series at the point of fault; in the latter case they are connected in parallel, as shown in Fig. 83 (*c*). The positive-sequence

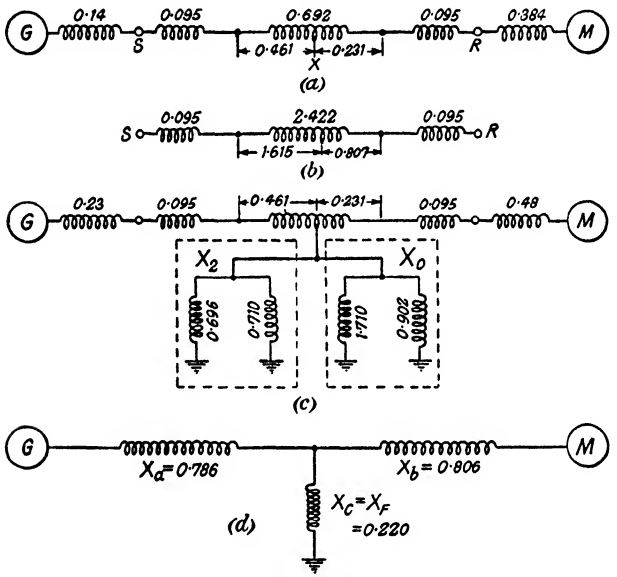

FIG. 83

network under fault conditions thus becomes a simple **T** circuit, as indicated in Fig. 83 (*d*), for which—

$$X_a = 0{\cdot}23 + 0{\cdot}095 + 0{\cdot}461 = 0{\cdot}786$$

$$X_b = 0{\cdot}48 + 0{\cdot}095 + 0{\cdot}231 = 0{\cdot}806$$

and $$X_c = X_F \begin{cases} = 0{\cdot}942 \text{ for a single line-to-earth fault} \\ = 0{\cdot}220 \quad \text{,, double ,, ,, ,,} \end{cases}$$

The transfer reactances of the system under these two fault conditions are given by equation (204) and have the values—

(*a*) $$X' = 0{\cdot}786 + 0{\cdot}806 + \frac{0{\cdot}786 \times 0{\cdot}806}{0{\cdot}942} = \underline{2{\cdot}264 \text{ per unit}}$$

and (*b*) $$X' = 0{\cdot}786 + 0{\cdot}806 + \frac{0{\cdot}786 \times 0{\cdot}806}{0{\cdot}22} = \underline{4{\cdot}471 \text{ per unit}}$$

The transfer reactances before the incidence and after the clearing of the fault are the same, namely—

$$X = X'' = X_a + X_b = 0{\cdot}786 + 0{\cdot}806 = \underline{1{\cdot}592 \text{ per unit}}$$

so that $r_2 = X/X'' = 1{\cdot}0$. The values of $r_1 = X/X'$ for the two types of fault are then—

(*a*) $r_1 = 1{\cdot}592/2{\cdot}264 = \underline{0{\cdot}703}$

and (*b*) $r_1 = 1{\cdot}592/4{\cdot}471 = \underline{0{\cdot}356}$

The maximum values of transmitted power which can be carried through a sustained fault of each type are found from Fig. 75, by putting $r = r_1$. Similarly the maximum power which can be transmitted without instability occurring, if the fault is cleared instantaneously, is given by putting $r = r_2$. The results are tabulated below.

Switching Time	r	$\sin\theta_0$	P_0* (per unit)	Limiting Transmitted Power (kW.)
∞	$r_1 = 0{\cdot}356$	0·292	0·195	11 700
∞	$r_1 = 0{\cdot}703$	0·635	0·496	29 750
0	$r_2 = 1{\cdot}000$	1·000	1·250	75 000

The final step in the calculation is the evaluation of the constant $c = \sqrt{(\pi f/HP_n)}$ in the basic relation $\tau' = c\sqrt{(r_1 P_m)} \cdot t$ between generalized time and actual time. In this case—

$$c = \sqrt{\frac{3{\cdot}1416 \times 50}{2{\cdot}46 \times 1{\cdot}0}} = 7{\cdot}99$$

Values of τ' corresponding to r_1 and r_2 as already found, and to successive values of $\sin\theta_0$, are extracted from the generalized switching-time curves given in Figs. 58 to 74. Values of P_0 and P_m corresponding to the same values of $\sin\theta_0$ are then taken from Fig. 82. The corresponding switching times are readily calculated from τ', r_1, and P_m. The results are tabulated below for the two types of fault considered.

(*a*) *Single Line-to-earth Fault* ($r_1 = 0{\cdot}703$; $r_2 = 1{\cdot}0$)

$\sin\theta_0$	P_0	P_m	$P_m' = r_1 P_m$	$7{\cdot}99\sqrt{r_1 P_m}$	τ'	t
1·00	1·250	—	—	—	—	0
0·90	0·913	1·015	0·714	5·390	1·06	0·197
0·85	0·797	0·940	0·661	5·190	1·54	0·297
0·80	0·710	0·887	0·624	5·032	2·06	0·409
0·75	0·636	0·848	0·596	4·931	2·69	0·546
0·70	0·572	0·817	0·575	4·840	3·61	0·746
0·65	0·512	0·788	0·554	4·752	(6·0)	(1·26)
0·635	0·496	—	—	—	—	∞

* From Fig. 82.

(*b*) *Double Line-to-earth Fault* ($r_1 = 0{\cdot}356$; $r_2 = 1{\cdot}0$)

$\sin \theta_0$	P_0	P_m	$P_m' = r_1 P_m$	$7{\cdot}99\sqrt{(r_1 P_m)}$	τ'	t
1·00	1·250	—	—	—	—	0
0·90	0·913	1·015	0·361	3·838	0·30	0·078
0·85	0·797	0·940	0·335	3·694	0·50	0·135
0·80	0·710	0·887	0·316	3·587	0·64	0·178
0·75	0·636	0·848	0·302	3·508	0·80	0·228
0·70	0·572	0·817	0·291	3·443	0·95	0·276
0·65	0·512	0·788	0·281	3·382	1·15	0·340
0·60	0·458	0·763	0·272	3·332	1·35	0·405
0·55	0·409	0·744	0·265	3·286	1·58	0·481
0·50	0·362	0·723	0·257	3·240	1·85	0·571
0·45	0·319	0·708	0·252	3·206	2·20	0·686
0·40	0·278	0·695	0·248	3·184	2·57	0·807
0·35	0·238	0·682	0·243	3·147	3·25	1·033
0·30	0·202	0·673	0·240	3·122	5·00	1·602
0·292	0·195	—	—	—	—	∞

The required relation between transmitted power (P_0) and the critical clearing time (t) is shown by the switching-time curves of Fig. 84.

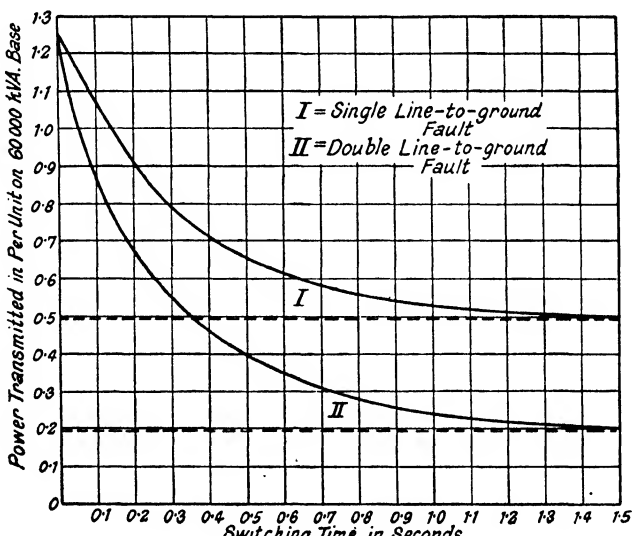

FIG. 84

Example 2. *The interconnection of two selected stations of the British "Grid" system is shown by the single-line circuit diagram of Fig.* 85. *Station A is a base load station the bulk of whose energy output is transmitted via two* 132 *kV. transmission lines to station B, which supplies a large industrial load area. Station A is also linked to stations C, D, E, and F by means of four* 132 *kV. interconnectors tied together at the high-tension busbars of the "Grid" substation at A. The outputs of the two stations are as follows:—*

STATION *A*

Export to station B.	180 000 *kW.*
Export to stations C, D, E, and F . .	10 000 *kW.*
Local load demand	30 000 *kW.*
Station output	220 000 *kW.*

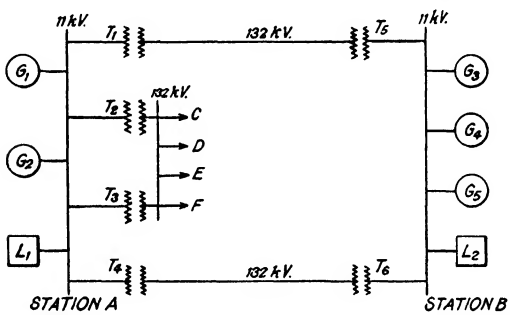

FIG. 85

STATION *B*

Station load demand	230 000 *kW.*
Import from station A	180 000 *kW.*
Station output	50 000 *kW.*

The interconnector transformers T_1, T_2, T_3, *and* T_4, *and the "Grid" substation transformers* T_5 *and* T_6 *each have a reactance of* 10 *per cent and are rated at* 45 000 *kVA. The two transmission lines each have a reactance of* 7·8 *ohms at* 50 *c/s. The ratings, speeds, and transient reactances of the several generators are as follows—*

STATION *A*

(G_1): *Two* 37 500 *kVA. units.* $N = 1\,500$ *r.p.m.* $x' = 22$ *per cent*
(G_2): *Three* 62 500 *kVA. units.* $N = 1\,500$ *r.p.m.* $x' = 28$ *per cent*

STATION *B*

(G_3): *Two* 23 435 *kVA. units.* $N = 1\,500$ *r.p.m.* $x' = 20{\cdot}4$ *per cent*
(G_4): *One* 22 500 *kVA. units.* $N = 1\,500$ *r.p.m.* $x' = 29$ *per cent*
(G_5): *One* 31 250 *kVA. units.* $N = 3\,000$ *r.p.m.* $x' = 23$ *per cent*

Rated voltage is maintained at the 11 kV. busbars of the two stations.

A flashover occurs on the high-tension side of one of the "Grid" substation transformers and immediately develops into a short circuit between all three phases.

(a) *Determine the time within which the fault must be cleared if stations A and B are to remain in synchronism.*

(b) *Using the step-by-step method, plot the appropriate swing curves for fault durations of* 0·2, 0·35, *and* 0·5 *second respectively.*

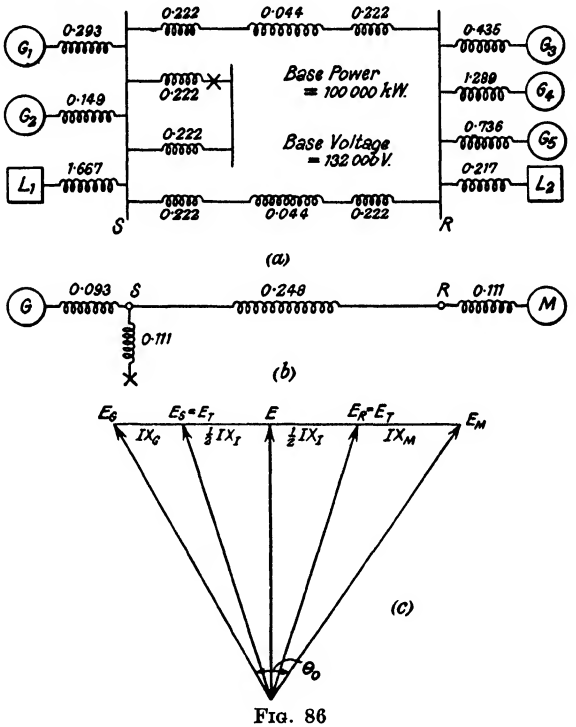

FIG. 86

Solution. It is first of all necessary to convert all reactances and H values to per unit on, say, a 100 000 kW. base. The station loads may be represented by synchronous machines having a reactance of 50 per cent on the kW rating and $H = 1{\cdot}95$ per unit.* The results are tabulated below. Fig. 86 (*a*) shows the per unit reactance diagram of the system, which reduces to the simple reactive tie of Fig. 86 (*b*). S and R are the station busbars, where the voltage is maintained constant at 11 kV. Referred to the nominal transmission pressure, $E_T = 132$ kV., as a voltage base, we thus have $E_S = E_R = 1{\cdot}0$ per unit. The initial transfer power is $P_0 = 180\,000$ kW. $= 1{\cdot}8$ per unit. Fig.

* See footnote on p. 179.

Item	kVA. Rating	Machine kVA. Base		System kVA. Base	
		x'	H*	x'	H
G_1	75 000	0·22	8.25	0·293	6·19
G_2	187 500	0·28	7·40	0·149	13·87
L_1	30 000	0·50	1·95	1·667	0·59
G_3	46 870	0·204	8·70	0·435	4·08
G_4	22 500	0·29	8·80	1·289	1·98
G_5	31 250	0·23	5·50	0·736	1·72
L_2	230 000	0·50	1·95	0·217	4·28
T	45 000	0·10	—	0·222	—

86 (*c*) shows the system vector diagram from which, with $P_0 = EI$ and $E^2 = E_T^2 - (\frac{1}{2}IX_l)^2$, one finds—

$$I^2 = \frac{2}{X_l^2}(E_T^2 - \sqrt{E_T^4 - P_0^2X_l^2})$$

$$= \frac{2}{0{\cdot}244^2}[1{\cdot}0 - \sqrt{1{\cdot}0 - (1{\cdot}8 \times 0{\cdot}244)^2}]$$

$$= 34{\cdot}15\,(1{\cdot}0 - \sqrt{0{\cdot}8103}) = 3{\cdot}408$$

and $E^2 = \frac{1}{2}(E_T^2 + \sqrt{E_T^4 - P_0X_l^2}) = 0{\cdot}5(1{\cdot}0 + 0{\cdot}9002) = 0{\cdot}9501$

Hence $E_G^2 = E^2 + I^2(X_G + \frac{1}{2}X_l)^2 = 1{\cdot}1062$; $\therefore E_G = \underline{1{\cdot}052 \text{ per unit}}$

and $E_M^2 = E^2 + I^2(X_M + \frac{1}{2}X_l)^2 = 1{\cdot}1135$; $\therefore E_M = \underline{1{\cdot}065 \text{ per unit}}$

(*a*) The transfer reactance of the system before the incidence of the fault is—

$$X = 0{\cdot}093 + 0{\cdot}244 + 0{\cdot}111 = \underline{0{\cdot}448 \text{ per unit}}$$

For a three-phase short circuit the equivalent fault reactance is zero, so that (Fig. 79) the transfer reactance during the fault is simply—

$$X' = 0{\cdot}093 + 0{\cdot}355 + \frac{0{\cdot}093 \times 0{\cdot}355}{0{\cdot}111} = \underline{0{\cdot}748 \text{ per unit}}$$

After the fault is cleared the system returns to its pre-fault configuration, so that $X'' = X$. Hence—

$$r_1 = 0{\cdot}448/0{\cdot}748 = 0{\cdot}599; \text{ and } r_2 = 1{\cdot}0$$

The maximum transfer power before the fault occurs is—

$$P_m = \frac{1{\cdot}052 \times 1{\cdot}065}{0{\cdot}448} = \underline{2{\cdot}51 \text{ per unit}}$$

so that the initial system angle is given by—

$$\sin\theta_0 = P_0/P_m = 1{\cdot}80/2{\cdot}51 = 0{\cdot}717$$

from which $\theta_0 = 45{\cdot}8°$. The maximum transfer power during the fault is

$$P_m' = r_1P_m = 0{\cdot}599 \times 2{\cdot}51 = \underline{1{\cdot}50 \text{ per unit}}$$

* The figures for the generators are taken from Fig. 77.

The critical clearing angle is defined by equation (150), which gives—

$$\cos\theta_1 = \frac{\left[\frac{\pi}{180}(180 - 91{\cdot}6) \times 0{\cdot}717\right] - [1{\cdot}599 \times 0{\cdot}697]}{0{\cdot}401}$$

$$= \frac{1{\cdot}106 - 1{\cdot}114}{0{\cdot}401} = -\frac{0{\cdot}008}{0{\cdot}401} = -0{\cdot}01995$$

Thus $\theta_1 = (180 - 88{\cdot}8) = \underline{91{\cdot}2 \text{ degrees}}$. Also we have from equation (188)—

$$T = 0{\cdot}717/0{\cdot}599 = 1{\cdot}19$$

Using pre-calculated angle/time curves (e.g. Fig. 57) one finds $\tau' = 1{\cdot}92$ for $\sin\theta_0 = 0{\cdot}717$, $T = 1{\cdot}19$, and $\theta_1 = 91{\cdot}1°$. Alternatively, with $r_1 = 0{\cdot}599$ and $r_2 = 1{\cdot}0$, the pre-calculated switching-time curves of Figs. 70 and 71 give—

$$\left.\begin{array}{l}\sin\theta_0 = 0{\cdot}70 \quad . \quad . \quad . \quad . \quad \tau' = 2{\cdot}11 \\ \sin\theta_0 = 0{\cdot}75 \quad . \quad . \quad . \quad . \quad \tau' = 1{\cdot}72\end{array}\right\}$$

from which $\tau' = 1{\cdot}98$ with $\sin\theta_0 = 0{\cdot}717$. Taking the mean of these two values for the generalized time, we have $\tau' = 1{\cdot}95$. The aggregate per unit stored energy of station A is—

$$H_1 = 6{\cdot}19 + 13{\cdot}87 + 0{\cdot}59 = 20{\cdot}65$$

while that of station B is—

$$H_2 = 4{\cdot}08 + 1{\cdot}98 + 1{\cdot}72 + 4{\cdot}28 = 12{\cdot}06$$

The corresponding figure for the equivalent generator at A when B is considered as an infinite bus is then—

$$H = \frac{H_1 H_2}{H_1 + H_2} = \frac{20{\cdot}65 \times 12{\cdot}06}{32{\cdot}71} = \underline{7{\cdot}61 \text{ per unit}}$$

The generalized time τ' is related to actual time t by the factor

$$\sqrt{\left(\frac{\pi f}{H} \cdot \frac{P_m'}{P_n}\right)} = \sqrt{\frac{50\pi}{7{\cdot}61}} \times \frac{1{\cdot}5}{1{\cdot}0} = 5{\cdot}56$$

Hence the time within which the fault must be cleared is—

$$t = 1{\cdot}95/5{\cdot}56 = \underline{0{\cdot}35 \text{ seconds}}$$

(*b*) In the step-by-step method of transient stability analysis a time interval of $\Delta t = 0{\cdot}05$ sec. does not generally lead to a large cumulative error in the computation of the appropriate swing curves, and this interval will accordingly be used for the present example. The inertia constant in this case is—

$$M = \frac{HP_n}{180f} = \frac{7{\cdot}61 \times 100\,000}{180 \times 50} = 84{\cdot}55 \text{ kW.-sec.}^2/\text{deg.},$$

or $$M = H/180f = 8{\cdot}455 \times 10^{-4} \text{ per unit},$$

so that the acceleration constant is—

$$k = \frac{(\Delta t)^2}{2M} = \frac{0{\cdot}05^2 \times 10^4}{2 \times 8{\cdot}455} = 1{\cdot}48 \text{ per unit.}$$

The step-by-step calculation schedules, based on equation (182), are given below. The three swing curves are shown in Fig. 87.

1. *Fault cleared at time* $t = 0{\cdot}2$ *sec.*

t	P_0	P_m	$P = P_m \sin\theta$	$\Delta P = P_0 - P$	$k \cdot \Delta P$	$\Delta\theta$	θ
0	1·8	1·504	1·078	0·722	1·07	0	45·81
0·05	1·8	1·504	1·097	0·703	1·04	1·07	46·88
0·10	1·8	1·504	1·153	0·647	0·96	3·18	50·06
0·15	1·8	1·504	1·235	0·565	0·84	5·18	55·24
0·20	1·8	2·511	2·221	− 0·421	− 0·62	6·98	62·22
0·25	1·8	2·511	2·350	− 0·550	− 0·81	7·20	69·42
0·30	1·8	2·511	2·428	− 0·628	− 0·93	5·77	75·19
0·35	1·8	2·511	2·466	− 0·666	− 0·99	4·03	79·22
0·40	1·8	2·511	2·482	− 0·682	− 1·01	2·11	81·33
0·45	1·8	2·511	2·482	− 0·682	− 1·01	0·11	81·44
0·50	1·8	2·511	2·469	− 0·669	− 0·99	− 1·91	79·53
0·55	1·8	2·511	2·432	− 0·632	− 0·93	− 3·91	75·62
0·60	1·8	2·511	2·354	− 0·554	− 0·82	− 5·83	69·79
0·65	1·8	2·511	2·217	− 0·417	− 0·62	− 7·58	62·25
0·70	1·8	2·511	2·005	− 0·205	− 0·30	− 9·02	53·23
0·75	1·8	2·511	1·681	0·119	− 0·18	− 9·94	42·29
0·80	1·8	2·511	1·163	0·637	0·94	− 14·42	27·87
0·85	1·8	2·511	0·604	1·196	1·77	− 13·66	13·21
0·90	1·8	2·511	0·043	1·757	2·60	− 10·93	2·26
0·95	1·8	2·511	− 0·159	1·959	2·88	− 6·58	− 4·32
1·00	1·8	2·511	− 0·209	2·009	2·96	− 1·10	− 5·42
1·05	1·8	2·511	0·000	1·800	2·56	4·70	− 0·72
1·10	1·8	2·511	0·444	1·356	2·00	10·22	9·50
1·15	1·8	2·511	1·057	0·743	1·10	14·78	24·28
1·20	1·8	—	—	—	—	17·88	42·16

2. *Fault cleared at time* $t = 0{\cdot}35$ *sec.*

t	P_0	P_m	$P = P_m \sin\theta$	$\Delta P = P_0 - P$	$k \cdot \Delta P$	$\Delta\theta$	θ
0·15	1·8	1·504	1·235	0·565	0·84	5·18	55·24
0·20	1·8	1·504	1·330	0·470	0·69	6·98	62·22
0·25	1·8	1·504	1·419	0·381	0·56	8·51	70·73
0·30	1·8	1·504	1·483	0·317	0·47	9·76	80·49
0·35	1·8	2·511	2·511	− 0·711	− 1·05	10·79	91·28
0·40	1·8	2·511	2·460	− 0·660	− 0·99	10·19	101·47
0·45	1·8	2·511	2·365	− 0·565	− 0·84	8·15	109·62
0·50	1·8	2·511	2·256	− 0·456	− 0·67	6·32	115·96
0·55	1·8	2·511	2·157	− 0·357	− 0·53	4·81	120·77
0·60	1·8	2·511	2·070	− 0·270	− 0·40	3·61	124·38
0·65	1·8	2·511	2·001	− 0·201	− 0·30	2·68	127·06
0·70	1·8	2·511	1·947	− 0·147	− 0·22	1·98	129·04
0·75	1·8	2·511	1·907	− 0·107	− 0·16	1·46	130·50
0·80	1·8	2·511	1·874	− 0·074	− 0·11	1·08	131·58
0·85	1·8	2·511	1·849	− 0·049	− 0·07	0·81	132·39
0·90	1·8	2·511	1·830	− 0·030	− 0·05	0·63	133·02
0·95	1·8	2·511	1·817	− 0·017	− 0·03	0·41	133·43
1·00	1·8	2·511	1·806	− 0·006	− 0·01	0·33	133·76
1·05	1·8	2·511	1·796	0·004	0·01	0·29	134·05
1·10	1·8	2·511	1·787	0·013	0·02	0·29	134·34
1·15	1·8	2·511	1·776	0·024	0·04	0·32	134·66
1·20	1·8	—	—	—	—	0·38	135·04

3. *Fault cleared at time* $t = 0{\cdot}5$ *sec.*

t	P_o	P_m	$P = P_m \sin\theta$	$\Delta P = P_o - P$	$k \cdot \Delta P$	$\Delta\theta$	θ
0·30	1·8	1·504	1·483	0·317	0·47	9·76	80·49
0·35	1·8	1·504	1·503	0·297	0·44	10·79	91·28
0·40	1·8	1·504	1·466	0·334	0·49	11·70	102·98
0·45	1·8	1·504	1·356	0·444	0·66	12·63	115·61
0·50	1·8	2·511	1·940	− 0·140	− 0·21	13·78	129·39
0·55	1·8	2·511	2·511	0·346	0·51	14·23	143·62
0·60	1·8	2·511	0·905	0·895	1·32	17·53	161·15
0·65	1·8	2·511	0·232	1·568	2·31	19·36	180·51
0·70	1·8	—	—	—	—	22·99	203·50

Example 3. *The transmission system shown in Fig.* 88 (*a*) *represents a hydro-electric generating station supplying power over a double-circuit* 220 *kV. transmission line to a power system whose effect is simulated by*

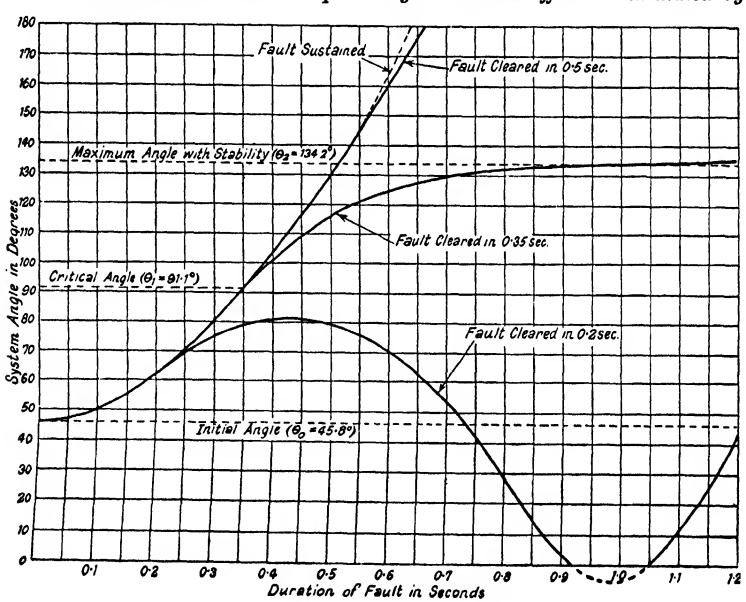

FIG. 87

an equivalent generating station and an equivalent load connected directly to the receiving-end busbars. The high-tension neutral points of the sending-end transformer banks are grounded through resistance, while those of the transformer banks at the receiving end are solidly earthed. The two transmission circuits are sectionalized by a bus-coupler at the mid point

of the line. The impedances of the several elements of the system, expressed in per unit on a 262 000 kVA. base, are as follows:—

HYDRO-ELECTRIC STATION (H)

Transient impedance ($\mathbf{Z}_{H_1}$)	$= 0{\cdot}004 + j0{\cdot}30$
Negative-sequence impedance ($\mathbf{Z}_{H_2}$)	$= 0{\cdot}12 + j0{\cdot}334$

STEAM STATION (S)

Transient impedance ($\mathbf{Z}_{S_1}$)	$= 0{\cdot}0026 + j0{\cdot}131$
Negative-sequence impedance ($\mathbf{Z}_{S_2}$)	$= 0{\cdot}0026 + j0{\cdot}0851$

TRANSFORMER BANKS

Sending-end transformer impedance ($\mathbf{Z}_{TS}$)	$= 0{\cdot}005 + j0{\cdot}100$
Earthing resistance (R_G)	$= 0{\cdot}10$
Receiving-end transformer impedance ($\mathbf{Z}_{TR}$)	$= 0{\cdot}0055 + j0{\cdot}109$

TRANSMISSION LINE (*two circuits in parallel*)

Positive-sequence impedance ($\mathbf{Z}_{TL_1}$)	$= 0{\cdot}043 + j0{\cdot}288$
Negative-sequence impedance ($\mathbf{Z}_{TL_2}$)	$= 0{\cdot}0043 + j0{\cdot}288$
Zero-sequence impedance ($\mathbf{Z}_{TL_0}$)	$= 0{\cdot}075 + j0{\cdot}504$

Under steady-state conditions the operating data of the system are as follows:—

Normal voltage at receiving-end busbars (E_R)	$= 1{\cdot}00$ *per unit*
Active power supplied by transmission line (P_{R_1})	$= 200\,000$ *kW.*
Reactive power supplied by transmission line (Q_{R_1})	$= 39\,000$ *kVAr.*
Active power supplied by equivalent steam station (P_{R_2})	$= 282\,000$ *kW.*
Reactive power supplied by equivalent steam station (Q_{R_2})	$= -\,264\,000$ *kVAr.*
Active power demand of equivalent load (P_L)	$= 482\,000$ *kW.*
Reactive power taken by equivalent load (Q_L)	$= -\,225\,000$ *kVAr.*

A double line-to-earth fault occurs on one of the transmission circuits near the sending-end busbars. Determine the time within which this fault must be cleared in order that the system may remain stable. Find also the steady-state power limit of the system.

Solution. (a) The positive-sequence network is a simple **T**-circuit, as shown in Fig. 88 (b), the impedances of which are

$$\mathbf{Z}_a = (\mathbf{Z}_{H_1} + \mathbf{Z}_{TS} + \mathbf{Z}_{TL_1} + \mathbf{Z}_{TR}),\ \mathbf{Z}_b = \mathbf{Z}_{S_1},\ \text{and}\ \mathbf{Z}_c = \mathbf{Z}_{L_1}$$

Taking the receiving-end busbar voltage as the axis of reference, we may write $\mathbf{E}_R = 1{\cdot}0\,\underline{|0°} = 1{\cdot}0 + j0$ per unit. Converting active and reactive power values to per unit on a 262 000 kVA. base, we find—

$$\mathbf{Z}_{L_1} = \frac{E_R^2}{P_L + jQ_L} = \frac{1{\cdot}0}{1{\cdot}841 - j0{\cdot}859} = 0{\cdot}446 + j0{\cdot}208 = 0{\cdot}492\,\underline{|25{\cdot}0°}$$

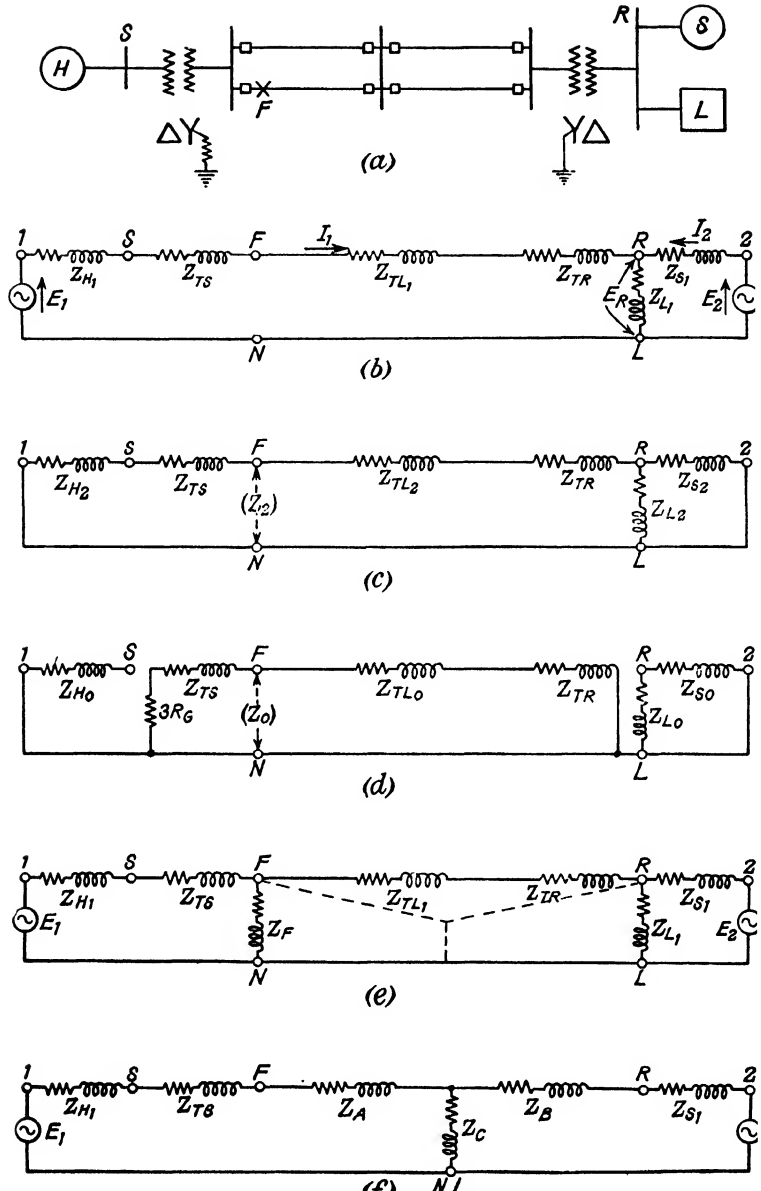
H
S
F
R
S
L
(a)
1
S
F
I_1
R
I_2
2
Z_{H_1}
Z_{TS}
Z_{TL_1}
Z_{TR}
Z_{S_1}
E_1
E_R
Z_{L_1}
E_2
N
L
(b)
1
S
F
R
2
Z_{H_2}
Z_{TS}
(Z_{L_2})
Z_{TL_2}
Z_{TR}
Z_{S_2}
Z_{L_2}
N
L
(c)
1
S
F
R
2
Z_{H_0}
Z_{TS}
$3R_G$
(Z_0)
Z_{TL_0}
Z_{TR}
Z_{S_0}
Z_{L_0}
N
L
(d)
1
S
F
R
2
Z_{H_1}
Z_{TS}
Z_{TL_1}
Z_{TR}
Z_{S_1}
E_1
Z_F
Z_{L_1}
E_2
N
L
(e)
1
S
F
R
2
Z_{H_1}
Z_{TS}
Z_A
Z_B
Z_{S_1}
E_1
Z_C
N, L
(f)

FIG. 88

Thus—

$$\mathbf{Z}_a = (0{\cdot}004 + j0{\cdot}300) + (0{\cdot}005 + j0{\cdot}100) + (0{\cdot}043 + j0{\cdot}288) + (0{\cdot}0055 + j0{\cdot}109)$$
$$= 0{\cdot}0575 + j0{\cdot}797 = 0{\cdot}799 \angle 85{\cdot}9°$$
$$\mathbf{Z}_b = 0{\cdot}0026 + j0{\cdot}131 = 0{\cdot}131 \angle 88{\cdot}6°$$
$$\mathbf{Z}_c = 0{\cdot}446 + j0{\cdot}208 = 0{\cdot}492 \angle 25{\cdot}0°$$

so that the driving-point impedances are—

$$\mathbf{Z}_1 = \mathbf{Z}_a + \frac{\mathbf{Z}_b\mathbf{Z}_c}{\mathbf{Z}_b + \mathbf{Z}_c} = 0{\cdot}799 \angle 85{\cdot}9° + \frac{0{\cdot}131 \angle 88{\cdot}6° \times 0{\cdot}492 \angle 25{\cdot}0°}{0{\cdot}449 + j0{\cdot}339}$$
$$= (0{\cdot}0575 + j0{\cdot}797) + (0{\cdot}0268 + j0{\cdot}111) = 0{\cdot}0842 + j0{\cdot}908$$
$$= 0{\cdot}913 \angle 84{\cdot}7°$$

and

$$\mathbf{Z}_2 = \mathbf{Z}_b + \frac{\mathbf{Z}_a\mathbf{Z}_c}{\mathbf{Z}_a + \mathbf{Z}_c} = 0{\cdot}131 \angle 88{\cdot}6° + \frac{0{\cdot}799 \angle 85{\cdot}9° \times 0{\cdot}492 \angle 25{\cdot}0°}{0{\cdot}504 + j1{\cdot}005}$$
$$= (0{\cdot}003 + j0{\cdot}131) + (0{\cdot}237 + j0{\cdot}259) = 0{\cdot}240 + j0{\cdot}390$$
$$= 0{\cdot}458 \angle 58{\cdot}4°$$

while the transfer impedance is—

$$\mathbf{Z} = \mathbf{Z}_a + \mathbf{Z}_b + \frac{\mathbf{Z}_a\mathbf{Z}_b}{\mathbf{Z}_c} = 0{\cdot}061 + j0{\cdot}928 + \frac{0{\cdot}799 \angle 85{\cdot}9° \times 0{\cdot}131 \angle 88{\cdot}6°}{0{\cdot}492 \angle 25{\cdot}0°}$$
$$= (0{\cdot}061 + j0{\cdot}928) + (-0{\cdot}183 + j0{\cdot}108) = -0{\cdot}123 + j1{\cdot}036$$
$$= 1{\cdot}043 \angle 96{\cdot}75°$$

(*b*) The negative-sequence network is shown in Fig. 88 (*c*). The impedance of the load $\mathbf{Z}_{L2}$ is not known, but may be assumed infinite without much error, as it is shunted by the low impedance $\mathbf{Z}_{S2}$. The impedance between 1 and the point of fault is—

$$\mathbf{Z}_{1F} = \mathbf{Z}_{L_2} + \mathbf{Z}_{TS} = (0{\cdot}12 + j0{\cdot}334) + (0{\cdot}005 + j0{\cdot}100)$$
$$= 0{\cdot}125 + j0{\cdot}434$$

while the impedance between 2 and the point of fault is—

$$\mathbf{Z}_{2F} = \mathbf{Z}_{TL_2} + \mathbf{Z}_{TR} + \frac{\mathbf{Z}_{L_2}\mathbf{Z}_{S_2}}{\mathbf{Z}_{L_2} + \mathbf{Z}_{S_2}} \cong \mathbf{Z}_{TL_2} + \mathbf{Z}_{TR} + \mathbf{Z}_{S_2}$$
$$= (0{\cdot}043 + j0{\cdot}288) + (0{\cdot}0055 + j0{\cdot}109) + (0{\cdot}0026 + j0{\cdot}0851)$$
$$= 0{\cdot}051 + j0{\cdot}482$$

The negative-sequence impedance of the system viewed from the point of fault is $\mathbf{Z}_N$, where

$$\frac{1}{\mathbf{Z}_N} = \frac{1}{\mathbf{Z}_{1F}} + \frac{1}{\mathbf{Z}_{2F}} = \frac{1}{0{\cdot}125 + j0{\cdot}434} + \frac{1}{0{\cdot}051 + j0{\cdot}482}$$
$$= (0{\cdot}61 - j2{\cdot}13) + (0{\cdot}22 - j2{\cdot}05) = 0{\cdot}83 - j4{\cdot}18$$

The zero-sequence network is shown in Fig. 88 (*d*). As the zero-sequence current in the neutral is the sum of the zero-sequence currents in all three phases, any neutral impedance has an effective value *per phase* of three times its actual value. The impedance per phase equivalent

to the neutral earthing resistance R_G is thus $3R_G$. The impedance to the left of the point of fault is—

$$\mathbf{Z}_{1F} = 3\mathbf{Z}_G + \mathbf{Z}_{TS} = (0{\cdot}3 + j0) + (0{\cdot}005 + j0{\cdot}100) = 0{\cdot}305 + j0{\cdot}100$$

while the impedance to the right of the point of fault is—

$$\mathbf{Z}_{2F} = \mathbf{Z}_{TL_0} + \mathbf{Z}_{TR} = (0{\cdot}075 + j0{\cdot}504) + (0{\cdot}006 + j0{\cdot}109)$$
$$= 0{\cdot}081 + j0{\cdot}613$$

The zero-sequence impedance of the system viewed from the point of fault is $\mathbf{Z}_0$, where

$$\frac{1}{\mathbf{Z}_0} = \frac{1}{\mathbf{Z}_{1F}} + \frac{1}{\mathbf{Z}_{2F}} = \frac{1}{0{\cdot}305 + j0{\cdot}100} + \frac{1}{0{\cdot}081 + j0{\cdot}613}$$
$$= (2{\cdot}96 - j0{\cdot}97) + (0{\cdot}21 - j1{\cdot}60) = 3{\cdot}17 - j2{\cdot}57$$

For a double line-to-ground fault the equivalent positive-sequence fault impedance $\mathbf{Z}_F$ is given by—

$$\frac{1}{\mathbf{Z}_F} = \frac{1}{\mathbf{Z}_N} + \frac{1}{\mathbf{Z}_0} = (0{\cdot}83 - j4{\cdot}18) + (3{\cdot}17 - j2{\cdot}57)$$
$$= 4{\cdot}00 - j6{\cdot}75$$

whence $\mathbf{Z}_F = 1/(4{\cdot}00 - j6{\cdot}75) = 0{\cdot}065 + j0{\cdot}110 = 0{\cdot}128\,\underline{|59{\cdot}5°}$

The positive-sequence network under fault conditions is accordingly as shown in Fig. 88 (*e*), in which the equivalent impedance $\mathbf{Z}_F$ is connected as a shunt at the point of fault. The delta-connected system of impedances $\mathbf{Z}_F$, $(\mathbf{Z}_{TL_1} + \mathbf{Z}_{TR})$, $\mathbf{Z}_{L_1}$ may be replaced by the equivalent star-connected system $\mathbf{Z}_A$, $\mathbf{Z}_B$, $\mathbf{Z}_C$, as shown in Fig. 88 (*f*). On putting

$$\mathbf{Z}_T = \mathbf{Z}_{TL1} + \mathbf{Z}_{TR} = (0{\cdot}043 + j0{\cdot}288) + (0{\cdot}006 + j0{\cdot}109)$$
$$= 0{\cdot}049 + j0{\cdot}397 = 0{\cdot}400\,\underline{|83{\cdot}0°}$$

and $$\Sigma\mathbf{Z} = \mathbf{Z}_F + \mathbf{Z}_T + \mathbf{Z}_{L_1} = 0{\cdot}560 + j0{\cdot}715 = 0{\cdot}908\,\underline{|51{\cdot}9°}$$

we then have—

$$\mathbf{Z}_A = \frac{\mathbf{Z}_F\mathbf{Z}_T}{\Sigma\mathbf{Z}} = \frac{0{\cdot}128 \times 0{\cdot}400}{0{\cdot}908}\,\underline{|59{\cdot}5° + 83{\cdot}0° - 51{\cdot}9°}$$
$$= 0{\cdot}0564\,\underline{|90{\cdot}6°} = -0{\cdot}0006 + j0{\cdot}0564$$

$$\mathbf{Z}_B = \frac{\mathbf{Z}_T\mathbf{Z}_{L_1}}{\Sigma\mathbf{Z}} = \frac{0{\cdot}400 \times 0{\cdot}492}{0{\cdot}908}\,\underline{|83{\cdot}0° + 25{\cdot}0° - 51{\cdot}9°}$$
$$= 0{\cdot}2167\,\underline{|56{\cdot}1°} = 0{\cdot}1207 + j0{\cdot}1800$$

$$\mathbf{Z}_C = \frac{\mathbf{Z}_{L_1}\mathbf{Z}_F}{\Sigma\mathbf{Z}} = \frac{0{\cdot}492 \times 0{\cdot}128}{0{\cdot}908}\,\underline{|25{\cdot}0 + 59{\cdot}5° - 51{\cdot}9°}$$
$$= 0{\cdot}0693\,\underline{|32{\cdot}6°} = 0{\cdot}0584 + j0{\cdot}0374$$

Fig. 88 (*f*) represents a simple T-circuit whose impedances are—

$$\mathbf{Z}_a' = \mathbf{Z}_{E1} + \mathbf{Z}_{TS} + \mathbf{Z}_A = 0{\cdot}0084 + j0{\cdot}4564 = 0{\cdot}457\,\underline{|88{\cdot}8°}$$
$$\mathbf{Z}_b' = \mathbf{Z}_B + \mathbf{Z}_{S_1} = 0{\cdot}1233 + j0{\cdot}3110 = 0{\cdot}334\,\underline{|68{\cdot}8°}$$
$$\mathbf{Z}_c' = \mathbf{Z}_C = 0{\cdot}0584 + j0{\cdot}0374 = 0{\cdot}0693\,\underline{|32{\cdot}6°}$$

The driving-point impedances of the system while the fault is on are thus—

$$\mathbf{Z}_1' = \mathbf{Z}_a' + \frac{\mathbf{Z}_b'\mathbf{Z}_c'}{\mathbf{Z}_b' + \mathbf{Z}_c'} = (0{\cdot}0084 + j0{\cdot}4564) + (0{\cdot}0457 + j0{\cdot}0370)$$
$$= 0{\cdot}0541 + j0{\cdot}4934 = 0{\cdot}496\,\underline{|83{\cdot}7^\circ}$$

$$\text{and } \mathbf{Z}_2' = \mathbf{Z}_b' + \frac{\mathbf{Z}_a'\mathbf{Z}_c'}{\mathbf{Z}_a' + \mathbf{Z}_c'} = (0{\cdot}1233 + j0{\cdot}3110) + (0{\cdot}0502 + j0{\cdot}0396)$$
$$= 0{\cdot}1735 + j0{\cdot}3506 = 0{\cdot}349\,\underline{|63{\cdot}7^\circ}$$

while the corresponding transfer impedance is—

$$\mathbf{Z}' = \mathbf{Z}_a' + \mathbf{Z}_b' + \frac{\mathbf{Z}_a'\mathbf{Z}_b'}{\mathbf{Z}_c'}$$
$$= (0{\cdot}1317 + j0{\cdot}7674) + (-\,1{\cdot}260 + j1{\cdot}799)$$
$$= -\,1{\cdot}128 + j2{\cdot}566 = 2{\cdot}803\,\underline{|113{\cdot}7^\circ}$$

(*c*) After the fault is cleared the impedance network of the system reverts to its original form, as shown by Fig. 88 (*b*), but the driving-point and transfer impedances are changed in value through the switching out of the faulty line section. The impedance of each double-circuit section is normally $\frac{1}{2}(0{\cdot}043 + j0{\cdot}288) = 0{\cdot}0215 + j0{\cdot}144$. After the faulty circuit is cleared the impedance of the affected section becomes twice the pre-fault value, viz. $0{\cdot}043 + j0{\cdot}288$. The new value of transmission-line impedance is thus—

$$\mathbf{Z}_{TL}'' = (0{\cdot}0215 + j0{\cdot}144) + (0{\cdot}043 + j0{\cdot}288) = 0{\cdot}0645 + j0{\cdot}432$$

Hence $\mathbf{Z}_a'' = \mathbf{Z}_{H_1} + \mathbf{Z}_{TS} + \mathbf{Z}_{TL}'' + \mathbf{Z}_{TR}$
$$= (0{\cdot}004 + j0{\cdot}300) + (0{\cdot}005 + j0{\cdot}100)$$
$$+ (0{\cdot}0645 + j0{\cdot}432) + (0{\cdot}0055 + j0{\cdot}109)$$
$$= 0{\cdot}079 + j0{\cdot}941 = 0{\cdot}945\,\underline{|85{\cdot}2^\circ}$$

The remaining impedances are unchanged in value, so that

$$\mathbf{Z}_b'' = \mathbf{Z}_b = 0{\cdot}003 + j0{\cdot}131 = 0{\cdot}131\,\underline{|88{\cdot}6^\circ}$$
$$\text{and } \mathbf{Z}_c'' = \mathbf{Z}_c = 0{\cdot}446 + j0{\cdot}208 = 0{\cdot}492\,\underline{|25{\cdot}0^\circ}$$

The driving-point and transfer impedances are thus—

$$\mathbf{Z}_1'' = \mathbf{Z}_a'' + \frac{\mathbf{Z}_b''\mathbf{Z}_c''}{\mathbf{Z}_b'' + \mathbf{Z}_c''} = 0{\cdot}945\,\underline{|85{\cdot}2^\circ} + 0{\cdot}1146\,\underline{|76{\cdot}55^\circ}$$
$$= 0{\cdot}108 + j1{\cdot}052 = 1{\cdot}058\,\underline{|84{\cdot}1^\circ}$$

$$\mathbf{Z}_2'' = \mathbf{Z}_b'' + \frac{\mathbf{Z}_a''\mathbf{Z}_c''}{\mathbf{Z}_a'' + \mathbf{Z}_c''} = 0{\cdot}131\,\underline{|88{\cdot}6^\circ} + 0{\cdot}3679\,\underline{|44{\cdot}8^\circ}$$
$$= 0{\cdot}265 + j0{\cdot}390 = 0{\cdot}472\,\underline{|55{\cdot}8^\circ}$$

$$\mathbf{Z}'' = \mathbf{Z}_a'' + \mathbf{Z}_b'' + \frac{\mathbf{Z}_a''\mathbf{Z}_b''}{\mathbf{Z}_c''} = (0{\cdot}082 + j1{\cdot}072) + 0{\cdot}251\,\underline{|148{\cdot}8^\circ}$$
$$= -\,0{\cdot}133 + j1{\cdot}202 = 1{\cdot}210\,\underline{|96{\cdot}3^\circ}$$

(*d*) The air-gap voltages of the generators (see Fig. 88 (*b*)) are given by—

$$\mathbf{E}_1 = \mathbf{E}_R + \mathbf{I}_1\mathbf{Z}_a$$
$$\mathbf{E}_2 = \mathbf{E}_R + \mathbf{I}_2\mathbf{Z}_b$$

where $$\mathbf{I}_1 = \frac{P_{R_1} + jQ_{R_1}}{E_R} = \frac{0{\cdot}764 + j0{\cdot}149}{1{\cdot}0\,\underline{|0°}}$$
$$= 0{\cdot}764 + j0{\cdot}149 = 0{\cdot}778\,\underline{|11{\cdot}0°}\text{ per unit*}$$

and $$\mathbf{I}_2 = \frac{P_{R_2} + jQ_{R_2}}{E_R} = \frac{1{\cdot}077 - j1{\cdot}008}{1{\cdot}0\,\underline{|0°}}$$
$$= 1{\cdot}077 - j1{\cdot}008 = 1{\cdot}475\,\underline{|-43{\cdot}1°}\text{ per unit*}$$

Hence $$\mathbf{E}_1 = 1{\cdot}0\,\underline{|0°} + (0{\cdot}778\,\underline{|11{\cdot}0°} \times 0{\cdot}799\,\underline{|85{\cdot}9°})$$
$$= (1{\cdot}0 + j0) + (-0{\cdot}075 + j0{\cdot}618)$$
$$= 0{\cdot}925 + j0{\cdot}618 = \underline{1{\cdot}112\,|33{\cdot}75°}\text{ per unit}$$

and $$\mathbf{E}_2 = 1{\cdot}0\,\underline{|0°} + (1{\cdot}475\,\underline{|-43{\cdot}1°} \times 0{\cdot}131\,\underline{|88{\cdot}6°})$$
$$= (1{\cdot}0 + j0) + (0{\cdot}135 + j0{\cdot}138)$$
$$= 1{\cdot}135 + j0{\cdot}138 = \underline{1{\cdot}142\,|6{\cdot}9°\text{ per unit}}$$

The initial system angle is thus—

$$\theta_0 = 33{\cdot}75° - 6{\cdot}9° = \underline{26{\cdot}85\text{ electrical degrees}}$$

The air-gap powers of the generators are then—

$$P_1 + jQ_1 = \mathbf{E}_1\mathbf{I}_1 = 1{\cdot}112\,\underline{|-33{\cdot}75°} \times 0{\cdot}778\,\underline{|11{\cdot}0°}$$
$$= 0{\cdot}865\,\underline{|-22{\cdot}75°} = 0{\cdot}798 - j0{\cdot}335\text{ per unit}$$
$$P_2 + jQ_2 = \mathbf{E}_2\mathbf{I}_2 = 1{\cdot}142\,\underline{|-6{\cdot}9°} \times 1{\cdot}475\,\underline{|-43{\cdot}1°}$$
$$= 1{\cdot}686\,\underline{|-50{\cdot}0°} = 1{\cdot}080 - j1{\cdot}191\text{ per unit.}$$

The mechanical inputs to the generators under these conditions are accordingly—

$$P_{M_1} = P_1 = 0{\cdot}798\text{ per unit} = 209\,000\text{ kW.}$$
$$P_{M_2} = P_2 = 1{\cdot}080\text{ per unit} = 283\,000\text{ kW.}$$

The assumption will here be made that the hydro-electric station contains five 50 000 kVA. generators whose aggregate output is thus (0·865 × 262 000) = 226 500 kVA. at a power factor of cos (22·75°) = 0·923 lagging, and that the steam station contains ten 45 000 kVA. units supplying (1·686 × 262 000) = 441 400 kVA. at a power factor of cos (50°) = 0·643 lagging. Taking $H_1 = 3{\cdot}5$ and $H_2 = 8{\cdot}1$ kW.-sec. per kVA. from Figs. 77 and 78, we have—

$$H_1 = 3{\cdot}5 \times 0{\cdot}865 = 3{\cdot}0\text{ per unit}$$
$$H_2 = 8{\cdot}1 \times 1{\cdot}686 = 13{\cdot}7\text{ per unit}$$
$$H = \frac{H_1H_2}{H_1 + H_2} = \frac{3 \times 13{\cdot}7}{16{\cdot}7} = \underline{2{\cdot}46\text{ per unit}}$$

* See footnote on p. 181.

Equation (162) then gives for the equivalent mechanical input—

$$P_M = \frac{H_2 P_{M_1} - H_1 P_{M_2}}{H_1 + H_2} = \frac{(13{\cdot}7 \times 0{\cdot}798) - (3{\cdot}0 \times 1{\cdot}080)}{3{\cdot}0 + 13{\cdot}7}$$
$$= \underline{0{\cdot}460 \text{ per unit}}$$

(*e*) The per unit air-gap powers of the two generators before the fault occurs are given by equations (155) and (156) as—

$$P_{E_1} = \frac{E_1^2}{Z_1} \sin \sigma_1 + \frac{E_1 E_2}{Z} \sin (\theta - \sigma)$$
$$= \frac{1{\cdot}112^2}{0{\cdot}913} \sin 5{\cdot}3° + \frac{1{\cdot}112 \times 1{\cdot}142}{1{\cdot}043} \sin (\theta + 6{\cdot}75°)$$
$$= 0{\cdot}125 + 1{\cdot}217 \sin (\theta + 6{\cdot}75°)$$

and
$$P_{E_2} = \frac{E_2^2}{Z_2} \sin \sigma^2 - \frac{E_1 E_2}{Z} \sin (\theta + \sigma)$$
$$= \frac{1{\cdot}142^2}{0{\cdot}458} \sin 31{\cdot}6° - 1{\cdot}217 \sin (\theta - 6{\cdot}75°)$$
$$= 1{\cdot}493 - 1{\cdot}217 \sin (\theta - 6{\cdot}75°)$$

[**Check.** When $\theta = \theta_0$, the air-gap powers become—

$$P_{E_1} = 0{\cdot}125 + 1{\cdot}217 \sin (26{\cdot}85° + 6{\cdot}75°) = 0{\cdot}80 = P_{M_1}$$
$$P_{E_2} = 1{\cdot}493 - 1{\cdot}217 \sin (26{\cdot}85° - 6{\cdot}75°) = 1{\cdot}08 = P_{M_2}$$

corresponding to the initial steady-state conditions of operation.]

The corresponding air-gap powers during the fault are, similarly—

$$P_{E_1}' = \frac{1{\cdot}112^2}{0{\cdot}496} \sin 6{\cdot}3° + \frac{1{\cdot}112 \times 1{\cdot}142}{2{\cdot}803} \sin (\theta + 23{\cdot}7°)$$
$$= 0{\cdot}264 + 0{\cdot}453 \sin (\theta + 23{\cdot}7°)$$

and
$$P_{E_2}' = \frac{1{\cdot}142^2}{0{\cdot}349} \sin 26{\cdot}3° - 0{\cdot}453 \sin (\theta - 23{\cdot}7°)$$
$$= 1{\cdot}655 - 0{\cdot}453 \sin (\theta - 23{\cdot}7°)$$

while after the fault has been cleared they become

$$P_{E_1}'' = \frac{1{\cdot}112^2}{1{\cdot}058} \sin 5{\cdot}9° + \frac{1{\cdot}112 \times 1{\cdot}142}{1{\cdot}210} \sin (\theta + 6{\cdot}3°)$$
$$= 0{\cdot}120 + 1{\cdot}050 \sin (\theta + 6{\cdot}3°)$$

and
$$P_{E_2}'' = \frac{1{\cdot}142^2}{0{\cdot}472} \sin 34{\cdot}2° - 1{\cdot}050 \sin (\theta - 6{\cdot}3°)$$
$$= 1{\cdot}551 - 1{\cdot}050 \sin (\theta - 6{\cdot}3°)$$

(*f*) Before the fault occurs the per unit separating powers are thus—

$$P_{0_1} = 0{\cdot}798 - 0{\cdot}125 = 0{\cdot}673$$
$$P_{0_2} = 1{\cdot}080 - 1{\cdot}493 = -0{\cdot}413$$

and during the fault they become—

$$P_{0_1}' = 0{\cdot}798 - 0{\cdot}264 = 0{\cdot}534$$
$$P_{0_2}' = 1{\cdot}080 - 1{\cdot}655 = -0{\cdot}575$$

After the fault is cleared the corresponding values are—

$$P_{0_1}'' = 0{\cdot}798 - 0{\cdot}120 = 0{\cdot}678$$

$$P_{0_2}'' = 1{\cdot}080 - 1{\cdot}551 = -0{\cdot}471$$

Equation (168) then gives for the equivalent separating powers—

$$P_0 = \frac{H_2P_{0_1} - H_1P_{0_2}}{H_1 + H_2} = \frac{(13{\cdot}7 \times 0{\cdot}673) + (3{\cdot}0 \times 0{\cdot}413)}{3{\cdot}0 + 13{\cdot}7}$$

$$= \underline{0{\cdot}625 \text{ per unit}}$$

$$P_0' = \frac{H_2P_{0_1}' - H_1P_{0_2}'}{H_1 + H_2} = \frac{(13{\cdot}7 \times 0{\cdot}534) + (3{\cdot}0 \times 0{\cdot}575)}{3{\cdot}0 + 13{\cdot}7}$$

$$= \underline{0{\cdot}546 \text{ per unit}}$$

$$P_0'' = \frac{H_2P_{0_1}'' - H_1P_{0_2}''}{H_1 + H_2} = \frac{(13{\cdot}7 \times 0{\cdot}678) + (3{\cdot}0 \times 0{\cdot}471)}{3{\cdot}0 + 13{\cdot}7}$$

$$= \underline{0{\cdot}640 \text{ per unit}}$$

so that the per unit equivalent driving-point powers are—

$$P_D = P_M - P_0 = 0{\cdot}460 - 0{\cdot}625 = -0{\cdot}166$$

$$P_D' = P_M - P_0' = 0{\cdot}460 - 0{\cdot}546 = -0{\cdot}086$$

$$P_D'' = P_M - P_0'' = 0{\cdot}460 - 0{\cdot}640 = -0{\cdot}180$$

The equivalent synchronizing-power maxima are found from equation (165) to be—

$$P_\mu = P_m\sqrt{\left(1 - \frac{4H^2}{H_1H_2}\sin^2\sigma\right)}$$

$$= 1{\cdot}217\sqrt{\left[1 - \frac{(2 \times 2{\cdot}46 \times \sin 6{\cdot}75°)^2}{3{\cdot}0 \times 13{\cdot}7}\right]} = \underline{1{\cdot}212 \text{ per unit}}$$

$$P_\mu' = 0{\cdot}453\sqrt{[1 - 0{\cdot}5895\ (\sin 23{\cdot}7°)^2]} = \underline{0{\cdot}431 \text{ per unit}}$$

$$P_\mu'' = 1{\cdot}050\sqrt{[1 - 0{\cdot}5895\ (\sin 6{\cdot}3°)^2]} = \underline{1{\cdot}046 \text{ per unit}}$$

while equation (166) gives for the corresponding equivalent displacement angles—

$$\tan\mu = \left(\frac{H_1 - H_2}{H_1 + H_2}\right)\tan\sigma = \left(\frac{3{\cdot}0 - 13{\cdot}7}{3{\cdot}0 + 13{\cdot}7}\right)\tan(-6{\cdot}75°)$$

$$= -0{\cdot}6408 \times -0{\cdot}1184 = 0{\cdot}0759; \quad \underline{\mu = 4{\cdot}3°}$$

$$\tan\mu' = -0{\cdot}6408\tan(-23{\cdot}7°) = 0{\cdot}2813; \quad \underline{\mu' = 15{\cdot}7°}$$

$$\tan\mu'' = -0{\cdot}6408\tan(-6{\cdot}3°) = 0{\cdot}0708; \quad \underline{\mu'' = 4{\cdot}0°}$$

The per unit air-gap powers of the equivalent generator are accordingly—

$$P_E = -0{\cdot}166 + 1{\cdot}212\sin(\theta + 4{\cdot}3°)$$

$$P_E' = -0{\cdot}086 + 0{\cdot}431\sin(\theta + 15{\cdot}7°)$$

$$P_E'' = -0{\cdot}180 + 1{\cdot}046\sin(\theta + 4{\cdot}0°)$$

[**Check.** When $\theta = \theta_0$, the air-gap power of the equivalent generator becomes—

$$P_E = -0{\cdot}166 + 1{\cdot}212\sin(26{\cdot}85° + 4{\cdot}3°) = 0{\cdot}46 = P_M$$

corresponding to the initial steady-state condition of operation.]

(*g*) Fig. 89 shows the equivalent power/angle diagram of the two-machine system of Fig. 88. To determine the critical clearing angle we have—

$$r_1 = \frac{P_{\mu}'}{P_{\mu}} = \frac{0{\cdot}431}{1{\cdot}212} = 0{\cdot}356$$

$$r_2 = \frac{P_{\mu}''}{P_{\mu}} = \frac{1{\cdot}046}{1{\cdot}212} = 0{\cdot}863$$

$$s_1 = \frac{P_0'}{P_0} = \frac{0{\cdot}546}{0{\cdot}626} = 0{\cdot}872$$

$$s_2 = \frac{P_0''}{P_0} = \frac{0{\cdot}640}{0\ 626} = 1{\cdot}022$$

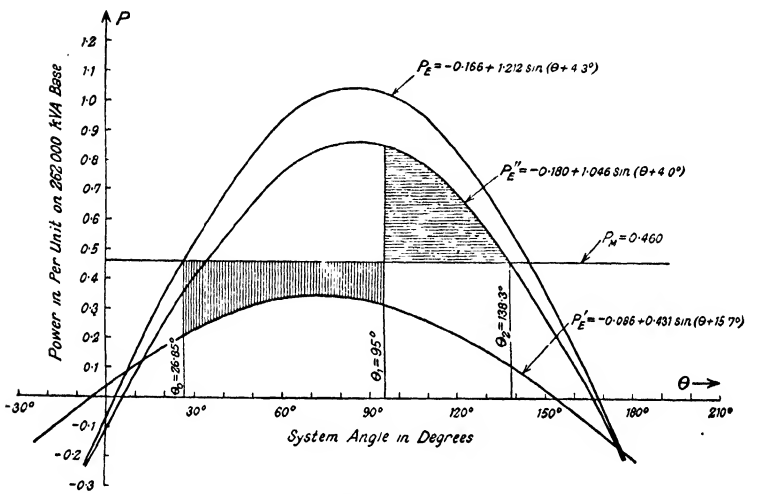

FIG. 89

Also, equation (176) gives—

$$\theta_2 = 180° - 4{\cdot}0° - \sin^{-1}(0{\cdot}640/1{\cdot}046) = 176{\cdot}0° - 37{\cdot}7° = 138{\cdot}3°$$

Hence $$\tan\gamma = \frac{r_2 \sin\mu'' - r_1 \sin\mu'}{r_2 \cos\mu'' - r_1 \cos\mu'} = -\frac{0{\cdot}038}{0{\cdot}520} = -0{\cdot}073$$

so that $\gamma = -4{\cdot}2°$. Furthermore—

$$r_1 \cos(\theta_0 + \mu') = 0{\cdot}356 \cos 42{\cdot}5° = 0{\cdot}260$$

$$r_2 \cos(\theta_2 + \mu'') = 0{\cdot}863 \cos 142{\cdot}3° = -0{\cdot}683$$

$$(s_2\theta_2 - s_1\theta_0)\sin(\theta_0 + \mu) = (141{\cdot}4 - 23{\cdot}4) \times \frac{\pi}{180} \times \frac{0{\cdot}626}{1{\cdot}212} = 1{\cdot}064$$

$$(s_1 - s_2)\,\theta_2 \,.\, \sin(\theta_0 + \mu) = -0{\cdot}15\theta_1 \times \frac{\pi}{180} \times \frac{0{\cdot}626}{1{\cdot}212} = -0{\cdot}00135\theta_1°$$

$$\sqrt{[r_1^2 + r_2^2 - 2r_1r_2\cos(\mu'' - \mu')]} = \sqrt{[(-0{\cdot}038)^2 + (0{\cdot}520)^2]} = 0{\cdot}521$$

Equation (177) accordingly gives for the critical clearing angle—

$$\cos(\theta_1^\circ - 4{\cdot}2^\circ) = \frac{1{\cdot}064 - 0{\cdot}001350\theta_1^\circ - 0{\cdot}260 - 0{\cdot}683}{0{\cdot}521}$$
$$= 0{\cdot}231 - 0{\cdot}00260\theta_1$$

the solution of which is $\theta_1 = 95{\cdot}0^\circ$. Introducing the variable θ' $= (\theta + \mu')$, we have—

$$\sin\theta_0' = \sin(26{\cdot}85^\circ + 15{\cdot}7^\circ) = \sin 42{\cdot}55^\circ = 0{\cdot}676$$
$$T = \frac{s_1 P_0}{r_1 P_\mu} = \frac{P_0'}{P_\mu'} = \frac{0{\cdot}546}{0{\cdot}431} = 1{\cdot}24$$
$$\theta_1' = (\theta_1 + \mu') = (95{\cdot}0^\circ + 15{\cdot}7^\circ) = 110{\cdot}7^\circ$$

From pre-calculated angle/time curves (e.g. Fig. 57) one finds $\tau' = 2{\cdot}24$ for the generalized time. Equation (193) finally gives—

$$t = \tau'\sqrt{\left(\frac{H}{\pi f} \cdot \frac{P_n}{P_\mu'}\right)}$$
$$= 2{\cdot}24 \times \sqrt{\left[\frac{2{\cdot}46}{50\pi} \times \frac{0{\cdot}431}{1{\cdot}0}\right]} = \underline{0{\cdot}43 \text{ sec.}}$$

If the system is to remain stable, therefore, the fault must be cleared within 21½ cycles.

The steady-state power limit is reached when $\theta = (90^\circ - 4{\cdot}3^\circ)$ $= 85{\cdot}7^\circ$, and its value is—

$$P_{max} = -0{\cdot}166 + 1{\cdot}212 = 1{\cdot}056 \text{ per unit}$$
$$= 1{\cdot}056 \times 262\,000 = \underline{276\,700 \text{ kW.}}$$

References

(1) *Cf.* A.I.E.E. Sub-committee's "First Report on Power System Stability," *Elec. Engineering*, 1937, Vol. 56, p. 261.

(2) *Vide* Edith Clarke and R. G. Lorraine: "Power Limits of Synchronous Machines," *Trans. A.I.E.E.*, 1934, Vol. 53, p. 1802.

(3) *Cf.* O. Muhleisen: "Power System Stability," *Elec. Journal*, 1930, Vol. 27, pp. 356 and 416; also R. H. Duval and L. J. Eastman: "System Stability Calculation Reduced to a Practical Basis," *Elec. World*, 1934, Vol. 103, pp. 514 and 620.

(4) *Trans. A.I.E.E.*, 1929, Vol. 48, p. 170.

(5) *Vide* O. G. C. Dahl: "Stability of the General Two-machine System," *Elec. Engineering*, 1935, Vol. 54, p. 185.

(6) *Vide* A. E. Kroneberg and Mabel MacFerran: "Power Limits of 220 kV. Transmission Lines," *Trans. A.I.E.E.*, 1934, Vol. 53, p. 1800, Appendix II.

(7) *Ibid.*, p. 1801, Appendix IV.

(8) *Vide* V. Bush and H. L. Hazen: "Integraph Solution of Differential Equations," *Journ. Franklin Inst.*, November, 1927, p. 575.

(9) *Vide* I. H. Summers and J. B. McClure: "Progress in the Study of System Stability," *Trans. A.I.E.E.*, 1930, Vol. 49, p. 132.

(10) *Vide* H. L. Byrd and S. R. Pritchard: "Solution of the Two-machine Stability Problem," *General Electric Review*, 1933, Vol. 36, p. 81.

(11) *Vide* R. T. Lythall: *Calculation of Fault Currents in Electrical Networks* (Pitman, London, 1940).

(12) *Vide* H. Rissik: "The Calculation of Unsymmetrical Short-circuits," *BEAMA Journal*, 1940: Part I—"Fundamental Principles and Methods of Analysis" (April); Part II—"Symmetrical Impedance Equivalents of Unsymmetrical Faults" (May); Part III—"The Phase-sequence Impedances of a Power Network" (June); Part IV—"Application of the Method to a Specific Example" (July); Part V—"Fault Current Distribution and System Voltage" (August).

(13) *Vide* I. T. Monseth and P. H. Robinson: *Relay Systems*, Ch. VII, pp. 212-38 (McGraw Hill Book Co., New York, 1935).

(14) *Vide* Reference (9), p. 149, Appendix V.

(15) *Trans. A.I.E.E.*, 1924, Vol. 43, p. 508.

(16) *Vide* Reference (9), p. 151, Appendix VI.

(17) *Vide* Reference (13), p. 121, Fig. 10.

(18) *Ibid.*, p. 125, Fig. 13.

(19) *Vide* Reference (4), Appendix I.

CHAPTER VI

LIMITATIONS OF A.C. POWER TRANSMISSION AND INTERCONNECTION

TOWARDS the end of 1938 the American Press commented upon an address given by the late Mr. J. D. Ross, President Roosevelt's chief technical adviser on power generation, transmission, and distribution, to the Engineers' Club of Seattle, the subject being the future possibility of linking all the varied sources of electric power in the United States by means of a trans-continental "grid." The climax to Mr. Ross's almost revolutionary exposition was the broad hint that such a vast interconnecting power network would, in all probability, operate as a super-tension d.c. system.* This statement coupled with the fact that tests have already been carried out on a 5 000 kW. experimental d.c. system, operating at 30 000 volts and transmitting power over a distance of 17 miles, once more raises doubts in the engineering mind as to the future of alternating current for the transport of electrical energy in bulk and over long distances.

For more than half a century the supremacy of alternating current in this sphere has remained unchallenged. The "battle of the systems" ended in the 'eighties of last century, and has been almost forgotten. But the question now arises whether that battle was decisive, in an absolute sense, or whether—as Lord Rayleigh prophesied to Kelvin† at the time—direct current will have its revenge in a final encounter, after which it will once more come into its own. We are living in a revolutionary age, an era of renaissance, embracing the whole complex of human achievement—economics, politics, science, technology. In the engineering sphere we are to-day witnessing the decline of electro-dynamics as the motivating factor in electrical development and its supersession by electronics. And it seems likely, therefore, that a future victory of direct current over alternating current in the field of power transmission

* See *inter alia* the *Scientific American*, December 1938.

† Kelvin himself declared as late as 1907: "I have never swerved from the opinion that the right system for long-distance transmission of power by electricity is the direct-current system."

will only be achieved by the aid of electronic devices of some kind. The advantages in favour of direct current are still largely theoretical.[1] In fact, at the moment d.c. transmission on the grand scale is barely a technical possibility, let alone an economic alternative to the present system of power transmission. Why, then, should responsible engineering opinion in the United States be giving serious consideration to high-tension direct current for this purpose? The answer is undoubtedly that the power limitation of a.c. transmission systems is no longer a matter of economics, but has become a question of a purely technical nature.

When considering the future possibilities of the present system of power transmission, it is necessary not only to bear in mind this change in emphasis from economic to technical considerations, but also to investigate its causes. In the past the economic limitation has been closely bound up with the attainment of higher transmission pressures. At first, no difficulty was experienced in utilizing the transmission-line conductors to the full extent of their power-carrying capacity. Transmission distances were short, and the amount of power transmitted was only a few thousand kilowatts. As time went on transmission pressures and distances gradually increased, and from accumulated experience it was found that the optimum economy from the points of view both of capital cost and of transmission losses was obtained with a line pressure of some 1 000 V. for every mile of transmission distance, and it was generally felt that any technical limitation was to be sought in the characteristics of generating plant and transformers rather than in those of the transmission line itself.

But the subsequent development in the United States, by 1920, of such long-distance transmission systems as the Big Creek and Pit River schemes, involving distances of 240 miles and operating at a pressure of 220 kV., for the first time clearly showed that the characteristics of the transmission line imposed a prior limitation. This new limitation arose from the fact that with transmission lines of such length sufficient power could not be transmitted—at any rate, not with the requisite degree of reliability—to justify the cost of the transmission system. Nearly twenty years ago, then, the accepted theory and practice of power transmission indicated that 250 miles represented about the maximum distance over which electrical energy could be transported in bulk; while subsequent

technical advance, as reflected in the Boulder Dam scheme, for example, which came into operation in 1936, and which involved a transmission voltage of 287 kV. and a distance of 267 miles, has done nothing to vitiate that conclusion. The reason for this purely technical limitation in the case of the present system of power transmission arises partly from considerations of finite system reactance and partly from the excitation requirements of the transmission line. Let us examine the latter aspect first, for a qualitative analysis brings out clearly the influence of line excitation upon the economics of the transmission problem.

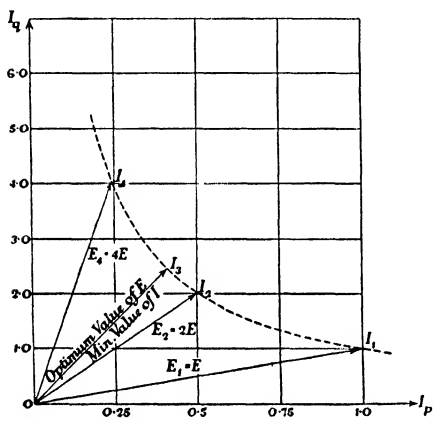

FIG. 90

Economic Aspects of the Transmission Problem. It is not generally realized that a transmission line requires excitation no less than a generator or a transformer. This excitation varies with the load, as in the case of a dynamo-electric machine, and its supply must be regulated by the generators or by additional synchronous condensers, or by both means. Moreover, it has a direct influence on the voltage at the receiving end of the transmission line, and it is precisely this interdependence between power transmitted, line voltage, and line excitation which leads to the difficulty of operating long-distance transmission lines. In this connection it is to be borne in mind that the excitation requirements of the line may be met partially, and in the case of very long lines wholly, by the charging current due to line capacitance. This charging current, being wattless, contributes only to the transmission losses, and for a given line there is an optimum value of transmission pressure for which these losses are a minimum. For line pressures below this value the power current is then too great, while for higher pressures the charging current becomes excessive. The bigger the line susceptance due to capacitance, the lower will be the optimum transmission pressure. As the capacitive susceptance is proportional to the length of the line

as well as to the system frequency, it is at once seen that the optimum value of the transmission voltage (i.e. the value for which the power losses are a minimum) can be raised, thus increasing the power-transmitting capacity of the line, by lowering the frequency. Here, then, we have the first indication as to the economic use of direct current as a means of long-distance power transmission.

The influence of the charging current on the transmission losses may, perhaps, be seen more clearly from Fig. 90. If E be the transmission pressure and I_p the load (power) current, then the power transmitted is $\sqrt{3}EI_p$. If I_q be the charging (quadrature) current, then the exciting kVAr. is, similarly, $\sqrt{3}EI_q$. The power losses are then $3I^2R = 3R\,(I_p^2 + I_q^2)$, where R is the line resistance per phase. By doubling the transmission voltage the charging current will be doubled also, but the load current will be halved (for the same transmitted power). The resultant line current will thus be reduced from I_1 to I_2. On raising the transmission voltage still further a point is eventually reached where the line current becomes a minimum, as shown at I_3 in Fig. 90. Any increase in voltage beyond this optimum value will result in an increase in the total current carried by the line, due to the preponderating effect of the charging current. Suppose now the length of the transmission line be, say, doubled. If E remains unchanged at the above optimum value, it is clear that the charging current I_q will also be doubled. Consequently the line current I will be increased, and the line will no longer be operating under the most favourable conditions. To reduce the line current to the optimum value necessitates a *decrease* in transmission voltage. But such a decrease would defeat its object, for it would require a corresponding increase in the load current I_p if the power transmitted were to remain the same. This would in turn result in increased line losses, over and above the doubling of these losses due to the twofold increase in transmission distance, and thus of the line resistance.

The only way out of this technical dilemma is to increase the conductor cross-section. By this means the condition of optimum transmission voltage may be retained, but at the expense of increased line material and supports, that is to say, of an increase in cost of the transmission line. The charging current thus directly enters into the economics of the transmission problem. This aspect of long-distance power

transmission is best shown by deriving an expression for a figure of merit for the transmission line which takes into account not only the line losses, but also the amount of line material. This figure of merit may be termed the "costliness factor" of the transmission line, and is then defined as the geometric mean of the per unit transmission losses and the weight of line material per kilowatt transmitted. The former term is a measure of the operating cost of the line, while the latter term is a measure of the capital outlay. The resistance per phase is $R = \rho D/A$, where ρ is the resistivity, A the cross-sectional area of the conductors, and D the transmission distance. If P be the power transmitted, then the per unit power loss is—

$$p = \frac{3I^2R}{P} = \frac{3\rho D}{AP}(I_p^2 + I_q^2) \quad . \quad . \quad (215)$$

The weight of line material is $W = 3\Delta DA$, where Δ is the density of the conductor material. The weight per kilowatt transmitted is thus—

$$w = \frac{W}{P} = \frac{3\Delta DA}{P} \quad . \quad . \quad . \quad (216)$$

From (215) and (216) the costliness factor of the transmission line is—

$$F = \sqrt{pw} = \frac{3D}{P}\sqrt{\rho\Delta(I_p^2 + I_q^2)}$$

$$= \frac{3D}{P}\sqrt{\rho\Delta} \cdot \sqrt{\left[\left(\frac{P}{\sqrt{3} \cdot E}\right)^2 + \left(2\pi fCD\frac{E}{\sqrt{3}}\right)^2\right]} \quad (217)$$

That is—

$$F = k_1\sqrt{\left[\left(\frac{D}{E}\right)^2 + \left(\frac{2\pi fCD^2E}{1\,000P}\right)^2\right]} \quad . \quad . \quad . \quad (217a)$$

$$= \sqrt{\left[k_2\left(\frac{D}{E}\right)^2 + k_3\left(\frac{fCD^2E}{P}\right)^2\right]} \quad . \quad . \quad . \quad (217b)$$

where k_1, k_2, and k_3 are constants, f is the system frequency, D is the transmission distance in miles, E is the line pressure in kilovolts, P is the transmitted power in kilowatts, and C is the line capacitance to neutral in microfarads per mile.

It is at once seen that in the case of d.c. transmission (when $f = 0$) or of short a.c. lines (for which $CD \approx 0$) the second term in the above expressions becomes zero, so that the figure of merit for the transmission line is then determined solely by the ratio of distance to voltage. As has already been

mentioned, past experience has gone to show that the optimum value of this ratio is in the neighbourhood of one mile per kV. The second term in equation (217*b*) becomes of importance whenever the effect of capacitive reactance begins to make itself felt, that is, as soon as the question of frequency enters into the transmission problem. The occurrence of this second term in the expression for the overall figure of merit F is in itself an indication that the transmission of power cannot take place so economically with alternating current as with direct current at the same voltage. Furthermore, as C is practically a constant, it is evident that with increasing transmission distance D the transmission of power becomes ever less economical.

Take, for example, the Boulder Dam line, for which $E = 287$ kV., $D = 267$ miles, and $P = 240$ MW. If the transmission distance were increased to 500 miles, the line voltage would have to be raised to 540 kV. in order that the first term in equation (217*b*) should remain unaltered. The simultaneous increase in D and E, however, raises the second term in equation (217*b*) to 6·5 times its former value. Hence P would have to be increased to 1 560 MW. in order to restore the costliness factor of the transmission line to the original figure. In the case of a 750-mile transmission line, the new values would be $E = 810$ kV. and $P = 5\,250$ MW. Under these circumstances we arrive at a state of affairs where with distances of 500 miles, let alone 750 or even 1 000 miles, the necessary transmitted power becomes fantastically large if the transmission system is to operate upon an economic basis. It is clear, therefore, that the question of line excitation is the determinating factor in the economics of the transmission problem.

Technical Aspects and Limitations. Let us now consider this problem from its technical aspects. In the first place, there is a limit to the transmission voltage, imposed by considerations of insulation. Probably the maximum figure attainable to-day is in the region of 500 kV. Secondly, there is a limit to the amount of power which can be transmitted over a given line, this limit being determined in the last analysis by its inductive reactance. As explained in Chapter IV, the maximum power which can be carried by a transmission line is—

$$P_m = \frac{E_1 E_2 \sin \theta}{X} \quad . \quad . \quad . \quad (218)$$

where X is the total line reactance, E_1 and E_2 are the voltages at the two ends of the line, and θ is the angle of displacement between them. The latter depends in a complicated manner on the ratio between the line reactance X and the generator and load reactances, as well as upon the inertias of the synchronous machines at the two ends of the line. Average values of the transmission angle θ lie between 30 and 60 electrical degrees, according to the length of the line. Such values correspond to the steady-state power limit of the transmission system, which is reached when the phase angle between the voltages behind the synchronous machine reactances attains 90°.* For example, the stability limit might be reached with an angle of 25° between the air-gap and terminal voltages of the generators, 36° between the terminal voltages at the two ends of the line (including transformers), and 29° between the terminal and air-gap voltages of the synchronous machinery at the receiving end of the line. Assuming that the receiving-end plant, whether generators or synchronous motors or condensers, provides for the necessary line excitation so that the two line terminal voltages are kept the same, and taking average figures of 0·7 ohm per mile for the line reactance and 35° for the transmission angle, then equation (218) becomes—

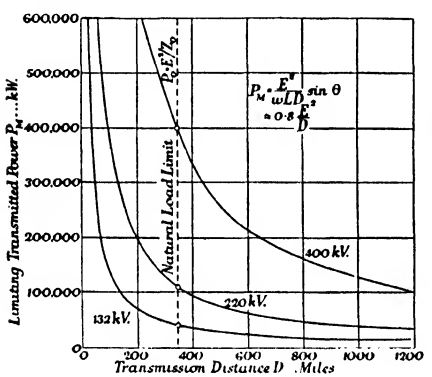

FIG. 91

$$P_m = \frac{E^2}{0{\cdot}7D} \times 0{\cdot}56 = 0{\cdot}8\,\frac{E^2}{D} \qquad . \qquad . \quad (218a)$$

This relation is shown graphically in Fig. 91. In the case of a 400-mile transmission line operating at 400 kV., for example, the power limit would thus be 320 000 kW. On the other hand, at 132 kV. the power limit for the same transmission distance would only be 35 000 kW. Assuming the same "costliness factor" as for the Boulder Dam line, the minimum

* Assuming all circuit resistance to be neglected, as in equation (218).

powers that can be economically transmitted in these two cases are, respectively, 1 370 000 kW. and 92 000 kW., as given by equation (217*a*), when taking $f = 50$ cycles and $C = 0{\cdot}014$ μF. per mile as an average value for modern high-tension transmission lines. The prior limitation imposed by stability considerations in the case of long-distance transmission is here clearly apparent.

The requirements of line excitation, which, as has already been shown, constitute the determining factor in the economics of long-distance transmission lines, are also reflected in the

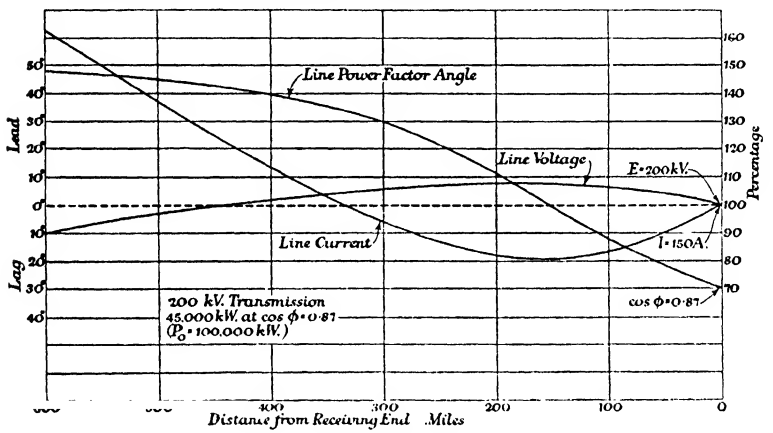

FIG. 92

voltage at the receiving end of the line. Due to the combined effect of capacitance and inductance, the receiving-end voltage depends to a very large extent upon the transmitted power and the load power factor.* Consider, for example, the case of a 600-mile line operating at 200 kV. and carrying a load of 45 000 kW. at 0·87 lagging power factor. Fig. 92 shows the variation in line voltage, line current, and line power-factor angle in terms of distance in miles from the receiving end. It is seen that the line current rapidly changes in magnitude, reaching a minimum value of 80 per cent of the normal at a distance of 150 miles. Due to the heavy lagging reactive component of the load current (50 per cent) and the high capacitance of the line, the phase angle between current and voltage also changes rapidly, passing through zero where the

* See Chapter I, Reference (4).

current is a minimum, and reaching nearly 50 degrees leading at the sending end of the line, where the current has risen to over 160 per cent of its normal value. The considerable effect of the charging current taken by long-distance transmission lines is clearly demonstrated by this rapid change, and it is seen that the low power factor at the sending end of the line results in a leading reactive kVA. requirement amounting to no less than 125 per cent of the power transmitted. Consideration of the variation in line voltage, on the other hand, reveals that the total variation is less than 20 per cent, the maximum increase above the receiving-end voltage being only about 7 per cent. This favourable variation is due to the highly inductive load.

Fig. 92 illustrates the general tendency of long high-tension transmission lines to show an overall rise in voltage from the sending end to the receiving end, provided the load is less than that corresponding to the so-called natural load condition of the line—a condition representing the maximum economy in the transmission of power. Consider for a moment an ideal transmission line having negligible resistance and leakage conductance. If the load could be gradually increased from zero, it would be found that there was a definite value of transmitted power for which both the current I and the voltage E remain constant in magnitude at all points along the line. This critical load is termed the natural load of the transmission line. The natural load condition is then defined by $E/\sqrt{3}\,I = Z_0 =$ constant, where Z_0 is the characteristic impedance of the line. The natural load is therefore—

$$P_0 = \sqrt{3}EI = \frac{E^2}{Z_0} \quad . \quad . \quad . \quad (219)$$

and is thus a function of the transmission pressure only, since the characteristic impedance Z_0 varies but little for different overhead transmission lines. The latter quantity is defined by—

$$Z_0 = \sqrt{\frac{Z}{Y}} = \sqrt{\left(\frac{R + j\omega C}{G + j\omega C}\right)} \approx \sqrt{\frac{L}{C}}$$

and in general has a value of some 400 ohms. Under natural load conditions, then, the voltage and current along the line each undergo the same increasing phase displacement with respect to their receiving-end vector positions, but remain

unchanged in relative phase displacement and, neglecting losses, in magnitude.

This relation may be expressed as—

$$\frac{\mathbf{E}_S}{\mathbf{E}_R} = \frac{\mathbf{I}_S}{\mathbf{I}_R} = \varepsilon^{j\Theta}; \quad \frac{E_S}{I_S} = \frac{E_R}{I_R} = \sqrt{3}Z_0 = \text{constant};$$

where $\Theta = pD$ and $p \simeq 2\pi f\sqrt{(LC)}$ is the propagation constant of the transmission line in radians per mile (if L and C are expressed per mile), while the subscripts S and R refer to the sending and receiving ends, respectively. The radical term $\sqrt{(LC)}$ is the reciprocal of v, the velocity of propagation, which is nearly that of light, viz. 186 000 miles per second for an overhead line. Hence the value of p for a 50-cycle transmission line is 0·17 radian, or 10·3 electrical degrees per 100 miles. The transmission angle Θ between the sending- and receiving-end voltages (and currents also) is thus given by—

$$\Theta = \frac{2\pi fD}{v} \text{ radians} = \frac{360}{\lambda} D \text{ deg.}$$

where λ is the natural wavelength of the transmission line, amounting to 3 700 miles at 50 c/s. The effect of resistance and leakage conductance, which has so far been neglected, is to cause an attenuation of the voltage and current along the line in accordance with an exponential law, due to the appearance of a real term in addition to the imaginary term $j\Theta$ in the index of the exponential ε. That is to say, in addition to a gradual and simultaneous shifting in phase of the voltage and current vectors, at the rate of 1° for every 10 miles of line, there occurs an exponential reduction in magnitude of these vectors which is also at the same rate for both.

When operating under "natural" load conditions, therefore, a transmission line behaves as a theoretically perfect conductor, permitting a specific amount of power to be transmitted over any desired distance. In fact, with unity load power factor at the receiving end, the electrical behaviour of such a line is almost the same as that of a d.c. line. However, in practice we are faced with the very real difficulty that the power to be transmitted can seldom be maintained at the value corresponding to the natural load of the line, which, putting $Z_0 = 400$ in equation (219), is given by $P_0 = 2{\cdot}5E^2$, where P_0 is in kilowatts and E in kilovolts. Any considerable deviation from this critical value upsets the delicate balance between line drop

due to inductance, and charging current due to capacitance. And as with long lines the reactance drop and charging current assume enormous proportions,* it is clear that any substantial deviation from the natural load condition will have a disastrous effect upon the sending-end voltage and reactive power consumption. If the power transmitted falls below the critical value, the reactive voltage drop decreases, but for the same sending-end terminal voltage, the charging current will remain unaltered. The latter, then, generates in the inductance of the line an in-phase voltage component which effects a rise in pressure at the receiving end—known as the "Ferranti effect." (In the case of a 600-mile line at no load, for which the charging current is equal to the natural load current, the voltage at the receiving end would be double the transmission pressure.) Conversely, if the load rises above the critical value, the reactive drop increases and results in a fall in voltage towards the receiving end.

A comparison of equations (218) and (219) reveals that there is a given transmission distance for which the maximum load determined by considerations of system stability (P_m) is equal to the natural load (P_0) and that this distance is independent of the transmission voltage. The limiting transmission distance is defined by—

$$D = \frac{Z_0 \sin\theta}{2\pi fL} = \frac{\sin\theta}{p} \quad . \quad . \quad . \quad (220)$$
$$= 590 \sin\theta \text{ miles}$$

Taking $\theta = 35°$ as an average value for the transmission angle, it is seen that the limiting distance over which power can be transmitted under the most favourable conditions from the operating standpoint is about 350 miles. This "natural load limit" is shown in Fig. 91, along with the "stability limit" curves based on equation (218*a*).

The Future Trend in Power System Interconnection. The future of the present system of power transmission is intimately bound up with the possibility of increasing the transmission distance beyond the limit of 300 to 400 miles. For it is but seldom that sources of cheap water power are within easy reach of industrial load centres, while the linking of existing

* A little consideration will show that the reactive voltage drop is $E_x = E\Theta$, while the charging current is similarly $I_c = I\Theta$, where Θ is expressed in radians.

power systems in the United States or in Europe, as was discussed at the 1930 World Power Conference, involves the construction of certain key tie lines whose length would considerably exceed the present limiting distance of some 350 miles. As already explained, this economic limit is dictated by considerations of stability, that is to say, by the maintenance of synchronism between the machines located in the generating stations at the two ends of the line. The synchronizing power keeping the two groups of machines in step is transmitted over the line by virtue of an angular displacement between the air-gap voltages (i.e. the e.m.f.'s behind the synchronous reactances) of the machines, and there is a critical angle beyond which synchronism is lost. It is this displacement angle upon which the stability of the transmission system as a whole, under steady load conditions, ultimately depends.

Considering the transmission system as a whole, therefore, the relation expressed by equation (218) for the transmission line alone becomes—

$$P_m = \frac{E_G E_M \sin \delta}{X_0\left(1 + \frac{R_0^2}{X_0^2}\right)} \quad . \quad . \quad . \quad (221)$$

where E_G and E_M are the generator (sending-end) and motor (receiving-end) air-gap voltages respectively, and δ is their mutual displacement.*

R_0 and X_0 are the resistance and reactance components of the transfer impedance of the transmission system. For purposes of discussion, however, the effect of resistance on system stability may be neglected, so that, with $R_0 = 0$, the critical angle is $\delta = 90°$. Equation (221) then becomes simply—

$$P_m = \frac{E_G E_M}{X_0} = \frac{E_G E_M}{X_G + X + X_M} \quad . \quad . \quad (222)$$

where X_G and X_M are the synchronous reactances of the generators and motors respectively, and X is the reactance of the intervening transmission line, including its terminal transformers.

The circuit parameter which particularly limits the amount of power that can be transmitted is the system reactance X_0. Usually the line reactance is not the most important element; for much more reactance is, as a rule (i.e. where the line is not

* *Cf.* Equation (40).

very long), associated with the terminal apparatus. The synchronous machines at each end of the system thus contribute to the power limitation of a transmission system to a very considerable extent. This is clearly shown by the example of Fig. 93, where the machine reactances are equivalent to an

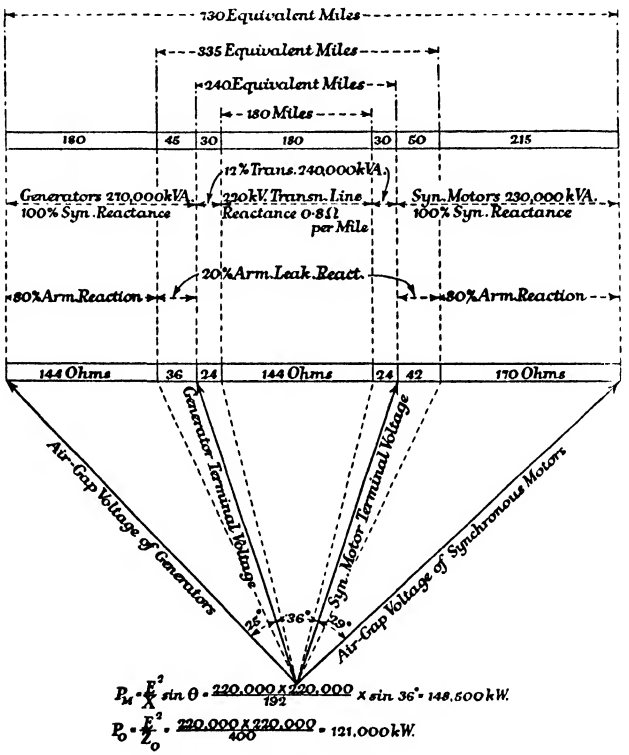

FIG. 93

extension of the transmission line amounting to 490 miles, or no less than 270 per cent of the line itself.

From the point of view of increasing the transmitted power as limited by stability considerations, it is therefore advantageous to employ low-reactance machines at both ends of the system. But this entails greater size, increased capital cost, and thus greater installed cost and lower efficiency as compared with synchronous machines of normal design. In addition, such special machines would give rise to fresh problems in

that under fault conditions the short-circuit currents would be greatly increased, thus necessitating circuit-breakers designed for much heavier duty.

The only remaining possibility of increasing the limiting power transmitted, therefore, lies either in reducing the total line reactance X or in neutralizing its effects by some means. Apart from the fact that little is to be gained from a reduction in transformer reactance, since this represents but a fraction of the total line reactance, this reactance is more or less fixed by other requirements of transformer design; while the line reactance itself, being proportional to the transmission distance and inversely proportional to the number of parallel circuits, can only be reduced by adding one or more circuits. This in turn makes the transmission line uneconomic; besides which, the increased charging current, due to the increase in line capacitance, upsets the stable operation of the generators and thus lowers the stability limit of the system as a whole.

So far consideration has only been given to the steady-state stability limit of the transmission system as determined by the angle δ of equation (221). It is obvious that under conditions of steady-load operation, a certain margin must be provided between the actual operating angle and the pull-out angle defined by $\delta = \tan^{-1}(X_0/R_0) \approx 90°$, as otherwise synchronism may be lost during a disturbance. The determination of the maximum operating angle consonant with the maintenance of system stability during disturbances, such as faults or switching operations, is a matter of considerable difficulty, and is involved in the general problem of transient stability which has been receiving so much attention in recent years. With modern systems of high-speed excitation, employing exciters having a build-up rate of 6 000 V. or more per second, the transient power limit can be raised to some 80 per cent of the steady-state limit given by equations (221) or (218), so that the curves of Fig. 91 must be looked upon as representing the ultimate power limits of a transmission system rather than limits actually attainable at the present time.

Methods of Compensating Transmission-line Reactance. It is by now generally recognized that the only hope for the a.c. system of power transmission lies in the possibility of extending these steady-state power limits to some new *ultima thule*, by providing special means for neutralizing the power-limiting effects of line reactance. The first attempt to solve this problem

was made in 1921 by F. G. Baum, whose paper entitled "Voltage Regulation and Insulation for Large-power Long-distance Transmission Systems" [2] was hailed as an especially important contribution to the art of power transmission and inspired a series of theoretical studies and experimental investigations, undertaken during the following five years, which laid the foundations of steady-state stability theory.

Baum's system of transmission rests on the principle of the intermediate synchronous condenser station, a principle which, broadly speaking, involves supplying to the transmission line, at intervals along it, the lagging reactive power necessary to compensate for the lagging reactive-power consumption due to line inductance. In Baum's view, moreover, these intermediate condenser stations are to be regarded as an integral part of the transmission system, and therefore their cost must be met by the increased economy of operation which their inclusion makes possible; but any similar equipment installed at the receiving end for the purpose of correcting the power factor of the load should not enter into the cost of transmitting power, for the reactive power consumption in that case is a characteristic of the receiving-end (load) network, and not of the transmission line.

One of the outstanding features of the Baum system of power transmission, in fact the main outstanding feature, is that the transmission line as a whole acquires the electrical characteristics of its individual sections. As the direct result of the reactive power compensation maintained by the several intermediate condenser stations, the voltage at each point of section is maintained constant and equal to the transmission pressure. The vector voltage difference between the sending-end and receiving-end voltages is thus subdivided into a number of successive voltage drops, each corresponding to a transmission angle θ which is only a fraction of the angle represented by the total voltage drop along the line (see Fig. 94). The consequent reduction in the angle δ between the internal voltages of successive synchronous machines means very greatly increased system stability, while for a given operating angle the amount of power which can be transmitted without danger of instability is a function of the distance between successive synchronous condenser stations, and not of the total transmission distance. In other words, with the Baum system of transmission the distance over which power may be transmitted

is no longer limited by technical considerations, but becomes purely a question of economics.

The Baum system of power transmission is, in effect, a method of "shunt excitation" of the transmission line. Apart from the vital question of the transient stability characteristics of the intermediate synchronous condensers, a question which does not as yet seem to have been satisfactorily answered, [3] there remains a fundamental drawback to the use of such shunt-connected machines: their size, and therewith their cost, increase as the square of the transmission voltage. And as a long-distance transmission line has to operate at really high voltages to justify its existence on economic grounds, it

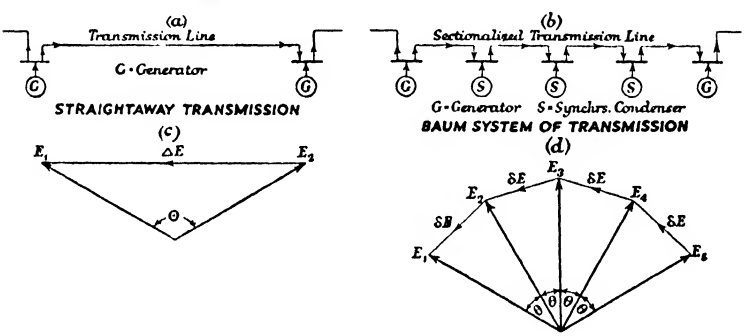

FIG. 94

is self-evident that there must be a prior limitation to the economic transmission distance imposed by the rapidly increasing cost of intermediate condenser stations.

Recognition of this prior limit some twenty years ago led to the investigation of alternative methods of compensating the inevitable line inductance, and culminated in the development of "series excitation" schemes, involving the insertion of capacitance in series with the line. Line compensation is in this case direct, being based on the principle of voltage resonance, and is obtained by the addition, at intervals along the line, of a series voltage equal and in phase opposition to the voltage drop due to the load current acting in the inductance of the individual line sections.

The first application of this method of line compensation to an actual transmission system was a series capacitor or static condenser installation for the voltage regulation of a

33 kV. line in 1928, [4] and the general circuit arrangement for one phase is shown in Fig. 95. Protection against fault conditions, such as a short circuit of the line on the load side, which would impress the full line voltage on the condenser bank, or a breakdown of the condenser dielectric, which would allow the load current to arc through the faulty section, is provided by a combination of a special sphere gap and a shunting contactor of high-speed type. The protective equipment is arranged to operate as soon as the voltage across the capacitor rises to 150 to 200 per cent of its rated value, thus affording overload protection as well. The high-speed contactor short-circuits the capacitor in under 10 milliseconds, and its rapid

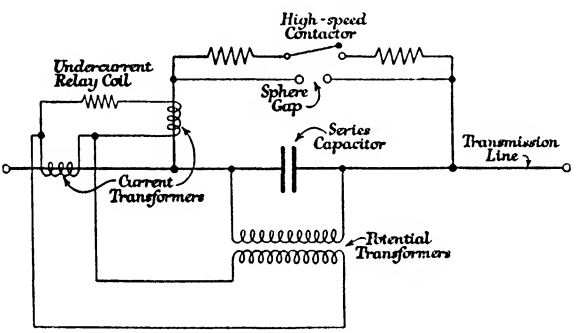

FIG. 95

operation ensures that under fault conditions the full line reactance is almost immediately available to limit the short-circuit current.

The success attending this installation led, in 1930, to the investigation of the effects of series capacitors upon the power available and the steady-state stability in the case of a 250-mile transmission line operating at 110 kV., and having a total inductive reactance (including transformers) of 263 ohms, necessitating a series capacitance of 10 μF. per phase. The results of this theoretical study indicated that the power limit could be raised from 53 000 kW. to 113 000 kW., representing an increase of 110 per cent.

The rather elaborate protective system required by such static condenser installations is done away with in an alternative method of series compensation put forward by T. H. Morgan in 1930, and illustrated in Fig. 96. Morgan's method

employs a synchronous motor-generator set, comprising a synchronous motor supplied from the transmission line through a transformer bank, and an "inductive compensating generator" from which a leading quadrature voltage, identical both in magnitude and phase with that produced by series capacitors, is obtained and, via a current-transformer bank, is injected into the transmission line. As this series voltage must at all times be proportional to the line current, a polyphase mercury-arc rectifier unit can be used to provide the excitation of the

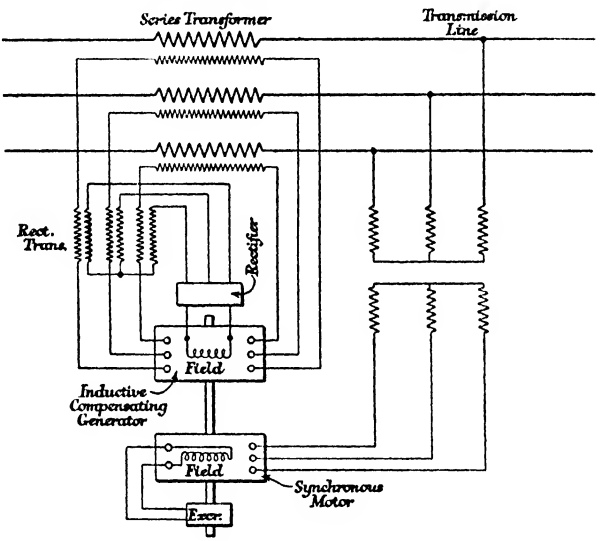

FIG. 96

compensating generator, the rectifier being fed from special current transformers connected in series with the primary windings of the main current transformer bank.

The rapid response in machine excitation obtained by this means is ideal from an operating standpoint, [5] while the magnetic saturation occurring under system short-circuit conditions limits the compensating effect of the machine and thus reduces the fault current by allowing the line reactance to exert a very considerable current-limiting influence. In fact, this inherent characteristic of the inductive compensating generator enables full compensation to be obtained up to a critical value of the line current, but almost no appreciable

increase in compensation will occur if the current exceeds this value.

Dual Compensation Systems. The kVAr requirements in compensating plant are the same whether the system of compensation is based on shunt or series excitation of the transmission line, [6] so that on that account there is little to choose between the two alternatives. From the operating standpoint, however, the series methods have the advantage that, being direct, the amount of compensation is automatically adjusted to the line current. Yet none of the foregoing systems of compensation attempts to nullify the effects of the charging current taken by long high-voltage transmission lines. As has already been shown, this wattless component of the total line current adversely affects the economic limit of power transmission, and only ceases to enter into the transmission problem in the case where, by appropriate compensation of line inductance, the stability limit is extended so as to make the maximum transmissible power coincide with the natural load of the transmission line for distances exceeding the present limiting value of some 350 miles. Hence, although compensation of line inductance enables us, technically at any rate, to transmit power over any distance we choose, the charging current will impose its own limitation on the transmission distance, because of the rapidly diminishing economy with which power transmission takes place under these circumstances.

Proposals taking into account this ultimate economic limitation were first put forward in 1932 by H. H. Skilling [7] on the basis of the tuned transmission line, that is, a power line operating under natural load conditions, and having a length equal to half or one-quarter of the natural wavelength (3 700 miles at 50 c/s). Skilling's original proposals envisaged the adoption of higher transmission frequencies so as to reduce the length of the half-wave or quarter-wave line to the particular transmission distance required. His subsequent proposals (1936) adhered to normal-frequency transmission, and provided for series capacitor compensation of line inductance together with what may be termed "shunt inductor" compensation of the line capacitance. In this way the transmission line may be artificially loaded so as to have a natural wavelength many times the actual transmission distance.

Skilling's view is that the shunt inductance of the terminal

transformers can be made to compensate the capacitance of the line. This is no doubt correct where relatively short lines are concerned. But the enormous charging currents taken by really long transmission lines—and we are here considering distances of the order of 500 to 1 000 miles—which necessarily would have to operate at pressures of from 400 to 600 kV., place such a proposal right out of court.

The most interesting method of dual compensation, and one which would appear to offer a complete solution of the transmission problem, is that put forward some years ago by Major A. M. Taylor, [8] and recently extended to cover the problem of transient instability [9] as described by him at the 1937 Congress of the C.I.G.R.E., where it created considerable interest.

Taylor's system* of power transmission makes use of special transformers, termed "quadrature boosters," which at intervals transfer the capacitance of the line from its natural shunt position between each line and neutral to the required position in series with the line inductance of each phase. In other words, the quadrature booster transformer converts the inherent shunt capacitance of the line into the series capacitance needed to compensate the line inductance.

As is well known, a three-phase transformer can be arranged so as to give a secondary voltage in leading phase quadrature with the voltage impressed on the primary. Quadrature booster transformers of this type have recently been used to obtain proper load sharing between two parallel branches of a transmission system, one of which also formed part of a trunk transmission line. [10] The essential feature of the quadrature boosters in the Taylor system of power transmission is the relationship between the secondary voltage neutralizing the inductive pressure drop in the line, and the primary current neutralizing the charging current of the line, whereby voltage resonance on the secondary side and current resonance on the primary side are simultaneously obtained, and thus complete "tuning" of the transmission line is effected.

This fundamental relationship is illustrated by Fig. 97, which represents one phase of a quadrature booster connected between two sections of line. If C is the line capacitance to neutral per section and L is the corresponding line inductance, then the charging current per section is $I_o = j\omega CE$, while the inductive voltage drop in each section of line is $E_x = IX$

* Brit. Pat. No. 459,121, 1938; U.S.A. Pat. No. 2,180,264, 1939.

$= j\omega LI$. Complete compensation of the line inductance then necessitates a quadrature boosting voltage from the transformer secondary defined by $E_B = -E_X$. Similarly, compensation of the charging current requires that the booster primary draws a current defined by $I_B = -I_C$. (The former will be a leading voltage and the latter a lagging current.) For these conditions to be fulfilled simultaneously, the reactive volt-amperes on

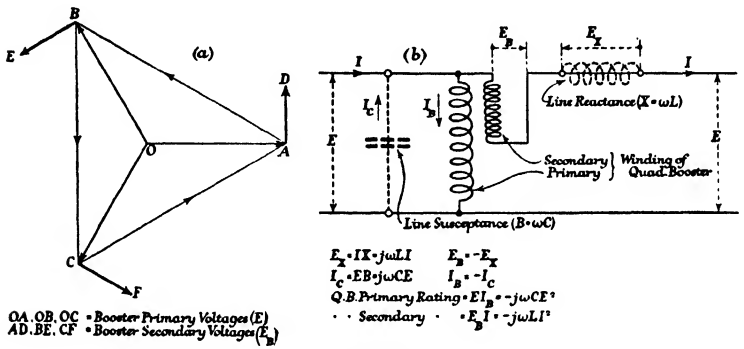

FIG. 97

the primary and secondary sides of the quadrature booster must be equal. Hence—

$$EI_B = IE_X; \text{ or } -j\omega CE^2 = -j\omega LI^2;$$

that is—

$$\frac{E}{I} = \sqrt{\frac{L}{C}} = Z_0,$$

so that complete dual compensation is only to be obtained when the load impedance is equal to the characteristic impedance of the transmission line; that is, when the line is operating under natural load conditions.

In the case of very long lines, with their enormous charging currents, it may not be possible—due to the increase in E necessitated on economic grounds by the increasing transmission distance—to obtain sufficiently high values of the load current I to maintain the requisite balance between the secondary and primary kVA. values of the quadrature booster. In other words, under these conditions the booster primary current—

$$I_B = j\frac{\omega LI^2}{E} \quad . \quad . \quad . \quad (223)$$

will tend to become less than the charging current $I_c = j\omega CE$.

Fortunately, however, in the case of super-power long-distance trunk lines, transmission is not commercially possible unless the amount of power transmitted is very large—of the order of megawatts—so that there is then in most cases a wide enough range within which balance between charging current and booster primary current can be maintained. For those somewhat extreme cases where, in spite of high values of transmitted power, I_B is yet less than I_C, Taylor's proposals include the insertion of ballast inductance in the line in order artificially to increase the value of L in equation (223) and so to obtain the requisite balance between I_B and I_C.

At first sight it would appear that at loads lower than full load the transmission pressure would have to be reduced in the same ratio as the load current in order to maintain the above balance. For example, if the load current I is halved, the booster secondary output kVAr. is reduced to one-quarter of its normal value. The corresponding reduction in primary input would thus involve halving the voltage E, and this reduction would have to be maintained throughout the whole length of the transmission line. This difficulty may be readily overcome, however, by raising the sending-end voltage somewhat above the value corresponding to the above ratio of reduction. The resulting unbalance between booster primary current and line-charging current then leaves a slight excess of leading quadrature current, which generates an in-phase voltage in the line inductance. [11]

The cumulative effect of this in-phase voltage rise along the line is to raise the receiving-end voltage to the normal value corresponding to the full-load condition. Fig. 98 is a numerical illustration of the Taylor system of power transmission applied to the problem of transmitting 1 000 MW. at unity power factor over a distance of 1 000 miles by means of a double-circuit 440 kV. line, and with five intermediate quadrature booster stations at 200-mile intervals. Diagram (*a*) shows the current and voltage relations at full load, while diagram (*b*) gives the corresponding relations at half-load* and with equal sending- and receiving-end voltages. Finally, diagram (*c*) depicts the "unbalanced condition" of half-load operation in

* i.e. 50 per cent load current. As the voltage is also 50 per cent below normal, the transmitted power is then one-quarter the full-load value, or 125 MW. per circuit.

which the sending-end voltage is two-thirds instead of one-half normal. It is seen that there is an excess charging current averaging 122 A. per 200-mile section which, in traversing the line reactance of 140 ohms per section, generates an in-phase voltage rise amounting to 86 kV. per phase for the five sections; so that the receiving-end voltage remains at its normal value in spite of the sending-end voltage being one-third less.

A comparison of the several methods of line compensation

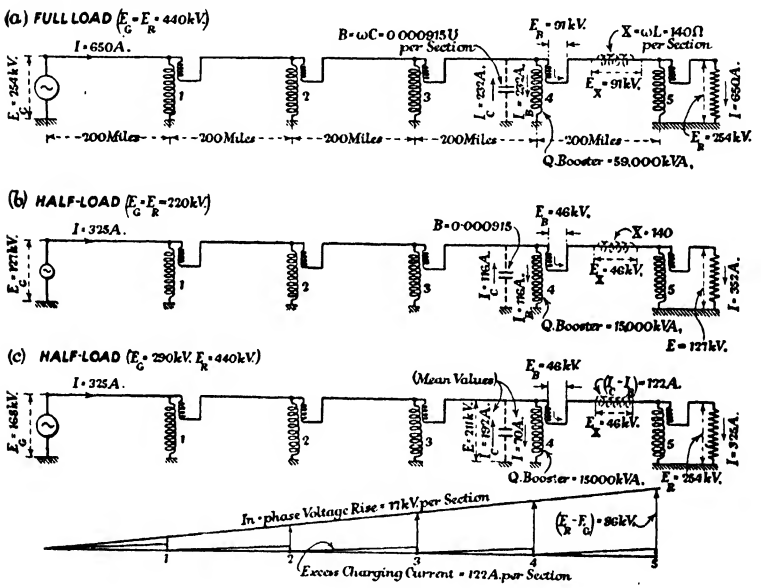

FIG. 98

is given in Fig. 99. Diagram (*a*) shows the normal transmission line in which all the circuit characteristics are operative. Diagram (*b*) illustrates the series method of line compensation, in which voltage resonance occurs between the line inductance L and the series capacitance C', so that the line behaves as if it possessed no inductance. The line capacitance, however, remains uncompensated, and the charging current therefore contributes seriously towards the line losses. Diagram (*c*) represents the so-called tuned transmission line, that is, a line operating under natural load conditions, in which mutual compensation of L and C takes place.

With such a line there remains, nevertheless, a displacement between E_G and E_R, amounting for 50 c/s to 360 degrees in 3 720 miles. Finally, diagram (*d*) illustrates Taylor's system of transmission, in which both series and shunt compensation occur, and in such a manner that the necessary compensating equipment is embodied in one piece of apparatus, namely, the quadrature booster transformer. The primary winding of the

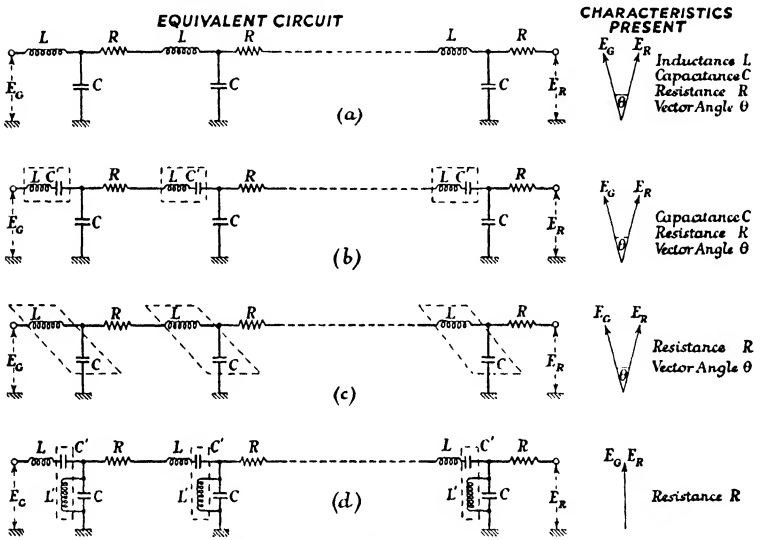

(a) *Normal Transmission Line.*
(b) *Series Compensated Line* ($\omega L = 1/\omega C'$).
(c) *Tuned Transmission Line* ($E/I = \sqrt{L/C} = Z_0$).
(d) *Taylor Transmission System* ($L/C = L'/C'$. $\omega L = 1/\omega C'$).

FIG. 99

booster is represented by the shunt inductance L', while the secondary winding is represented by the series capacitance C'. It is seen that with this arrangement complete compensation of L and C takes place, so that the circuit is equivalent to a d.c. line whose only characteristic is the resistance R.

REFERENCES

(1) *Vide* H. Rissik: "Some Aspects of the Electrical Transmission of Power by Means of Direct Current at Very High Voltages," *Journ. I.E.E.*, 1934, Vol. 75, p. 1; also "Super-power Transmission," *Electrical Review*, 1940, Vol. 126, p. 125.

(2) *Trans., A.I.E.E.*, 1921, Vol. 40, p. 1017.

(3) *Cf.* I. H. Summers and J. B. McClure: "Progress in the Study of System Stability," *Trans. A.I.E.E.*, 1930, Vol. 49, p. 132.

(4) *Vide* E. K. Skelton: "The Series Capacitor Installation at Ballston, N.Y.," *General Electric Review*, 1928, Vol. 31, p. 432; also J. W. Butler and C. Concordia: "Series Capacitor Application Problems," *Elec. Engineering*, 1937, Vol. 56, p. 975; and R. C. Buell: "Improved Voltage Regulation with Series Capacitors," *General Electric Review*, 1937, Vol. 40, p. 174.

(5) *Cf.* H. Rissik: "High-speed Rectifier Excitation Systems," *Elec. Times*, 1939.

(6) *Elektrotechnische Zeitschrift*, 1929, Vol. 50, p. 978.

(7) *Trans. A.I.E.E.*, 1932, Vol. 51, p. 51.

(8) *Vide* A. M. Taylor: "Ultra-long-distance Power Transmission," *Engineering*, 1937, Vol. 143, p. 311; also H. Rissik: "Long-distance Transmission," *Electrical Review*, 20th October, 1939, p. 517.

(9) *Cf.* A. M. Taylor: "Quadrature Boosters and Transmission," *Electrician*, 1940, Vol. 124, p. 390.

(10) *Vide* W. J. Lyman and J. R. North, *Trans. A.I.E.E.*, 1938, Vol. 57, p. 579; also *Brown Boveri Review*, March, 1938, p. 43.

(11) *Vide* H. Rissik: "Long-distance Power Transmission," *Electrician*, 1940, Vol. 124, p. 317.

BIBLIOGRAPHY

1920–23

"Electrical Calculations of Long-distance H.-V. Transmission Systems." A. McKinstry, *J. I.E.E.*, **57** (Supp.), 92.

"Stability of High-power Generating Stations." C. P. Steinmetz, *J. Am. I.E.E.*, **39**, 554.

"Power Control and Stability of Electric Generating Stations." C. P. Steinmetz. *Trans. Am. I.E.E.*, **39**, 1215.

"Voltage Regulation and Insulation for Large-power Long-distance Transmission Systems." F. G. Baum. *Trans. Am. I.E.E.*, **40**, 1017.

"Transmission-line Circuit Constants and Resonance." R. D. Evans and H. K. Sels. *Elec. J.*, **18**, 306, 356, 530; and **19**, 53.

"Interconnection of A.C. Power Stations." L. Romero and J. B. Palmer. *J. I.E.E.*, **60**, 287.

"Electrical Characteristics of Transmission Systems." H. B. Dwight. *Trans. Am. I.E.E.*, **41**, 781.

"Qualitative Analysis of Transmission Lines." H. Goodwin. *Trans. Am. I.E.E.*, **42**, 24.

1924

"Superpower Transmission." P. H. Thomas. *Trans. Am. I.E.E.*, **43**, 1.

"Some Theoretical Considerations of Transmission Systems." C. L. Fortescue and C. F. Wagner. *Trans. Am. I.E.E.*, **43**, 16.

"Power Limitations of Transmission Systems." R. D. Evans and H. K. Sels. *Trans. Am. I.E.E.*, **43**, 26.

"Experimental Analysis of Stability and Power Limitations." R. D. Evans and R. C. Bergvall. *Trans. Am. I.E.E.*, **43**, 39.

"Limitations of Output of Power Systems Involving Long Transmission Lines." E. B. Shand. *Trans. Am. I.E.E.*, **43**, 59.

"Analytical Solution of Networks." R. D. Evans. *Elec. J.*, **22**, 149, 208.

1925

"Artificial Representation of Power Systems." H. H. Spencer and H. L. Hazen. *Trans. Am. I.E.E.*, **44**, 72.

"Power System Transients." V. Bush and R. D. Booth. *Trans. Am. I.E.E.*, **44**, 80.

"Fundamental Considerations of Power Limits of Transmission Systems." R. E. Doherty and H. H. Dewey. *Trans. Am. I.E.E.*, **44**, 972.

"Transmission Stability." C. L. Fortescue. *Trans. Am. I.E.E.*, **44**, 984.

"Single-phase Short-circuit Calculations." W. W. Lewis. *G.E. Review*, **28**, 489.

"Stability of Long Transmission Lines." C. D. Gibbs. *Elec. World*, **85**, 143.

1926

"Investigation of Transmission-system Power Limits." C. A. NICKLE and F. L. LAWTON. *Trans. Am. I.E.E.*, **45**, 1.

"Calculation of Steady-state Stability in Transmission Systems." E. CLARKE. *Trans. Am. I.E.E.*, **45**, 22.

"Further Studies of Transmission Stability." R. D. EVANS and C. F. WAGNER. *Trans. Am. I.E.E.*, **45**, 51.

"Circle Diagram of a Transmission Network." F. E. TERMAN. *Trans. Am. I.E.E.*, **45**, 1081.

"Stability Characteristics of Alternators." O. E. SHIRLEY. *Trans. Am. I.E.E.*, **45**, 1108.

"Synchronizing Power in Synchronous Machines under Steady-state and Transient Conditions." H. V. PUTMAN. *Trans. Am. I.E.E.*, **45**, 1116.

"Calculation of 1-phase Short-circuits by the Method of Symmetrical Components." A. P. MACKERRAS. *G.E. Review*, **29**, 218, 468.

"Mechanical Analogy to the Problem of Transmission Stability." S. B. GRISCOM. *Elec. J.*, **23**, 230.

"Stability of A.C. Turbine Generators with Fluctuating Loads." J. STRASSER. *Elec. J.*, **23**, 413.

1927

"Stability of Large Power Systems." F. H. CLOUGH. *J. I.E.E.*, **65**, 653.

"Baum Principle of Transmission." C. L. FORTESCUE. *Elec. World*, **89**, 954.

"Problems Arising from the Expansion and Interconnection of Power Systems." F. C. HANKER. *Elec. J.*, **24**, 96.

"Oscillation Stability of Synchronous Machines in Parallel." M. OLLENDORF and W. PETERS. *Wiss. Veröff. Siemens-Konzern*, **5**, 11.

1928

"Static Stability Limits and the Intermediate Condenser Station." C. F. WAGNER and R. D. EVANS. *Trans. Am. I.E.E.*, **47**, 94.

"Alternator Characteristics under Conditions Approaching Instability." J. T. H. DOUGLAS and E. W. KANE. *Trans. Am. I.E.E.*, **47**, 275.

"Reactances of Synchronous Machines." R. H. PARK and B. L. ROBERTSON. *Trans. Am. I.E.E.*, **47**, 514.

"Quantitative Mechanical Analysis of Power-system Transient Disturbances." R. C. BERGVALL and P. H. ROBINSON. *Trans. Am. I.E.E.*, **47**, 915.

1929

"System Stability as a Design Problem." R. H. PARK and E. H. BANCKER. *Trans. Am. I.E.E.*, **48**, 170.

"Elementary Conception of Stability." C. A. POWEL. *Elec. J.*, **26**, 279.

"Developments in Generators and Systems as they Affect System Reliability." R. E. POWERS and L. A. KILGORE. *Elec. J.*, **26**, 480.

"Long-distance Power Transmission." R. RÜDENBERG. *E.T.Z.*, **50**, 978.

1930

"Progress in the Study of System Stability." I. H. SUMMERS and J. B. MCCLURE. *Trans. Am. I.E.E.*, **49**, 132.

"Stability of Synchronous Machines." C. A. NICKLE and C. A. PIERCE. *Trans. Am. I.E.E.*, **49**, 338.

"General Circle Diagram of Electrical Machinery." F. E. TERMAN. *Trans. Am. I.E.E.*, **49**, 376.

"Transient Torque/Angle Characteristics of Synchronous Machines." W. V. LYON and H. E. EDGERTON. *Trans. Am. I.E.E.*, **49**, 686.

"Calculation of Alternator Swing Curves—Step-by-Step Method." F. R. LONGLEY. *Trans. Am. I.E.E.*, **49**, 1129.

"Power System Stability—A Non-mathematical Review." R. D. BOOTH and O. G. C. DAHL. *G.E. Review*, **33**, 677, and **34**, 131.

"Theory of Power-system Stability." O. MUEHLEISEN. *Elec. J.*, **27**, 356, 416.

"Parallel Operation of any Number of Synchronous Machines." G. GALMICHE. *Rev. gén. d'Él.*, **28**, 3, 43.

1931

"Calculation of Synchronous Machine Constants." L. A. KILGORE. *Trans. Am. I.E.E.*, **50**, 1201.

"Determination of Sychronous Machine Constants by Test." S. H. WRIGHT. *Trans. Am. I.E.E.*, **50**, 1331.

"Power System Stability." F. A. HAMILTON. *Eng. J.*, **14**, 227.

"Transient Operation of Interconnected Generating Stations." L. BARBILLION. *Rev. gén. d'Él.*, **30**, 943.

1932

"Tuned Power Lines." H. H. SKILLING. *Trans. Am. I.E.E.*, **51**, 51.

"Equivalent Circuits." F. M. STARR. *Trans. Am. I.E.E.*, **51**, 287.

"Generalized Stability Solution for Metropolitan-type Systems." S. B. GRISCOM, W. A. LEWIS and W. R. ELLIS. *Trans. Am. I.E.E.*, **51**, 363.

"Torque/Angle Characteristics of Synchronous Machines Following Transient Disturbances." S. B. CRARY and M. L. WARING. *Trans. Am. I.E.E.*, **51**, 764.

"Out-of-step Conditions on a Synchronous System." A. A. KRONEBERG. *Elec. Eng.*, **51**, 769.

"Synchronous Machine Reactances—A Fundamental and Physical Viewpoint." L. P. SCHILDNECK. *G.E. Review*, **35**, 560.

1933

"Power Limits of a Transmission System." W. S. PETERSON. *Elec. Eng.*, **52**, 569.

"Power Limits of 220-kV. Transmission Lines." A. A. KRONEBERG and M. MCFERRAN. *Elec. Eng.*, **52**, 758.

"Power Limits of Synchronous Machines." E. CLARKE and R. G. LORRAINE. *Elec. Eng.*, **52**, 780.

"Steady-state Stability of Composite Systems." S. B. CRARY. *Elec. Eng.*, **52**, 787.

"Solution of the Two-machine Stability Problem." H. L. BYRD and S. R. PRITCHARD. *G.E. Review*, **36**, 81.
"Calculation of the Transient Stability of Power Systems." R. MAYER. *E.T.Z.*, **54**, 678.

1934

"Control of the Voltage and Power Factor in Interconnected Systems." O. HOWARTH. *J.I.E.E.*, **76**, 353.
"Earth Faults—Analysis by the Method of Phase-sequence Components." G. A. ROBERTSON. *Electrician*, **113**, 95, 241, 433, 573, 797; and **114**, 183, 341, 599.
"Graphical Solution of Steady-state Stability." H. B. DWIGHT. *Trans. Am. I.E.E.*, **53**, 566.
"Equivalent Circuits in System Stability Studies." O. G. C. DAHL and A. E. FITZGERALD. *Trans. Am. I.E.E.*, **53**, 1272.
"Calculation of 2-machine Stability with Resistance." S. R. PRITCHARD and E. CLARKE. *G.E. Review*, **37**, 87.
"System Stability Reduced to a Practical Basis." R. H. DUVAL and L. T. EASTMAN. *Elec. World*, **103**, 514, 620.

1935

"Stability Characteristics of Alternators and Large Interconnected Systems." W. D. HORSLEY. *J.I.E.E.*, **77**, 577.
"Stability of the General 2-machine System." O. G. C. DAHL. *Trans. Am. I.E.E.*, **54**, 185.
"Engineering Features of the Boulder Dam—Los Angeles Line." O. M. SCATTERGOOD. *Trans. Am. I.E.E.*, **54**, 361, 494.

1936

"Requirements of Direct Interconnectors Between Generating Stations." R. H. COATES. *M.-V. Gazette*, **16**, 51.
"Negative-phase-sequence Reactance of Synchronous Machines." W. A. THOMAS. *Elec. Eng.*, **55**, 1378.
"Impedance Measurements on Underground Cables." R. L. WEBB and O. W. MANZ. *Elec. Eng.*, **55**, 359.
"Free Oscillations Between Two Synchronous Machines." R. WIDEROE. *Arch. für Elektrot.*, **30**, 825.
"Network Reactance for Short-circuit Calculations." H. MAASS. *Siemens Zeits.*, **16**, 115.

1937

"Ultra-long-distance Power Transmission." A. M. TAYLOR. *Engineering*, **143**, 311, 354.
"Notes on the Calculation of Network Short-circuits." C. J. O. GARRARD. *G.E.C. Journal*, Feb., 62.
"Stability of 3-phase Power Systems." W. WANGER. *Brown Boveri Rev.*, **24**, 99.
"Contributions to Synchronous Machine Theory." A. S. LANGSDORF. *Elec. Eng.*, **56**, 41.
"Rectifier Circuit for Measuring Small Power/Angle Oscillations." T. A. ROGERS and B. L. ROBERTSON. *Elec. Eng.*, **56**, 339.

"Power System Faults to Ground." C. L. GILKESON, P. A. JEANNE and J. C. DAVENPORT. *Elec. Eng.*, **56**, 421, 428.
"Fundamental Concepts of Synchronous Machine Reactance." B. R. PRENTICE. *Trans. A.I.E.E.*, **56** (Supp.), 1.
"Stability of 3-phase Power Systems Under Transient Disturbances." W. WANGER. *C.I.G.R.E.*, No. 120.
"Voltage Stability of Parallel-connected Asynchronous and Synchronous Machines." A. LEONHARD. *Arch. für Elektrot.*, **31**, 24.
"Transient Stability of Synchronous Machines." W. WANGER. *Bull. Assoc. Suisse Elect.*, **28**, 41.
"Sudden Load Changes with Synchronous Machines in Parallel." F. HELLER. *Rev. Gén. d'Él.*, **41**, 67, 163.

1938

"Voltage Control and Power Limits of Transmission Lines." H. RISSIK. *Elec. Times*, **93**, 387.
"Constant-voltage Transmission." H. RISSIK. *Elec. Times*, **94**, 109.
"Transient Stability and its Requirements." A. M. TAYLOR. *Electrician*, **122**, 531.
"Parallel Operation." H. RISSIK. *Elec. Review*, **122**, 751.
"System Analysis for Peterson Coil Applications." W. C. CHAMPE and F. VON VOIGTLANDER. *Trans. Am. I.E.E.*, **57**, 663.
"Factors Influencing Synchronous Stability of Transmission Systems." B. L. GOODLET. *Trans. S. Afr. I.E.E.*, **29**, 166.
"Stability Conditions in the Operation of Asynchronous Machines over Long Lines." A. LEONHARD. *E. und M.*, **56**, 405.
"Long-distance Transmission at Half-wave Frequency." A. LEONHARD. *E. und M.*, **56**, 542.
"On the Theory of Parallel Running of Synchronous Machines." F. GUERY. *Bull. Soc. Franç. Élec.*, **8**, 1077.

1939

"Synchronizing Power, and Long-distance Power Transmission." H. RISSIK. *Elec. Review*, **124**, 953, and **125**, 517.
"Phase-angle Control of System Interconnections." R. E. PIERCE and B. W. HAMILTON. *Trans. Am. I.E.E.*, **58**, 83.
"Static Power Limits of Synchronous Machines." C. F. DALZIEL. *Trans. Am. I.E.E.*, **58**, 93.
"Regulating Transformers in Power-system Analysis." J. E. HOBSON and W. A. LEWIS. *Trans. Am. I.E.E.*, **58**, 874.
"Comparison of Stability of Synchronous and Asynchronous Machines on Long Lines." A. LEONHARD. *E. und M.*, **57**, 77.

1940

"Long-distance Power Transmission." H. RISSIK. *Electrician*, **124**, 317.
"Quadrature Boosters and Transmission." A. M. TAYLOR. *Electrician*, **124**, 390.
"Calculation of Unsymmetrical Short-circuits." H. RISSIK. *Beama J.*, **46**, 100, *et seq.*

"Superpower Transmission." H. RISSIK. *Elec. Review*, **126**, 125.
"Power Transfer between Interconnected Energy Sources." V. GENKIN. *Rev. Gén. d'Él.*, **47**, 437.

1941

"Control of Power in Large Interconnected Electrical Supply Systems." T. F. WALL. *Engineering*, **152**, 1, 41, 81, 121, 161, 221, 264.
"System Stability." F. W. GAY. *Trans. Am. I.E.E.*, **60**, 168.
"System Load Swings." H. A. BAUMAN, O. W. MANZ, J. E. MCCORMACK and H. B. SEELEY. *Trans. Am. I.E.E.*, **60**, 541.
"Interconnected Transmission Systems." H. RISSIK. *Electrician*, **126**, 243.
"Semi-graphical Method of Determining the Power Limits of an Interconnector. H. RISSIK. *J. I.E.E.*, **88** (II), 568.
"Stability of 3-phase Long-distance Transmission Systems." W. WANGER and W. FREY. *Brown Boveri Rev.*, **28**, 264.

1942

"Long-distance Power Transmission by A.C." E. FRIEDLAENDER and C. J. O. GARRARD. *Engineering*, **153**, 1, 21, 41.
"Problems of Long-distance High-power D.C. Transmission." C. EHRENSPERGER. *Bull. Assoc. Suisse Élect.*, **33**, 145.
"A.C. Transmission of very High Powers over Great Distances." W. WANGER. *Bull. Assoc. Suisse Élect.*, **33**, 115.
"Facilities for the Supply of Kilowatts and Kilovars." H. K. SELS and T. SEELY. *Trans. Am. I.E.E.*, **61**, 249.
"Control of Tie-line Power Swings." C. CONCORDIA, H. S. SHOTT and C. N. WEYGANDT. *Trans. Am. I.E.E.*, **61**, 306.
"Stability Study of A.C. Power Transmission Systems." J. G. HOLM. *Trans. Am. I.E.E.*, **61**, 893.
"Series Capacitors for Transmission Circuits." E. C. STARR and R. D. EVANS. *Trans. Am. I.E.E.*, **61**, 963.
"Stability Limitations of Long-distance A.C. Power Transmission Systems." E. CLARKE and S. B. CRARY. *Trans. Am. I.E.E.*, **61**, 1051.
"Static and Dynamic Stability of Synchronous Machines in Interconnected Supply Systems." J. MÜLLER-STROBEL. *Arch. für Elektrot.*, **36**, 573.

1943

"Limits of Power Transmission over the Lines of a Rigid Network." W. ZORN. *Arch. für Elektrot.*, **37**, 171.
"Load Distribution Between Interconnected Power Stations." P. G. KAUFMANN. *J. I.E.E.*, **90** (II), 119.

1944

"Static Stability of a Network with a Number of Synchronous Machines." W. FREY. *Brown Boveri Rev.*, **31**, 167.
"Power Limits of a Transmission Line in a Closely-coupled Network." R. LANGLOIS-BERTHELOT. *Rev. Gén. d'Él.*, **53**, 269.

"Static Stability of 3-phase Power-transmission Systems." A. DELLA VERDE. *Elettrotecnica*, **31**, 305, 325.
"Measured Electric Constants of a 270-mile 154-kV. Transmission Line." C. A. STREIFUS, C. S. ROADHOUSE and R. B. GOW. *Trans. Am. I.E.E.*, **63**, 538.

1945

"Stability of Networks, and Associated Problems." F. CAHEN. *Bull. Soc. Franç. Élect.*, **5**, 87.
"Comparative Study of Some Problems of A.C. and D.C. Power Transmission." C. EHRENSPERGER. *Brown Boveri Rev.*, **32**, 284, 322.
"Power Geometry of General Transmission Systems." W. ALTAR. *Trans. Am. I.E.E.*, **64**, 312.
"New Transmission-line Diagrams." A. C. SCHWAGER and P. Y. WANG. *Trans. Am. I.E.E.*, **64**, 610.
"Overhead-line Charts." J. S. FORREST. *Elec. Review*, **136**, 893 *et seq.*

1946

"High-voltage D.C. Transmission." C. EHRENSPERGER. *C.I.G.R.E.*, No. 103.
"Long-distance Transmission of Energy and the Artificial Stabilization of A.C. Systems." G. DARRIEUS. *C.I.G.R.E.*, No. 110.
"High-voltage D.C. Transmission." W. BORGQUIST. *C.I.G.R.E.*, No. 132.
"Artificial Stability of Synchronous Machines for Long-distance Power Transmission." W. FREY. *C.I.G.R.E.*, No. 317.
"Long-distance Power Transmission as Influenced by Excitation Systems." C. CONCORDIA, S. B. CRARY and F. J. MAGINNISS. *Trans. Am. I.E.E.*, **65**, 974.
"Characteristics of a 400-mile 230-kV. Series-capacitor-compensated Transmission System." B. V. HOARD. *Trans. Am. I.E.E.*, **65**, 1102.
"Evolution of Load-distribution Methods in Interconnected Networks." J. DANIEL. *Rev. Gén. d'Él.*, **55**, 403.
"Fundamental Investigations of the most Economical Voltage for Long-distance Power Transmission." W. FREY. *Brown Boveri Rev.*, **33**, 354.

1947–48

"Critical Analysis of the Possibilities of High-voltage D.C. Transmission." W. G. THOMPSON. *G.E.C. Journ.*, **14**, 239.
"A.C. Power Transmission Economics." S. B. CRARY and I. B. JOHNSON. *Elect. Eng.*, **66**, 793.
"Methods of Transmitting 2 000 000 kW. of Electric Power 600 km." *F.I.A.T. Report*, No. 1119.
"Technical Problems of 3-phase Long-distance Transmission at 400 kV." H. ROSER. *E.T.Z.*, **69**, 7.
"Technical and Economic Aspects of the Transmission of Electrical Energy over Long Distances." W. WANGER. *J.I.E.E.*, **95** (I), 340.
"Influence of Earthing on Network Power-system Stability." W. FREY. *Brown Boveri Rev.*, **35**, 100.
"Transmission of Electric Power at Extra-high Voltages." P. SPORN and A. C. MONTEITH. *Trans. Am. I.E.E.*, **66**, 1571.

INDEX

TRANSIENTS IN ELECTRIC CIRCUITS

By W. B. COULTHARD, B.Sc. (Eng.), A.M.I.E.E. Engineers interested in this subject can be sure of finding all the available information in this book. **21s.** net.

SWITCHGEAR HANDBOOK

Edited by W. A. COATES, M.I.E.E., F.A.I.E.E., and H. PEARCE, B.Sc. (Eng.), M.I.E.E. A group of sixteen engineers specializing in various branches of the subject have combined to write this book. It deals exhaustively with the design and construction of switchgear, and provides a mass of useful data.

Vol. I. Apparatus. **18s.** net.
Vol. II. Application. **30s.** net.

OUTDOOR HIGH-VOLTAGE SWITCHGEAR

By R. W. TODD, A.M.I.E.E., and W. H. THOMPSON, A.M.I.E.E. Engineers and designers concerned with high-voltage switchgear will welcome this reliable and exhaustive treatise. **42s.** net.

CURRENT COLLECTING BRUSHES IN ELECTRICAL MACHINES

By M. E. HAYES. An invaluable book for dynamo-electric machine designers and operating engineers and all concerned with the correct functioning of electrical machines. **21s.** net.

ALTERNATING CURRENT BRIDGE METHODS

By B. HAGUE, D.Sc. (Lond.), Ph.D., F.C.G.I., etc. A theoretical and practical handbook for the use of advanced students. Includes the Measurement of Inductance, Capacitance, and Effective Resistance at Low and Telephonic Frequencies. **30s.** net.

DICTIONARY OF ELECTRICAL TERMS

Including Electrical Communication

By S. R. ROGET, M.A., A.M.Inst.C.E. A complete and up-to-date dictionary of electrical engineering terms in the English language. It includes the general science of electricity and magnetism. **12s. 6d.** net.